frontiers | Research Topics

Current advancements in real-time plant pathogen diagnostics: From lab assays to in-field detection

Edited by
Ravinder Kumar, Milan Kumar Lal, Pramod Prasad and Rahul Kumar Tiwari

Published in
Frontiers in Plant Science

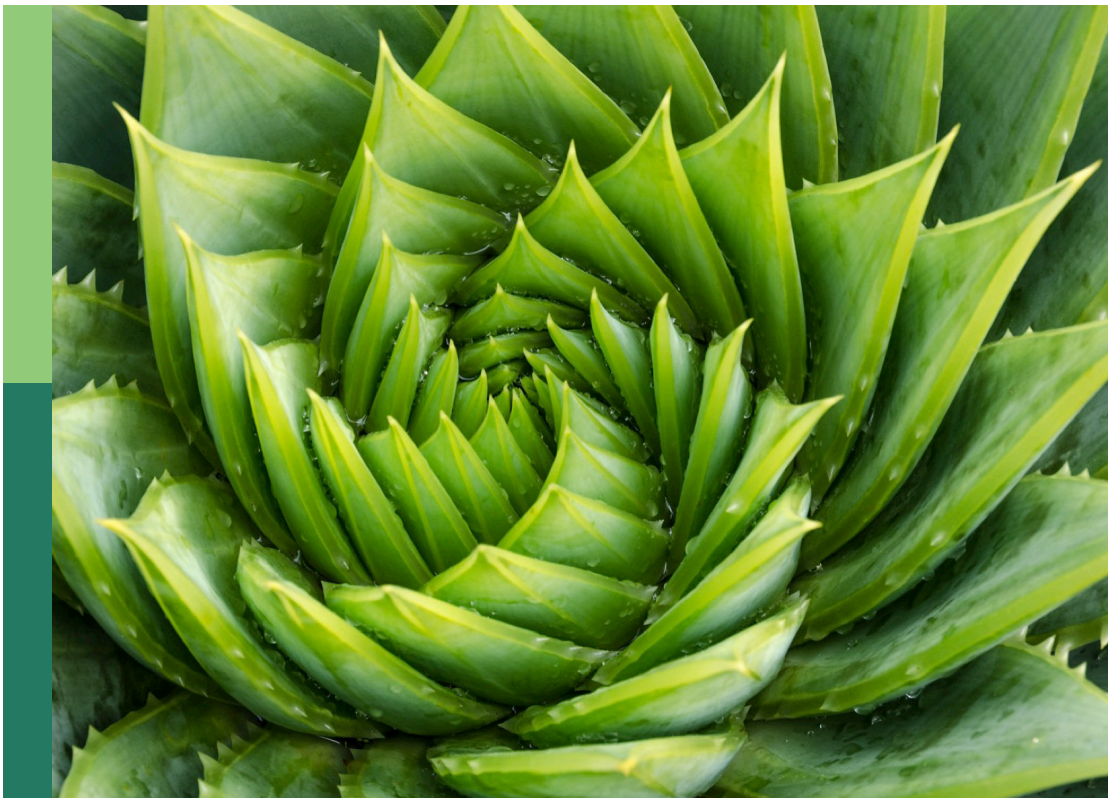

ISSN 1664-8714
ISBN 978-2-8325-3268-3
DOI 10.3389/978-2-8325-3268-3

About Frontiers

Frontiers is more than just an open access publisher of scholarly articles: it is a pioneering approach to the world of academia, radically improving the way scholarly research is managed. The grand vision of Frontiers is a world where all people have an equal opportunity to seek, share and generate knowledge. Frontiers provides immediate and permanent online open access to all its publications, but this alone is not enough to realize our grand goals.

Frontiers journal series

The Frontiers journal series is a multi-tier and interdisciplinary set of open-access, online journals, promising a paradigm shift from the current review, selection and dissemination processes in academic publishing. All Frontiers journals are driven by researchers for researchers; therefore, they constitute a service to the scholarly community. At the same time, the *Frontiers journal series* operates on a revolutionary invention, the tiered publishing system, initially addressing specific communities of scholars, and gradually climbing up to broader public understanding, thus serving the interests of the lay society, too.

Dedication to quality

Each Frontiers article is a landmark of the highest quality, thanks to genuinely collaborative interactions between authors and review editors, who include some of the world's best academicians. Research must be certified by peers before entering a stream of knowledge that may eventually reach the public - and shape society; therefore, Frontiers only applies the most rigorous and unbiased reviews. Frontiers revolutionizes research publishing by freely delivering the most outstanding research, evaluated with no bias from both the academic and social point of view. By applying the most advanced information technologies, Frontiers is catapulting scholarly publishing into a new generation.

What are Frontiers Research Topics?

Frontiers Research Topics are very popular trademarks of the *Frontiers journals series*: they are collections of at least ten articles, all centered on a particular subject. With their unique mix of varied contributions from Original Research to Review Articles, Frontiers Research Topics unify the most influential researchers, the latest key findings and historical advances in a hot research area.

Find out more on how to host your own Frontiers Research Topic or contribute to one as an author by contacting the Frontiers editorial office: frontiersin.org/about/contact

Current advancements in real-time plant pathogen diagnostics: From lab assays to in-field detection

Topic editors

Ravinder Kumar — Central Potato Research Institute (ICAR), India
Milan Kumar Lal — Central Potato Research Institute (ICAR), India
Pramod Prasad — ICAR-Indian Institute of Wheat and Barley Research, Regional Station, Himachal Pradesh, India
Rahul Kumar Tiwari — Central Potato Research Institute (ICAR), India

Citation

Kumar, R., Lal, M. K., Prasad, P., Tiwari, R. K., eds. (2023). *Current advancements in real-time plant pathogen diagnostics: From lab assays to in-field detection*. Lausanne: Frontiers Media SA. doi: 10.3389/978-2-8325-3268-3

Table of contents

frontiers | Frontiers in Plant Science

TYPE Editorial
PUBLISHED 04 August 2023
DOI 10.3389/fpls.2023.1255654

OPEN ACCESS

EDITED BY
Carla M R Varanda,
Instituto Politécnico de Santarém, Portugal

REVIEWED BY
Patrick Materatski,
University of Evora, Portugal
Margarida Espada,
University of Évora, Portugal

*CORRESPONDENCE
Milan Kumar Lal
milan2925@gmail.com
Rahul Kumar Tiwari
rahultiwari226@gmail.com

RECEIVED 09 July 2023
ACCEPTED 25 July 2023
PUBLISHED 04 August 2023

CITATION
Kumar R, Kumar Lal M, Prasad P and Tiwari RK (2023) Editorial: Current advancements in real-time plant pathogen diagnostics: from lab assays to in-field detection. *Front. Plant Sci.* 14:1255654. doi: 10.3389/fpls.2023.1255654

Editorial: Current advancements in real-time plant pathogen diagnostics: from lab assays to in-field detection

Ravinder Kumar[1], Milan Kumar Lal[1]*, Pramod Prasad[2] and Rahul Kumar Tiwari[1]*

[1]Division of Plant Protection, ICAR-Central Potato Research Institute, Shimla, Himachal Pradesh, India, [2]Plant Pathology, ICAR-Indian Institute of Wheat and Barley Research, Regional Station, Shimla, Himachal Pradesh, India

KEYWORDS

plant disease, plant pathogen, detection, field level diagnostics, fungi, bacteria, viruses

Editorial on the Research Topic
Current advancements in real-time plant pathogen diagnostics: from lab assays to in-field detection

Introduction

Food security and increased global population have driven agricultural activities to strive for higher productivity. There are however numerous invasive plant pathogens that cause plant diseases and reduce crop yields, including viruses, fungi, nematodes, mycoplasma, bacteria and others (Raigond et al., 2022; Chikh-Ali and Karasev, 2023; Thakur et al., 2023). Approximately, $220 billion is lost to the global economy each year as a result of plant diseases caused by these pathogens (Lal et al., 2021; Tiwari et al., 2021; Raigond et al., 2022). Diseases of plants are historically diagnosed by looking at their symptoms and appearance, often at advanced stages when they are difficult to manage and treat. Single or mixed infections can occur with pathogens (Shah et al., 2020). The most effective way to manage plant diseases is to use healthy, disease-free plants. To ensure food security and minimize crop losses, continuous and immediate monitoring and pathogen identification efforts must be undertaken before planting crops in the field (Kumar et al., 2017; Bhardwaj et al., 2019; Kumar et al., 2020b; Tiwari et al., 2020; Tiwari et al., 2022; Rahman et al., 2023).

Increasing sensitivity and specificity of disease monitoring in the field have been enabled by advances in real-time diagnostics. There are several techniques available for detecting plant pathogens, such as enzyme-linked immunosorbent assay (ELISA), polymerase chain reaction (PCR), real-time PCR, fluorescence *in situ* hybridization (FISH), and flow cytometry. However, these methods often suffer from certain limitations, including being time-consuming, costly, and requiring highly skilled personnel for their execution (Kumar et al., 2020a; Kumar et al., 2022). Therefore, plant pathology is focusing on rapid, accurate, and cost-effective diagnostics, especially for emerging diseases or elusive pathogens with subtle initial symptoms.

Moreover, diagnostic laboratories have become increasingly dependent on innovative diagnostic tools designed for field use in an interconnected global environment. The tools used ensure that instruments and techniques are operationally relevant. Nanotechnology and biosensor-based diagnostics, along with portable systems integrated with the Internet of Things (IoT), have revolutionized the field of pathogen detection. These advancements have led to the development of isothermal amplification-based nucleic acid visual detection systems, which are highly efficient in identifying pathogens. Key technologies within this framework include Loop-mediated isothermal amplification (LAMP), rolling circle amplification (RCA), recombinase polymerase assay (RPA), and CRISPR/Cas (Raigond et al., 2020; Kumar et al., 2021; Watpade et al., 2023).

The latest advancements in real-time plant pathogen diagnostics

To prevent an outbreak of plant diseases, farmers worldwide must detect them quickly and accurately. Rapid diagnosis of pathogens is, therefore, necessary to reduce yield losses. We gathered the latest research on field-level diagnostics for real-time identification and timely management of plant diseases in crops for this Research Topic. The eleven research articles on diagnostics cover a broad range of topics, including the diagnosis and management of bacterial, fungal, viral, phytoplasma, and nonparasitic diseases.

Cheng et al. identified the proteins unaffected by Pst DC3000 infection by mass spectrometry-based label-free quantification (LFQ) and demonstrated the capability of this to quantify protein abundance and the possibility of extending protein expression studies to transcripts in Arabidopsis. Ren et al. tested 100 inter simple sequence repeats (ISSR) primers and generated a species-specific fragment (515 bp) with ISSR 827 against *Tilletia caries*. In addition, they developed a super-sensitive quantitative real-time polymerase chain reaction (qRT-PCR) with a detection limit of 2.4 fg/µL, and droplet digital PCR (ddPCR) with a detection limit of 0.24 fg/µL. In a study by Logeshwari et al., a LAMP was developed for highly sensitive detection of *Sarocladium oryzae* at concentrations as low as 10 fg in 30 minutes at 65°C. LAMP was validated using live infected tissues, weeds and seeds collected from different locations in Tamil Nadu. Using reverse transcription recombinase-amplification (RT-RAA) and CRISPR/Cas12a-based lateral flow assays, Lei et al. developed a rapid detection method that can detect 2.5 copies of the coat protein gene of MCMV, using 0.96 pg of total RNA extracted from maize leaves infected with MCMV. To make the method more feasible for field detection, crude virus extraction of plant RNA combined with one-tube RT-RAA/CRISPR-Cas12a reaction was implemented on a portable metal incubator (37-42 ^{0}C).

Awan et al. conducted antifungal bioassays, and the metabolites extracted from BS-01 exhibited the most potent inhibition of fungal biomass. The extracellular metabolites displayed an impressive inhibition range of 69-98%, while the intracellular metabolites showed inhibition ranging from 48% to 85%. In comparison, the metabolites extracted using n-hexane demonstrated inhibition percentages of 63-88% for extracellular metabolites and 35-62% for intracellular metabolites. Similarly, the use of dichloromethane resulted in inhibition percentages of 41-74% for extracellular metabolites and 42-74% for intracellular metabolites. In growth chamber bioassays, both foliar application and seed application of BS-01 significantly reduced *Alternaria solani* load on inoculated tomato foliage. To improve Plant parasitic nematodes (PPNs) identification and detection, Shao et al. reviewed the latest research advances and diagnostic approaches and techniques. Morphological characters alone are not sufficient to identify PPNs because they often have interspecific overlays and wide intraspecific variations. PPNs can now be diagnosed directly in the field using newly developed isothermal amplification technologies and remote sensing methods. Lal et al. studied the worldwide research on real-time PCR-based pathogen detection from 2001 to 2021 that was used for any diagnostic assay or gene expression level study. According to the analysis, research on RT-PCR-based pathogen detection is booming and should be strengthened by using modern diagnostic tools and collaboration among labs equipped with the necessary equipment. Using crude sap lysed in 0.5M NaOH solution as a template and purified DNA/cDNA as a primer, Kishan et al. developed an isothermal-based recombinase polymerase amplification (RPA) method for the detection of Grapevine geminivirus A (GGVA) in grapevine samples. This assay has the advantage of not requiring purification or isolation of viral DNA and can be performed at a wide range of temperatures (18-46°C) for 10-40 minutes, making it an effective and rapid way to detect grapevine GGVA. Buttar et al. demonstrated that three applications of Trifloxystrobin+ Tebuconazole 75% WG @ 0.07% were the most effective against pod rot disease on two mungbean cultivars, ML 2056 and SML 668. ML 2524, among the tested genotypes, exhibited resistance to pod rot disease, with an incidence of 15.62% and a severity of 7.69%. A new protocol was developed by Moran et al. that does not require nucleic acid purification or specialized equipment, making it ideal for field use. Primer and probe targeting a region of the fusA gene show 94-100% specificity both *in vitro* and in silico for the `Ca. Liberibacter´ species associated with HLB. HLB-infected plant and insect material can be detected with a reliable limit of 101 copies per microliter using the new protocol. Chauhan et al. studied biochemical mechanisms associated with cotton leaf curl disease (CLCuD) resistance. High-diseased plants of the susceptible hybrid HS 6 had a value of 0.7 mg g-1 at 60 DAS. At 90 DAS, resistant cultivars exhibited the highest phenol content (0.70 mg g-1). HS 6 (9.4 mg g-1) and RCH 134 BG-II (10.5 mg g-1) showed the lowest protein activity at 120 DAS. CLCuV protection in cotton begins with protein activity, one of the primary biochemical compounds. In cotton, phenol and tannin are the secondary levels of defense, showing significant increases in their levels while imparting resistance against CLCuV.

Conclusions and perspectives

In conclusion, the Research Topic addresses the critical need for early detection and accurate diagnosis of plant pathogens to mitigate crop losses and ensure food security. It emphasizes the development of diagnostic techniques and tools that are simple, specific, rapid, and cost-effective. The focus was on advancing field-deployable molecular diagnostics that enable on-the-spot pathogen detection and immediate response. Isothermal amplification techniques such as RPA have gained prominence in field-deployable diagnostics. This technique amplifies targeted nucleic acids of pathogens at a constant temperature, eliminating the need for complex thermal cycling equipment. They are simple, fast, and robust, making them suitable for on-site detection even in resource-limited settings. CRISPR/Cas technologies have also shown promise in plant pathogen detection. These methods leverage the Cas enzyme's ability to target and cleave specific sequences in the pathogen's DNA or RNA. Coupled with a detection system, CRISPR-based diagnostics enable rapid identification of pathogens in the field, facilitating real-time disease monitoring and control. Overall, these advancements in field-deployable molecular diagnostics, including portable systems interconnected with isothermal amplification techniques like LAMP and RPA, and CRISPR/Cas technologies, are revolutionizing the field of plant pathology. They provide rapid, reliable, and on-the-spot pathogen detection capabilities, empowering farmers, researchers, and agricultural professionals to make informed decisions and take immediate action to protect crops from the devastating effects of plant pathogens.

Author contributions

RK: Conceptualization, Resources, Visualization, Writing – original draft, Writing – review & editing, MKL: Conceptualization, Resources, Visualization, Writing – original draft, Writing – review & editing, PP: Conceptualization, Resources, Visualization, Writing – original draft, Writing – review & editing. RKT: Data curation, Formal Analysis, Investigation, Methodology, Resources, Software, Writing – original draft, Writing – review & editing.

Conflict of interest

The authors declare that the research was conducted in the absence of any commercial or financial relationships that could be construed as a potential conflict of interest.

Publisher's note

References

Bhardwaj, V., Sood, S., Kumar, A., Patil, V., Sharma, S., Sundaresha, S., et al. (2019). Efficiency and reliability of marker assisted selection for resistance to major biotic stresses in potato. *Potato J.* 46, 56–66.

Chikh-Ali, M., and Karasev, A. V. (2023). Virus diseases of potato and their control. *Potato Prod. Worldw.* 199–212. doi: 10.1016/B978-0-12-822925-5.00008-6

Kumar, R., Jeevalatha, A., and Raigond, B. (2017). Viral Diseases and their Management in Seed Potato Production. Pp. 181-189. In: Advances in quality potato production and post-harvest management (NK Panday, DK Singh, BP Singh, Jeevalatha A, Baswaraj R. and B Singh). Agrotech publishing academy, Udaipur

Kumar, R., Jeevalatha, A., Raigond, B., and Tiwari, R. K. (2020a). Viral and viroid diseases of potato and their management. In: Singh AK, Chakrabarti SK, Singh B, Sharma J, Dua VK (eds) Potato Science & Technology for Sub Tropics, Ist edn. New India Publishing Agency, New Delhi, pp 267–292

Kumar, R., Kaundal, P., Arjunan, J., Sharma, S., and Chakrabarti, S. K. K. (2020b). Development of a visual detection method for Potato virus S by reverse transcription loop-mediated isothermal amplification. *3 Biotech.* 10, 219–225. doi: 10.1007/S13205-020-02214-4

Kumar, R., Kaundal, P., Tiwari, R. K., Siddappa, S., Kumari, H., Chandra Naga, K., et al. (2021). Rapid and sensitive detection of potato virus X by one-step reverse transcription-recombinase polymerase amplification method in potato leaves and dormant tubers. *Mol. Cell. Probes* 58, 101743. doi: 10.1016/J.MCP.2021.101743

Kumar, R., Kaundal, P., Tiwari, R. K., Siddappa, S., Kumari, H., Lal, M. K., et al. (2022). Establishment of a one-step reverse transcription recombinase polymerase amplification assay for the detection of potato virus S. *J. Virol. Methods* 307, 114568. doi: 10.1016/J.JVIROMET.2022.114568

Lal, M. K., Tiwari, R. K., Kumar, R., Naga, K. C., Kumar, A., Singh, B., et al. (2021). Effect of potato apical leaf curl disease on glycemic index and resistant starch of potato (Solanum tuberosum L.) tubers. *Food Chem.* 359, 129939. doi: 10.1016/j.foodchem.2021.129939

Rahman, M., Borah, S. M., Borah, P. K., BORA, P., Sarmah,, B. K., Lal, M. K., et al. (2023). Deciphering the antimicrobial activity of multifaceted rhizospheric biocontrol agents of solanaceous crops viz., Trichoderma harzianum MC2 and Trichoderma harzianum NBG. *Frontiers in Plant Science*, 14:1141506. doi: 10.3389/fpls.2023.1141506

Raigond, B., Jeevalatha, A., Kumar, R., and Verma, G. (2020). *Potato in Sub-tropics : A Saga of Success.*

Raigond, B., Verma, G., Kumar, R., and Tiwari, R. K. (2022). Serological and Molecular Diagnosis of Potato Viruses: An Overview. In: Chakrabarti, S.K., Sharma, S., Shah, M.A. (eds) Sustainable Management of Potato Pests and Diseases. 337–352. Springer, Singapore. doi: 10.1007/978-981-16-7695-6_13

Shah, M. A., Kumar, R., Kaundal, P., and Sharma, S. (2020). *Prevalence of Natural Infection of Potato Viruses in Weeds and Other Crops.*

Thakur, R., Devi, R., Lal, M. K., Tiwari, R. K., Sharma, S., and Kumar, R. (2023). *Morphological, ultrastructural and molecular variations in susceptible and resistant genotypes of chickpea infected with Botrytis grey mould*. 1–18. doi: 10.7717/peerj.15134

Tiwari, R. K., Bashyal, B. M., Shanmugam, V., Lal, M. K., Kumar, R., Sharma, S., et al. (2022). First report of dry rot of potato caused by Fusarium proliferatum in India. *J. Plant Dis. Prot.* 129, 173–179. doi: 10.1007/s41348-021-00556-6

Tiwari, R. K., Kumar, R., Naga, K. C., Sagar, V., Kumar, D., Lal, M. K., Chourasia, K. N., and Sharma, S. (2021). Recent Advancements in Integrated Management of Potato Diseases. In: More, SJ; Giri, NA; Suresh, KJ; Visalakshi, CC & Tadigiri, S (eds) Recent Advances in Root and Tuber Crops. Brillion Publishing, New Delhi, pp. 185–203.

Tiwari, R. K., Kumar, R., Sharma, S., Naga, K. C., Subhash, S., Sagar, V., et al. (2020). Continuous and emerging challenges of silver scurf disease in potato. *Int. J. Pest Manage.* 0, 1–13. doi: 10.1080/09670874.2020.1795302

Watpade, S., Naga, K. C., Pramanick, K. K., Tiwari, R. K., Kumar, R., Shukla, A. K., et al. (2023). First report of powdery mildew of pomegranate (Punica granatum) caused by Erysiphe punicae in India. *J. Plant Dis. Prot.* 130 (3), pp. 651–656. doi: 10.1007/s41348-023-00718-8

frontiers | Frontiers in Plant Science

TYPE Original Research
PUBLISHED 29 September 2022
DOI 10.3389/fpls.2022.1001920

OPEN ACCESS

EDITED BY
Pramod Prasad,
ICAR-Indian Institute of Wheat and Barley Research, Regional Station, India

REVIEWED BY
Rupam Kumar Bhunia,
National Agri-Food Biotechnology Institute, India
Jay Jayaraman,
The New Zealand Institute for Plant and Food Research Ltd., New Zealand

*CORRESPONDENCE
Yee-Shan Ku
ysamyku@cuhk.edu.hk
Hon-Ming Lam
honming@cuhk.edu.hk

SPECIALTY SECTION
This article was submitted to Plant Pathogen Interactions, a section of the journal Frontiers in Plant Science

RECEIVED 24 July 2022
ACCEPTED 29 August 2022
PUBLISHED 29 September 2022

CITATION
Cheng S-S, Ku Y-S, Cheung M-Y and Lam H-M (2022) Identification of stably expressed reference genes for expression studies in *Arabidopsis thaliana* using mass spectrometry-based label-free quantification.
Front. Plant Sci. 13:1001920.
doi: 10.3389/fpls.2022.1001920

Identification of stably expressed reference genes for expression studies in *Arabidopsis thaliana* using mass spectrometry-based label-free quantification

Sau-Shan Cheng, Yee-Shan Ku*, Ming-Yan Cheung and Hon-Ming Lam*

Centre for Soybean Research of the State Key Laboratory of Agrobiotechnology and School of Life Sciences, The Chinese University of Hong Kong, Shatin, Hong Kong SAR, China

Arabidopsis thaliana has been used regularly as a model plant in gene expression studies on transcriptional reprogramming upon pathogen infection, such as that by *Pseudomonas syringae* pv. *tomato* DC3000 (*Pst* DC3000), or when subjected to stress hormone treatments including jasmonic acid (JA), salicylic acid (SA), and abscisic acid (ABA). Reverse transcription-quantitative polymerase chain reaction (RT-qPCR) has been extensively employed to quantitate these gene expression changes. However, the accuracy of the quantitation is largely dependent on the stability of the expressions of reference genes used for normalization. Recently, RNA sequencing (RNA-seq) has been widely used to mine stably expressed genes for use as references in RT-qPCR. However, the amplification step in RNA-seq creates an intrinsic bias against those genes with relatively low expression levels, and therefore does not provide an accurate quantification of all expressed genes. In this study, we employed mass spectrometry-based label-free quantification (LFQ) in proteomic analyses to identify those proteins with abundances unaffected by *Pst* DC3000 infection. We verified, using RT-qPCR, that the levels of their corresponding mRNAs were also unaffected by *Pst* DC3000 infection. Compared to commonly used reference genes for expression studies in *A. thaliana* upon *Pst* DC3000 infection, the candidate reference genes reported in this study generally have a higher expression stability. In addition, using RT-qPCR, we verified that the mRNAs of the candidate reference genes were stably expressed upon stress hormone treatments including JA, SA, and ABA. Results indicated that the candidate genes identified here had stable expressions upon these stresses and are suitable to be used as reference genes for RT-qPCR. Among the 18 candidate reference genes reported in this study, many of them had greater expression stability than the commonly used reference genes, such as *ACT7*, in previous studies. Here, besides proposing more appropriate reference genes for Arabidopsis expression studies, we also demonstrated the capacity of mass spectrometry-based LFQ to quantify protein abundance and the possibility to extend protein expression studies to the transcript level.

KEYWORDS

pathogen infection, jasmonic acid, salicylic acid, abscisic acid, expression study, label-free quantification, RT-qPCR, reference gene

Introduction

Pathogen infection of plants has been a major cause of yield loss in agriculture (Gorshkov and Tsers, 2022). Upon pathogen infection, plants perceive the signal elicited by the secretions from the pathogens known as pathogen-associated molecular patterns (PAMPs) or microbe-associated molecular patterns (MAMPs; Medzhitov and Janeway, 1997), through pattern recognition receptors (PRRs). The signal perception triggers a series of defense responses including the generation of reactive oxygen species (ROS), fluctuations in the cellular calcium level, activation of proteins, such as mitogen-activated protein kinases (MAPKs), and GTP-binding proteins (G-proteins), and synthesis of stress hormones such as jasmonic acid (JA), salicylic acid (SA), and ethylene (Zhang and Zhou, 2010; Li et al., 2016b; Ku et al., 2020). These signaling events regulate the expressions of defense-related genes such as *Pathogenesis-Related* (*PR*) genes (Zhang and Zhou, 2010; Li et al., 2016b; Ku et al., 2020). PAMP-triggered immunity (PTI) describes the general pathogen resistance responses in plants (Zhang and Zhou, 2010; Li et al., 2016b; Ku et al., 2020). Some plants are known to have specific pathogen recognition mechanisms termed effector-triggered immunity (ETI; Dodds and Rathjen, 2010). ETI triggers hypersensitive response (HR) and usually leads to programmed cell death (PCD) at the area of infection to prevent the invading pathogens from spreading. In HR, ROS is produced to cause a series of cellular events including the disruption of cell membrane, thickening of the cell wall, and the production of stress hormones such as JA and SA. PTI and ETI lead to systemic acquired resistance (SAR) against a broad spectrum of pathogens (Dodds and Rathjen, 2010; Zhang and Zhou, 2010; Li et al., 2016b; Ku et al., 2020). The interactions among different signaling pathways, such as those of JA, SA, and abscisic acid (ABA), result in further complexity of the regulatory processes when under stress (Ku et al., 2018). These cellular events involve extensive transcriptional reprogramming (Li et al., 2016a). RNA sequencing (RNA-seq) has been used as the platform to study the global gene expression changes in plants upon pathogen infection (Zhu et al., 2013; Martin et al., 2016; Matic et al., 2016; Gupta and Senthil-Kumar, 2017; Poretti et al., 2021). Reverse transcription-quantitative polymerase chain reaction (RT-qPCR) is regarded as the gold standard for quantifying gene expressions due to its sensitivity, accuracy, and reproducibility (Gökmen-Polar, 2019). Although digital PCR (dPCR) has been shown to out-perform RT-qPCR in terms of sensitivity, accuracy, and reproducibility (Gökmen-Polar, 2019), RT-qPCR remains a more common approach for routine gene expression quantification due to the lower cost compared to dPCR. However, the accuracy of expression quantification by RT-qPCR is largely dependent on the expression stability of the reference gene used for normalization.

RNA-seq is commonly employed to mine reference genes for RT-qPCR (Yim et al., 2015; Kudo et al., 2016; Carmona et al., 2017; Zhou et al., 2017; Pombo et al., 2019). However, the accuracy of RNA-seq data has been a concern. PCR bias and GC content bias are hurdles for the accurate quantitative analysis of high-throughput sequencing data. In addition, the accuracy of quantitative gene expression analyses is highly influenced by the algorithms and pipelines for RNA-seq data analyses (Benjamini and Speed, 2012; Parekh et al., 2016; Corchete et al., 2020). In an attempt to assess the different RNA-seq data analysis pipelines, it was found that each of the 192 pipelines examined in the study had its advantages and disadvantages for quantitative gene expression analysis (Corchete et al., 2020).

Many previous researches have attempted to determine the correlation between mRNA and protein levels in plants. It was concluded that the correlation between mRNA levels and protein abundances is largely dependent on the plant species, tissue type, developmental stage, and stress condition of the plant (Nakaminami et al., 2014; Ponnala et al., 2014; Wang et al., 2017; Ding et al., 2020; Ren et al., 2022). Nevertheless, a significant correlation between mRNA and protein levels has been reported (Arefian et al., 2019; Ding et al., 2020; Shu et al., 2022; Zhu et al., 2022). Recent technologies have enabled high-throughput proteomic analyses through mass spectrometry, which does not involve amplification steps and thus may complement the limitations due to biased quantification in RNA-seq. In this study, we employed mass spectrometry-based label-free quantification (LFQ) to search for proteins that have stable abundances in *Arabidopsis thaliana* despite *Pseudomonas syringae* pv. *tomato* DC3000 (*Pst* DC3000) infection and tested the expression stability of their corresponding mRNAs by RT-qPCR. Compared to reference genes commonly used in previous studies, the mRNA levels of these proteins were generally more stable upon *Pst* DC3000 infection. We then extended the assessment of the stability of mRNA levels of these proteins to stress hormone treatments, including JA, SA and ABA. Altogether, 18 candidate reference genes were identified and tested. Using *A. thaliana* as the model, we revealed a set of more suitable reference genes for expression studies on *Pst* DC3000 infection and stress hormone treatments. We also demonstrated the advantage of using mass spectrometric analysis for mining genes which have stable protein and mRNA abundances upon various treatments.

Materials and methods

Plant materials and treatment conditions

For *Pst* DC3000 inoculation, *A. thaliana* plants (Col-0) were grown on Floragard potting soil in a growth chamber under these conditions: 22–24°C, light intensity 80–120 μE with a 16-h light:8-h dark cycle; relative humidity 70–80%. The rosette leaves of 5-week-old plants were inoculated with *Pst* DC3000 according to the protocol reported in previous studies (Cheung et al., 2013; Mi et al., 2013). At 0 day and 3 days post-inoculation (dpi), the aerial parts of the inoculated plants were collected, snap-frozen in liquid nitrogen, and stored at −80°C. The tissues of three individual plants were pooled as one biological replicate for total protein or total RNA extraction. A total of three biological

replicates per treatment were collected for total protein extraction while two biological replicates per treatment were collected for total RNA extraction.

For JA treatment, the seeds of *A. thaliana* Col-0 were surface-sterilized by shaking in 100% household bleach for 3 min. After that, the bleach was removed, and the seeds were rinsed three times with sterilized water. The surface-sterilized seeds were then placed on Murashige & Skoog (MS) agar plates supplemented with 3% sucrose with or without 5 μM JA (Zhang et al., 2017). The seeded agar plates were then kept at 4°C in the dark for 2 days to break dormancy. After that, the plates were moved into a growth chamber under these conditions: 22°C–24°C, light intensity 80–120 μE with a 16-h light:8-h dark cycle, for 17 days. Then the seedlings were removed from the agar plates, frozen in liquid nitrogen, and stored at −80°C before total RNA extraction. Samples for two biological replicates per treatment were collected. Each biological replicate consisted of at least seven seedlings pooled together for total RNA extraction.

For SA treatment, the seeds of *A. thaliana* Col-0 were surface-sterilized as described above. The surface-sterilized seeds were then placed on MS agar plates without sucrose and with or without 50 μM SA (Sakurai et al., 2011; Sugano et al., 2016; Zhang et al., 2017). The seeded plates were then kept at 4°C in the dark for 2 days before being moved into a growth chamber under the same growth conditions as above for 17 days. After that, the seedlings were harvested from the agar plates, frozen in liquid nitrogen, and stored at −80°C before total RNA extraction. Two biological replicates per treatment were collected. Each biological replicate consisted of at least seven seedlings pooled together for total RNA extraction.

For ABA treatment, the seeds of *A. thaliana* Col-0 were sown on Floragard potting soil in a growth chamber under the same growth conditions as described above. Then the rosette leaves of 4-week-old plants were detached and floated on a perfusion solution (50 mM KCl, 10 mM MES, pH 7.0) under light for 2 h before being treated with ABA. ABA was first dissolved in 10% (v/v) methanol (MeOH) before being added to the perfusion solution to reach a final concentration of ABA at 10 μM and MeOH at 0.1% (v/v). The detached leaves were treated with ABA under light for 2 h. Then they were frozen in liquid nitrogen and stored at −80°C before total RNA extraction. Two biological replicates were sampled for each treatment, and each biological replicate consisted of the rosette leaves of at least three plants pooled together for total RNA extraction.

Protein extraction and protein profile analysis by liquid chromatography–tandem mass spectrometry (LC–MS/MS)

Total protein was extracted from the plant samples according to a previously described protocol (Marx et al., 2016; Cheng et al., 2022), with minor modifications. The plant samples were ground to a fine powder in liquid nitrogen using mortar and pestle. Around 100 mg of the powder was resuspended in five volumes of total protein extraction buffer [290 mM sucrose, 250 mM Tris (pH 7.6), 50 mM Na pyrophosphate, 25 mM EDTA (pH 8.0), 25 mM NaF, 10 mM KCl, 1 mM $(NH_4)_6Mo_7O_{24}$, 1 mM phenylmethylsulfonyl fluoride (PMSF), and 1X Halt™ Protease Inhibitor Cocktail (Cat#78430, Thermo Fisher Scientific, Waltham, MA, United States)]. The plant proteins in the extract were precipitated using the chloroform/methanol method (Wessel and Flügge, 1984). After that, the protein pellet was lyzed with five volumes of lysis buffer (w/v) [8 M urea, 50 mM Tris–HCl (pH 8.0), 30 mM NaCl, 20 mM sodium butyrate, 1 mM $CaCl_2$, and 1X Halt™ Protease Inhibitor Cocktail (Cat#78430, Thermo Fisher Scientific, Waltham, MA, United States)]. The protein concentration was determined using the Pierce™ BCA Protein Assay Kit (Cat#23225, Thermo Fisher Scientific, Waltham, MA, United States). Then, 10 μg of each protein sample was reduced with 5 mM dithiothreitol (DTT) at 37°C for 30 min, alkylated with 20 mM iodoacetamide at room temperature for 30 min, and underwent a final reduction with 5 mM DTT at 37°C for 30 min. Then the protein mixture was incubated with trypsin in a ratio of 1/20 (w/w) of the protein amount at 37°C overnight.

The peptides resulting from trypsin digestion were desalted using Pierce™ C18 Spin Column (Cat#89873, Thermo Fisher Scientific, Waltham, MA, United States), and each sample was analyzed independently for protein identification using LC–MS/MS. Five hundred nanograms of desalted peptides from each sample were injected into the LC Ultimate 3000 RSLCnano system equipped with a C-18 μ-precolumn (300-μm i.d. × 5 mm) with an Acclaim Pepmap RSLC nanoViper C-18 column (75 μm × 25 cm) coupled to the Orbitrap Fusion Lumos Tribrid mass spectrometer (Thermo Fisher Scientific, Waltham, MA, United States). The peptide samples were separated against the gradient profile with a 50°C chamber at a flow rate of 0.3 $\mu L min^{-1}$, using a mixture of ultrapure water with 1.9% acetonitrile and 0.1% formic acid as mobile phase A and ultrapure water with 2% acetonitrile and 0.1% formic acid as mobile phase B, with the following gradient profile setting in the LC: 0% mobile phase B for the initial 5 min; at 5–8 min, 0–6% mobile phase B; 8–48 min, 6–18% mobile phase B; 48–58 min, 18–30% mobile phase B; 58–65 min, 30–80% mobile phase B; and then at 65–75 min, 0% mobile phase B for re-equilibration of the column. Each desalted peptide sample was analyzed twice (as technical replicates) to eliminate the instrumental variations.

The raw data files were generated using Xcalibur software (Thermo Fisher Scientific, Waltham, MA, United States) for MS/MS identification using Proteome Discoverer v2.4 (Thermo Fisher Scientific, Waltham, MA, United States) against the *A. thaliana* protein database (TAIR10) with the built-in SEQUEST HT program at the following settings: MS precursor mass tolerance of 10 ppm, fragment mass tolerance of 0.02 Da, a maximum of 2 missed trypsin cleavage, fixed N-terminal protein acetylation (+42.011 Da), dynamic cysteine carbamidomethylation (+57.021 Da) and methionine oxidation (+15.995 Da). Peptide validation using the built-in Percolator program was accepted at

a false discovery rate (FDR) with a q-value <0.01. Samples were compared using the LFQ method according to the protocol in Proteome Discoverer v2.4 (Thermo Fisher Scientific, Waltham, MA, United States). The proteomic dataset was deposited to PRIDE (PRoteomics IDEntifications Database; Project accession: PXD035677). The grouping of the protein samples from different treatments was presented using PCA plot (Supplementary Figure S1). Proteins appearing in all biological replicates with an adjusted value of $p > 0.05$ for the difference in the abundance (using the Benjamini-Hochberg correction) between 0 and 3 dpi with *Pst* DC3000, i.e., no significant difference in abundance, were short-listed as possible reference gene candidates. Among the short-listed candidates, 18 proteins were highly ranked as stably expressed by Proteome Discoverer v2.4 (Thermo Fisher Scientific, Waltham, MA, United States) and were included in the final list of candidate reference genes (Supplementary Table S1).

Primer design

Primers for RT-qPCR were designed according to the mRNA sequences of the candidate reference genes. The primer specificity was determined by the Primer-BLAST function on the NCBI platform against the *A. thaliana* genome (taxid: 3702) and validated by melting curve analysis after RT-qPCR (Supplementary Figure S2). For references genes commonly used in previous studies, the primer sequences were adopted from the corresponding publications (Czechowski et al., 2005; Jeong et al., 2011; Huang et al., 2013; Chen et al., 2014; Cheong et al., 2014; Cuéllar Pérez et al., 2014; Kim and Hwang, 2014; Zhang et al., 2015; Huot et al., 2017; Jia et al., 2018; Wu et al., 2019; Cui et al., 2021; Romero-Pérez et al., 2021; Gao et al., 2022). The primer sequences are listed in Supplementary Table S1.

Total RNA extraction, cDNA synthesis, and RT-qPCR

The plant samples were ground in liquid nitrogen to a fine powder. After that, total RNA was extracted using Trizol™ Reagent (Cat#15596018, Thermo Fisher Scientific, Waltham, MA, United States) according to the manufacturer's protocol. Then, the RNA was quantitated using the Qubit™ RNA Broad Range (BR) Assay Kit (Cat#Q10211, Thermo Fisher Scientific, Waltham, MA, United States) with the use of Qubit 2.0 Fluorometer (Cat#Q32866, Thermo Fisher Scientific, Waltham, MA, United States) according to the manufacturer's protocol. For *Pst* DC3000 infection and ABA treatment, 320 ng of total RNA was used for cDNA synthesis. For JA and SA treatments, 640 ng of total RNA was used for cDNA synthesis. For cDNA synthesis, the RNA was first treated with DNase I according to the manufacturer's protocol (Cat#18068015, Thermo Fisher Scientific, Waltham, MA, United States). The DNase I-treated RNA was then subjected to cDNA synthesis using the High-Capacity cDNA Reverse Transcription Kit with RNase Inhibitor (Cat#4374966, Thermo Fisher Scientific, Waltham, MA, United States) according to the manufacturer's protocol, with the random primers being replaced by oligo$(dT)_{20}$ to make up a final concentration of 20 μM oligo$(dT)_{20}$. After that, the cDNA was diluted 30 folds before being used for qPCR. For qPCR, 3 μl diluted cDNA was added to a 20-μL qPCR reaction mix with 1X SsoAdvanced Universal SYBR Green Supermix (Cat#1725270, Bio-Rad, Hercules, CA, United States) and 0.15 μM each of forward and reverse primers. Quantitative PCR and melting curve analyses (from 95°C to 65°C) were performed using a CFX96 Touch Real-Time PCR system (Bio-Rad, Hercules, CA, United States).

Stability analysis of the candidate reference genes and reference genes commonly used in previous studies

In each treatment, three technical replicates of the qPCR were performed for each primer pair. The six C_t values from the six technical replicates in total of two biological replicates were used as the inputs for stability analyses using programs including geNorm *via* the R-based package ctrlGene (ver. 1.0.0; Vandesompele et al., 2002; Zhong, 2019), Normfinder *via* RefFinder (Andersen et al., 2004; Xie et al., 2012), BestKeeper (Pfaffl et al., 2004), the comparative ΔC_t method (Silver et al., 2006), and RefFinder (Xie et al., 2012) with default parameters.

Results

Identification of stably expressed proteins unaffected by *Pst* DC3000 infection

Five-week-old *A. thaliana* plants (Col-0) were inoculated with *Pst* DC3000. Total protein was extracted from the inoculated plants at 0 and 3 dpi, and then subjected to mass spectrometry-based LFQ analyses. Eighteen proteins were found to have stable abundances between 0 and 3 dpi (Figure 1). The gene names and accession numbers corresponding to the proteins are listed in Supplementary Table S1. The abundance of the proteins corresponding to 12 reference genes commonly used in previous studies (Czechowski et al., 2005; Jeong et al., 2011; Huang et al., 2013; Chen et al., 2014; Cheong et al., 2014; Cuéllar Pérez et al., 2014; Kim and Hwang, 2014; Zhang et al., 2015; Huot et al., 2017; Jia et al., 2018; Wu et al., 2019; Cui et al., 2021; Romero-Pérez et al., 2021; Gao et al., 2022) were also investigated using the protein dataset. The gene names and accession numbers are listed in Supplementary Table S1. Among the 12 reference genes commonly used in previous studies, ACT1, ACT8, PP2AA3, UBQ5, UBC9, and TIP41 were found from the protein dataset. The abundances of ACT1, ACT8, PP2AA3, and UBQ5 did not

show statistically significant difference between 0 dpi and 3 dpi, the abundance of UBC9 was higher at 0 dpi compared to 3 dpi, while the abundance of TIP41 was too low to be quantified (Supplementary Figure S3). The protein abundance could be found from the protein dataset deposited to PRIDE (PRoteomics IDEntifications Database; Project accession: PXD035677). The chromatograms of the LC/MS–MS analyses are shown in Supplementary Figures S4, S5.

Amplification specificity and efficiency

To test the abundance of the mRNAs corresponding to the stably expressed proteins shown in Figure 1, specific primers were designed based on their mRNA sequences. The specificity of each primer pair was first determined using the Primer-BLAST function on the NCBI platform against the *A. thaliana* genome (taxid: 3702) and validated by melting curve analyses after RT-qPCR (Supplementary Figure S2).

Using RT-qPCR, we analyzed the expression levels of the 18 candidate reference genes and 12 reference genes commonly used in previous studies (Supplementary Table S1; Czechowski et al., 2005; Jeong et al., 2011; Huang et al., 2013; Chen et al., 2014; Cheong et al., 2014; Cuéllar Pérez et al., 2014; Kim and Hwang, 2014; Zhang et al., 2015; Huot et al., 2017; Jia et al., 2018; Wu et al., 2019; Cui et al., 2021; Romero-Pérez et al., 2021; Gao et al., 2022) at 0 and 3 dpi with *Pst* DC3000 inoculation. We also evaluated the expression stability of these candidate reference genes in stress hormone treatments, including JA, SA, and ABA. The distributions of the C_t values of the candidate reference genes were shown by boxplots (Figure 2). In *Pst* DC300 infection, the average expression values of the reference genes commonly used in previous studies ranged from the $\log_2$ values of 4.71 and 5.14 (Figure 2A), which are equivalent to C_t values of 26.26 to 35.38. Meanwhile, the average expression values of the candidate reference genes predicted in this study ranged from the $\log_2$ values of 4.41–5.05 (Figure 2A), which are equivalent to C_t values of 21.20-33.21. In *Pst* DC3000 infection, the expression levels of the reference genes commonly used in previous studies are generally lower than those of the candidate reference genes predicted in this study. Considering all the treatments, the average expression values of the candidate reference genes predicted in this study were in the

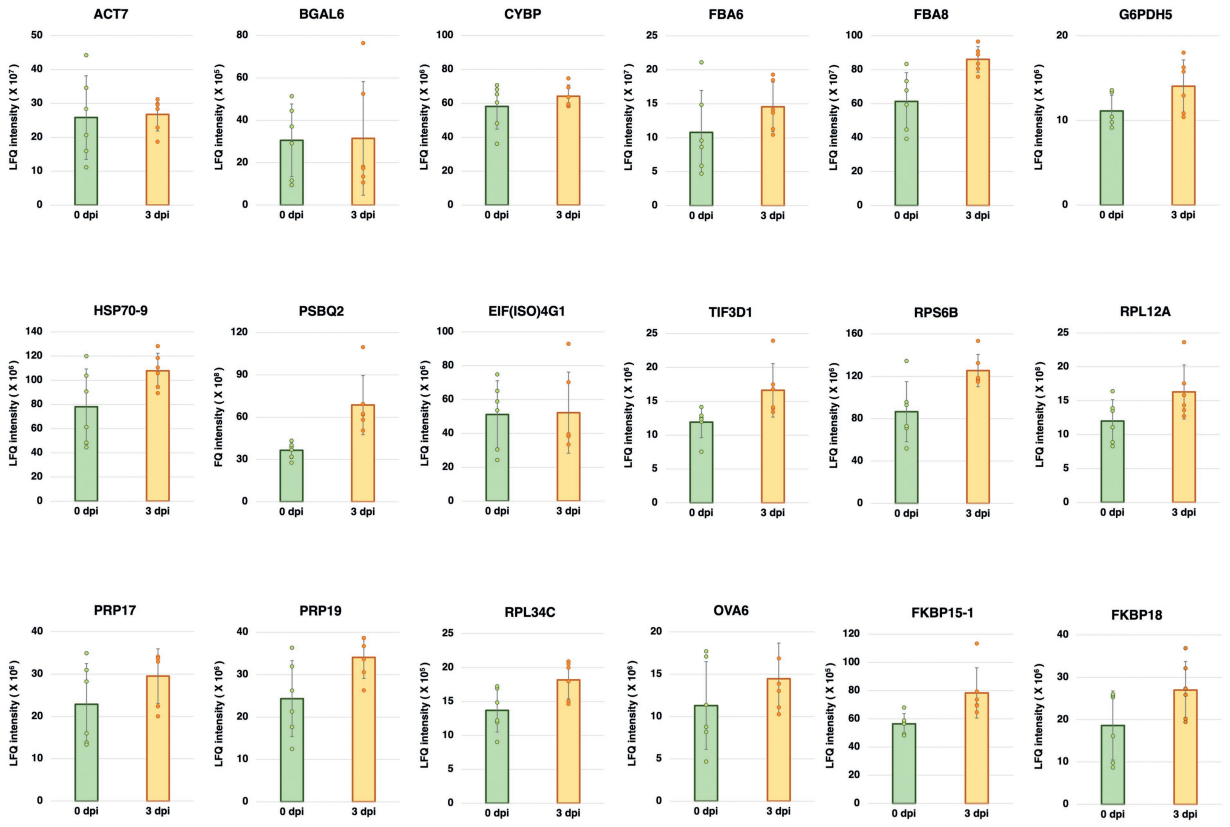

FIGURE 1
Label-free quantification (LFQ) intensities of the candidate reference genes having stable abundances between 0 and 3days post-inoculation (dpi) with *Pseudomonas syringae* pv. *tomato* DC3000 (*Pst* DC3000) in 5-week-old *A. thaliana* ecotype Col-0. The protein abundance levels of these candidate reference genes, calculated from LFQ using Proteome Discoverer v2.4 (Thermo Fisher Scientific, Waltham, MA, United States), were not statistically different between 0 and 3 dpi (p>0.05). Three individual plants were pooled as one biological replicate, each with two technical repeats of LFQ analysis. Error bar represents the standard deviation of a total of six technical repeats based on three biological replicates.

range of $\log_2$ values of 4.40–5.10, equivalent to the C_t values of 21.12–34.22. Based on the C_t values obtained from RT-qPCR and the LFQ intensities obtained from the mass spectrometry-based proteomic analysis, the mRNA level was found to be positively correlated to the protein abundance (Supplementary Figure S6).

Stability analysis of the mRNAs

Expression stability comparison between the candidate reference genes and reference genes commonly used in previous studies upon *Pst* DC3000 infection

To compare the expression stabilities of the 18 candidate reference genes predicted in this study and those of the 12 reference genes commonly used in previous studies, the expression stabilities were ranked using geNorm (Vandesompele et al., 2002) and RefFinder (Xie et al., 2012).

Stability analysis by geNorm

In geNorm analysis, the expression stability of the candidate reference genes was calculated using pairwise comparisons (Vandesompele et al., 2002), and presented in the form of the average expression stability value (M), with a lower M representing a higher stability (Vandesompele et al., 2002). Genes with $M < 1.5$ are commonly considered stably expressed (Vandesompele et al., 2002; Walker et al., 2009; Jin et al., 2019; Fu et al., 2022). All the candidate reference genes and the reference genes commonly used in previous studies showed $M < 1.5$ (Figure 3). However, the M values of the candidate reference genes reported in this study were generally lower than those of the reference genes commonly used in previous studies (Figure 3).

Using geNorm analysis, the optimal number of reference genes required for expression normalization in RT-qPCR was determined by the pairwise variation calculation (V_n/V_{n+1}), in which n represents the number of reference genes required for expression normalization in RT-qPCR. All the candidate reference genes and the reference genes commonly used in previous studies showed V_n/V_{n+1} values smaller than 0.15, which is the cut-off value indicating the expression stability (Vandesompele et al., 2002; Figure 4). However, the candidate reference genes predicted in this study showed general smaller V values compared to the reference genes commonly used in previous studies (Figure 4).

Comprehensive stability analysis by RefFinder

The results of geNorm analysis suggest that the candidate reference genes predicted in this study are generally more stable than the reference genes commonly used in previous studies upon *Pst* DC3000 infection. The stabilities were further analyzed using RefFinder (Xie et al., 2012), which calculates the comprehensive gene stability by integrating the algorithms of geNorm, NormFinder, BestKeeper, and the comparative ΔC_t method (Xie et al., 2012). The result from RefFinder also suggests that the candidate reference genes reported in this study are generally more stable than the reference genes commonly used in previous studies upon *Pst* DC3000 infection (Figure 5). Among all the genes, *ACT7*, *TIF3D1*, and *RPS6B*, which are candidate reference genes reported in this study, were the most stably expressed upon *Pst* DC3000 infection (Figure 5).

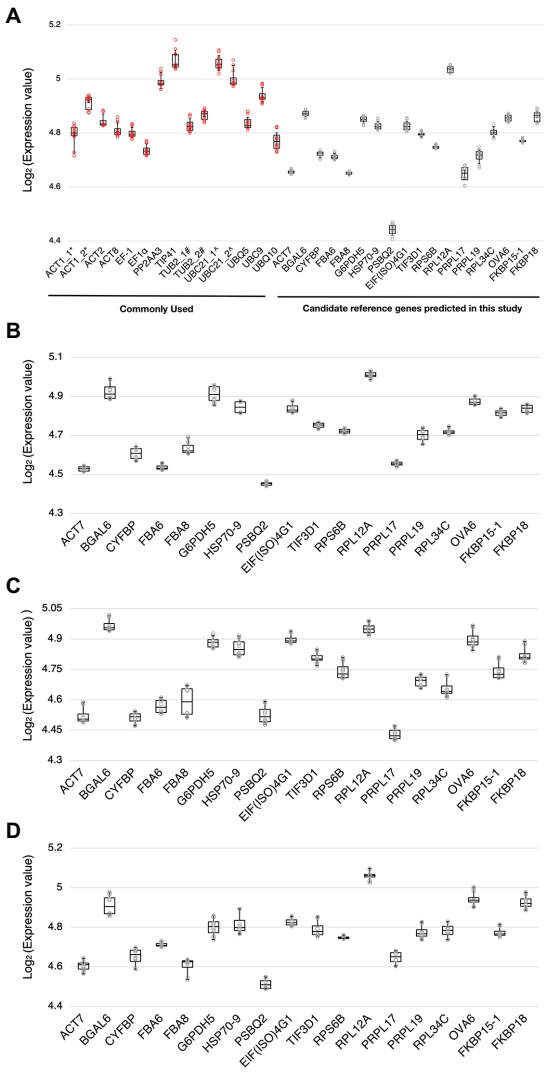

FIGURE 2
Ranges of expression levels of the candidate reference genes and reference genes commonly used in previous studies. **(A)** A boxplot showing the range of expression values [$\log_2$(C_t value)] of the candidate reference genes and the reference genes commonly used in previous studies obtained by RT-qPCR when subjected to *Pst* DC3000 at 0 dpi and 3 dpi. **(B–D)** Boxplots showing the range of expression values [$\log_2$(C_t value)] of the candidate reference genes when subjected to jasmonic acid (JA) **(B),** salicylic acid (SA) **(C)**, and abscisic acid (ABA) **(D)** treatments and the corresponding mock control treatments. The solid line inside each box represents the median expression value and the lower and upper edges of the boxes denote the 25th and 75th percentiles, while the whiskers represent the maximum and the minimum values. Each dot represents the expression value calculated from each technical replicate of RT-qPCR. Three technical repeats were performed for each biological replicate, with two biological replicates in total.

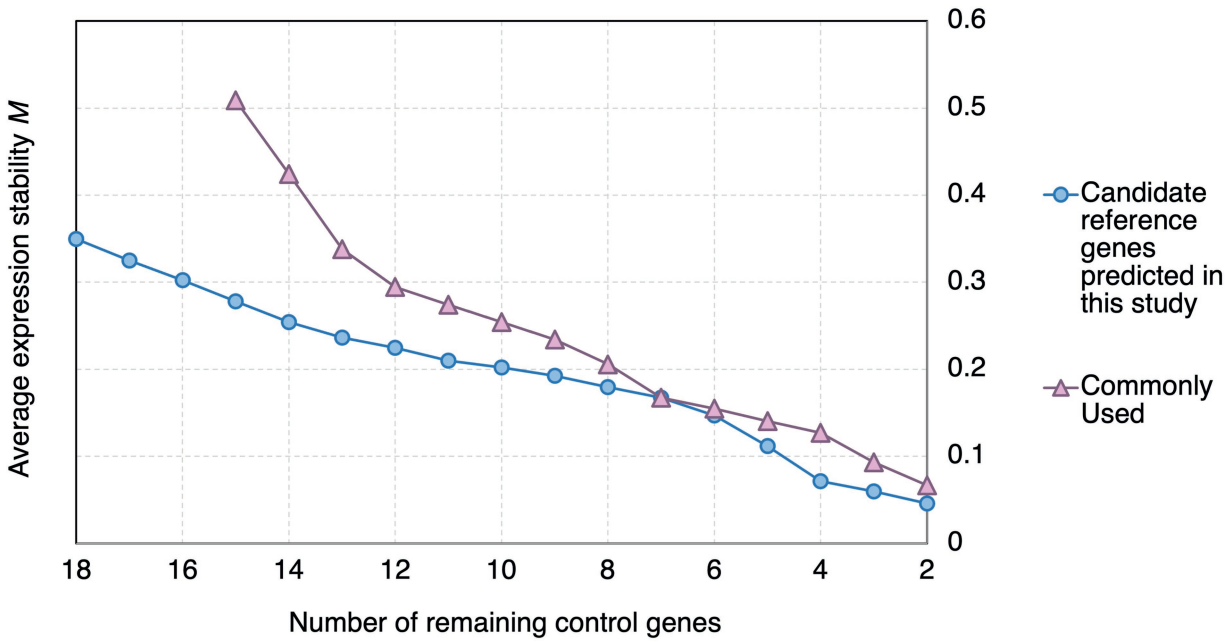

FIGURE 3
geNorm analysis of the average stability values of the candidate reference genes predicted in this study and reference genes commonly used in previous studies upon *Pst* DC3000 infection. Average expression stability values (*M*) of the remaining control genes during the step exclusion of the least stable control among the reference gene candidate upon *Pst* DC3000 infection using geNorm. The higher the average *M*, the lower rank of the expression stability of the reference gene candidate.

Expression stability analyses of the candidate reference genes in various treatments

The above results suggest that the expressions of the candidate reference genes predicted in this study are generally more stable than those of the reference genes commonly used in previous studies. In addition to *Pst* DC3000 infection, we further analyzed the expression stabilities of the candidate reference genes in stress hormone treatments including JA, SA, and ABA. To rank the expression stability of the 18 candidate references genes under different treatments, programs including geNorm (Vandesompele et al., 2002), NormFinder (Andersen et al., 2004), BestKeeper (Pfaffl et al., 2004), and RefFinder (Xie et al., 2012) were used.

Stability analysis by geNorm

In geNorm analysis, all the 18 candidate reference genes had *M* values <1 in all the different treatments (Figure 6; Supplementary Table S2). The *M* values in *Pst* DC3000 infection are generally lower than those in other treatment (Supplementary Table S2). In *Pst* DC3000 infection, among the candidate genes, *RPS6B* and *FKBP15-1* were the most stably expressed ($M = 0.046$) while *PRPL17* was the least stably expressed ($M = 0.35$; Supplementary Table S2). For gene expression analyses using RT-qPCR, multiple reference genes are usually required for accurate expression normalization if the expression stability of the reference gene is low (Vandesompele et al., 2002). Among the 18 candidate reference genes, all the V_n/V_{n+1} values were much lower than the cut-off value of 0.15 (Figure 7). Such results suggest that using two reference genes would be good enough, eliminating the need of a third one, for expression normalization (Vandesompele et al., 2002).

Stability analysis by NormFinder

The expression stability values for each candidate reference gene was also analyzed using the linear mixed-effect model-based NormFinder, in which the variations between the input C_t values are considered in testing the gene expression stability (Andersen et al., 2004). Similar to geNorm, a higher stability value represents a lower expression stability of the reference gene candidate. The range of the stability values varied among treatments. It ranged between 0.041 and 0.528 under *Pst* DC3000 infection, between 0.088 and 0.765 with JA treatment, between 0.266 and 1.333 with SA treatment, and between 0.316 and 1.18 with ABA treatment (Supplementary Table S2). These results mean that the expression stability of the candidate reference genes varied under different treatments, but all had the highest stability upon *Pst* DC3000 infection.

Stability analysis by BestKeeper

The stability of the reference gene candidates was also tested using BestKeeper, in which the standard descriptive statistics for the genes are considered (Pfaffl et al., 2004). The BestKeeper algorithm suggests excluding those candidate reference genes with a standard deviation (SD) > 1.0 in C_t due to low expression stability (Pfaffl et al., 2004; Piehler et al., 2010). Among all the candidate reference genes for all the treatments, only *FBA8* under SA treatment had an $SD > 1$ ($SD = 1.125$) in its C_t values while all the

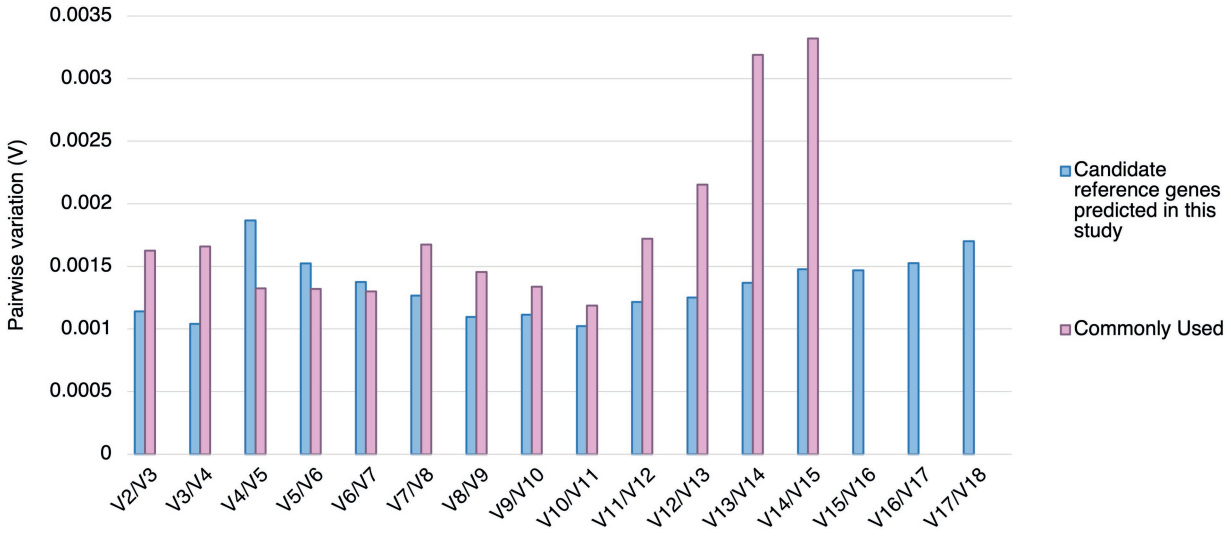

FIGURE 4
Pairwise variation (V) of the candidate reference genes predicted in this study and reference genes commonly used in previous studies calculated by geNorm. The pairwise variation representing (V_n/V_{n+1}). The threshold value of V for accessing the optimal number of the reference genes for RT-qPCR normalization is 0.15. n represents the number of reference gene required for expression normalization in RT-qPCR.

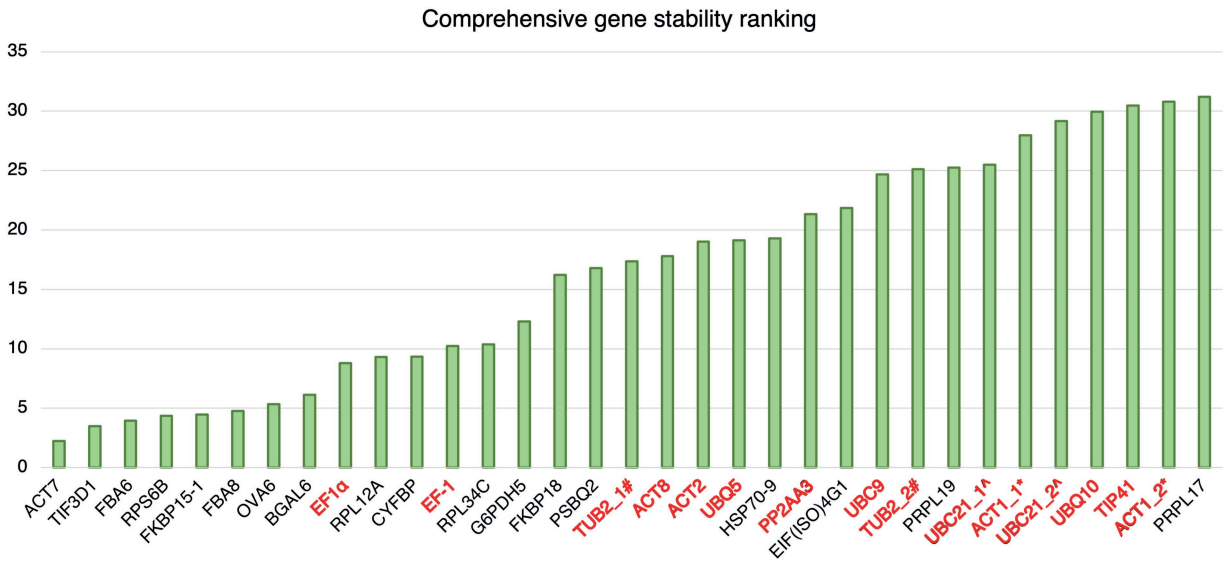

FIGURE 5
Comprehensive gene stability ranking of the predicted reference gene candidates and the commonly used reference gene for *Pst* DC3000 inoculation. The stability ranking was generated using the RefFinder. A lower stability ranking refers to a higher stability of the reference gene. Gene names in black: candidate reference genes reported in this study; gene names in red: reference genes commonly used in previous studies. #TUB2_1 and TUB2_2 refer to two different primer pairs for TUB2 (Wu et al., 2019; Gao et al., 2022). ^UBC21_1 and UBC21_2 refer to two different primer pairs for UBC21 (Cuéllar Pérez et al., 2014; Gao et al., 2022) *ACT1_1 and ACT1_2 refer to two different primer pairs for ACT1 (Kim and Hwang, 2014; Zhang et al., 2015).

other genes had their $SD < 1$ for all the treatments (Supplementary Table S2). Similar to the results from NormFinder, results from BestKeeper suggest that the expression stability of the reference genes varies under different treatments, but with the highest stability upon *Pst* DC3000 infection in general. Nevertheless, the results strongly suggest the stability of all the candidate genes was acceptable as reference genes under all the treatment conditions tested.

Stability analysis by the comparative ΔC_t method

We also used the comparative ΔC_t method (Silver et al., 2006) to evaluate the relative stability of the candidate

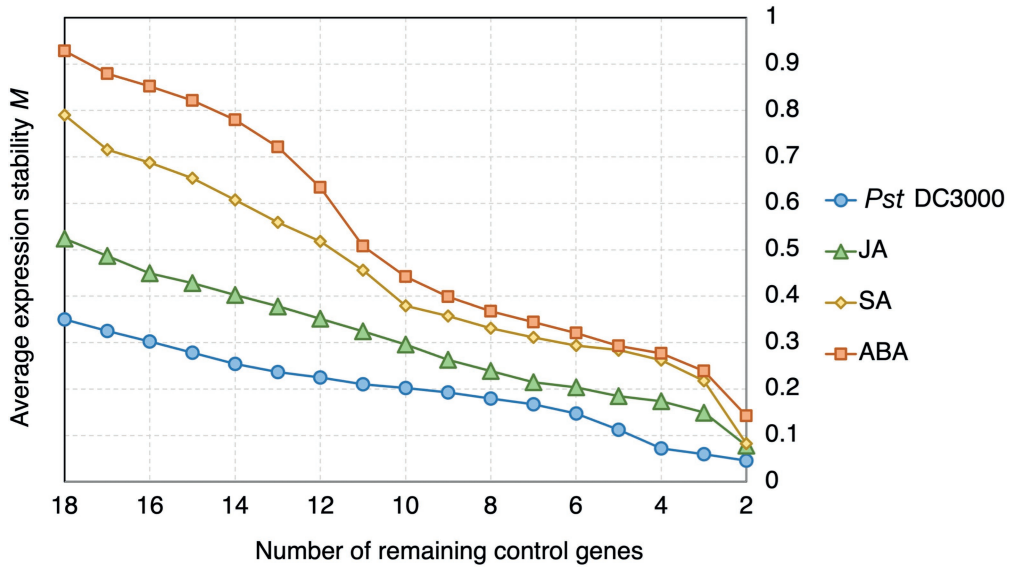

FIGURE 6
geNorm analysis of the average expression stability values of the candidate reference genes under *Pst* DC3000, JA, SA, and ABA treatments. Average expression stability values (*M*) of the remaining control genes were calculated by a stepwise exclusion of the least stable control gene among the reference gene candidates under each treatment using geNorm. The higher the *M* value, the lower is the ranking of the reference gene candidate in terms of expression stability.

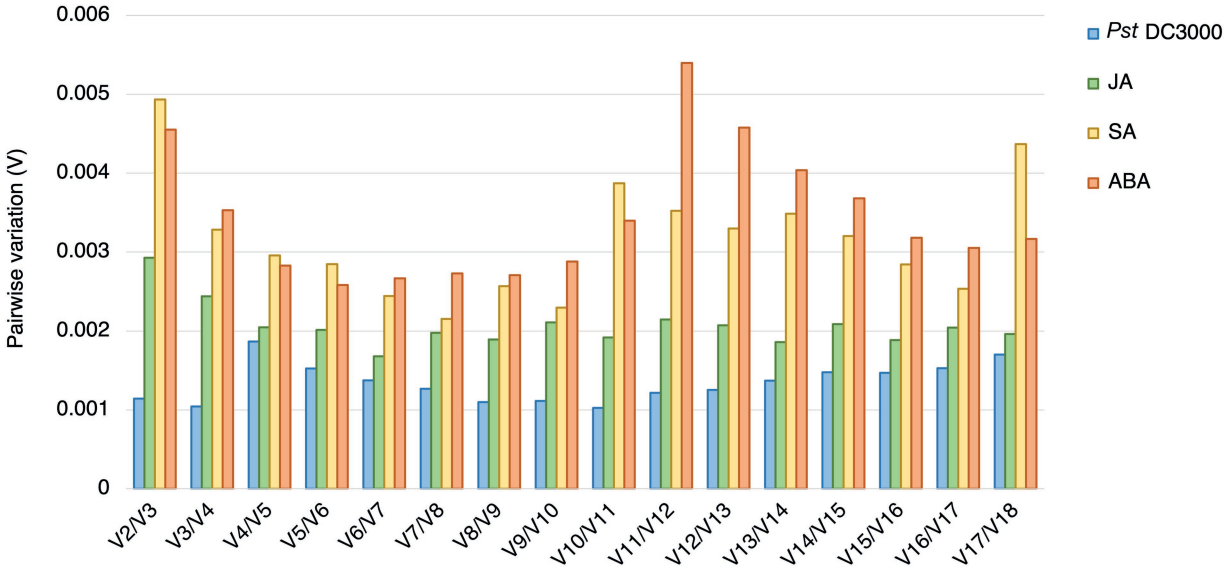

FIGURE 7
Pairwise variations (V) of the candidate reference genes. The pairwise variations (V) of the candidate reference genes calculated using geNorm, and $V=V_n/V_{n+1}$, where *n* is the number of reference genes required for expression normalization in RT-qPCR. The threshold value of V for achieving the optimal number of reference genes for RT-qPCR normalization is 0.15. All the candidate genes had V values well below the threshold value under all the treatments, indicating a minimal number of reference genes from among these candidates is required for normalization in RT-qPCR.

reference genes. The method compares the relative expression fluctuation of the two reference gene by measuring differences between their ΔC_t values (Silver et al., 2006; Nagy et al., 2017). The average SD of the 18 candidate reference genes ranged from 0.26 to 0.55 for *Pst* DC3000 treatment, 0.39 to 0.82 for JA treatment, 0.62 to 1.39 for SA treatment and 0.73 to 1.33 for ABA treatment (Supplementary Table S2). Among all the candidates, *TIF3D1* was the most stably expressed in both *Pst* DC3000 and SA treatments while *RPS6B* and *FKBP15-1* were the most stable with JA and ABA treatments, respectively (Supplementary Table S2). Similar to the results from NormFinder and BestKeeper, the results in the comparative

ΔC_t method showed that the stability of the reference genes varied with treatments, but they all had the highest expression stability upon *Pst* DC3000 infection.

Stability analysis by RefFinder

To gain a comprehensive view of the stability ranking of the 18 candidate reference genes, the results from geNorm, NormFinder, BestKeeper, and the comparative ΔC_t method were integrated using RefFinder (Xie et al., 2012; Supplementary Table S2). The results showed that the candidate reference genes had different degrees of expression stability under different treatments (Supplementary Table S2). Based on the comprehensive ranking, *TIF3D1*, *RPS6B*, and *FKBP15-1* were the most stably expressed under *Pst* DC3000 treatment, *RPS6B*, *PSBQ2*, and *FKBP15-1* most stably expressed with JA treatment, *TIF3D1*, *CYFBP*, and *FBA6* most stably expressed under SA treatment, and *PRPL17*, *PSBQ2,* and *FKBP15-1* most stably expressed with ABA treatment (Supplementary Table S2).

To see whether a single reference gene would be suitable for expression normalization for samples treated with different stresses, we estimated the geometric means of the rankings from RefFinder of each reference gene under different treatment combinations and suggested the most suitable candidate reference genes under these treatments (Table 1).

Discussion

In this study, we employed mass spectrometry-based LFQ and identified the *A. thaliana* proteins having stable abundances upon *Pst* DC3000 treatment. The candidate proteins fell into these categories: structural protein [ACT7 (Paez-Garcia et al., 2018)], basal metabolism-related proteins [BGAL6 (Dwevedi and Kayastha, 2010), CYFBP (Daie, 1993), FBA6 (Carrera et al., 2021), FBA8 (Lu et al., 2012), G6PDH5 (Sharkey and Weise, 2016), and PSBQ2 (Yi et al., 2006), protein-folding regulators HSP70-9 (Sung et al., 2001), FKBP15-1 and FKBP18 (Harrar et al., 2001)], and translation regulatory proteins [EIF(ISO)4G1 (Martínez-Silva et al., 2012), TIF3D1 (Raabe et al., 2019), RPS6B (Horiguchi et al., 2012), RPL12A, RPL17, RPL19, and RPL34C (Martinez-Seidel et al., 2020), and OVA6 (Berg et al., 2005)]. The results are consistent with the notion that genes involved in the maintenance of basal cellular functions tend to have stable expressions (Eisenberg and Levanon, 2013). It was therefore reasonable to expect the levels of the mRNAs encoding these proteins to also be relatively stable and that the study of expression stability upon pathogen infection could be applied to other treatments. The protein abundance and the mRNA level were found to be positively correlated (Supplementary Figure S6). In addition to the positive correlation, the slope of the line of best fit (Supplementary Figure S6) suggests that the mass spectrometry-based LFQ in proteomic analysis is more sensitive than RT-qPCR for expression quantitation. Such a high sensitivity of the mass spectrometry-based LFQ in proteomic analysis will enable accurate quantitation particularly if the experimental data fit the line of best fit well.

For the reference genes commonly used in previous studies, upon *Pst* DC3000 infection, the expression levels were generally lower than those of the candidate reference genes used in this study (Figure 2). The result is consistent with the lower abundance of the proteins compared to the proteins corresponding to the candidate reference genes reported in this study (Figure 1; Supplementary Figure S3). It is possible that proteins having higher abundances are more easily detectable by LC–MS/MS. In

TABLE 1 Appropriate *A. thaliana* reference genes for expression normalization under different combinations of treatments, including *Pseudomonaas syringae* pv. *tomato* DC3000 (*Pst* DC3000), jasmonic acid (JA), salicylic acid (SA), and abscisic acid (ABA).

Treatment(s)				Suggested reference genes		
Pst DC3000	JA	SA	ABA	*RPS6B* (1.41)	*TIF3D1* (2.71)	*PRPL19* (3.16)
Pst DC3000	JA	SA		*PRPL19* (2.55)	*RPS6B* (2.59)	*FKBP18* (2.99)
Pst DC3000	JA		ABA	*RPS6B* (1.57)	*PSBQ2* (2.78)	*RPL12A* (3.44)
Pst DC3000		SA	ABA	*FKBP15-1* (2.06)	*RPS6B* (2.3)	*PRPL19* (3.83)
Pst DC3000	JA			*RPS6B* (1.19)	*FKBP18* (2.3)	*PSBQ2* (3.31)
Pst DC3000		SA		*TIF3D1* (2.21)	*PRPL19* (2.38)	*G6PDH5* (3.6)
Pst DC3000			ABA	*RPS6B* (1)	*FBA6* (1.68)	*FKBP15-1* (3)
Pst DC3000				*RPS6B* (1.32)	*FKBP15-1* (2)	*FBA8* (2.45)
	JA	SA	ABA	*RPS6B* (2)	*ACT7* (2.24)	*PSBQ2* (2.66)
	JA	SA		*PRPL19* (2)	*ACT7* (2.28)	*RPS6B* (2.94)
	JA		ABA	*RPS6B* (1.63)	*PSBQ2* (2.11)	*ACT7* (3)
	JA			*RPS6B* (2.55)	*PSBQ2* (3.16)	*ACT7* (3.46)
		SA	ABA	*ACT7* (2.43)	*FKBP15-1* (3.46)	*RPS6B* (3.56)
		SA		*CYFBP* (2.17)	*TIF3D1* (2.34)	*EIF(ISO)4G1* (4.86)
			ABA	*FBA6* (2.06)	*RPS6B* (2.38)	*FKBP15-1* (3.08)

The geometric means of the RefFinder rankings of each candidate reference gene under the corresponding pair of treatment conditions are in brackets. The shade means blank.

other words, the mass spectrometry-based proteomic analysis favors the detection of highly expressed proteins, which may imply the high levels of the corresponding mRNAs. The use of highly expressed genes for expression normalization in RT-qPCR facilitates the expression analysis when the input amount of cDNA or RNA is low.

The expression levels of the candidate reference genes were in a reasonably detectable range (Figure 2). The expression stability of the candidate reference genes was estimated using multiple programs including geNorm *via* the R-based package ctrlGene (ver. 1.0.0; Vandesompele et al., 2002; Zhong, 2019), Normfinder *via* RefFinder (Andersen et al., 2004; Xie et al., 2012), BestKeeper (Pfaffl et al., 2004) and the comparative ΔC_t method (Silver et al., 2006). Since different programs employ different algorithms, they assigned different rankings to the same candidate reference genes (Supplementary Table S2). Similar observations were also reported in previous studies in which different reference genes were selected (Jia et al., 2019; Jin et al., 2019; Dudziak et al., 2020; Fu et al., 2022). To have a comprehensive view of expression stability, we employed RefFinder (Xie et al., 2012), in which an overall final ranking of the genes was generated based on the rankings in geNorm, Normfinder, BestKeeper, and the comparative ΔC_t method.

The overall stability of the mRNA levels of the candidate reference genes was most closely reflected by the results from geNorm. The *M* values of the reference genes determined in previous studies using RNA-seq approaches ranged from 0.3 to 2.1 (Jin et al., 2019; Dudziak et al., 2020; Mao et al., 2021; Fu et al., 2022), compared to *M* values of 0.046–0.350 under *Pst* DC3000 infection, 0.078–0.524 with JA treatment, 0.082–0.790 with SA treatment, and 0.142–0.929 with ABA treatment in this study (Supplementary Table S2). As lower *M* values indicate higher expression stability, our results from this study showed that the candidate reference genes discovered here have a higher stability than the previously reported ones.

The results from NormFinder, BestKeeper, and the comparative ΔC_t method all showed that these candidate reference genes had the highest expression stability upon *Pst* DC3000 infection compared to other treatments. This is to be expected, as these candidates were discovered based on the proteomic dataset upon *Pst* DC3000 infection. Although the stabilities of the candidate reference genes from other treatments were lower than those with *Pst* DC3000 infection, all the genes in all the treatments, except *FBA8* with SA treatment, are regarded as suitable reference genes, according to the algorithm of BestKeeper.

Among the 18 candidate reference genes, only *ACT7* (Czechowski et al., 2005) in *A. thaliana* and *OVA6* in potato (Castro-Quezada et al., 2013) were previously reported to be suitable for being used as reference genes for RT-qPCR in multiple-treatment experiments. Based on the overall final ranking generated using RefFinder, *ACT7* was out-performed by *TIF3D1*, *RPS6B*, *FKBP15-1*, and *FBA8* in *Pst* DC3000 infection, by *RPS6B*, *PSBQ2*, and *FKBP15-1* in JA treatment, by all candidate reference genes except *RPS6B*, *OVA6*, *FKBP15-1*, *HSP70-9*, and *FBA8* in SA treatment, and by *PRPL17*, *PSBQ2*, and *FKBP15-1* in ABA treatment (Supplementary Table S2). In previous studies on *A. thaliana-Pst* DC3000 interaction, depending on the stress responses, the plant samples may be harvested from 1 to 5 dpi (Mackey et al., 2003; Chow and Ng, 2017; Zhang et al., 2017; Cheng et al., 2022). Although the current study only addressed the expression stability of the candidate reference genes between 0 dpi and 3 dpi, the general expression stability of the genes upon various treatments may suggest the potential of these candidate reference genes for expression normalization at different time points after *Pst* DC3000 infection. For *A. thaliana*, *Pst* DC3000 has been commonly employed as the model bacterial pathogen (Xin and He, 2013). Besides being used as the model for studying plant-bacterium interaction, *A. thaliana* is also commonly used as the model for other plant-pathogen interactions. For example, *A. thaliana-Hyaloperonospora arabidopsidis*, *A. thaliana-Alternaria brassicicola* conidia, and *A. thaliana-Cucumber mosaic virus* have been employed as the models for plant-oomycete interaction, plant-fungus interaction, and plant-virus interactions, respectively, (Coates and Beynon, 2010; Pochon et al., 2012; Montes et al., 2019). Although the expression stability of the candidate reference genes was not tested upon the infection by the other pathogens, the expression stability of these candidate reference genes upon the treatment of various stress hormones was demonstrated. Since JA, SA, and ABA are major hormones regulating plant-pathogen interactions (Ku et al., 2018), the results may suggest the potential of these candidate reference genes for expression normalization upon the infection by other pathogens.

In conclusion, the results in this study suggest that mass spectrometry-based LFQ in proteomic analysis is an effective approach for mining proteins and their corresponding mRNAs with stable expression levels under different conditions. Compared to RNA-seq, mass spectrometry-based LFQ does not involve amplification steps which have been known to create biases that affect the accuracy of quantification. In addition, genes involved in the maintenance of basic cellular functions generally have stable expression levels. These factors enable the identification of elite reference genes from the proteomic dataset under different experimental treatments. The expression stability of the candidate reference genes in various treatments may suggest the potential of the genes to be employed as the reference genes in treatment conditions yet to be covered in the current study. The homologs of the candidate reference genes in other plant species may also be the potential candidates of reference genes for expression studies.

Data availability statement

The data presented in the study are deposited in PRIDE (PRoteomics IDEntifications Database, accession number PXD035677).

Author contributions

S-SC, Y-SK, and M-YC conducted the experiments and analyzed the data. S-SC and Y-SK drafted the manuscript. Y-SK and H-ML finalized the manuscript. H-ML acquired the funding. All authors contributed to the article and approved the submitted version.

Funding

This work was supported by the Hong Kong Research Grants Council: General Research Fund (14164617).

Acknowledgments

Jee-Yan Chu copy-edited this manuscript. Any opinions, findings, conclusions, or recommendations expressed in this publication do not reflect the views of the Government of the Hong Kong Special Administrative Region or the Innovation and Technology Commission.

Conflict of interest

The authors declare that the research was conducted in the absence of any commercial or financial relationships that could be construed as a potential conflict of interest.

Publisher's note

Supplementary material

The Supplementary material for this article can be found online at: https://www.frontiersin.org/articles/10.3389/fpls.2022.1001920/full#supplementary-material

References

Andersen, C. L., Jensen, J. L., and Ørntoft, T. F. (2004). Normalization of real-time quantitative reverse transcription-PCR data: a model-based variance estimation approach to identify genes suited for normalization, applied to bladder and colon cancer data sets. *Cancer Res.* 64, 5245–5250. doi: 10.1158/0008-5472.CAN-04-0496

Arefian, M., Vessal, S., Malekzadeh-Shafaroudi, S., Siddique, K. H. M., and Bagheri, A. (2019). Comparative proteomics and gene expression analyses revealed responsive proteins and mechanisms for salt tolerance in chickpea genotypes. *BMC Plant Biol.* 19:300. doi: 10.1186/s12870-019-1793-z

Benjamini, Y., and Speed, T. P. (2012). Summarizing and correcting the GC content bias in high-throughput sequencing. *Nucleic Acids Res.* 40:e72. doi: 10.1093/nar/gks001

Berg, M., Rogers, R., Muralla, R., and Meinke, D. (2005). Requirement of aminoacyl-tRNA synthetases for gametogenesis and embryo development in Arabidopsis. *Plant J.* 44, 866–878. doi: 10.1111/j.1365-313X.2005.02580.x

Carmona, R., Arroyo, M., Jiménez-Quesada, M. J., Seoane, P., Zafra, A., Larrosa, R., et al. (2017). Automated identification of reference genes based on RNA-seq data. *Biomed. Eng. Online* 16:65. doi: 10.1186/s12938-017-0356-5

Carrera, D. Á., George, G. M., Fischer-Stettler, M., Galbier, F., Eicke, S., Truernit, E., et al. (2021). Distinct plastid fructose bisphosphate aldolases function in photosynthetic and non-photosynthetic metabolism in Arabidopsis. *J. Exp. Bot.* 72, 3739–3755. doi: 10.1093/jxb/erab099

Castro-Quezada, P., Aarrouf, J., Claverie, M., Favery, B., Mugniéry, D., Lefebvre, V., et al. (2013). Identification of reference genes for normalizing RNA expression in potato roots infected with cyst nematodes. *Plant Mol. Biol. Rep.* 31, 936–945. doi: 10.1007/s11105-013-0566-3

Chen, C. C., Chien, W. F., Lin, N. C., and Yeh, K. C. (2014). Alternative functions of *Arabidopsis YELLOW STRIPELIKE3*: from metal translocation to pathogen defense. *PLoS One* 9:e98008. doi: 10.1371/journal.pone.0098008

Cheng, S.-S., Ku, Y.-S., Cheung, M.-Y., and Lam, H.-M. (2022). AtGAP1 promotes the resistance to *pseudomonas syringae* pv. *Tomato* DC3000 by regulating cell-wall thickness and stomatal aperture in Arabidopsis. *Int. J. Mol. Sci.* 23:7540. doi: 10.3390/ijms23147540

Cheong, M. S., Kirik, A., Kim, J. G., Frame, K., Kirik, V., and Mudgett, M. B. (2014). AvrBsT acetylates *Arabidopsis* ACIP1, a protein that associates with microtubules and is required for immunity. *PLoS Pathog.* 10:e1003952. doi: 10.1371/journal.ppat.1003952

Cheung, M. Y., Li, M. W., Yung, Y. L., Wen, C. Q., and Lam, H. M. (2013). The unconventional P-loop NTPase OsYchF1 and its regulator OsGAP1 play opposite roles in salinity stress tolerance. *Plant Cell Environ.* 36, 2008–2020. doi: 10.1111/pce.12108

Chow, H. T., and Ng, D. W.-K. (2017). Regulation of miR163 and its targets in defense against *Pseudomonas syringae* in *Arabidopsis thaliana*. *Sci. Rep.* 7:46433. doi: 10.1038/srep46433

Coates, M. E., and Beynon, J. L. (2010). *Hyaloperonospora arabidopsidis* as a pathogen model. *Annu. Rev. Phytopathol.* 48, 329–345. doi: 10.1146/annurev-phyto-080508-094422

Corchete, L. A., Rojas, E. A., Alonso-López, D., De Las Rivas, J., Gutiérrez, N. C., and Burguillo, F. J. (2020). Systematic comparison and assessment of RNA-seq procedures for gene expression quantitative analysis. *Sci. Rep.* 10:19737. doi: 10.1038/s41598-020-76881-x

Cuéllar Pérez, A., Nagels Durand, A., Vanden Bossche, R., De Clercq, R., Persiau, G., Van Wees, S. C. M., et al. (2014). The non-JAZ TIFY protein TIFY8 from *Arabidopsis thaliana* is a transcriptional repressor. *PLoS One* 9:e84891. doi: 10.1371/journal.pone.0084891

Cui, B., Xu, S., Li, Y., Umbreen, S., Frederickson, D., Yuan, B., et al. (2021). The *Arabidopsis* zinc finger proteins SRG2 and SRG3 are positive regulators of plant immunity and are differentially regulated by nitric oxide. *New Phytol.* 230, 259–274. doi: 10.1111/nph.16993

Czechowski, T., Stitt, M., Altmann, T., Udvardi, M. K., and Scheible, W.-R. (2005). Genome-wide identification and teseting of superior refernece genes for transcript normalization in Arabidopsis. *Plant Physiol.* 139, 5–17. doi: 10.1104/pp.105.063743

Daie, J. (1993). Cytosolic fructose-1,6-bisphosphatase: a key enzyme in the sucrose biosynthetic pathway. *Photosynth. Res.* 38, 5–14. doi: 10.1007/BF00015056

Ding, H., Mo, S., Qian, Y., Yuan, G., Wu, X., and Ge, C. (2020). Integrated proteome and transcriptome analyses revealed key factors involved in tomato (*Solanum lycopersicum*) under high temperature stress. *Food Energy Secur.* 9:e239. doi: 10.1002/fes3.239

Dodds, P. N., and Rathjen, J. P. (2010). Plant immunity: towards an integrated view of plant-pathogen interactions. *Nat. Rev. Genet.* 11, 539–548. doi: 10.1038/nrg2812

Dudziak, K., Sozoniuk, M., Szczerba, H., Kuzdraliński, A., Kowalczyk, K., Börner, A., et al. (2020). Identification of stable reference genes for qPCR studies in common wheat (*Triticum aestivum* L.) seedlings under short-term drought stress. *Plant Methods* 16:58. doi: 10.1186/s13007-020-00601-9

Dwevedi, A., and Kayastha, A. M. (2010). Plant β-galactosidases: physiological significance and recent advances in technological applications. *J. Plant Biochem. Biotechnol.* 19, 9–20. doi: 10.1007/bf03323431

Eisenberg, E., and Levanon, E. Y. (2013). Human housekeeping genes, revisited. *Trends Genet.* 29, 569–574. doi: 10.1016/j.tig.2013.05.010

Fu, N., Li, J., Wang, M., Ren, L., Zong, S., and Luo, Y. (2022). Identification and validation of reference genes for gene expression analysis in different development stages of *Amylostereum areolatum*. *Front. Microbiol.* 12, 1–9. doi: 10.3389/fmicb.2021.827241

Gao, Y., Li, Z., Yang, C., Li, G., Zeng, H., Li, Z., et al. (2022). *Pseudomonas syringae* activates *ZAT18* to inhibit salicylic acid accumulation by repressing *EDS1* transcription for bacterial infection. *New Phytol.* 233, 1274–1288. doi: 10.1111/nph.17870

Gökmen-Polar, Y. (2019). "Overview of PCR-based technologies and multiplexed gene analysis for biomarker studies," in *Predictive Biomarkers in Oncology*. eds. S. Badve and G. L. Kumar (Cham: Springer Nature Switzerland AG), 63–73. doi: 10.1007/978-3-319-95228-4

Gorshkov, V., and Tsers, I. (2022). Plant susceptible responses: the underestimated side of plant–pathogen interactions. *Biol. Rev.* 97, 45–66. doi: 10.1111/brv.12789

Gupta, A., and Senthil-Kumar, M. (2017). Transcriptome changes in *Arabidopsis thaliana* infected with *Pseudomonas syringae* during drought recovery. *Sci. Rep.* 7:9124. doi: 10.1038/s41598-017-09135-y

Harrar, Y., Bellini, C., and Faure, J.-D. (2001). FKBPs: at the crossroads of folding and transduction. *Trends Plant Sci.* 6, 426–431. doi: 10.1016/s1360-1385(01)02044-1

Horiguchi, G., Van Lijsebettens, M., Candela, H., Micol, J. L., and Tsukaya, H. (2012). Ribosomes and translation in plant developmental control. *Plant Sci.* 191-192, 24–34. doi: 10.1016/j.plantsci.2012.04.008

Huang, T. Y., Desclos-Theveniau, M., Chien, C. T., and Zimmerli, L. (2013). *Arabidopsis thaliana* transgenics overexpressing *IBR3* show enhanced susceptibility to the bacterium *Pseudomonas syringae*. *Plant Biol. J.* 15, 832–840. doi: 10.1111/j.1438-8677.2012.00685.x

Huot, B., Castroverde, C. D. M., Velásquez, A. C., Hubbard, E., Pulman, J. A., Yao, J., et al. (2017). Dual impact of elevated temperature on plant defence and bacterial virulence in *Arabidopsis*. *Nat. Commun.* 8, 1808–1811. doi: 10.1038/s41467-017-01674-2

Jeong, H. J., Kim, Y. J., Kim, S. H., Kim, Y. H., Lee, I. J., Kim, Y. K., et al. (2011). Nonsense-mediated mRNA decay factors, UPF1 and UPF3, contribute to plant defense. *Plant Cell Physiol.* 52, 2147–2156. doi: 10.1093/pcp/pcr144

Jia, D. H., Wang, B., Li, X. L., Tan, W., Gan, B. C., and Peng, W. H. (2019). Validation of reference genes for quantitative gene expression analysis in *Auricularia cornea*. *J. Microbiol. Methods* 163:105658. doi: 10.1016/j.mimet.2019.105658

Jia, X., Zeng, H., Wang, W., Zhang, F., and Yin, H. (2018). Chitosan oligosaccharide induces resistance to *Pseudomonas syringae* pv. *tomato* DC3000 in *Arabidopsis thaliana* by activating both salicylic acid–and jasmonic acid–mediated pathways. *Mol. Plant Microbe Interact.* 31, 1271–1279. doi: 10.1094/MPMI-03-18-0071-R

Jin, Y., Liu, F., Huang, W., Sun, Q., and Huang, X. (2019). Identification of reliable reference genes for qRT-PCR in the ephemeral plant *Arabidopsis pumila* based on full-length transcriptome data. *Sci. Rep.* 9, 8408–8411. doi: 10.1038/s41598-019-44849-1

Kim, D. S., and Hwang, B. K. (2014). An important role of the pepper phenylalanine ammonia-lyase gene (PAL1) in salicylic acid-dependent signalling of the defence response to microbial pathogens. *J. Exp. Bot.* 65, 2295–2306. doi: 10.1093/jxb/eru109

Ku, Y.-S., Cheng, S.-S., Gerhardt, A., Cheung, M.-Y., Contador, C. A., Poon, L.-Y. W., et al. (2020). Secretory peptides as bullets: effector peptides from pathogens against antimicrobial peptides from soybean. *Int. J. Mol. Sci.* 21, 1–26. doi: 10.3390/ijms21239294

Ku, Y.-S., Sintaha, M., Cheung, M.-Y., and Lam, H.-M. (2018). Plant hormone signaling crosstalks between biotic and abiotic stress responses. *Int. J. Mol. Sci.* 19:3206. doi: 10.3390/ijms19103206

Kudo, T., Sasaki, Y., Terashima, S., Matsuda-Imai, N., Takano, T., Saito, M., et al. (2016). Identification of reference genes for quantitative expression analysis using large-scale RNA-seq data of *Arabidopsis thaliana* and model crop plants. *Genes Genet. Syst.* 91, 111–125. doi: 10.1266/ggs.15-00065

Li, B., Meng, X., Shan, L., and He, P. (2016a). Transcriptional regulation of pattern-triggered immunity in plants. *Cell Host Microbe* 19, 641–650. doi: 10.1016/j.chom.2016.04.011

Li, L., Yu, Y., Zhou, Z., and Zhou, J. M. (2016b). Plant pattern-recognition receptors controlling innate immunity. *Sci. China Life Sci.* 59, 878–888. doi: 10.1007/s11427-016-0115-2

Lu, W., Tang, X., Huo, Y., Xu, R., Qi, S., Huang, J., et al. (2012). Identification and characterization of fructose 1,6-bisphosphate aldolase genes in Arabidopsis reveal a gene family with diverse responses to abiotic stresses. *Gene* 503, 65–74. doi: 10.1016/j.gene.2012.04.042

Mackey, D., Belkhadir, Y., Alonso, J. M., Ecker, J. R., and Dangl, J. L. (2003). *Arabidopsis* RIN4 is a target of the type III virulence effector AvrRpt2 and modulates RPS2-mediated resistance. *Cell* 112, 379–389. doi: 10.1016/S0092-8674(03)00040-0

Mao, M., Xue, Y., He, Y., Zhou, X., Hu, H., Liu, J., et al. (2021). Validation of reference genes for quantitative real-time PCR normalization in *Ananas comosus* var. *bracteatus* during chimeric leaf development and response to hormone stimuli. *Front. Genet.* 12:716137. doi: 10.3389/fgene.2021.716137

Martin, K., Singh, J., Hill, J. H., Whitham, S. A., and Cannon, S. B. (2016). Dynamic transcriptome profiling of bean common mosaic virus (BCMV) infection in common bean (*Phaseolus vulgaris* L.). *BMC Genom.* 17:613. doi: 10.1186/s12864-016-2976-8

Martinez-Seidel, F., Beine-Golovchuk, O., Hsieh, Y. C., and Kopka, J. (2020). Systematic review of plant ribosome heterogeneity and specialization. *Front. Plant Sci.* 11:948. doi: 10.3389/fpls.2020.00948

Martínez-Silva, A. V., Aguirre-Martínez, C., Flores-Tinoco, C. E., Alejandri-Ramírez, N. D., and Dinkova, T. D. (2012). Translation initiation factor AteiF(iso)4E is involved in selective mRNA translation in *Arabidopsis thaliana* seedlings. *PLoS One* 7:e31606. doi: 10.1371/journal.pone.0031606

Marx, H., Minogue, C. E., Jayaraman, D., Richards, A. L., Kwiecien, N. W., Siahpirani, A. F., et al. (2016). A proteomic atlas of the legume *Medicago truncatula* and its nitrogen-fixing endosymbiont *Sinorhizobium meliloti*. *Nat. Biotechnol.* 34, 1198–1205. doi: 10.1038/nbt.3681

Matic, S., Bagnaresi, P., Biselli, C., Orru, L., Carneiro, G. A., Siciliano, I., et al. (2016). Comparative transcriptome profiling of resistant and susceptible rice genotypes in response to the seedborne pathogen *Fusarium fujikuroi*. *BMC Genom.* 17:608. doi: 10.1186/s12864-016-2925-6

Medzhitov, R., and Janeway, C. A. (1997). Innate immunity: the virtues of a nonclonal system of recognition. *Cell* 91, 295–298. doi: 10.1016/S0092-8674(00)80412-2

Mi, H., Muruganujan, A., Casagrande, J. T., and Thomas, P. D. (2013). Large-scale gene function analysis with the panther classification system. *Nat. Protoc.* 8, 1551–1566. doi: 10.1038/nprot.2013.092

Montes, N., Alonso-Blanco, C., and García-Arenal, F. (2019). *Cucumber mosaic virus* infection as a potential selective pressure on *Arabidopsis thaliana* populations. *PLoS Pathog.* 15:e1007810. doi: 10.1371/journal.ppat.1007810

Nagy, N. A., Németh, Z., Juhász, E., Póliska, S., Rácz, R., Kosztolányi, A., et al. (2017). Evaluation of potential reference genes for real-time qPCR analysis in a biparental beetle, *Lethrus apterus* (Coleoptera: Geotrupidae). *PeerJ.* 5, 1–16. doi: 10.7717/peerj.4047

Nakaminami, K., Matsui, A., Nakagami, H., Minami, A., Nomura, Y., Tanaka, M., et al. (2014). Analysis of differential expression patterns of mRNA and protein during cold-acclimation and de-acclimation in *Arabidopsis*. *Mol. Cell. Proteomics* 13, 3602–3611. doi: 10.1074/mcp.M114.039081

Paez-Garcia, A., Sparks, J. A., de Bang, L., and Blancaflor, E. B. (2018). "Plant actin cytoskeleton: new functions from old scaffold," in *Concepts in Cell Biology - History and Evolution*. eds. V. P. Sahi and F. Baluška (London, UK: Springer Nature), 103–137.

Parekh, S., Ziegenhain, C., Vieth, B., Enard, W., and Hellmann, I. (2016). The impact of amplification on differential expression analyses by RNA-seq. *Sci. Rep.* 6:25533. doi: 10.1038/srep25533

Pfaffl, M. W., Tichopad, A., Prgomet, C., and Neuvians, T. P. (2004). Determination of stable housekeeping genes, differentially regulated target genes and sample integrity: BestKeeper - excel-based tool using pair-wise correlations. *Biotechnol. Lett.* 26, 509–515. doi: 10.1023/B:BILE.0000019559.84305.47

Piehler, A. P., Grimholt, R. M., Øvstebø, R., and Berg, J. P. (2010). Gene expression results in lipopolysaccharide-stimulated monocytes depend significantly on the choice of reference genes. *BMC Immunol.* 11:21. doi: 10.1186/1471-2172-11-21

Pochon, S., Terrasson, E., Guillemette, T., Iacomi-Vasilescu, B., Georgeault, S., Juchaux, M., et al. (2012). The *Arabidopsis thaliana-Alternaria brassicicola* pathosystem: a model interaction for investigating seed transmission of necrotrophic fungi. *Plant Methods* 8:16. doi: 10.1186/1746-4811-8-16

Pombo, M. A., Ramos, R. N., Zheng, Y., Fei, Z., Martin, G. B., and Rosli, H. G. (2019). Transcriptome-based identification and validation of reference genes for plant-bacteria interaction studies using *Nicotiana benthamiana*. *Sci. Rep.* 9:1632. doi: 10.1038/s41598-018-38247-2

Ponnala, L., Wang, Y., Sun, Q., and van Wijk, K. J. (2014). Correlation of mRNA and protein abundance in the developing maize leaf. *Plant J.* 78, 424–440. doi: 10.1111/tpj.12482

Poretti, M., Sotiropoulos, A. G., Graf, J., Jung, E., Bourras, S., Krattinger, S. G., et al. (2021). Comparative transcriptome analysis of wheat lines in the field reveals multiple essential biochemical pathways suppressed by obligate pathogens. *Front. Plant Sci.* 12:720462. doi: 10.3389/fpls.2021.720462

Raabe, K., Honys, D., and Michailidis, C. (2019). The role of eukaryotic initiation factor 3 in plant translation regulation. *Plant Physiol. Biochem.* 145, 75–83. doi: 10.1016/j.plaphy.2019.10.015

Ren, H., Li, X., Guo, L., Wang, L., Hao, X., and Zeng, J. (2022). Integrative transcriptome and proteome analysis reveals the absorption and metabolism of selenium in tea alants [*Camellia sinensis* (L.) O. Kuntze]. *Front. Plant Sci.* 13:848349. doi: 10.3389/fpls.2022.848349

Romero-Pérez, A., Ameye, M., Audenaert, K., and Van Damme, E. J. M. (2021). Overexpression of F-box Nictaba promotes defense and anthocyanin accumulation in *Arabidopsis thaliana* after *Pseudomonas syringae infection*. *Front. Plant Sci.* 12:692606. doi: 10.3389/fpls.2021.692606

Sakurai, T., Kondou, Y., Akiyama, K., Kurotani, A., Higuchi, M., Ichikawa, T., et al. (2011). RiceFOX: a database of Arabidopsis mutant lines overexpressing rice full-length cDNA that contains a wide range of trait information to facilitate analysis of gene function. *Plant Cell Physiol.* 52, 265–273. doi: 10.1093/pcp/pcq190

Sharkey, T. D., and Weise, S. E. (2016). The glucose 6-phosphate shunt around the Calvin-Benson cycle. *J. Exp. Bot.* 67, 4067–4077. doi: 10.1093/jxb/erv484

Shu, J., Ma, X., Ma, H., Huang, Q., Zhang, Y., Guan, M., et al. (2022). Transcriptomic, proteomic, metabolomic, and functional genomic approaches of *Brassica napus* L. during salt stress. *PLoS One* 17:e0262587. doi: 10.1371/journal.pone.0262587

Silver, N., Best, S., Jiang, J., and Thein, S. L. (2006). Selection of housekeeping genes for gene expression studies in human reticulocytes using real-time PCR. *BMC Mol. Biol.* 7:33. doi: 10.1186/1471-2199-7-33

Sugano, S., Hayashi, N., Kawagoe, Y., Mochizuki, S., Inoue, H., Mori, M., et al. (2016). Rice OsVAMP714, a membrane-trafficking protein localized to the chloroplast and vacuolar membrane, is involved in resistance to rice blast disease. *Plant Mol. Biol.* 91, 81–95. doi: 10.1007/s11103-016-0444-0

Sung, D. Y., Kaplan, F., and Guy, C. L. (2001). Plant Hsp70 molecular chaperones: protein structure, gene family, expression and function. *Physiol. Plant.* 113, 443–451. doi: 10.1034/j.1399-3054.2001.1130402.x

Vandesompele, J., De Preter, K., Pattyn, F., Poppe, B., Van Roy, N., De Paepe, A., et al. (2002). Accurate normalization of real-time quantitative RT-PCR data by geometric averaging of multiple internal control genes. *Genome Biol.* 3:research0034. doi: 10.1186/gb-2002-3-7-research0034

Walker, C. G., Meier, S., Mitchell, M. D., Roche, J. R., and Littlejohn, M. (2009). Evaluation of real-time PCR endogenous control genes for analysis of gene expression in bovine endometrium. *BMC Mol. Biol.* 10:100. doi: 10.1186/1471-2199-10-100

Wang, J., Islam, F., Li, L., Long, M., Yang, C., Jin, X., et al. (2017). Complementary RNA-sequencing based transcriptomics and iTRAQ proteomics reveal the mechanism of the alleviation of quinclorac stress by salicylic acid in *Oryza sativa* ssp. *japonica*. *Int. J. Mol. Sci.* 18:1975. doi: 10.3390/ijms18091975

Wessel, D., and Flügge, U. I. (1984). A method for the quantitative recovery of protein in dilute solution in the presence of detergents and lipids. *Anal. Biochem.* 138, 141–143. doi: 10.1016/0003-2697(84)90782-6

Wu, Z., Han, S., Zhou, H., Tuang, Z. K., Wang, Y., Jin, Y., et al. (2019). Cold stress activates disease resistance in *Arabidopsis thaliana* through a salicylic acid dependent pathway. *Plant Cell Environ.* 42, 2645–2663. doi: 10.1111/pce.13579

Xie, F., Xiao, P., Chen, D., Xu, L., and Zhang, B. (2012). miRDeepFinder: a miRNA analysis tool for deep sequencing of plant small RNAs. *Plant Mol. Biol.* 80, 75–84. doi: 10.1007/s11103-012-9885-2

Xin, X. F., and He, S. Y. (2013). *Pseudomonas syringae* pv. *tomato* DC3000: a model pathogen for probing disease susceptibility and hormone signaling in plants. *Annu. Rev. Phytopathol.* 51, 473–498. doi: 10.1146/annurev-phyto-082712-102321

Yi, X., Hargett, S. R., Frankel, L. K., and Bricker, T. M. (2006). The PsbQ protein is required in *Arabidopsis* for photosystem II assembly/stability and photoautotrophy under low light conditions. *J. Biol. Chem.* 281, 26260–26267. doi: 10.1074/jbc.M603582200

Yim, A. K.-Y., Wong, J. W.-H., Ku, Y.-S., Qin, H., Chan, T.-F., and Lam, H.-M. (2015). Using RNA-seq data to evaluate reference genes suitable for gene expression studies in soybean. *PLoS One* 10:e0136343. doi: 10.1371/journal.pone.0136343

Zhang, H., Huang, L., Dai, Y., Liu, S., Hong, Y., Tian, L., et al. (2015). *Arabidopsis* AtERF15 positively regulates immunity against *Pseudomonas syringae* pv. *tomato* DC3000 and *Botrytis cinerea*. *Front. Plant Sci.* 6:686. doi: 10.3389/fpls.2015.00686

Zhang, R., Qi, H., Sun, Y., Xiao, S., and Lim, B. L. (2017). Transgenic *Arabidopsis thaliana* containing increased levels of ATP and sucrose is more susceptible to *Pseudomonas syringae*. *PLoS One* 12:e0171040. doi: 10.1371/journal.pone.0171040

Zhang, J., and Zhou, J. M. (2010). Plant immunity triggered by microbial molecular signatures. *Mol. Plant* 3, 783–793. doi: 10.1093/mp/ssq035

Zhong, S. (2019). ctrlGene: assess the stability of candidate housekeeping genes. Available at: https://cran.r-project.org/web/packages/ctrlGene/ (Accessed June 1, 2022).

Zhou, Z., Cong, P., Tian, Y., and Zhu, Y. (2017). Using RNA-seq data to select reference genes for normalizing gene expression in apple roots. *PLoS One* 12:e0185288. doi: 10.1371/journal.pone.0185288

Zhu, Y., Qiu, W., He, X., Wu, L., Bi, D., Deng, Z., et al. (2022). Integrative analysis of transcriptome and proteome provides insights into adaptation to cadmium stress in *Sedum plumbizincicola*. *Ecotoxicol. Environ. Saf.* 230:113149. doi: 10.1016/j.ecoenv.2021.113149

Zhu, Q.-H., Stephen, S., Kazan, K., Jin, G., Fan, L., Taylor, J., et al. (2013). Characterization of the defense transcriptome responsive to *Fusarium oxysporum*-infection in *Arabidopsis* using RNA-seq. *Gene* 512, 259–266. doi: 10.1016/j.gene.2012.10.036

frontiers | Frontiers in Plant Science

TYPE Original Research
PUBLISHED 21 November 2022
DOI 10.3389/fpls.2022.1077328

OPEN ACCESS

EDITED BY
Ravinder Kumar,
Central Potato Research Institute (ICAR), India

REVIEWED BY
Sanjay Kumar Goswami,
Indian Institute of Sugarcane Research (ICAR), India
Ho-jong Ju,
Jeonbuk National University, South Korea

*CORRESPONDENCE
C. Gopalakrishnan
pcgopalagri@gmail.com

SPECIALTY SECTION
This article was submitted to Plant Pathogen Interactions, a section of the journal Frontiers in Plant Science

RECEIVED 22 October 2022
ACCEPTED 31 October 2022
PUBLISHED 21 November 2022

CITATION
Logeshwari R, Gopalakrishnan C, Kamalakannan A, Ramalingam J and Saraswathi R (2022) A colorimetric hydroxy naphthol blue based loop-mediated isothermal amplification detection assay targeting the β-tubulin locus of *Sarocladium oryzae* infecting rice seed. *Front. Plant Sci.* 13:1077328. doi: 10.3389/fpls.2022.1077328

A colorimetric hydroxy naphthol blue based loop-mediated isothermal amplification detection assay targeting the β-tubulin locus of *Sarocladium oryzae* infecting rice seed

R. Logeshwari[1], C. Gopalakrishnan[1]*, A. Kamalakannan[1], J. Ramalingam[2] and R. Saraswathi[3]

[1]Department of Plant Pathology, Tamil Nadu Agricultural University, Coimbatore, India,
[2]Department of Plant Biotechnology, Tamil Nadu Agricultural University, Coimbatore, India,
[3]Department of Plant Genetic Resources, Tamil Nadu Agricultural University, Coimbatore, India

Sarocladium oryzae is a widely prevalent seed-borne pathogen of rice. The development of a rapid and on-site detection method for *S. oryzae* is therefore important to ensure the health of rice seeds. Loop-mediated isothermal amplification (LAMP) is ideal for field-level diagnosis since it offers quick, high-specific amplification of target template sequences at a single temperature. We designed primers based on the β-tubulin region of *S. oryzae*. The LAMP technique devised was extremely sensitive, detecting the presence of the *S. oryzae* template at concentrations as low as 10 fg in 30 minutes at 65°C. The assay specificity was confirmed by performing the experiment with genomic DNA isolated from 22 different phytopathogens. Through the addition of hydroxy naphthol blue in the reaction process prior to amplification, a colour shift from violet to deep sky blue was seen in the vicinity of the target pathogen only. Finally, the LAMP assay was validated using live infected tissues, weeds and different varieties of seeds collected from different locations in Tamil Nadu, India. If developed into a detection kit, the LAMP assay developed in this study has potential applications in seed health laboratories, plant quarantine stations, and on-site diagnosis of *S. oryzae* in seeds and plants.

KEYWORDS

Sarocladium oryzae*, seed, β-tubulin, HNB dye, Loop-mediated isothermal amplification, *Oryza sativa

1 Introduction

Rice (*Oryza sativa* L.) is a substantial food crop that contributes significantly to the global economy. It is the primary food crop for almost two-thirds of the world's population, coming in third place globally behind maize and wheat in terms of production (Abbade, 2021). According to a comprehensive survey made by the International Food Policy Research Institute, rice production will need to increase by 38% by 2030 to feed the world's growing population, yet available arable land is being lost to housing and industrialization (Zhang et al., 2019). Even if the annual rise in rice output is high, there are still several production barriers, such as pests and diseases. Diseases have caused a significant loss in rice output, amounting up to 80% of the entire rice crop in severe cases (Nasruddin and Amin, 2013). The maintenance of rice seed health is crucial to secure food availability and achieving significant export because the number of organisms that threaten rice cultivation is abundant (Teng, 1994; Reddy and Sathyanarayana, 2001; Dossou and Silue, 2018).

A significant loss in quality and yield can be caused by seed-borne pathogens, which may also serve as an unnoticed source for the spread of pathogens (Tiwari, 2016). Early detection of seed-borne fungal infections is critical to minimize uncontrolled pathogen propagation *via* long-distance exchange of such material, as well as to avoid economic losses and superfluous application of fungicide (Mancini et al., 2016). Rice Sheath Rot incited by *Sarocladium oryzae*, one of the most damaging rice seed-borne fungal diseases, resulting in significant economic losses in rice-growing countries. The pathogen was first reported in 1922 in Taiwan (Mathur, 1981; Mew and Gonzales, 2002; Ayyadurai et al., 2005; Bigirimana et al., 2015). This pathogen thrives well in rainfed rice fields and is prevalent in lowland and medium-land habitats (Pearce et al., 2001; Sarangi and Islam, 2019). The losses were in the form of qualitative as well as quantitative *i.e.*, loss of yield including discoloration of grain that renders it unfit for export (Gopalakrishnan et al., 2010; Zhang et al., 2019).

The detection of seed-borne *S. oryzae* is vital during seed certification and allows for the implementation of early containment and control measures. Early detection of RSR is crucial for regulating the spread of the disease, minimizing direct and indirect economic losses like the excessive application of fungicides, and preventing excessive pathogen spread. The common method used for diagnosis of *S. oryzae* in the laboratory is standard blotter tests. However, it requires laboratory facilities and incubation for several days. Nucleic acid-based approaches have become widely used to identify pathogens more quickly. To address this, LAMP is an isothermal nucleic acid amplification technology that has several benefits in diagnostic research. Due to the lack of thermal cycling and the tendency of the enzymes to replicate more quickly than PCR, reactions can be carried out using portable, battery-operated platforms. The LAMP test utilizes four to six oligonucleotide primers that were intended to recognize a total of six distinct regions of the target gene, and two loop primers positioned in the loop region might speed up the amplification (Notomi et al., 2000; Zhang et al., 2016) together with the strand displacement activity of *Bst* DNA polymerase, which may amplify precise DNA sequences with great specificity (Wastling et al., 2000).

In this investigation, LAMP assay was established for the quick, facile, specific and highly sensitive detection of *S. oryzae* in rice seeds. With these assays, *S. oryzae* may be rapidly detected in infected rice tissues in the field as well as in seeds.

2 Materials and method

2.1 Sample collection, isolation of pathogen and DNA extraction

Fifty *S. oryzae* isolates were isolated from rice grain samples which were randomly collected from farmer's field, storage godowns and research centres from different locations of Tamil Nadu, India, labeled appropriately and brought to the laboratory for further studies. Each isolates were incubated at 27 ± 2°C for 10- 20 days on potato dextrose agar (PDA) media. For extracting DNA from fungal mycelia, cultures were grown in a 250 ml conical flask with 100 ml of potato dextrose broth that had been autoclaved at 121°C and 15 psi. The fungal mycelial discs (4 no.) were then inoculated into flasks and incubated at 27 ± 2°C for 7-10 days. The mycelial mat was taken from the broth and dried on filter paper. The modified CTAB method was used to extract total genomic DNA (Doyle, 1991). A Nano-drop Spectrophotometer (ND-1000) was used to measure the concentration and purity of each genomic DNA, and the quality of all extracted DNA was determined by measuring its absorbance at 260 and 280 nm. Agarose gel electrophoresis was done to confirm DNA concentrations. On an agarose gel with a 1.2% (w/v) concentration and 0.1 µg/mL of ethidium bromide, ten microliters of purified DNA were run. The Biorad Gel Doc was used to visualize the DNA. The DNA was kept at -20°C for further use.

2.2 PCR detection and sequencing

PCR analysis was carried out in a 25 µL reaction mixture containing 1 µL of genomic DNA, 12.5 µL of 2X Master mix (RR310 EmeraldAmp), and 2.5 µL of both forward and reverse primer (ITS 1F and ITS 4R). Nuclease-free water was added to bring the total amount to 25 µL. DNA amplification was accomplished in an Eppendorf thermocycler (Germany) under

the following cycling conditions: primary denaturation at 95°C for 2 min; 35 cycles of denaturation at 95°C for 30 s; annealing at 55°C for 30 s; elongation at 72°C for 60 s and terminal elongation 72°C for 10 min. The DNA bands were separated by gel electrophoresis in a 1.2% agarose (Himedia) gel stained with 0.1 µg/mL of ethidium bromide. The UV gel documentation system was used to visualize the DNA bands resolved on agarose gel. By contrasting the amplicons with a 100 bp DNA ladder (3422A Takara) on an agarose gel, the amplicons sizes were estimated. The amplified PCR product was sequenced at Biokart India Pvt. Ltd. (Bangalore, India) by Sanger's dideoxy method. The sequences were compared with other ITS region of *S. oryzae* available at NCBI database to assess for their variability (Supplementary Table 1).

2.3 Primer design and *in silico* validation

The software tool PRIMER EXPLORER V5 (http://primerexplorer.jp/e/) which is accessible on the Eiken Genome website was used to design LAMP primers. A critical part in LAMP primer designing is the selection of a potential target gene with high nucleotide variability among related species. LAMP primers were designed by utilizing the β-tubulin gene of *S. oryzae*. A set of six primers was designed by using the sequences retrieved from NCBI GenBank (Accession number MZ614962.1). Each parameter was set to its default value. The primer sequences utilized in this experiment are furnished in Table 1. Figure 1 depicts LAMP primer's structure and its complement target DNA used in this work. In addition, β-Tubulin sequences of *S. oryzae* strain Sor-3 (MZ614962.1), *S. oryzae* strain Sor-2 (MZ614961.1), *S. oryzae* strain Sor-1 (MZ614960.1), *S. strictum* (KM249114.1), *S. kiliense* (MZ833455.1) and *S. spirale* (LC464483.1) were acquired from the NCBI website (http://www.ncbi.nlm.nih.gov) to verify the specificity of primers against other three *Sarocladium* spp. (Figure 2). Oligo Evaluator™ (Sigma Aldrich) was employed to verify developed primers for secondary structure formation (hairpins, palindromes, repetitions, dimers, cross dimers and runs), primer dimerization (primer-dimer), % GC and GC clamp (https://www.sigmaaldrich.com) (Zaczek-Moczydłowska et al., 2020). The specificity of each primer was confirmed by comparing the primer sequences with the NCBI GenBank nucleotide and genome databases by employing the BLASTn programme (Altschul et al., 1990).

2.4 LAMP reaction

The LAMP reagents were standardized in various concentrations (Table 2) in order to determine the best conditions for the reaction. The final LAMP reactions were accomplished in a 25 µL LAMP reaction mixture that contained 1.5 µL of target DNA (~ 120 ng), 2.5 µL of Thermopol reaction buffer (10x), 1.4 mM of each dNTPs, 0.2 mM of both outer primers, 0.4 mM of both loop primers, 1.4 M of both inner primers, 1.2 M betaine, 8 mM $MgSO_4$, 2 U *Bst* polymerase (0.08 U/µL) and 120 µM hydroxyl naphthol blue. Instead of using a DNA template, the nuclease-free water served as the negative control. The reactions were performed in an Eppendorf thermal cycler for 30 min at a constant temperature of 65°C, and then the reaction was ceased by thermal denaturation for 2 min at 80°C.

A visual evaluation of the colour was done after termination. The quantity of amplification product as evaluated by 2% agarose gel electrophoresis was used to choose the optimal condition (Supplementary Figure 1). Protocols with varying amplification temperature (56-70°C) and amplification time (10-150 min) were investigated to optimize the LAMP assay (Supplementary Figure 2).

2.5 Sensitivity of LAMP assay

Genomic DNA that had been serially diluted ten times (100 ng/l to 1 fg/l) was used to assess the amplification potency and sensitivity of the LAMP primers. This experiment was carried out thrice (Table 3; Figure 3).

2.6 Specificity of LAMP assay

Genomic DNA samples from 22 different phytopathogens (Table 4), which were obtained from the Culture Collection Centre, Department of Plant Pathology at Tamil Nadu

TABLE 1 Sequence of oligonucleotide primer sets used for amplification of target sequence in β-tubulin gene in this study.

Primer name	Primer type	Sequence 5'→3'	Primer length (nt)	GC (%)	GC clamp	3'ΔG
Tub-F3	Forward outer	CGTGGTTGGATTTGCAAACC	20	50	2	-4.77
Tub-B3	Backward outer	GGCCGAAAACGAAGTTGTCA	20	50	2	-4.58
Tub-FIP (F1c-F2)	Forward inner	CTTGTTGCCGGAGGCCTGAAG-GACGAGATGCCCATAACGC	40	60	3	-4.79
Tub-BIP(B1c-B2)	Backward inner	GTCCTCGTCGATCTTGAGCCTG-GAAAAGCTGACCGAAGGGA	41	56	3	-5.64
Tub-LF	Forward loop	GGGTTCATAGCAAGCAAGAGAC	22	50	3	-4.59
Tub-LB	Backward loop	TACCATGGACGCCGTCCGT	19	63	3	-6.18

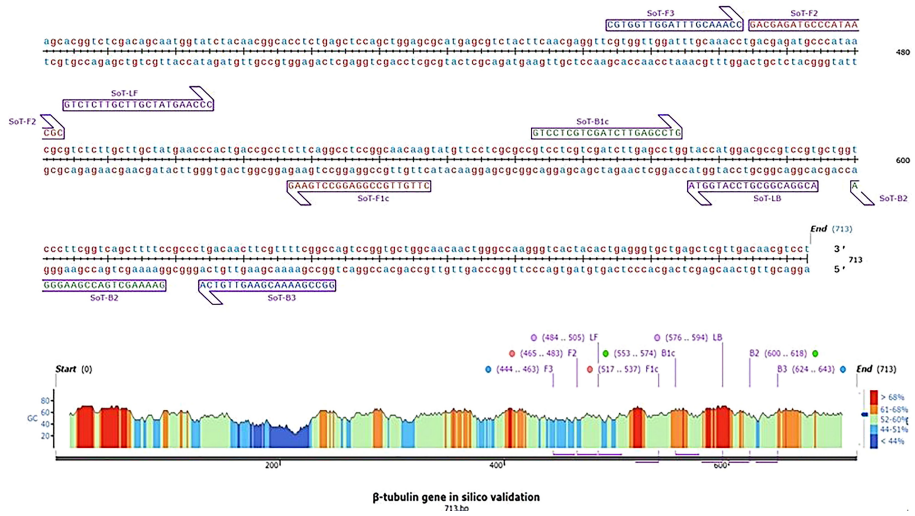

FIGURE 1
Diagrammatic illustration of *in silico* hybridization of LAMP primers positioned within the β-tubulin (713 bp) domain of the pathogen *Sarocladium oryzae* visualized using SnapGene viewer® 6.1.1. Outer primers: F3 and B3 (blue), loop primers: LF and LB (purple), inner primers: F2 and F1c (Red) and B1c and B2 (green).

Agricultural University in Coimbatore, India were tested to ascertain the specificity of the LAMP assay (Figure 4).

2.7 Validation of LAMP assay with different isolates of *S. oryzae*

The LAMP assay technique developed was validated with different isolates of *S. oryzae* collected from various locations of Tamil Nadu (Table 5; Supplementary Figure 3). As mentioned earlier, genomic template was extracted using a modified CTAB technique. The LAMP assay was carried out on the DNA of 50 fungal isolates, with nuclease-free water serving as a negative control. The LAMP reaction mixture was incubated at 65°C for 30 min, and then the reaction was ceased by heating it at 80°C for 2 min. The results were visualized by HNB dye, and the experiments were carried out thrice.

2.8 Validation of LAMP assay with naturally and artificially infected samples

The LAMP assay was validated with field samples using naturally infected rice seeds and artificial pathogen inoculation in seeds. For naturally infected seeds, seeds from the infected panicle were collected from rice fields in the districts of Coimbatore, Trichy and Villupuram. Three samples were collected from each district, and apparently healthy seeds collected from the panicle showing no

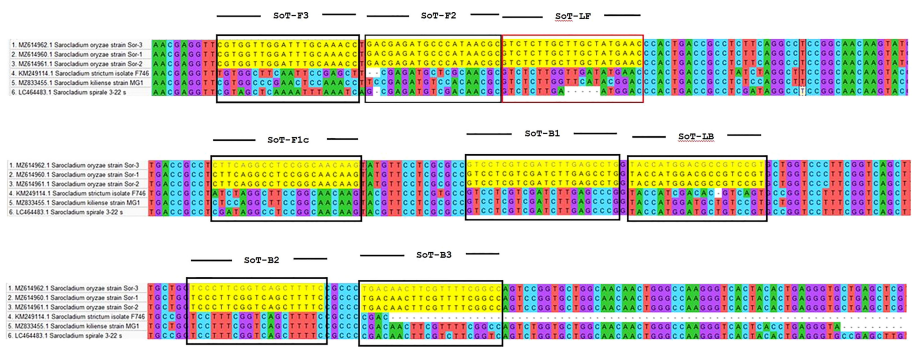

FIGURE 2
Comparison of the β-tubulin region of *S. oryzae* with other *Sarocladium* spp.

TABLE 2 Standardization of reagents used in LAMP assay.

S. No.	Reagent	Stock Conc.	Concentration of Tested Reagents/1 µL Reaction Volume				
1.	$MgSO_4$ (New England BioLabs)	100 mM	2mM	4 mM	6 mM	**8 mM**	10 mM
2.	dNTP Mix (Genei)	10 mM	0 mM	0.6 mM	0.8 mM	1.2 mM	**1.4 mM**
3.	Betaine (Sigma Aldrich)	5M	0 M	0.6 M	0.8 M	**1.2 M**	1.4 M
4.	*Bst* DNA polymerase Large Fragments (New England BioLabs)	8U	0 U	**2 U**	4 U	6 U	8 U
5.	HNB dye	400 µM	80 µM	100 µM	**120 µM**	148 µM	300 µM

The values (bold) indicated optimal reagents concentrations selected for LAMP assay.

TABLE 3 Sensitivity of LAMP assay for the detection of *S. oryzae* targeting β-tubulin gene.

S. No.	Concentration of genomic DNA template	LAMP assay
1.	100 ng	+
2.	10 ng	+
3.	1 ng	+
4.	100 pg	+
5.	10 pg	+
6.	1 pg	+
7.	100 fg	+
8.	10 fg	+
9.	1 fg	–

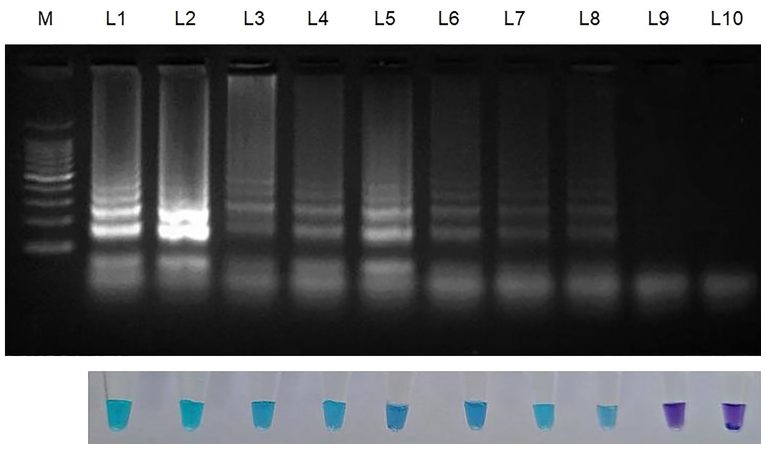

FIGURE 3
Sensitivity of LAMP assay using ten-fold serially diluted genomic DNA (from 100ng to 1 fg) from *Sarocladium oryzae* isolate OM841519 as template and nuclease free water as negative control. Upper panel in the figure shows agarose gel electrophoresis results whereas lower panel shows reaction tubes for colorimetric detection. M- 100bp Ladder; Lane 1: 100 ng; Lane 2: 10 ng; Lane 3: 1 ng; Lane 4: 100 pg; Lane 5: 10 pg; Lane 6: 1 pg; Lane 7: 100 fg; Lane 8: 10fg; Lane 9: 1 fg; Lane 10: Nuclease free water (Control).

infection were kept as a control. Contrarily, for artificial inoculation, seeds were surface sterilized with a 3% sodium hypochlorite solution for 5 minutes, followed by three washes with sterile water. *S. oryzae* spore suspension was added to rice seeds 24 hours before DNA extraction and dried overnight to remove the excess spore suspension on seed surface. Using the CTAB method, genomic DNA was extracted from rice seeds. According to Liang et al., 2016, 2 mg of rice seeds were ground in a mortar and pestle with 150 µL of extraction buffer (200 mmol/L Tris-Cl (pH 8.0), 50 mol/L ethylenediaminetetraacetic acid (EDTA; pH 8.0), 2.8 mol/L NaCl, 4% CTAB, and 2% sodium dodecyl sulphate). The obtained genomic DNA sample was digested with

TABLE 4 Specificity of LAMP assay for the detection of *S. oryzae* targeting β-tubulin gene.

S. No.	Organism	NCBI genbank Accession number	Host	Result
1.	*Sarocladium oryzae*	OM841519	Paddy	+
2.	*Sarocladium attenuatum*	OP099851	Paddy	-
3.	*Sarocladium strictum*	OP377063	Paddy	-
4.	*Bipolaris oryzae*	MZ995432	Paddy	-
5	*Magnaporthe oryzae*	OP303344	Paddy	-
6.	*Rhizoctonia solani*	OP412773	Paddy	-
7.	*Ustilaginoidea virens*	MZ157263	Paddy	-
8.	*Exserohilum rostratum*	OM891473	Paddy	-
9.	*Simplicillium obclavatum*	OP501088	Paddy	-
10.	*Bipolaris sorokianiana*	OP303316	Wheat	-
11.	*Pyricularia grisea*	ON116174	Cumbu	-
12.	*Exserohilum turcicum*	ON524816	Maize	-
13.	*Macrophomina phaseolina*	ON945550	Groundnut	-
14.	*Sclerotium rolfsii*	ON945552	Groundnut	-
15.	*Sclerotinia sclerotiorum*	ON025544	Cabbage	-
16.	*Colletotrichum gloeosporioides*	ON799265	Mango	-
17.	*Colletotrichum scovillea*	ON182070	Chilli	-
18.	*Colletotrichum truncatum*	ON182072	Chilli	-
19.	*Fusarium oxysporum* f. sp. *cubense*	OM103052	Banana	-
20.	*Phytophthora infestans*	ON705720	Potato	-
21.	*Puccinia arachidis*	OL437026	Groundnut	-
22.	*Uncinula nector*	MK637521	Grapes	-
23.	*Pantoea dispersa*	OP378111	Paddy	-
24.	Nuclease free water	–	–	–

10 µg/mL of RNase to remove any RNA contamination and stored at -20°C. The 2 µL final solution was directly used as a DNA template for the LAMP assay.

2.9 Validation of LAMP assay using weed species and different rice seed varieties

Following the procedure mentioned in section 2.3, template DNA was extracted from the weeds randomly collected from bunds of sheath rot infected fields. The LAMP assay was carried out using templates following the previously stated optimal conditions. When testing rice seeds of different varieties, 2 µl of total genomic DNA was utilized for the assay while maintaining all other parameters unchanged.

3 Results

3.1 PCR assay

In a PCR assay, fifty isolates of *S. oryzae* collected from diverse locations were amplified using the ITS 1 and 4 primers. The sequenced products were evaluated against other *S. oryzae* sequences found in the NCBI database. A similarity search was done in NCBI using the BLAST tool, the nucleotide sequence of the study isolate's ITS region revealed 100% identity with other *S. oryzae* isolates and significantly very less similarity with other *Sarocladium* isolates.

3.2 Primer design

Using the Primer explorer V5 software programme, at least five different primer sets were predicted for unique sequences and used to build LAMP assay specific for *S. oryzae*. The primers were designed to allow *S. oryzae*-specific amplification showed 100% identity with 100% query coverage for *S. oryzae*. The G values of the 3′ end were determined during the design of LAMP primers and were less than -4 Kcal/mole. One pair of primers with a stable DNA construct and no primer-dimer formation were seen from *in silico* evaluation of the five designed primer sets generated by the software. Eventually, a set of six primers with high species specificity and sensitivity that targeted the *S. oryzae* β-tubulin sequences were elected for future investigation. The potential for the development of very weak to moderate secondary structures were found for the outer primers (forward-F3 and reverse-B3), moderate to weak secondary structures were

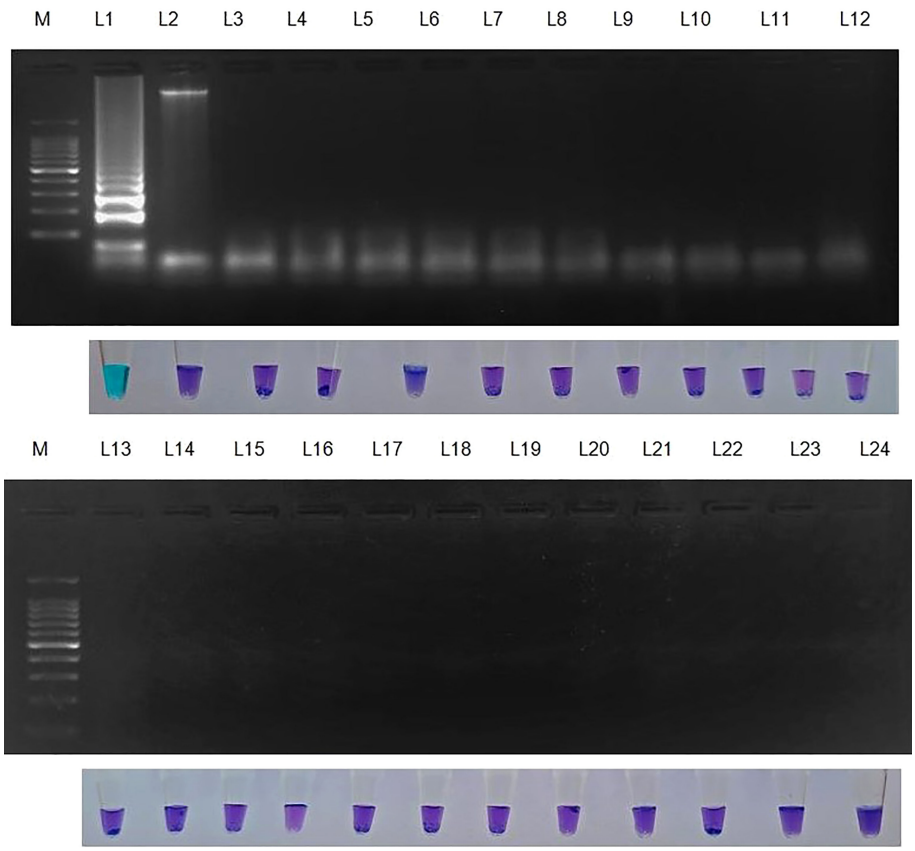

FIGURE 4
Specificity of LAMP assay using *Sarocladium oryzae* isolate OM841519 as template and nuclease free water as negative control. Upper panel in the figure shows agarose gel electrophoresis results whereas lower panel shows reaction tubes for colorimetric detection. M- 100bp Ladder; Lane 1: *Sarocladium oryzae*; Lane 2: *Sarocladium attenuatum*; Lane3: *Sarocladium strictum;* Lane 4: *Bipolaris oryzae*; Lane 5: *Magnaporthe oryzae*; Lane 6: *Rhizoctonia solani*; Lane 7: *Ustilaginoidea virens*; Lane 8: *Exserohilum rostratum*; Lane 9: *Simplicillium obclavatum*; Lane 10: *Pyricularia grisea*; Lane 11: *Helminthosporium turcicum*; Lane 12: *Macrophomina phaseolina*; Lane 13: *Sclerotium rolfsii*; Lane 14: *Sclerotinia sclerotiorum*; Lane 15: *Colletotrichum gloeosporioides*; Lane 16: *C. scovillea*; Lane 17: *C. truncatum*; Lane 18: *Fusarium oxysporum* f. sp. *cubense*; Lane 19: *Phytophthora infestans*; Lane 20: *Puccinia arachidis*; Lane 21: *Uncinula nector*; Lane 22: *Pantoea dispersa*; Lane 23: *Ralstonia solanacearum*; Lane 24: Nuclease free water (Negative control).

identified for inner primers (FIP and BIP) whereas no to strong secondary structures were identified for loop primers (LF and LB) (Supplementary Table 2). The 3' end of the primers was clamped with 2 to 3 guanine or/and cytosine bases (Table 1).

In silico hybridization of the primers revealed that the following six primers annealed to unique locations in 713 bp of the specific β -tubulin target sequence: F3 (444-463 bp), F2 (465-483 bp), LF (484-505 bp), F1c (517-537 bp), B1c (553-574 bp), LB (576-594 bp), B2 (600-618 bp) and B3 (624-643 bp). In Figure 2, binding positions of the primers were highlighted.

3.3 Optimization of LAMP assay reaction components and conditions

The critical components that could affect the effectiveness of the detection include the concentrations of $MgSO_4$, betaine, *Bst* polymerase, dNTPs, and HNB dye. Magnesium ions in particular have a significant impact on the activity of DNA polymerase and primer annealing (Saiki et al., 1988; Yeh et al., 2005). Reuter et al. (2020) reported that the colour shift in the LAMP assay is due to the chelation of Mg^{2+} ions by dNTPs. During the LAMP assay, the development of sky-blue colour signifies the positive reaction in the suspect samples (Supplementary Figure 1), whereas the violet colour signifies the negative reaction. The LAMP response was strongly impacted by the $MgSO_4$ concentration. Colour change was established as the major benchmark for the optimization of $MgSO_4$ concentration. The $MgSO_4$ at 8 mM Conc. exhibited a deep sky blue colour in the LAMP reaction. The intensity of the sky blue colour decreased with either an increase or decrease from the optimal $MgSO_4$ concentration. The intensity of sky blue decreased at concentrations of 4 mM, 6 mM, and 10 mM. Furthermore, the LAMP assay failed to produce colour at 0 mM

TABLE 5 Validation of LAMP assay for the detection of different isolates of *S. oryzae*.

S. No.	Isolate code	Location	Latitude	Longitude	Result
1.	So 1	PBS, Coimbatore	11.0137°N	76.9354°E	Positive
2.	So 2	Thirukovilur	11.9687°N	79.2086°E	Positive
3.	So 3	Vasanthakrishnapuram	12.0455°N	79.2232°E	Positive
4.	So 4	Wetland, Coimbatore	11.0031°N	76.9249°E	Positive
5	So 5	Chidambaram	11.3909°N	79.6662°E	Positive
6.	So 6	Emappur	11.8698°N	79.3702°E	Positive
7.	So 7	Thiruvannamalai	12.2286°N	79.0665°E	Positive
8.	So 8	Kondathur	11.1792°N	79.7079°E	Positive
9.	So 9	Vellimalaipattinam, CBE	10.9779°N	76.7610°E	Positive
10.	So 10	Thiruvennainallur	11.8570°N	79.3682°E	Positive
11.	So 11	Mayiladuthurai	10.9010°N	79.1472°E	Positive
12.	So 12	Kallakurichi	11.7652°N	79.0706°E	Positive
13.	So 13	Sathyamangalam	10.9386°N	79.2375°E	Positive
14.	So 14	Someshwarapuram	10.9020°N	79.0989°E	Positive
15.	So 15	Thirupazhanam	10.8905°N	79.1343°E	Positive
16.	So 16	Sirkazhi	11.1616°N	79.7046°E	Positive
17.	So 17	Papanasam	10.9251°N	79.2708°E	Positive
18.	So 18	Puduchatiram	10.8528°N	78.9463°E	Positive
19.	So 19	Saliyantoppu	11.3672°N	79.6978°E	Positive
20.	So 20	Tanjore	10.8871°N	79.1230°E	Positive
21.	So 21	Vadakurangaduthurai	10.9230°N	79.1984°E	Positive
22.	So 22	Pudhur, S	11.2700°N	79.7213°E	Positive
23.	So 23	Ganapathiagaram	10.9061°N	79.1602°E	Positive
24.	So 24	Rayampettai,Tanjore	10.8871°N	79.1230°E	Positive
25.	So 25	Aduthurai	10.9932°N	79.4909°E	Positive
26.	So 26	Athukudi	11.1729°N	79.7078°E	Positive
27.	So 27	Sivapuri, Chidambaram	11.3838°N	79.7092°E	Positive
28.	So 28	Kallanai, Tanjore	10.8554°N	78.9412°E	Positive
29.	So 29	Govindhanallucheri	10.9374°N	79.2237°E	Positive
30.	So 30	Thiruvidaimaruthur	10.9979°N	79.4572°E	Positive
31.	So 31	Chellapatty, Madurai	9.94700°N	77.8899°E	Positive
32.	So 32	Bhavanisagar	11.4739°N	77.1465°E	Positive
33.	So 33	Dindugal	10.4091°N	78.0410°E	Positive
34.	So 34	Kodikulam, Madurai	9.9569°N	78.1607°E	Positive
35.	So 35	Samayapuram	10.9076°N	78.7065°E	Positive
36.	So 36	Perambalur	11.2300°N	78.8799°E	Positive
37.	So 37	Palaiyur, Thiruvarur	10.6648°N	79.4507°E	Positive
38.	So 38	Purathakudi	10.9360°N	78.7763°E	Positive
39.	So 39	Aduthurai	11.0139°N	79.4810°E	Positive
40.	So 40	Perugamani, Trichy	10.8708°N	78.5943°E	Positive
41.	So 41	Kumaramangalam	10.7403°N	78.6804°E	Positive
42.	So 42	Perugamani	10.8854°N	78.5414°E	Positive
43.	So 43	Orayur	10.8378°N	78.6483°E	Positive
44.	So 44	Vayalur	10.8240°N	78.6230°E	Positive
45.	So 45	Yethapur, Salem	11.5862°N	78.6992°E	Positive
46.	So 46	K. Sathanoor	10.8360°N	78.6591°E	Positive
47.	So 47	Maruthandakurichi	10.8372°N	78.6480°E	Positive
48.	So 48	Mochakottapalayam	10.9643°N	78.0242°E	Positive

(Continued)

TABLE 5 Continued

S. No.	Isolate code	Location	Latitude	Longitude	Result
49.	So 49	Melur, Madurai	10.0313°N	78.3382°E	Positive
50.	So 50	Kulithalai	10.8389°N	78.6523°E	Positive
51.	Nuclease free water	-	–	–	Negative

and 2 mM concentration, indicating that $MgSO_4$ is highly imperative for the LAMP assay. The results were validated using 2% agarose gel electrophoresis. In the presence of 8 mM $MgSO_4$, a distinctive ladder-like pattern was visible; however, no such ladder-like pattern was found in the samples containing 0 mM, 2 mM, and 10 mM $MgSO_4$ (Supplementary Figure 1A). Similarly, betaine at 0.8 mM concentration generated a characteristic ladder-like pattern, but other concentrations did not, implying negative results (Supplementary Figure 1B). The LAMP assay results at varying concentrations of *Bst* DNA polymerase (0U, 2U, 4U, 6U, and 8U) implied amplification at all doses except at 0 U. The best amplification, however, was found at a concentration of 2U *Bst* polymerase (Supplementary Figure 1C). The amplification improved noticeably when the dNTPs dose increased from 0.6 mM to 1.4 mM, as evidenced by brighter bands on 2% agarose gels (Supplementary Figure 1D). Hydroxy naphthol blue (HNB), an indicator dye for LAMP-based detection was utilized for the LAMP assay to enable visualization in the current work. According to the result of a range of HNB dye concentration test, concentration less than 120 µM have an impact on the visual detection of LAMP results but have no impact on the ladder-like pattern on 2% agarose gel. However, at greater concentrations affected the visualization as well as the ladder-like pattern (Supplementary Figure 1E).

A short range of temperatures (56°C to 70°C) (Supplementary Figure 2A) and minimum time (10-150 min) (Supplementary Figure 2B) were used to accurately assess the colour intensity using template DNA from the *S. oryzae* to find the optimum temperature and reaction time for the assay. The assay performed well at various temperatures. The outcomes were also evaluated on a 2% agarose gel. Positive results were seen after 30 min of incubation; however, no amplification was seen during the incubation period of 10 or 20 min. In case of different temperature range tested, positive results were obtained in all the cases but with varying range of colorimetric reaction and degree of amplification. However, conspicuous amplification and colorimetric reaction was seen at a temperature of 65°C. Therefore, *S. oryzae* was best detected at 65°C for 30 minutes under optimal circumstances.

3.4 Sensitivity of the LAMP assay

After establishing that the primer targeting the β-Tubulin gene became unique for *S. oryzae*, the lowest detection limit was interpreted with the use of 10-fold serial dilutions of *S. oryzae* DNA (100 ng to 1 fg). The least possible detection limit for *S. oryzae* as per reaction within 30 min incubation was 10 fg and was confirmed by colouration shift from violet to sky blue and reconfirmed by way of characteristic ladder-like pattern on 2% gel electrophoresis (Figure 3; Table 3). This experiment was repeated thrice.

3.5 Specificity of the LAMP assay

S. oryzae isolate and non-target DNA samples from 22 different phytopathogens listed in Table 5 were used to test the primers' specificity. The LAMP assay successfully identified *S. oryzae*, as shown by a colour change from violet to sky blue in the reaction solution, and did not cross-react with non-target phytopathogens, which retained their original violet colour. The specificity of the *S. oryzae* LAMP assay was validated by electrophoresis on 2% agarose gels stained with ethidium bromide. A characteristic ladder-like pattern was observed in reactions with genomic DNA from *S. oryzae* but not with DNA from other non-target phytopathogens. The findings demonstrated the great specificity of the newly designed LAMP primer targeting the β-Tubulin gene in identifying *S. oryzae* (Figure 4; Table 4).

3.6 Validation of LAMP assay

Primarily based on the colour development, the LAMP assay was initially optimized for *S. oryzae* pathogen to confirm the facilitative evaluation of a reaction with different isolates collected from different locations of Tamil Nadu. And it was reconfirmed by subjecting the samples to 2% agarose gel electrophoresis. A deep sky blue colour was visualized from the tubes retaining template DNA and HNB indicator dye. Meanwhile the violet colour indicated the absence of *S. oryzae* in the tubes with nuclease-free water (Supplementary Figure 3).

The initial validation of the LAMP assay technique was performed on the *S. oryzae* culture sample. 30 samples were collected from several farmers' fields and seed godowns for implementation at the field level. The LAMP assay was validated for field samples in each location using uninfected sample as a healthy control. The seeds from the infected panicle and the seeds with discolouration showed a positive

reaction (deep sky blue colour), whereas the samples without infection showed a negative reaction (violet colour). In case of artificially inoculated seed samples, those seeds which are inoculated with pathogen showed colour development whereas, those which are surface sterilized didn't developed colour resulting in negative reaction. Similar negative results were seen in nuclease-free water, which served as the negative control (Figure 5).

When weed samples were evaluated utilizing Tub LAMP primer sets, all weed species and rice sheath rot infected samples generated positive outcomes. However, the degree of amplification varied among the weed species. No amplification was observed in NTC (Figure 6 and Table 6).

Rice seeds from 11 of 13 rice varieties have showed positive reaction for *S. oryzae* (Table 7). Two varieties namely, TRY 43 and RNR 15048 did not exhibit amplification (Figure 7) along with NTC.

4 Discussion

Seeds are the prime carriers of numerous phytopathogens that cause most plant diseases, resulting in significant agricultural output loss (Neergaard, 1977). Notably, it is well admitted that both major and minor fungal pathogens of rice were spread by seeds. *S. oryzae* is one of the rice seed-borne infections that cause the catastrophic disease called sheath rot, which is widespread in the major rice-producing countries (Richardson, 1981; Reddy and Sathyanarayana, 2001; Dossou and Silue, 2018). To reduce the possibility of disease

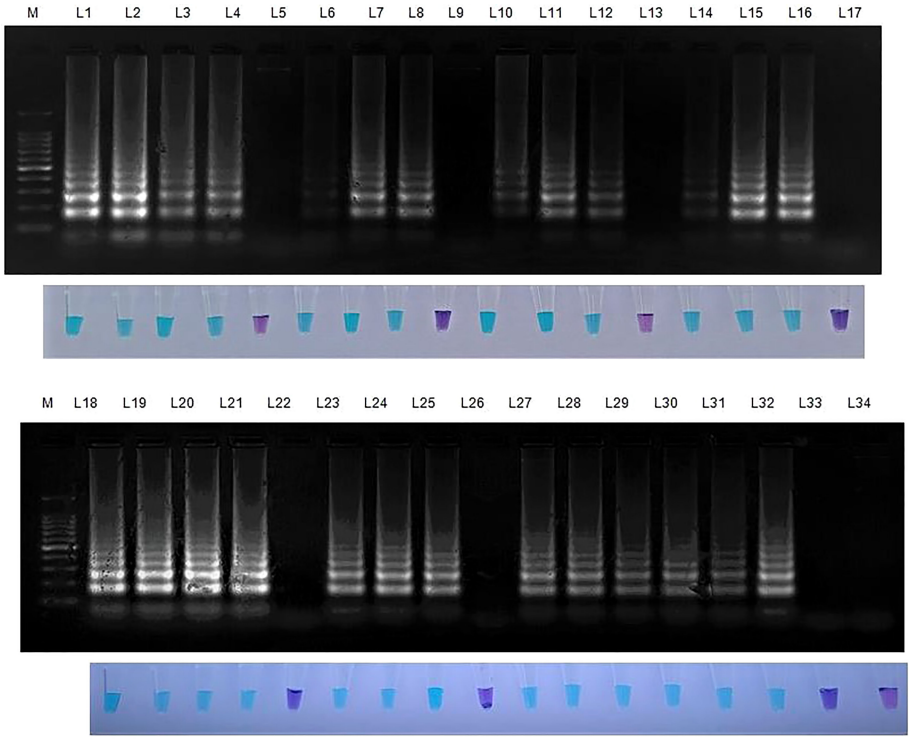

FIGURE 5
Validation of LAMP assay with *S. oryzae* infected field samples. Bright sky blue colour represents positive reaction while the violet colour indicates the negative reaction. Upper panel in the figure shows agarose gel electrophoresis results whereas lower panel shows reaction tubes for colorimetric detection. M- 100bp Ladder; Lane 1: *Sarocladium oryzae* isolate OM841519 (Positive control); Lane 2: Coimbatore infected sheath sample 1; Lane 3: Coimbatore infected sheath sample 2; Lane 4: Coimbatore infected sheath sample 3; Lane 5: Coimbatore healthy sheath sample; Lane 6: Coimbatore infected seed sample 1; Lane 7: Coimbatore infected seed sample 2; Lane 8: Coimbatore infected seed sample 3; Lane 9: Coimbatore healthy seed sample; Lane 10: Villupuram infected sheath sample 1; Lane11: Villupuram infected sheath sample 2; Lane 12: Villupuram infected sheath sample 3; Lane 13: Villupuram healthy sheath sample; Lane 14: Villupuram infected seed sample 1; Lane 15: Villupuram infected seed sample 2; Lane 16: Villupuram infected seed sample 3; Lane 17: Villupuram healthy seed sample; Lane 18: *Sarocladium oryzae* isolate OM841519 (Positive control); Lane 19: Trichy infected sheath sample 1; Lane 20: Trichy infected sheath sample 2; Lane 21: Trichy infected sheath sample 3; Lane 22: Trichy healthy sheath sample; Lane 23: Trichy infected seed sample 1; Lane 24: Trichy infected seed sample 2; Lane 25: Trichy infected seed sample 3; Lane 26: Trichy healthy seed sample; Lane 27: *Sarocladium oryzae* isolate OM841519 (Positive control); Lane 28: Artificially inoculated seed sample 1; Lane 29: Artificially inoculated seed sample 2; Lane 30: Artificially inoculated seed sample 3; Lane 31: Artificially inoculated seed sample 4; Lane 32: Artificially inoculated seed sample 5; Lane 33: Surface sterilized uninoculated seed sample; Lane 34: Nuclease free water (Negative Control).

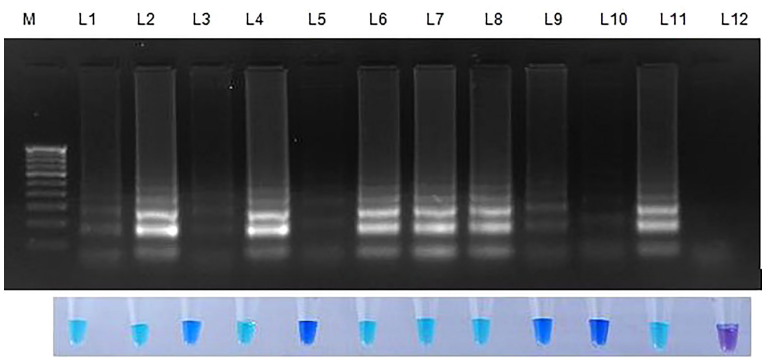

FIGURE 6
Validation of LAMP assay with *S. oryzae* infected paddy and weed samples. Bright sky blue colour represents positive reaction while the violet colour indicates the negative reaction. Total DNA isolated from fungi was used as the positive control. Upper panel in the figure shows agarose gel electrophoresis results whereas lower panel shows reaction tubes for colorimetric detection. M- 100bp Ladder; Lane 1: *Oryza sativa*; Lane 2: *Echinchloa crusgalli*: Lane 3: *Cyperus difformis*; Lane 4: *Eleusine indica*; Lane 5: *Dactyloctenium aegyptium*; Lane 6: *Cyperus iris*; Lane 7: *Eragrostis amabilis*; Lane 8: *Leersia hexandra*; Lane 9: *Phalaris minor*; Lane 10: *Brachiaria mutica*; Lane 11: *Sarocladium oryzae* isolate OM841519 (Positive control); Lane 12: Nuclease free water.

TABLE 6 Validation of LAMP with weeds collected from paddy fields.

S. No.	Weeds	Results
1.	*Echinchloa crusgalli*	+
2.	*Cyperus difformis*	+
3.	*Eleusine indica*	+
4.	*Dactyloctenium aegyptium*	+
5.	*Cyperus iris*	+
6.	*Eragrostis amabilis*	+
7.	*Leersia hexandra*	+
8.	*Phalaris minor*	+
9.	*Brachiaria mutica*	+
10.	Nuclease free water	-

TABLE 7 Validation of LAMP assay with different varieties of rice.

S. No.	Rice seed variety	Results
1.	Co 39	+
2.	Co 51	+
3.	Co 52	+
4.	Co 53	+
5.	Co 54	+
6.	Co 55	+
7.	ADT 37	+
8.	ADT 43	+
9.	RNR 15048	-
10.	TN 1	+
11.	TPS 5	+
12.	TRY 43	-
13.	ASD 16	+
14.	Nuclease free water	-

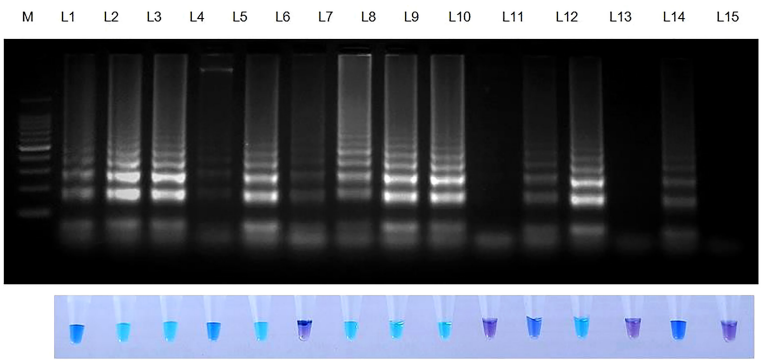

FIGURE 7
Validation of LAMP assay with naturally infected seeds of different varieties. Bright sky blue colour represents positive reaction while the violet colour indicates the negative reaction. Upper panel in the figure shows agarose gel electrophoresis results whereas lower panel shows reaction tubes for colorimetric detection. M- 100bp Ladder; Lane 1: *Sarocladium oryzae* isolate OM841519 (Positive control); Lane 2: Co 39; Lane 3: Co 51; Lane 4: Co 52; Lane 5: Co 53; Lane 6: Co 54; Lane 7: Co 55; Lane 8: ADT 37; Lane 9: ADT 43; Lane 10: RNR 15048; Lane11: TN 1; Lane 12: TPS 5; Lane 13: TRY 43; Lane 14: ASD 16; Lane 15: Nuclease free water (Negative Control).

outbreaks, it is crucial to identify the seed-borne inoculum so that early control measures like seed treatment, seed certification and quarantine legislation may be implemented.

Presently, the International Seed Testing Association, 2017 (ISTA) proposes the technique of blotting a working sample of 400 seeds divided into 25 seed subsamples onto a 90 mm filter paper saturated with distilled water and documenting the proportion of diseased seed after incubating for 7 days at 27 ± 2°C in alternate 12 hr. cycles of light and darkness followed by validation with stereoscopic observation of each seed. Despite the simplicity of the blotting procedure and its widespread usage in diagnostic labs, a proper inspection calls for skilled diagnosticians who can spot the conidia of the ensuing fungal growth *via* a stereomicroscope. One factor to consider during this process is the prevalence of other conidia with indistinguishable morphological traits as in saprophytic fungus *Verticillium* spp. that might be misdiagnosed as *S. oryzae*. Any enterprise seeking to certify the absence of pathogens in rice seed faces economic losses as a result of misdiagnosis. In addition, blotting requires a lengthy incubation period of seven days, which is another drawback of this technique. The tests also necessitate the use of vast, high-priced and controlled-environment chambers.

To tackle this challenge, quick and reliable identification of *S. oryzae* is crucial for elucidating the pathogenic determinants and core mechanisms. Consequently, corresponding disease management strategies can be devised. Rapid and precise detection of an appropriately low amount of pathogen is crucial to diagnose *S. oryzae* at the seed for disease surveillance and management activities.

In well-equipped laboratories, PCR-based procedures are frequently employed to perform routine identification tests. However, these technologies are sophisticated and time-consuming, as it decreases the likelihood of on-site sampling and detection, prolonging the period between sampling and results (Boonham et al., 2008). Also, PCR-based approach has a few limitations, one of which is its vulnerability to inhibitors, which might affect the specificity and potentially yield false negative results. These inhibitors include a diverse range of compounds like phenols, polysaccharides, melanin, humic or tannic acids, and rice seed proteins that have received little research (Tian et al., 2004; Schrader et al., 2012). The LAMP test has excellent characteristics since it provides for quick, sensitive, specific, and simplistic field detection and is perhaps less susceptible to inhibitors (Kaneko et al., 2007).

Another prime flaw of PCR is that it only detects two amplicons in the target gene; therefore there is a higher likelihood of false-positive reactions occurring. Whereas, LAMP uses a set of six primers to amplify six different target regions, it is highly specific and has a reduced chance of false-positive results than traditional PCR (Marimuthu et al., 2020).

LAMP technique is strongly recommended as a fast diagnostic method since it may amplify the DNA in less than 60 minutes, which is significantly faster than traditional PCR (Notomi et al., 2000). Since LAMP amplifies DNA in an isothermal condition, it may be completed in a single reaction under visual examination. Magnesium pyrophosphate being deposited during the reaction period results in an increase in the turbidity of the amplified products (a positive reaction), which in turn cuts down on the amount of time needed for reconfirmation under gel electrophoresis (Fukuta et al., 2004).

The majority of formerly described LAMP assays for fungi target areas with significant interspecies similarity, like the ITS (Zeng et al., 2017), which tends to have less interspecific variability and may impede the synthesis of species-specific primers. LAMP primers were developed using the sequence of the conserved β-tubulin gene to achieve excellent *S. oryzae*

specificity. The primers developed for this study were more precise and sensitive in distinguishing *Sarocladium oryzae* from other fungal phytopathogens. The developed LAMP primers were capable of detecting *S. oryzae* DNA at inoculum levels as low as 10 fg. This reveals that this assay is 100 times more sensitive than traditional PCR. Because of its extreme sensitivity, LAMP was an exemplary technique for diagnosing *S. oryzae* even at minimal concentrations.

Prasannakumar et al., 2021 reported *S. oryzae* identification using RNA polymerase II largest subunit region-based LAMP analysis. In this technique, the LAMP methodology was used for onsite detection of *S. oryzae* seed-borne inoculum through the construction of a LAMP based foldable device, and it was shown that the LAMP assay was more sensitive and has a detection limit of up to 50 fg of genomic DNA when compared to traditional PCR (100 pg). They investigated the specificity of the LAMP assay with six other phytopathogens and concluded that RNA polymerase II largest subunit-based LAMP primer solely unique to *S. oryzae*. Moreover, our findings also exhibit a significant correlation with Ghosh et al. (2015) and Lakshmi et al. (2022), who devised the LAMP assay for the detection of *Fusarium oxysporum* f. sp. *ciceris*, the causative agent of chickpea wilt and *Bipolaris oryzae*, the causal organism of brown spot of rice.

The LAMP test was performed at 65°C for 30 minutes and did not require the use of a programmed thermocycler. Before amplification, the LAMP was optimized by adding a visualization indicator, hydroxy naphthol blue (HNB) dye. This was done to avoid the use of intercalating dyes like SYBR green (Parida et al., 2005), which can exacerbate the frequencies of aerosol contamination when the tubes were opened to add. Most of the non-specific detection and misleading false positive/negative result that occurs during LAMP reaction was mainly due to cross-contamination that may arise because of the possibility of cis and trans priming of primer (Zaczek-Moczydłowska et al., 2020). This has been circumvented by the effective use of metal ion indicators such as calcein and HNB dye, to visualize the final result of the LAMP reaction (Tomita et al., 2008; Wang et al., 2012). The results of the assay were indicated by the colour shift when this metal ion indicator was added to the pre-reaction solution. In the presence of magnesium ions, the HNB metal indicator changes colour from violet to sky blue (Goto et al., 2009). The LAMP reaction results in the depletion of magnesium ions in the solution which causes a colour shift from violet to blue, signifying a positive reaction. This colour change was due to the interaction of magnesium ions with pyrophosphate produced by dNTPs during the LAMP reaction resulting in a precipitate (Marimuthu et al., 2020; Reuter et al., 2020). The detection limit of the HNB-LAMP test was reported to be analogous to that of the assay employing SYBR green dye by Goto et al. (2009) while comparing the LAMP assay using HNB, SYBR green and calcein dyes. Contrarily, Balne et al. (2013) reported the detection threshold of the LAMP test containing calcein was 10 times lower than that of other assays.

The sensitivity of the LAMP test was confirmed for DNA samples at different concentration. Also, LAMP precisely recognized only *S. oryzae* DNA, and no cross response was observed in other phytopathogens used in this study. Owing to this, only the LAMP test will allow for the early and accurate detection of seed-borne *S. oryzae*.

To validate the LAMP assay, naturally infected and uninfected field samples collected from three distinct villages were screened for *S. oryzae* detection. All the collected samples were tested using LAMP assay, and all infected samples showed positive result when compared to the healthy control, which indicates the detection efficiency of *S. oryzae* in a short period. In addition, weeds around the sheath rot-infected rice field and seeds of several rice kinds were tested for *S. oryzae* detection for final validation.

As the LAMP technique is remarkably simplistic, efficient and incredibly specific, it is ideal for the development of diagnostic tools for accurate and timely detection of *S. oryzae* in seeds as well as for the forecasting of disease outbreaks. This assay will aid in the successful management of rice sheath rot by detecting the *S. oryzae* infected seeds in quarantine station and seed testing laboratories and implementing prophylactic steps in the field.

5 Conclusion

It is concluded that the LAMP technique has a very high specificity and sensitivity for the detection of *S. oryzae*. The LAMP approach eliminates the requirement for sophisticated equipment such as PCR machines, gel electrophoresis, or gel imaging systems for detection and visualization. Finally, the LAMP primers are specific for the detection of *S. oryzae*. This assay has the potential to be a future on-site diagnostic tool since it is fast, sensitive, needs less equipment, and requires less specialized labour. Our findings will contribute to the body of knowledge on reliable approaches for the early detection of *S. oryzae* from seeds, facilitating the adoption of appropriate prophylactic measures, maintaining high-quality seed standards, and preventing catastrophic field epidemics.

Data availability statement

The datasets presented in this study can be found in online repositories. The names of the repository/repositories and accession number(s) can be found in the article/Supplementary Material.

Author contributions

CG devised and planned the experiments. RL carried out the experiments, collected the data, and wrote the initial draft of the manuscript. The manuscript's initial draft was revised by CG. RL updated and refined the draft. All authors contributed to the article and approved the submitted version.

Acknowledgments

We gratefully acknowledge the DST-FIST Lab, Tamil Nadu Agricultural University, Coimbatore, Tamil Nadu, India. Thanks to Dr. M. Jayakanthan of the Department of Plant Molecular Biology and Bioinformatics, Tamil Nadu Agricultural University, Coimbatore, India for his guidance on targeting gene and primer designing.

Conflict of interest

The authors declare that the research was conducted in the absence of any commercial or financial relationships that could be construed as a potential conflict of interest.

Publisher's note

All claims expressed in this article are solely those of the authors and do not necessarily represent those of their affiliated organizations, or those of the publisher, the editors and the reviewers. Any product that may be evaluated in this article, or claim that may be made by its manufacturer, is not guaranteed or endorsed by the publisher.

Supplementary material

The Supplementary Material for this article can be found online at: https://www.frontiersin.org/articles/10.3389/fpls.2022.1077328/full#supplementary-material

References

Abbade, E. B. (2021). Estimating the potential for nutrition and energy production derived from maize (*Zea mays* l.) and rice (*Oryza sativa* l.) losses in Brazil. *Waste Manage.* 134, 170–176. doi: 10.1016/j.wasman.2021.08.009

Altschul, S. F., Gish, W., Miller, W., Myers, E. W., and Lipman, D. J. (1990). Basic local alignment search tool. *J. Mol. Biol.* 215, 403–410. doi: 10.1016/S0022-2836(05)80360-2

Ayyadurai, N., Kirubakaran, S. I., Srisha, S., and Sakthivel, N. (2005). Biological and molecular variability of *Sarocladium oryzae*, the sheath rot pathogen of rice (*Oryza sativa* l.). *Curr. Microbiol.* 50, 319–323. doi: 10.1007/s00284-005-4509-6

Balne, P. K., Barik, M. R., Sharma, S., and Basu, S. (2013). Development of a loop-mediated isothermal amplification assay targeting the mpb64 gene for diagnosis of intraocular tuberculosis. *J. Clin. Microbiol.* 51, 3839–3840. doi: 10.1128/JCM.01386-13

Bigirimana, V. P., Hua, G. K., Nyamangyoku, O. I., and Höfte, M. (2015). Rice sheath rot: An emerging ubiquitous destructive disease complex. *Front. Plant Sci.* 6. doi: 10.3389/fpls.2015.01066

Boonham, N., Glover, R., Tomlinson, J., and Mumford, R. (2008). "Exploiting generic platform technologies for the detection and identification of plant pathogens," in *Sustainable disease management in a European context* (Dordrecht: Springer), 355–363.

Dossou, B., and Silue, D. (2018). Rice pathogens intercepted on seeds originating from 11 African countries and from the USA. *Seed Sci. Technol.* 46, 31–40. doi: 10.15258/sst.2018.46.1.03

Doyle, J. (1991). "DNA Protocols for plants," in *Molecular techniques in taxonomy* (Berlin, Heidelberg: Springer), 283–293.

Fukuta, S., Mizukami, Y., Ishida, A., Ueda, J., Hasegawa, M., Hayashi, I., et al. (2004). Real-time loop-mediated isothermal amplification for the CaMV-35S promoter as a screening method for genetically modified organisms. *Eur. Food Res. Technol.* 218, 496–500. doi: 10.1007/s00217-003-0862-5

Ghosh, R., Nagavardhini, A., Sengupta, A., and Sharma, M. (2015). Development of loop-mediated isothermal amplification (LAMP) assay for rapid detection of *Fusarium oxysporum* f. sp. *ciceris*-wilt pathogen of chickpea. *BMC Res. Notes* 8, 1–10. doi: 10.1186/s13104-015-0997-z

Gopalakrishnan, C., Kamalakannan, A., and Valluvaparidasan, V. (2010). Effect of seed-borne *Sarocladium oryzae*, the incitant of rice sheath rot on rice seed quality. *J. Plant Prot. Res.* 50, 98–102. doi: 10.2478/v10045-010-0017-1

Goto, M., Honda, E., Ogura, A., Nomoto, A., and Hanaki, K. I. (2009). Colorimetric detection of loop-mediated isothermal amplification reaction by using hydroxy naphthol blue. *Biotechniques* 46, 167–172. doi: 10.2144/000113072

ISTA (International Seed Testing Association) (2017). "International rules for seed testing. proceedings of the international seed testing association," in *Bassersdorf* (Switzerland: Seed Science and Technology).

Kaneko, H., Kawana, T., Fukushima, E., and Suzutani, T. (2007). Tolerance of loop-mediated isothermal amplification to a culture medium and biological substances. *J. Biochem. Biophys. Methods* 70, 499–501. doi: 10.1016/j.jbbm.2006.08.008

Lakshmi, K. R., Kamalakannan, A., Gopalakrishnan, C., Rajesh, S., Panneerselvam, S., and Ganapati, P. S. (2022). Loop-mediated isothermal amplification assay: A specific and sensitive tool for the detection of *Bipolaris oryzae* causing brown spot disease in rice. *Phytoparasitica* 50, 543–553. doi: 10.1007/s12600-022-00979-3

Liang, H., Deng, Y., Wang, C., and Xu, X. (2016). A high-throughput DNA extraction method from rice seeds. *Biotechnol. Biotechnol. Equip.* 30, 32–35. doi: 10.1080/13102818.2015.1088401

Mancini, V., Murolo, S., and Romanazzi, G. (2016). Diagnostic methods for detecting fungal pathogens on vegetable seeds. *Plant Pathol.* 65, 691–703. doi: 10.1111/ppa.12515

Marimuthu, K., Ayyanar, K., Varagur Ganesan, M., Vaikuntavasan, P., Uthandi, S., Mathiyazhagan, K., et al. (2020). Loop-mediated isothermal amplification assay for the detection of plasmopara viticola infecting grapes. *J. Phytopathol.* 168, 144–155. doi: 10.1111/jph.12866

Mathur, S. C. (1981). Observations on diseases of dryland rice in Brazil. *Int. Rice Res. Newsl.* 6, 11–12.

Mew, T. W., and Gonzales, P. (2002). *A handbook of rice seedborne fungi* (Philippines: International Rice Research Institute).

Nasruddin, A., and Amin, N. (2013). Effects of cultivar, planting period, and fungicide usage on rice blast infection levels and crop yield. *J. Agric. Sci.* 5, 160. doi: 10.5539/jas.v5n1p160

Neergaard, P. (1977). "Economic significance of seed-borne diseases," in *The seed pathology* (Palgrave, London: Red Globe Press), 3–39.

Notomi, T., Okayama, H., Masubuchi, H., Yonekawa, T., Watanabe, K., Amino, N., et al. (2000). Loop-mediated isothermal amplification of DNA. *Nucleic Acids Res.* 28, 63. doi: 10.1093/nar/28.12.e63

Parida, M., Horioke, K., Ishida, H., Dash, P. K., Saxena, P., Jana, A. M., et al. (2005). Rapid detection and differentiation of dengue virus serotypes by a real-time reverse transcription-loop-mediated isothermal amplification assay. *J. Clin. Microbiol.* 43, 2895–2903. doi: 10.1128/JCM.43.6.2895-2903.2005

Pearce, D. A., Bridge, P. D., and Hawksworth, D. L. (2001). "Species concept in sarocladium, the causal agent of sheath rot in rice and bamboo blight," in *Major fungal diseases of rice* (Dordrecht: Springer), 285–292.

Prasannakumar, M. K., Parivallal, P. B., Pramesh, D., Mahesh, H. B., and Raj, E. (2021). LAMP-based foldable microdevice platform for the rapid detection of *Magnaporthe oryzae* and *Sarocladium oryzae* in rice seed. *Sci. Rep.* 11, 1–10. doi: 10.1038/s41598-020-80644-z

Reddy, O. R., and Sathyanarayana, N. (2001). "Seed-borne fungi of rice and quarantine significance," in *Major fungal diseases of rice* (Dordrecht: Springer), 331–345.

Reuter, C., Slesiona, N., Hentschel, S., Aehlig, O., Breitenstein, A., Csáki, A., et al. (2020). Loop-mediated amplification as promising on-site detection approach for *Legionella pneumophila* and legionella spp. *App. Microbiol. Biotechnol.* 104, 405–415. doi: 10.1007/s00253-019-10286-3

Richardson, M. J. (1981). *Supplement 1 to an annotated list of seed-borne diseases. 3rd ed* (Zurich, Switzerland: The International Seed Testing Association).

Saiki, R. K., Gelfand, D. H., Stoffel, S., Scharf, S. J., Higuchi, R., Horn, G. T., et al. (1988). Primer-directed enzymatic amplification of DNA with a thermostable DNA polymerase. *Science* 239, 487–491. doi: 10.1126/science.2448875

Sarangi, S. K., and Islam, M. R. (2019). "Advances in agronomic and related management options for sundarbans," in *The sundarbans: a disaster-prone eco-region* (Cham: Springer), 225–260.

Schrader, C., Schielke, A., Ellerbroek, L., and Johne, R. (2012). PCR inhibitors – occurrence, properties and removal. *J. Appl. Microbiol.* 113, 1014–1026. doi: 10.1111/j.1365-2672.2012.05384.x

Teng, P. S. (1994). Integrated pest management in rice. *Exp. Agric.* 30, 115–137. doi: 10.1017/S001447970002408X

Tian, C., Wan, P., Sun, S., Li, J., and Chen, M. (2004). Genome-wide analysis of the GRAS gene family in rice and *Arabidopsis*. *Plant Mol. Biol.* 54, 519–532. doi: 10.1023/B:PLAN.0000038256.89809.57

Tiwari, A. K. (2016). *Current trends in plant disease diagnostics and management practices* (Berlin: Springer), 207–219. doi: 10.1007/978-3-319-27312-9

Tomita, N., Mori, Y., Kanda, H., and Notomi, T. (2008). Loop-mediated isothermal amplification (LAMP) of gene sequences and simple visual detection of products. *Nat. Protoc.* 3, 877–882. doi: 10.1038/nprot.2008.57

Wang, X., Zhang, Q., Zhang, F., Ma, F., Zheng, W., Zhao, Z., et al. (2012). Visual detection of the human metapneumovirus using reverse transcription loop-mediated isothermal amplification with hydroxynaphthol blue dye. *Virol. J.* 9, 1–6. doi: 10.1186/1743-422X-9-138

Wastling, S. L., Picozzi, K., Kakembo, A. S. L., and Welburn, S. C. (2000). LAMP for human African trypanosomiasis: a comparative study of detection formats. *PloS Neglec. Trop. D.* 4, 865. doi: 10.1371/journal.pntd.0000865

Yeh, H. Y., Shoemaker, C. A., and Klesius, P. H. (2005). Evaluation of a loop-mediated isothermal amplification method for rapid detection of channel catfish *Ictalurus punctatus* important bacterial pathogen *Edwardsiella ictaluri*. *J. Microbiol. Methods* 63, 36–44. doi: 10.1016/j.mimet.2005.02.015

Zaczek-Moczydłowska, M. A., Mohamed-Smith, L., Toldrà, A., Hooper, C., Campàs, M., Furones, M. D., et al. (2020). A single-tube HNB-based loop-mediated isothermal amplification for the robust detection of the ostreid herpesvirus 1. *Int. J. Mol. Sci.* 21, 6605. doi: 10.3390/ijms21186605

Zeng, D., Ye, W., Xu, M., Lu, C., Tian, Q., and Zheng, X. (2017). Rapid diagnosis of soya bean root rot caused by *Fusarium culmorum* using a loop-mediated isothermal amplification assay. *J. Phytopathol.* 165, 249–256. doi: 10.1111/jph.12556

Zhang, S. Y., Dai, D. J., Wang, H. D., and Zhang, C. Q. (2019). One-step loop-mediated isothermal amplification (LAMP) for the rapid and sensitive detection of *Fusarium fujikuroi* in bakanae disease through NRPS31, an important gene in the gibberellic acid bio-synthesis. *Sci. Rep.* 9, 1–9. doi: 10.1038/s41598-019-39874-z

Zhang, X., Harrington, T. C., Batzer, J. C., Kubota, R., Peres, N. A., and Gleason, M. L. (2016). Detection of *Colletotrichum acutatum* sensu lato on strawberry by loop-mediated isothermal amplification. *Plant Dis.* 100, 1804–1812. doi: 10.1094/PDIS-09-15-1013-RE

frontiers | Frontiers in Plant Science

TYPE Original Research
PUBLISHED 25 November 2022
DOI 10.3389/fpls.2022.1031611

OPEN ACCESS

EDITED BY
Ravinder Kumar,
Central Potato Research Institute (ICAR), India

REVIEWED BY
Meinan Wang,
Washington State University, United States
Malkhan Singh Gurjar,
Indian Agricultural Research Institute (ICAR), India

*CORRESPONDENCE
Li Gao
xiaogaosx@hotmail.com

SPECIALTY SECTION
This article was submitted to Plant Pathogen Interactions, a section of the journal Frontiers in Plant Science

RECEIVED 06 September 2022
ACCEPTED 18 October 2022
PUBLISHED 25 November 2022

CITATION
Ren Z, Chen R, Muhae-Ud-Din G, Fang M, Li T, Yang Y, Chen W and Gao L (2022) Development of real-time PCR and droplet digital PCR based marker for the detection of *Tilletia caries* inciting common bunt of wheat. *Front. Plant Sci.* 13:1031611. doi: 10.3389/fpls.2022.1031611

Development of real-time PCR and droplet digital PCR based marker for the detection of *Tilletia caries* inciting common bunt of wheat

Zhaoyu Ren[1], Rongzhen Chen[1,2], Ghulam Muhae-Ud-Din[1], Mingke Fang[1,3], Tianya Li[2], Yazheng Yang[3], Wanquan Chen[1] and Li Gao[1]*

[1]State Key Laboratory for Biology of Plant Disease and Insect Pests, Institute of Plant Protection, Chinese Academy of Agricultural Sciences, Beijing, China, [2]Department of Plant Protection, Shenyang Agricultural University, Liaoning, China, [3]College of Life Sciences, Yangtze University, Jingzhou, China

This is the first study reporting droplet digital PCR and quantitative real time PCR for detection of *Tilletia caries* (syn. *T. tritici*), which causes common bunt of wheat and leads to yield losses of 80% in many wheat growing areas worldwide. To establish an accurate, rapid and quantifiable detection method, we tested 100 inter simple sequence repeats (ISSR) primers and obtained a species-specific fragment (515 bp) generated by ISSR 827. Then, a specific 266 bp band for the sequence characterized amplified region (SCAR) marker was produced from *T. caries*. The detection limit reached 50 pg/μL. Based on the SCAR marker, we further developed a higher sensitivity of quantitative real time-polymerase chain reaction (qRT-PCR) with a detection limit of 2.4 fg/μL, and droplet digital PCR (ddPCR) with a detection limit of 0.24 fg/μL. Both methods greatly improved the detection sensitivity of *T. caries*, which will be contribute a lot for quickly and accurately detection of *T. caries*, which causes wheat common bunt.

KEYWORDS

droplet digital PCR, SCAR marker, qRT-PCR, ISSR, *Tilletia caries*, wheat common bunt

Introduction

Tilletia caries (syn. *T. tritici*) causes common bunt of wheat (*Triticum aestivum* L.), which is a seed-borne disease (Menzies et al., 2006; Goates, 2012) that appears in wheat-growing areas worldwide (Albughobeish, 2015). A typical symptom of the disease is that wheat kernel turns into millions of teliospores generated by the pathogen; the grains are then referred to as "bunt balls" (Mourad et al., 2018). The teliospore-released trimethylamine, which emits a fishy smell, seriously affecting the taste and quality of wheat flour (Gaudet et al., 2007). The teliospores of *T. caries* is very similar to *T. laevis*, and *T. controversa*, especially *T. controversa* is characterized as a quarantine pathogen (Peterson et al., 2009; Bishnoi et al., 2020). Therefore, accurate, and efficient detection methods to differentiate *T. caries* and *T. controversa* are important regarding management practices, and global trade of cereals. The traditional methods for identification are mainly based on the characterization of teliospores and germination features (5°C at 40 days and 15°C at 10 days for *T. controversa* and *T. caries*, respectively) (Boyd and Carris, 1998). However, it is very difficult to differentiate both pathogens based on the characterization of teliospores, both the measurements of teliospores and its reticulum of *T. caries* and *T. controversa* have big overlap. Overall, both methods mentioned above were laborious, time-cost and unable to quickly meet the demand for diagnosis, especially for the plant quarantine pathogen *T. controversa*. In previous studies, some methods based on internal transcription spacers (ITSs), specific DNA fragments, and DNA molecular diagnosis technology were used for the identification of different *Tilletia* spp. (Kochanová et al., 2004; Eibel et al., 2005; Carris et al., 2006), but all these methods have low sensitivity to identify *T. caries* successfully. Thus, it is of great significance and essential to develop a rapid, effective and high sensitivity detection method for *T. caries*.

With the development of molecular diagnosis technology, PCR has been widely used to differentiate *Tilletia* spp. Kochanová et al. (Kochanová et al., 2004) developed a PCR detection method for *T. caries* and *T. controversa*. The repetitive extragenic palindromic PCR (Rep-PCR) fingerprinting technique used for the identification of *Tilletia* spp. (McDonald et al., 2000; Župunski et al., 2011). Nian et al. (Nian et al., 2007) developed multiple PCRs to distinguish *T. controversa* from *T. caries*, and the lowest detectable concentration was 10 fg/μL. The qRT-PCR is characterized by its multiplexing capacity and wide range of detection with high sensitivity (Lillsunde Larsson and Helenius, 2017), but it has also been criticized for inevitably producing false-positives (Suo et al., 2020). Moreover, the results of qRT-PCR cannot be easily analyzed without a standard reference curve. The ddPCR have been reported to be used to detect a variety of plant pathogens, such as *Aspergillus flavus* (Schamann et al., 2022), *Fusarium oxysporum* f. sp.*vasinfectum* (Davis et al., 2022), *Monilinia fructicola and Monilinia laxa* (Raguseo et al., 2021), *T. controversa* (Liu et al., 2020), and *T. laevis* (Xu et al., 2020) which demonstrates the practicability and potential of ddPCR detection methods, especially in the context of a small number of target organisms. The ddPCR can still play an important role because of its sensitivity. Due to the dilution and distribution of samples across many reaction droplets, ddPCR results are more accurate and reliable than those obtained with other methods. Target DNA could be detected by a specific fluorescent labeling probe at a relatively low concentration (Hindson et al., 2011). Similarly, ddPCR technology has been applied for the identification of *T. controversa* and *T. laevis*, with detection limits of 2.1 copies/μL and 1.5 copies/μL, respectively (Liu et al., 2020; Xu et al., 2020).

In this study, we successfully developed the sequence characterized amplified region (SCAR) marker method for the identification of *T. caries*, and based on the SCAR marker, qRT-PCR and ddPCR detection methods were also successfully developed with high sensitivity. This is the first report on the detection of teliospores of *T. caries* by qRT-PCR and ddPCR method which based on SCAR marker from ISSR.

Materials and methods

Fungal isolates and DNA extraction

In this study, five wheat pathogens (Blumeria graminis, F. graminearum, Puccinia graminis var. tritici, P. striiformis and P. triticina) and six Tilletia-related fungi (Ustilago tritici, U. hordei, U. maydis, T. laevis and T. controversa, T. caries) were used to detect the specificity. Information on the pathogens listed in Table S1. The DNA of all the strains was extracted by the CTAB method (Xu et al., 2020). Then, a NanoDrop 3300 fluorospectrometer (Biotech, USA) was used to evaluate the purity and quantitation of DNA with an OD_{260}/OD_{280} between 1.8 and 2.0. The integrity of the DNA was examined by agarose gel electrophoresis with λDNA/HindIII labeling. Finally, the DNA were stored at −20°C for further use.

ISSR-PCR amplification

To obtain the species-specific DNA fragment, 100 ISSR primers published by the University of British Columbia (https://www.michaelsmith.ubc.ca/services/NAPS/PrimerSets) were used to amplify the DNA of all the tested pathogens. The primers were synthesized by Tsingke Biotechnology Co., Ltd. (Beijing, China), and are listed in Table 1. ISSR-PCR was

TABLE 1 Primers used in the study.

Name	Primer sequences
M13F	5'-GTTTTCCCAGTCACGAC-3'
M13R	5'-CAGGAAACAGCTATGAC-3'
ISSR827	5′- ACA CAC ACA CAC ACA CG -3′
Erc 19F	5'-CTTGTCCAAGCACGTACC-3'
Erc 19R	5'-CTGCGCAGCGAGAGTAG-3'
Qerc19F	5'-GCTTTCTGTTGTTTGCTGTTGA-3'
Qerc19R	5'-ATCGGCTGGCTGATGTCTATA-3'
WX-F	5'-AGGAGTCAGTAGTCAGTAGTCAG-3'
WX-R	5'-GGGAGTCGGTGGTGTAATTT-3'
Probe primer WX-P	FAM 5'-CTTTGGCCGTGGTGGATACCTATAGC-3' TAMRA

performed in a programmable optics module thermocycler (Bio-Rad, USA) with a total reaction volume of 25 μL, which included 2 μL of primer (10 μM), 1 μL of template DNA (100 ng/μL), 12.5 μL of 2 × Pro Taq Master Mix (dye plus) (Vazyme Biotech Co., Ltd., China), and 9.5 μL of ddH_2O. The PCR amplification programs were as follows: predenaturation at 94°C for 30 s; followed by 35 cycles of denaturation at 98°C for 10 s, annealing at 45–65°C (depending on the primers) for 30 s, and extension at 72°C for 1 min; and final extension step at 72°C for 2 min. The PCR products were electrophoresed on 2% agarose gel electrophoresis containing ethidium bromide at 150 V for 20 min and visualized by a gel documentation system (WSE-5200 Printgraph 2 M, ATTO, Korea).

Cloning species-specific DNA fragment and SCAR marker development

The DNA fragment (515 bp) specific to *T. caries* produced by the ISSR 827 primer was isolated from the gel and purified with a TIANgel Purification Kit (TianGen Biochemical Technology Co., Ltd., China). Then, a *pCloone007* Versatile Simple Vector Kit (Tsingke Biotechnology Co., Ltd., China) was used to ligate the specific DNA fragment with the *pUC19* vector and transform it into chemically competent *Escherichia coli* DH5α cells (Tsingke Biotechnology Co., Ltd.). The cloned fragment was sequenced with primers M13F and M13R by Tsingke Biotechnology Co., Ltd. The *E. coli* plasmid was then extracted by a TIANprep Mini Plasmid Kit (TianGen Biochemical Technology Co., Ltd., China), and the concentration calculated by the NanoDrop 3300 fluorospectrometer (Biotech, USA) was 240 ng/μL. Based on the sequencing results, SCAR marker primers Erc19F and Erc19R were designed by Primer Premier 6 and synthesized by Tsingke Biotechnology Co., Ltd. (Beijing, China).

Specificity of the SCAR marker

Five wheat pathogens and five fungi closely related to *T. caries* were used as controls in this study. SCAR-based PCR amplification was carried out with a total volume of 25 μL, including 1 μL DNA template (100 ng/μL), 1 μL SCAR primer Erc19F (10 μM), 1 μL SCAR primer Erc19R (10 μM), 12.5 μL of 2 × Pro Taq Master Mix II (dye plus) (Vazyme Biotech Co., Ltd., China) and 9.5 μL ddH_2O. The PCR amplification programs were as follows: predenaturation at 94°C for 30 s; followed by 35 cycles of denaturation at 98°C for 10 s, annealing at 61.5°C for 30 s, and extension at 72°C for 1 min; and final extension step at 72°C for 2 min. The PCR products were electrophoresed as mentioned above.

Sensitivity of the SCAR marker

A series of diluted DNA concentrations (100 ng/μL, 50 ng/μL, 25 ng/μL, 10 ng/μL, 5 ng/μL, 1 ng/μL, 0.5 g/μL, 0.1 ng/μL, 50 pg/μL, 25 pg/μL, 10 pg/μL and 1 pg/μL) were used as templates for sensitivity. The amplification system, programs and agarose gel electrophoresis conditions were consistent with those mentioned above.

Specificity and sensitivity of quantitative real time PCR detection method

According to the specific DNA fragment generated by ISSR 827, qRT-PCR primers Qerc19F and Qerc19R were designed and synthesized by Tsingke Biotechnology Co., Ltd. (Beijing, China). To verify the specificity of the primers, we used 10 sets of *T. laevis* DNA (100 ng/μL) and 3 sets of *T. caries* DNA (100 ng/μL) to perform qPCR. The reaction was carried out by using an ABI 7500 real-time PCR system (Applied Biosystems, Carlsbad, CA, USA) machine. The reaction was performed in 20 μL, including 1 μL DNA, 0.4 μL Qerc19F (10 μM), 0.4 μL of Qerc19R (10 μM), 8.2 μL of nuclease-free water (TransGen Biotech, China) and 10 μl of 2 × TransStart Top Green qPCR SuperMix (+DyeI/+DyeII) (TransGen Biotech, China). The program settings were as follows: 95°C for 5 min, followed by 40 cycles of 95°C for 10 s and 58°C for 30 s. Then, a series of 10-fold diluted plasmids (2.4 pg-0.24 fg) were used as templates. Three repeats for every concentration and 2 μL of nuclease-free water (TransGen Biotech, China) were used as controls for each repeat. The reaction system was the same as mentioned above.

DdPCR detection method

Based on the success of the SCAR marker and qRT-PCR for the detection of *T. caries*, we successfully developed ddPCR detection method. Pairs of the primers WX-F and WX-R and probe primer WX-P were synthesized by Tsingke Biotechnology Co., Ltd. (Beijing, China). The probe primer WX-FRP was generated by mixing WX-F, WX-R and WX-P at a ratio of 1:1:0.5 (10 μL of WX-F, 10 μL of WX-R, 5 μL of probe primer WX-P and 225 μL of ddH_2O). The reaction was performed in 20 μL, containing, 10 μL Prenix EX Taq (Probe qPCR) (Takara, Japan), 4 μL WX-FRP, 4 μL ddH_2O and 2 μL DNA template (240 ng/μL), was mixed with 35 μL of droplet-generating oil (186-3005, Bio-Rad, USA) and moved to a droplet-generating card (186-4007, Bio-Rad, USA) to generate droplets in a droplet generator (QX200, Bio-Rad, USA). The products were transferred to a 96-well PCR plate (Eppendorf, Germany), and ddPCR was performed in a C1000 touch thermal cycler (Bio-Rad, USA) with the following program: predenaturation at 95°C for 5 min, 40 cycles of denaturing at 95°C for 30 s, followed by 60 s of annealing at 58°C, and extension at 98°C for 10 min. The products were diluted 10-fold in 10 gradients and transferred to a droplet reader (QX200, Bio-Rad, Hercules, CA, US). Quanta Soft (Version, 1.7.4, Bio-Rad, provided with the ddPCR system) analysis was used to generate data, and the florescence amplitude threshold was set by the JavaScript program "dedinetherain" (Jones et al., 2014) to improve the accuracy and credibility of the results to follow the previous studies (Kubista et al., 2006; Jones et al., 2014). In this experiment, we tested the *T. caries* samples with plasmid concentrations ranging from 2.4 pg/μL to 0.24 fg/μL in 3 replicates per sample, 7 repeats of *T. controversa* and *T. laevis*, and 2 repeats of ddH_2O as negative controls.

Results

Specific ISSR marker screening and SCAR marker development

Among the 100 ISSR primers from the University of British Columbia, ISSR 827 amplified a polymorphic profile (515 bp) in *T. caries* but not in the other investigated pathogens (Figure 1). Primer Premier 6 was used to analyze the specific DNA sequence of *T. caries*, and pairs of SCAR marker primers named Erc 19F and Erc 19R were designed. The primers amplified a specific 266 bp band from the DNA of *T. caries* (Figure 2).

Specificity and detection limit of the SCAR marker

Some related pathogens (B. graminis, F. graminearum, P. graminis var. tritici, P. striiformis f. sp. tritici, P. triticina, U. tritici, U. hordei, U. maydis, T. caries, T. laevis and T. controversa) were used to detect the specificity of the designed SCAR primers. The specific band (266 bp) occurred only in T. caries and in none of the other tested pathogens (Figure 3). In addition, we tested the sensitivity of the SCAR marker using a series of diluted DNA template concentrations of T. caries (100 ng/μL, 50 ng/μL, 25 ng/μL, 10 ng/μL, 5 ng/μL, 1 ng/μL, 0.5 ng/

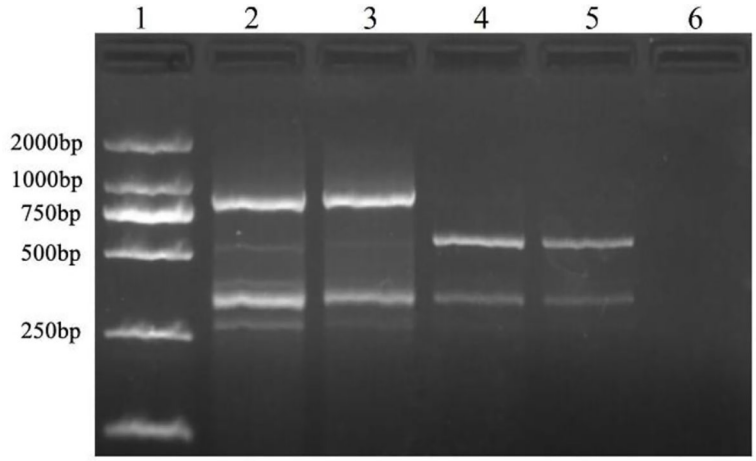

FIGURE 1
Specific fragment of *T. caries* obtained with an inter simple sequence repeat primer (ISSR827). Lane 1: DL2000 DNA ladder; lane 2: *T. controversa*; lane 3: *T. laevis*; lanes 4-5: *T. caries*; and lane 6: ddH_2O.

5'-CTTGTCCAAGCACGTACCGTAGATGCAGTAAGTAGATACAGTCAGGAAG
TATCTAAGCACAGTACATCCATACACCCATACATACATACAGGAGTCAGTAG
TCAGTAGTCAGTATCTACAGTAGTCAGTATCTACTTATCTACTTAGGTACTAC
AGTGTAGTAAGAACATGCGTGATCGCTATAGGTATCCACCACGGCCAAAGC
CCCAAAAATTACACCACCGACTCCCGGCCGGCGACGCTTCCCCCCTACTCT
CGCTGCGCAG-3'

FIGURE 2
Sequence of the SCAR marker produced by Erc 19F and Erc 19R. The sequences under line are the amplification primers (Erc 19F and Erc 19R).

μL, 0.1 ng/μL, 50 pg/μL, 25 pg/μL, 10 pg/μL, and 1 pg/μL), resulting in a sensitivity of 50 pg/μL of the Erc19F/Erc19R primer (Figure 4).

Development of qRT- PCR detection method

Based on the specific sequence, primers Qerc19F and Qerc19R were designed to perform qRT-PCR with SYBR Green I. For the specific of the primers, 10 sets of T. laevis DNA and 3 sets of T. caries DNA were used as templates to carry out qPCR. The results showed that 10 sets of T. laevis DNA failed to amplify the target sequence, while 3 sets of T. caries DNA successfully amplified the target sequence (Supplementary Figure S1). For the sensitivity of the detection, 10-fold serial dilutions of plasmids were used as templates (2.4 pg to 0.24 fg) and the detection limit concentration was 2.4 fg/μL (Figure 5A). Furthermore, a standard curve with correlation coefficient of the standard curve reached 0.997, suggesting successful development of the SYBR Green I qRT-PCR detection method (Figure 5B).

The ddPCR detection method

We used 10,000 droplets to increase the accuracy and reliability of the experiment. The increase in the number of positive droplets (blue points) in the DNA samples indicated a greater copy number in the ddPCR products, which suggested that the concentration of *T. caries* in the DNA samples was increased. In contrast, the lack of positive droplets indicated that

FIGURE 3
Specificity of the SCAR marker on *T. caries*. Lane 1: DL2000 DNA ladder; lanes 2–5: *T. caries;* lanes 6–9: *T. controversa*; lanes 14–17: *Ustilago maydis*; lanes 18–21: *Ustilago tritici*; lanes 22–25: *Ustilago hordei*; lane 26: DL2000 DNA ladder; lanes 27–30: *Puccinia striiformis* f. sp. *tritici;* lanes 31–34: *Puccinia triticina*; lanes 35–38: *Puccinia graminis* f. sp. *tritici*; lanes 39–42: *Blumeria graminis*; lanes 43–46: *Fusarium graminearum*; and lanes 47–50: ddH_2O.

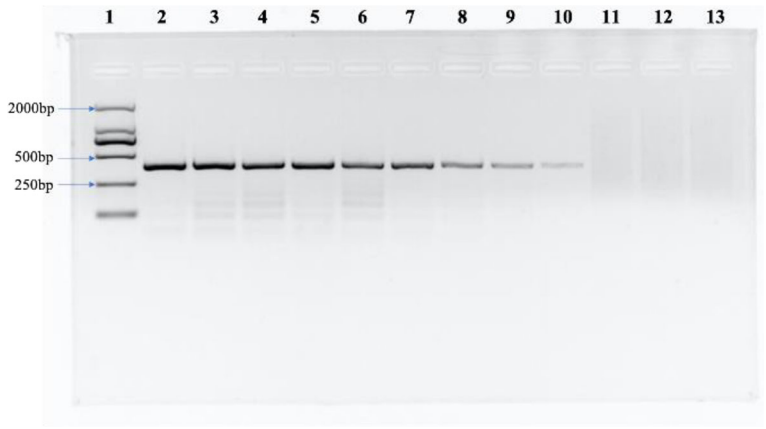

FIGURE 4
The sensitivity of the SCAR marker. Lane 1: DL2000 DNA ladder, lane 2: 100 ng/μL, lane 3: 50 ng/μL, lane 4: 25 ng/μL, lane 5: 10 ng/μL, lane 6: 5 ng/μL, lane 7: 1 ng/μL, lane 8: 0.5 ng/μL, lane 9: 0.1 ng/μL, lane 10: 50 pg/μL, lane 11: 25 pg/μL, lane 12: 10 pg/μL, and lane 13: ddH_2O.

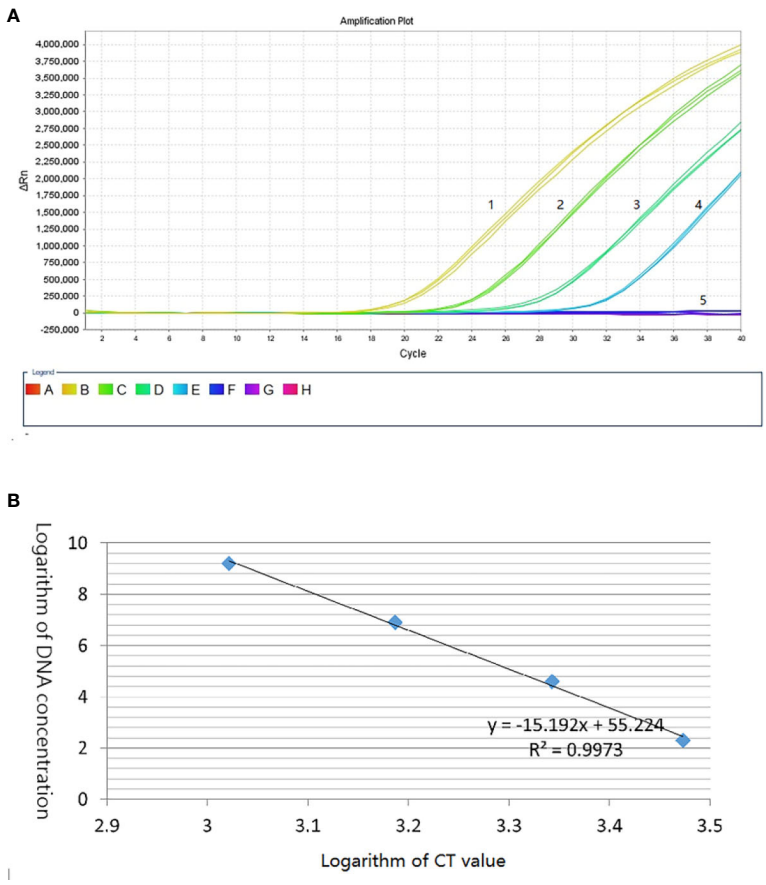

FIGURE 5
Establishment of *T. caries* standard curve by SYBR Green I real-time PCR. **(A)** Quantitative real-time amplified curves. Lanes 1–4: tenfold dilutions of recombinant plasmid DNA (2.4 pg–0.24 fg); lane 5: negative control (ddH_2O). **(B)** Standard curve.

T. caries was not detected (Supplementary Figure S2). The results showed that the detection limit of ddPCR was 0.7 copies/μl (0.24 fg/μL) (Figure 6). Furthermore, we conducted a statistical analysis of the number of positive droplets, and the results showed that ddPCR detection is a precise and effective method for the detection of *T. caries* (Figure 7).

Discussion

Until now, this is the first report on detection *T. caries* by ddPCR and qRT-PCR, even these methods were reported on *T. caries* and *T. laevis* previously (Liu et al., 2020; Xu et al., 2020). Actually, quickly detection of *T. caries* is also very important; it is difficult to differentiate *T. caries* and *T. controversa* with morphological characters. Moreover, the size and reticulum of teliospores of *T. caries* overlapped with those of *T. controversa*, a quarantine fungus of wheat in most countries.

In this research, based on the species-specific DNA band (515 bp) by ISSR 827, we developed SCAR marker (primers Erc 19F and Erc 19R). A specific band (266 bp) was amplified by the DNA of *T. caries*, but not in other related wheat pathogens, indicating the great specificity of the SCAR marker, and the detection limit of the SCAR marker was 50 pg/μL. In addition, we further developed a qRT-PCR method with a detection limit of 2.4 fg/μL, which had a higher sensitivity than the SCAR marker. The detection limit of SCAR marker and qRT-PCR was 797 and 7.97 copies/μL (1.8 and 0.018 fg/μL) for *T. controversa* respectively (Liu et al., 2020), and was 5 ng/μl and 100 fg/μl for *T. laevis* (Xu et al., 2020), while for the detection limit of our research on *T. caries*, the sensitivity of SCAR marker (50 pg/μL) and qRT-PCR (2.4 fg/μL)are higher than *T. laevis*, while lower than *T. controversa.*

The qRT-PCR can only achieve relative quantification with a standard curve, while ddPCR can achieve absolute quantification. DdPCR is more accurate and reliable than qRT-PCR (Kubista et al., 2006; Hindson et al., 2011; Pinheiro et al., 2012; Jones et al., 2014; Pavšič et al., 2016). Pieczul et al. (Pieczul et al., 2018) described the loop-mediated isothermal DNA amplification (LAMP) method for the identification of *T. caries*, *Tilletia laevis* and *T. controversa* but could not differentiate between *T. laevis*, *T. caries*, and *T. controversa*. Similarly, qPCR was used to detect the spores of *T. indica*, but could not differentiate the other bunt pathogens at the same time (Gurjar et al., 2017). However, ddPCR can differentiate *T. caries* from other bunt pathogens. Thus, we performed ddPCR for the

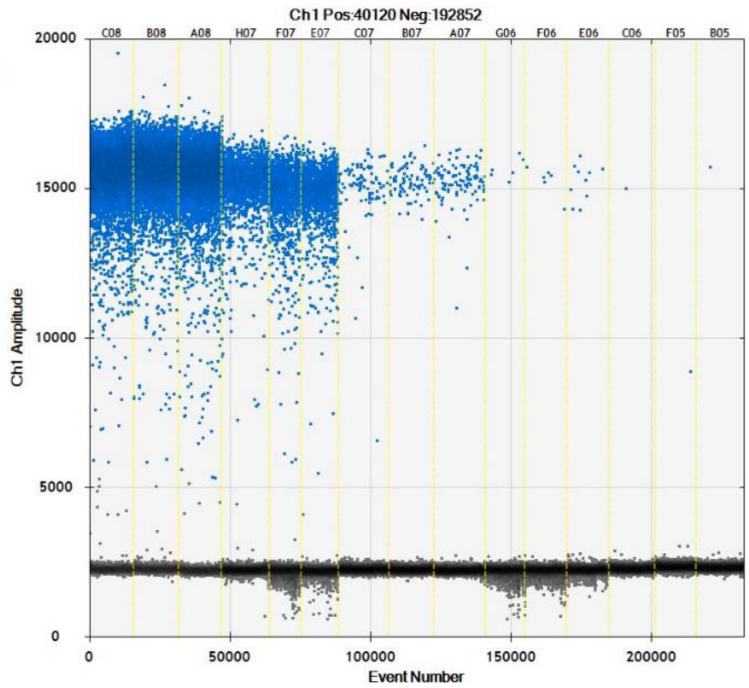

FIGURE 6
Distribution diagram of droplets of *T. caries* isolates obtained by droplet digital PCR. C08–A08, DNA template of *T. caries* (2.4 pg/μL); H07–E07, DNA template of *T. caries* (0.24 pg/μL); C07–A07, DNA template of *T. caries* (24 fg/μL); G06–E06, DNA template of *T. caries* (2.4 fg/μL), C06–B05, and DNA template of *T. caries* (0.24 fg/μL). The blue dots are positive droplets, and the black dots are negative controls.

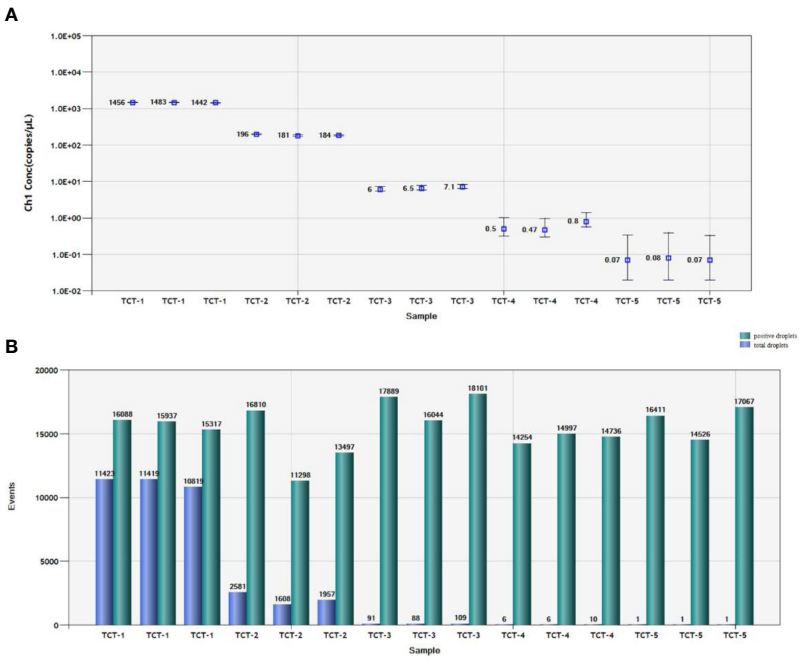

FIGURE 7
Statistical analysis by ddPCR. **(A)** Positive copy number analysis for detection of *T. caries* by copy number; TCT-1, DNA template of *T. caries* (2.4 pg/μL); TCT-2, DNA template of *T. caries* (0.24 pg/μL); TCT-3, DNA template of *T. caries* (24 fg/μL); TCT-4, DNA template of *T. caries* (2.4 fg/μL); TCT-5, DNA template of *T. caries* (0.24 fg/μL). **(B)**. Number analysis of *T. caries* isolates; TCT-1, DNA template of *T. caries* (2.4 pg/μL); TCT-2, DNA template of *T. caries* (0.24 pg/μL); TCT-3, DNA template of *T. caries* (24 fg/μL); TCT-4, DNA template of *T. caries* (2.4 fg/μL); TCT-5, DNA template of *T. caries* (0.24 fg/μL). The green pillars are the number of positive droplets, and the blue pillars indicate the number of total droplets (positive + negative).

detection of *T. caries*. The results showed that the detection limit was 0.7 copies/μL (0.24 fg/μL), which is 10-fold more sensitive than the qRT-PCR method and the detection sensitivity was higher than the previous method used for *T. controversa* (2.1 copies/μL (Liu et al., 2020) and *T. laevis* (1.5 copies/μL (Xu et al., 2020). In addition, we only found droplets with the samples of *T. caries* while not in other two similar pathogens, *T. controversa* and *T. laevis*, and can also found droplets with 0.7 copies/μL (0.24 fg/μL), which indicate the reliability of this method and reliability of the detection threshold. All the methods developed in this study showed great specificity and sensitivity and could be used as powerful tools for *T. caries* detection in the future.

Conclusion

We successfully developed ddPCR and qRT-PCR detection method for *T. caries*, the teliospores of *T. caries* is very similar to the teliospores of *T. controversa*. Based on the results of this study, ddPCR is more sensitive than qRT-PCR based on SCAR marker. This is the first study to develop ddPCR technique and qRT-PCR detection method for *T. caries*, which caused common bunt of wheat.

Data availability statement

The original contributions presented in the study are included in the article/Supplementary Material. Further inquiries can be directed to the corresponding author.

Author contributions

Conceptualization, LG. Methodology, RC. Validation, ZR, MF, YY. Resources, WC. Writing—original draft preparation, LG and RC. Writing—review and editing, LG and GM-u-D. All authors contributed to the article and approved the submitted version.

Funding

This research was funded by National Natural Science Foundation of China (grant numbers 31761143011 and 31571965), China Agriculture Research System (CARS-3), and Agricultural Science and Technology Innovation Program (CAAS-ASTIP).

Conflict of interest

The authors declare that the research was conducted in the absence of any commercial or financial relationships that could be construed as a potential conflict of interest.

Publisher's note

All claims expressed in this article are solely those of the authors and do not necessarily represent those of their affiliated organizations, or those of the publisher, the editors and the reviewers. Any product that may be evaluated in this article, or claim that may be made by its manufacturer, is not guaranteed or endorsed by the publisher.

Supplementary material

The Supplementary Material for this article can be found online at: https://www.frontiersin.org/articles/10.3389/fpls.2022.1031611/full#supplementary-material

SUPPLEMENTARY FIGURE 1
Specificity of quantitative real time PCR detection method. Lanes 1: DNA of *T. caries*; lane 2: DNA of *T. laevis* and *T. controversa*

SUPPLEMENTARY FIGURE 2
Amplification of *T. controversa* and *T. laevis*. A02-H02, DNA template of *T. controversa*; A03-B03, ddH_2O; A04-G04, DNA template of *T. laevis*

References

Albughobeish, N., and Jorf, S. A. M. (2015). New races of *Tilletia laevis* and *T. caries*, the causal agents of wheat common bunt in khuzestan province, Iran. *J. Crop Prot.* 4, 59–68.

Bishnoi, S. K., He, X., Phuke, R. M., Kashyap, P. L., Alakonya, A., Chhokar, V., et al. (2020). Karnal bunt: A re-emerging old foe of wheat. *Front. Plant Sci.* 11. doi: 10.3389/fpls.2020.569057

Boyd, M. L., and Carris, L. M. (1998). Enhancement of teliospore germination in wheat- and wild grass-infecting species of *Tilletia* on activated charcoal medium. *Phytopathol* 88, 260–264. doi: 10.1094/PHYTO.1998.88.3.260

Carris, L. M., Castlebury, L. A., and Goates, B. J. (2006). Nonsystemic bunt fungi—*Tilletia indica* and *T. horrida* : A review of history, systematics, and biology. *Annu. Rev. Phytopathol.* 44, 113–133. doi: 10.1146/annurev.phyto.44.070505.143402

Davis, R. LII, Isakeit, T., and Chappell, T. M. (2022). DNA-Based quantification of *Fusarium oxysporum* f. sp. *vasinfectum* in environmental soils to describe spatial variation in inoculum density. *Plant Dis.* 106, 1653–1659. doi: 10.1094/PDIS-08-21-1664-RE

Eibel, P., Wolf, G. A., and Koch, E. (2005). Detection of *Tilletia caries*, causal agent of common bunt of wheat, by ELISA and PCR. *J. Phytopathol.* 153, 297–306. doi: 10.1111/j.1439-0434.2005.00973.x

Gaudet, D. A., Lu, Z. X., Leggett, F., Puchalski, B., and Laroche, A. (2007). Compatible and incompatible interactions in wheat involving the bt-10 gene for resistance to *Tilletia tritici*, the common bunt pathogen. *Phytopathol* 97, 1397–1405. doi: 10.1094/PHYTO-97-11-1397

Goates, B. J. (2012). Identification of new pathogenic races of common bunt and dwarf bunt fungi, and evaluation of known races using an expanded set of differential wheat lines. *Plant Dis.* 96, 361–369. doi: 10.1094/PDIS-04-11-0339

Gurjar, M. S., Aggarwal, R., Jogawat, A., Sharma, S., Kulshreshtha, D., Gupta, A., et al. (2017). Development of real time PCR assay for detection and quantification of teliospores of *Tilletia indica* in soil. *Indian J. Exp. Biol.* 55, 549–554.

Hindson, B. J., Ness, K. D., Masquelier, D. A., Belgrader, P., Heredia, N. J., Makarewicz, A. J., et al. (2011). High-throughput droplet digital PCR system for absolute quantitation of DNA copy number. *Anal. Chem.* 83, 8604–8610. doi: 10.1021/ac202028g

Jones, M., Williams, J., Gärtner, K., Phillips, R., Hurst, J., and Frater, J. (2014). Low copy target detection by droplet digital PCR through application of a novel open access bioinformatic pipeline, "definetherain". *J. Virol. Methods* 202, 46–53. doi: 10.1016/j.jviromet.2014.02.020

Kochanová, M., Zouhar, M., Prokinová, E., and Ryšánek, P. (2004). Detection of *Tilletia controversa* and *Tilletia caries* in wheat by PCR method. *Plant Soil Environ.* 50, 75–77. doi: 10.17221/3684-pse

Kubista, M., Andrade, J. M., Bengtsson, M., Forootan, A., Jonák, J., Lind, K., et al. (2006). The real-time polymerase chain reaction. *Mol. Aspects Med.* 27, 95–125. doi: 10.1016/j.mam.2005.12.007

Lillsunde Larsson, G., and Helenius, G. (2017). Digital droplet PCR (ddPCR) for the detection and quantification of HPV 16, 18, 33 and 45 - a short report. *Cell. Oncol.* 40, 521–527. doi: 10.1007/s13402-017-0331-y

Liu, J., Li, C., Muhae-ud-din, G., Liu, T., and Chen, W. (2020). Development of the droplet digital PCR to detect the teliospores of *Tilletia controversa* kühn in the soil with greatly enhanced sensitivity. *Front. Microbiol.* 11. doi: 10.3389/fmicb.2020.00004

McDonald, J. G., Wong, E., and White, G. P. (2000). Differentiation of *Tilletia* taxa by rep-PCR genomic fingerprinting. *EPPO Bull.* 30, 549–553. doi: 10.1111/j.1365-2338.2000.tb00945.x

Menzies, J. G., Knox, R. E., Popovic, Z., and Procunier, J. D. (2006). Common bunt resistance gene Bt10 located on wheat chromosome 6D. *Can. J. Plant Sci.* 86, 1409–1412. doi: 10.4141/p06-106

Mourad, A., Mahdy, E., Bakheit, B. R., Abo-Elwafaa, A., and Baenziger, P. S. (2018). Effect of common bunt infection on agronomic traits in wheat (*Triticum aestivum* L.). *J. Plant Genet. Breed* 2, 1–7.

Nian, S. J., Yin, Y. P., Yuan, Q., Xia, Y. X., and Wang, Z. K. (2007). Selection of differential DNA fragment of *Tilletia controversa* kühn and establishment of molecular detection approach. *Acta Microbiologica Sinica (In Chin)* 47, 725–728.

Pavšič, J., Žel, J., and Milavec, M. (2016). Assessment of the real-time PCR and different digital PCR platforms for DNA quantification. *Anal. Bioanal. Chem.* 408, 107–121. doi: 10.1007/s00216-015-9107-2

Peterson, G. L., Whitaker, T. B., Stefanski, R. J., Podleckis, E. V., Phillips, J. G., Wu, J. S., et al. (2009). A risk assessment model for importation of united states milling wheat containing *Tilletia contraversa*. *Plant Dis.* 93, 560–573. doi: 10.1094/PDIS-93-6-0560

Pieczul, K., Perek, A., and Kubiak, K. (2018). Detection of *Tilletia caries*, t*illetia laevis* and *Tilletia controversa* wheat grain contamination using loop-mediated isothermal DNA amplification (LAMP). *J. Microbiol. Methods* 154, 141–146. doi: 10.1016/j.mimet.2018.10.018

Pinheiro, L. B., Coleman, V. A., Hindson, C. M., Herrmann, J., Hindson, B. J., Bhat, S., et al. (2012). Evaluation of a droplet digital polymerase chain reaction format for DNA copy number quantification. *Anal. Chem.* 84, 1003–1011. doi: 10.1021/ac202578x

Raguseo, C., Gerin, D., Pollastro, S., Rotolo, C., Rotondo, P. R., Faretra, F., et al. (2021). A duplex-droplet digital PCR assay for simultaneous quantitative detection of *Monilinia fructicola* and *Monilinia* laxa on stone fruits. *Front. Microbiol.* 12. doi: 10.3389/fmicb.2021.747560

Schamann, A., Schmidt-Heydt, M., and Geisen, R. (2022). Analysis of the competitiveness between a non-aflatoxigenic and an aflatoxigenic *Aspergillus flavus* strain on maize kernels by droplet digital PCR. *Mycotoxin Res.* 38, 27–36. doi: 10.1007/s12550-021-00447-7

Suo, T., Liu, X., Feng, J., Guo, M., Hu, W., Guo, D., et al. (2020). ddPCR: a more accurate tool for SARS-CoV-2 detection in low viral load specimens. *Emerg. Microbes Infect.* 9, 1259–1268. doi: 10.1080/22221751.2020.1772678

Xu, T., Yao, Z., Liu, J., Zhang, H., Din, G. M. U., Zhao, S., et al. (2020). Development of droplet digital PCR for the detection of *Tilletia laevis*, which causes common bunt of wheat, based on the SCAR marker derived from ISSR and real-time PCR. *Sci. Rep.* 10, 16106. doi: 10.1038/s41598-020-72976-7

Župunski, V., Ignjatović-Micić, D., Nikolić, A., Stanković, S., Jevtić, R., Lević, J., et al. (2011). Identification of tilletia species using rep-PCR fingerprinting technique. *Genetika* 43, 183–195. doi: 10.2298/GENSR1101183Z

frontiers | Frontiers in Plant Science

TYPE Review
PUBLISHED 24 January 2023
DOI 10.3389/fpls.2023.1106784

OPEN ACCESS

EDITED BY
Rahul Kumar Tiwari,
Indian Council of Agricultural Research (ICAR), India

REVIEWED BY
Ashish Kumar Singh,
Vivekananda Parvatiya Krishi Anusandhan Sansthan (ICAR), India
Lee Robertson,
National Institute of Agricultural and Food Research and Technology, Spain

*CORRESPONDENCE
Huan Peng
penghuan@caas.cn
Enliang Liu
liuenliang@cau.edu.cn

†These authors have contributed equally to this work and share first authorship

SPECIALTY SECTION
This article was submitted to Plant Pathogen Interactions, a section of the journal Frontiers in Plant Science

RECEIVED 24 November 2022
ACCEPTED 10 January 2023
PUBLISHED 24 January 2023

CITATION
Shao H, Zhang P, Peng D, Huang W, Kong L-a, Li C, Liu E and Peng H (2023) Current advances in the identification of plant nematode diseases: From lab assays to in-field diagnostics.
Front. Plant Sci. 14:1106784.
doi: 10.3389/fpls.2023.1106784

Current advances in the identification of plant nematode diseases: From lab assays to in-field diagnostics

Hudie Shao[1,2†], Pan Zhang[2†], Deliang Peng[1], Wenkun Huang[1], Ling-an Kong[1], Chuanren Li[2], Enliang Liu[3*] and Huan Peng[1*]

[1]State Key Laboratory for Biology of Plant Diseases and Insect Pests, Institute of Plant Protection, Chinese Academy of Agricultural Sciences, Beijing, China, [2]College of Agriculture, Yangtze University, Jingzhou, Hubei, China, [3]Grain Crops Institute, XinJiang Academy of Agricultural Sciences, Urumqi, China

Plant parasitic nematodes (PPNs) cause an important class of diseases that occur in almost all types of crops, seriously affecting yield and quality and causing great economic losses. Accurate and rapid diagnosis of nematodes is the basis for their control. PPNs often have interspecific overlays and large intraspecific variations in morphology, therefore identification is difficult based on morphological characters alone. Instead, molecular approaches have been developed to complement morphology-based approaches and/or avoid these issues with various degrees of achievement. A large number of PPNs species have been successfully detected by biochemical and molecular techniques. Newly developed isothermal amplification technologies and remote sensing methods have been recently introduced to diagnose PPNs directly in the field. These methods have been useful because they are fast, accurate, and cost-effective, but the use of integrative diagnosis, which combines remote sensing and molecular methods, is more appropriate in the field. In this paper, we review the latest research advances and the status of diagnostic approaches and techniques for PPNs, with the goal of improving PPNs identification and detection.

KEYWORDS

plant parasitic nematodes, diagnosis, PCR, Isothermal amplification, remote sensing, field detection

1 Introduction

The phylum Nematoda is one of the largest in the animal kingdom, including many species and a wide variety of lifestyles. More than 25 000 nematode species are currently known (Zhang, 2013). Of these, 50% are marine salt water and 25% dwell in soil and freshwater. (Hassan et al., 2015). Over 4100 species of PPNs have been described to date (Decraemer and Hunt, 2006) representing an important constraint on global food security. They parasitize a wide range of plant species, including monocots and dicots, and are one of the most severe limiting factors for major crops, causing an estimated annual crop loss of at

least 80$ billion worldwide (Nicol et al., 2011). Nematode diseases are difficult to control because their symptoms could be largely inapparent, hence, they are often overlooked. Nematode identification and differentiation can allow accurate decisions for the control of these plant parasites and the conservation of non-parasitic nematodes.

The challenge in differentiating nematodes is not only the selection of the most accurate and suitable methods, but also due to other factors possibly effects the performance of the identification assays, such as the small size of the nematode, the high number of nematodes found in the samples, and/or the lack of particular morphological characteristics. (Floyd et al., 2002; Chitwood, 2003). The traditional classification of PPNs is based on morphological characteristics combined with morphometric values. The variations in some of these morphological and morphometric features are often conjectural, subtle, and have overlapping characteristics or show intraspecific variation that compromises accurate identification or may result in mistaken identification of species (Oliveira et al., 2011). Moreover, morphological identification is complex and time-consuming, requiring specialized and experienced researchers to be accurate (Carneiro et al., 2017).

The recent rapid development of Polymerase Chain Reaction (PCR)-based methods has facilitated their wide use for the detection and identification of PPNs. Since its invention, PCR has been one of the most prevalent and essential molecular biology methods. Currently, the PCR detection techniques applied to PPNs mainly include DNA barcoding, restriction fragment length polymorphism of the internal transcribed spacer region of ribosomal DNA (ITS-RFLP), sequence characterized amplified regions (SCAR), random amplified polymorphic DNA (RAPD), and Real-time Quantitative Polymerase Chain Reaction (RT-qPCR). Many target genes for PCR methods have been used to identify PPNs using the universal primers (Table 1),such as rDNA -ITS, rDNA - intergenic spacer region (IGS) (Wishart et al., 2002), 28S D2-D3 (Vallejo et al., 2021), heat shock proteins (Green et al., 2019), 18S (small subunit; SSU) (Floyd et al., 2002), and mitochondrial DNA (mtDNA) (Stanton et al., 1997). These molecular approaches compensate for the failings of traditional morphological identification to a certain extent. One or more nematode species can be detected in a mixed sample by a PCR assay, reducing the time and cost of diagnosis (Keçici et al., 2022).

The advent of detection techniques for isothermal amplification, including loop-mediated isothermal amplification (LAMP) and recombinase polymerase amplification (RPA), provides additional options for the identification of PPNs. These technologies are characterized by high specificity and sensitivity. These two methods combined with the Lateral Flow Dipstick (LFD) allow for the clear visualization of the amplification products in the field, which can be identified by the naked eye (Yao et al., 2021). They also work well for field or point-of-service-based nematode detection and diagnosis. The combination of CRISPR Cas12a with RPA and LAMP methods has a detection sensitivity at the attomolar level. The specificity is enhanced by the isothermal detection technique (Gootenberg et al., 2017). CRISPR/Cas12a-based nucleic acid detection technology has been successfully used to test *Heterodera schachtii* (Yao et al., 2021), *H. avenae*, and *H. filipjevi* (Shao et al., 2022). Additionally, the development of remote sensing technology has brought new opportunities for extensive field monitoring and management of nematodes.

This article is a review of common methods for the identification of PPNs, which focuses on new isothermal amplification technologies and remote sensing methods capable of revolutionizing the approach for PPNs detection in the field.

2 Biochemical detection methods for PPNs

2.1 Isozymes analyses

Enzyme phenotyping methods, also named multifocal enzyme electrophoresis (MEE), were determined by the transport modes of isozymes, as variations in charges, molecular volumes and conformations arise from slight changes in their amino acid composition (Bogale et al., 2020). This method has the advantages of high stability, high polymorphism, and accuracy (Carneiro et al., 2017). It was first applied in the early 1970s for the identification of several common root-knot nematodes (*Meloidogyne* spp.) (Dickson et al., 1970). Many root-knot nematodes including *Meloidogyne javanica*, *M. incognita*, *M. arenaria*, *M. exigua*, and *M. paranaensis* have been identified using isozyme techniques (Carneiro et al., 2004; Carneiro et al., 2008; Muniz et al., 2008). Although this technique has been studied for other nematodes such as *H. glycines*, *Ditylenchus triformic*, and *Aphelenchus avenae* (Dickson et al., 1970), it has been best applied only for root-knot nematodes. The main reason is that certain proteins are only expressed at specific stages of the nematode life cycle, hence the isozyme extraction has strict requirements vis a vis the worm's state (Esbenshade and Triantaphyllou, 1985; Esbenshade and Triantaphyllou, 1990). Generally, only young females can be used. Except for root-knot nematodes, young females of other plant nematode species are relatively difficult to obtain.

2.2 Mass spectral analyses

Matrix-assisted laser desorption/ionization time-of-flight mass spectrometry (MALDI-TOF MS) has been widely used as a diagnostic technology in laboratories for the analysis of complex molecules, by producing protein fingerprint signatures from protein extracts of organisms (Bizzini et al., 2010). MALDI-TOF MS is a highly sensitive, rapid, and reliable diagnosis method (Seng et al., 2009; Sandrin et al., 2013). Recently, researchers have discovered that MALDI biotechnology can be used for viruses, protozoa, and arthropods in addition to bacteria, mycobacteria, and fungi (Sjöholm et al., 2008; Yssouf et al., 2016; Angeletti, 2017; Vega-Rúa et al., 2018). Today, MALDI-TOF MS has also been applied for the identification of the PPNs *Anguina tritici*, *A. funesta*, *M. javanica* and *M. incognita* (Perera et al., 2005; Ahmed et al., 2011). With the increasing development of MALDI-TOF MS technology, the reduction of instrument cost, and the improvement of related databases, the technique will become a powerful tool for PPNs identification soon.

10.3389/fpls.2023.1106784

TABLE 1 Some universal primer combinations used for amplification of ribosomal RNA genes of PPNs.

Primercombination and code(direction)	Primersequence(5′-3′)	Amplified region	References
G18SU(f)	GCTTGCCTCAAAGATTAAGCC	18SrRNA	(Blaxter et al., 1998)
R18Tyl1(r)	GGTCCAAGAATTTCACCTCTC		(Chizhov et al., 2006)
F18Tyl2(f)	CAGCCGCGGTAATTCCAGC	18SrRNA	(Chizhov et al., 2006)
R18Tyl2(r)	CGGTGTGTACAAAGGGCAGG		
988F(f)	CTCAAAGATTAAGCCATGC	18SrRNA	(Holterman et al., 2006)
1912R(r	TTTACGGTCAGAACTAGGG		
1096F(f)	GGTAATTCTGGAGCTAATAC	18SrRNA	(Holterman et al., 2006)
1912R(r)	TTTACGGTCAGAACTAGGG		
1813F(f)	CTGCGTGAGAGGTGAAAT	18SrRNA	(Holterman et al., 2006)
2646R(r)	GCTACCTTGTTACGACTTTT		
SSU_F_04	GCTTGTCTCAAAGATTAAGCC	18SrRNA	(Blaxter et al., 1998)
SSU_R_09	AGCTGGAATTACCGCGGCTG		
SSU_F_22	TCCAAGGAAGGCAGCAGGC	18SrRNA	(Blaxter et al., 1998)
SSU_R_13	GGGCATCACAGACCTGTTA		
SSU_F_23	ATTCCGATAACGAGCGAGA	18SrRNA	(Blaxter et al., 1998)
SSU_R_81	TGATCCWKCYGCAGGTTCAC		
designated Nem_18S_F	CGCGAATRGCTCATTACAACAGC	18SrRNA	(Floyd et al., 2005)
Nem_18S_R	GGGCGGTATCTGATCGCC		
18S-CL-F3	CTTGTCTCAAAGATTAAGCCATGCAT	18SrRNA+ ITS1-5.8S- ITS2rRNA+ 28SrRNA	(Carta and Li, 2018; Carta and Li, 2019)
28S-CL-R	CAGCTACTAGATGGTTCGATTAGTC		
18S(f)	TTGATTACGTCCCTGCCCTTT	ITS1-rRNA	(Vrain et al., 1992)
rDNA1.58S(r)	ACGAGCCGAGTGATCCACCG		(Szalanski et al., 1997)
TW81(f)	GTTTCCGTAGGTGAACCTGC	ITS1-rRNA	(Curran et al., 1994)
5.8SM5(r)	GGCGCAATGTGCATTCGA		(Zheng et al., 2000)
18S(f)	TTGATTACGTCCCTGCCCTTT	ITS1-5.8S- ITS2rRNA	(Vrain et al., 1992)
26S(r)	TTTCACTCGCCGTTACTAAGG		
F194(f)	CGTAACAAGGTAGCTGTAG	ITS1-5.8S- ITS2rRNA	(Ferris et al., 1993)
F195(r)	TCCTCCGCTAAATGATATG		
TW81(f)	GTTTCCGTAGGTGAACCTGC	ITS1-5.8S- ITS2rRNA	(Curran et al., 1994)
AB21(r)	ATATGCTTAAGTTCAGCGGGT		
D2A(f)	ACAAGTACCGTGAGGGAAAGTTG	D2-D3of28S rRNA	(Nunn, 1992)
D3B(r)	TCGGAAGGAACCAGCTACTA		
D2Tyl(f)	GAGAGAGTTAAANAGBACGTGA	D2-D3of28S	(Chizhov et al., 2012)
D3B(r)	TCGGAAGGAACCAGCTACTA	rRNA	(Nunn, 1992)
D2A(f)	ACAAGTACCGTGAGGGAAAGTTG	D2of 28S rRNA	(Nunn, 1992)
D2A(r)	GACCCGTCTTGAAACACGGA		

3 Molecular diagnosis of PPNs

3.1 Traditional PCR methods

3.1.1 RFLP

RFLP uses restriction enzymes to either digest genomic DNA or amplified fragments, producing DNA banding patterns based on sequence divergence (Brown, 1981). The RFLP technique has the characteristics of high sensitivity, a requirement for a low amount of DNA, rapidity, and accuracy (Jarcho, 2001). The technique was first applied to the identification of nematode species by Curran et al. (1985). This method has been applied successively to identify root-knot nematodes and their physiological subspecies (Curran et al., 1986; Powers and Sandall, 1988; Zijlstra et al., 1995), *Xiphinema aameracanum* (Vrain, 1993), *Diylenchus* spp. (Wendt et al., 1993; Mahmoudi et al., 2020), *Bursaphelenchus* spp. (Aikawa et al., 2013), and *Heterodera* spp. (Zheng et al., 2003; Ou et al., 2008b; Baklawa et al., 2015). Although this method is valid in differentiating nematode isolates, it is less frequently used today owing to the complicated nature of its technique and the need for significant numbers of target DNA, usually requiring pre-culture of nematode populations (Currie et al., 2000).

3.1.2 RAPD and SCAR

The RAPD method was invented by Williams et al. (1991) and is a novel genetic marker. The method involves PCR amplification of target DNA using a random sequence of 9–10 nucleotides as a primer. Polymorphism can occur due to a difference of one base in the DNA sequence from the complementary oligonucleotide primer. The use of RAPD markers for PPNs identification has the benefits of rapidity, ease, and sensitivity. Caswell-Chen et al. (1992) distinguished *H. curicifrae* from *H. schachtii* by RAPD and detected differences among six geographic populations of *H. schachtii*. Subsequently, this method was studied on both root-knot nematodes and cyst nematodes (Cenis, 1993). Because the RAPD assay is performed at a low temperature, creating a lower degree of severity for primer reductions, and replicability, in particular between laboratories. It also imposes a restriction, making it impossible to use in the field.

To compensate for the shortcomings of RAPD, it can be converted into a SCAR marker technique as proposed and applied by Paran and Michelmore in 1993. This technique not only has the characteristics of high specificity and sensitivity of the RAPD method, but has the advantages of good stability and reproducibility (Li et al., 2022). This method solves the problem of long primers and a high annealing temperature for RAPD. Fullaondo et al. (1999) transformed RAPD markers into SCAR markers to differentiate between *Globodera rostochiensis* and *G. pallida*. Subsequently, SCAR markers have been successfully used to identify *Meloidogyne* spp. (Lecouls et al., 1999; Zijlstra et al., 2000; Randig et al., 2002), *Heterodera* spp. (Ou et al., 2008a; Qi et al., 2012; Liu et al., 2014; Jiang et al., 2021), and *Bursaphelenchus* spp. (Chen et al., 2011; Feng et al., 2011).

3.1.3 DNA barcoding

The DNA barcoding technique was first proposed by Hebert et al. (2003), and it uses a universal barcode to build a barcode database and analyze DNA data based on sample information to achieve identification. The advantages of this method are high primer versatility, a stable amplification system, a convenient fragment size, and low DNA sample quality requirements (Ahmed et al., 2015). DNA barcoding techniques have recently been used to study the species and phylogenetic relationships of nematodes including *Meloidogyne* spp. (Rashidifard et al., 2019), *Heterodera* spp. (Subbotin et al., 2019), and *Bursaphelenchus* spp. (Wang et al., 2015). Metabarcoding is a combination of barcoding and high-throughput sequencing (NGS). Metabarcoding was described by Taberlet et al. (2012) as the automatic identification of multiple species from a single bulk sample including several different taxa. Waite et al. (2003) used this method for community analysis of nematodes using 18S rDNA. Palomares-Rius et al. (2017) applied barcoding methods using mtDNA and rDNA regions to the phylogenetic analysis of PPNs from *Longidoridae* (Nematoda, Enoplea). There are several difficulties in the analysis of DNA metabarcoding of environmental DNA (eDNA). The eDNA is susceptible to contamination during sampling, extraction, and storage; the availability of species-specific DNA barcodes relies on the mass of the available databases. The identification of PPNs species is difficult due to the lack of available data for DNA barcoding of most known plant nematodes (Sikder et al., 2020). DNA barcoding is a tool with much potential for taxonomy. Currently, the metabarcoding technique is little utilized for PPNs detection and can be more developed in the future for PPNs identification.

3.1.4 Quantitative real-time PCR (qPCR)

The fluorescent qPCR technique adds fluorescent moieties to a PCR reaction system and monitors the entire PCR process in real-time by the accumulation of the fluorescent signal. The qPCR method allows continuous monitoring of the sample during PCR using fluorescence probes or double-stranded dyes such as SYBR Green I. The method is used to quantify the unknown template by means of a standard curve. The qPCR method has the advantages of sensitivity, reliability, safety, and allowing high throughput (Smith and Osborn, 2009). A quantitative PCR technique has been developed for targeting PPNs, containing *M. enterolobii* (Kiewnick et al., 2015), *M. javanica*, *Xiphinema elongatum*, and *Pratylenchus zeae* (Berry et al., 2008), *P. penetrans* (Sato et al., 2007), *H. avenae* and *H. latipons* (Toumi et al., 2013), *H. schachtii* (Madani et al., 2005), and *H. glycines* (Goto et al., 2009; Baidoo et al., 2017). Specific technologies for PPNs identification and quantification directly from the soil or plant tissues before DNA extraction and amplification have been recently explored (Goto et al., 2009; Lopez-Nicora et al., 2012; Li et al., 2014; Jian et al., 2022). These molecular detection methods can reduce the time and labor required for identification since they eliminate the need to extract nematodes from the soil and microscopy. Although qPCR is a sensitive method for detecting low concentrations of target DNA, its use for the identification of PPNs is hampered by its cost and dependence on expensive equipment.

3.1.5 Droplet digital PCR (ddPCR) technology

The concept of digital PCR was first described in 1992 by Sykes et al. (1992). It quantifies DNA molecules using a combination of the Poisson distribution and the dilution of templates to the single

molecule level (Espy et al., 2006). The principle of ddPCR is to reduce a traditional PCR reaction mixture, which is like the Taqman assay, into a smaller reaction system either by diluting it in microwell plates, oil emulsion, or capillaries (Rougemont et al., 2004). It has the advantage of being very accurate at very low concentrations, with less contamination, and may be easier to sample for some diseases that are difficult to diagnose accurately (Li et al., 2018). Compared to qPCR, the ddPCR system could be used for the absolute quantitation of DNA copy numbers. The ddPCR method has high sensitivity and does not depend on a pre-enrichment for templates in extremely low concentrations. The ddPCR method has been successfully introduced into the clinic for the diagnosis of infectious diseases. Also the ddPCR has been utilized for the identification of a variety of plant pathogens including fungi, bacteria, and viruses. (Rani et al., 2019). Currently, this method has been applied to *M. enterolobii* (Chen et al., 2022).

3.2 Isothermal amplification technologies

3.2.1 LAMP

LAMP is designed on based on automated cycling and high DNA strand replacement activity mediated by Bst polymerase. It uses 4-6 oligonucleotide primers to produce a significant amount of amplicons within 10-20min (Notomi et al., 2000). LAMP is becoming a popular assay for the detection of PPNs, because it is rapid, sensitive and easy to use in a point-of-service environment (Ahuja, 2020). The inclusion of a fluorescent dye in a positive LAMP reaction generated a color difference that enabled observation by the naked eye. (He et al., 2013). Moreover, it has also been advanced by using Lateral flow devices (LFDs) to confirm visually the existence of amplicons (Kiatpathomchai et al., 2008; Ding et al., 2010). The LAMP-LFD method allows both nucleic acid amplification and amplicon visualization to be conducted without any complex or costly equipment, which promises to enhance usability for field investigations and common field monitoring. However, the disadvantage of LAMP is that once the tube is opened, aerosol contamination can easily form, causing more serious problem of false positives. In combination with a real-time turbidimeter, LAMP results can be measured accurately and contamination can be avoided (Mori et al., 2004). With these benefits, LAMP technology has been packaged in commercially available assay kits for the testing of a diversity of pathogens which include viruses, fungi and bacteria. (Mori et al., 2001). The use of this method on PPNs has been very popular in recent years. In particular, LAMP technology has been developed for diagnosing many species of PPNs including *Bursaphelenchus* spp., *Meloidogyne* spp., *Anguina* spp., *Radopholus* spp., *Ditylenchus* spp., and *Tylenchulus* spp. (Table 2).

3.2.2 RPA

RPA is a novel, highly sensitive, isothermal DNA amplification and detection assay (Piepenburg et al., 2006). The technique is performed at 37-42°C and only requires a minimum number of DNA samples to amplify 1-10 target copies of DNA within 20 minutes (Sabate del Rio et al., 2017). RPA products can be detected by using fluorescent probes in real-time or by agarose gel electrophoresis or a lateral flow assay (Lobato and O'sullivan, 2018). The main advantages of RPA technology over other PCR detection technologies are that it is quick, sensitive, simple, and easy to use in the field. Compared to the LAMP, which needs 6-8 primers for amplification, RPA technology is simpler and requires only one pair of primers to finish amplification. RPA has been successfully applied to different species of target organisms including viruses, fungi, bacteria, animals and plants. (Lobato and O'sullivan, 2018). It has recently been reported to be highly effective in testing for a large range of PPNs including *M. javanica* (Chi et al., 2020), *M. enterolobii* (Subbotin, 2019), *M. hapla* (Subbotin and Burbridge, 2021), *B.*

TABLE 2 The application of the LAMP technique to plant parasitic nematodes.

Genus name	Nematode species	Target region	Host	References
Bursaphelenchus	*B. xylophilus*	ITS-rDNA	Pine	(Kikuchi et al., 2009)
	B. xylophilus	ITS-rDNA	Pinus armandii var.	(Kanetani et al., 2011)
	B. xylophilus	Pectate lyase-3	Pine	(Kang et al., 2015)
	B. cocophilus	D2-D3 of rDNA	coconut and oil palm trees	(Ide et al., 2017)
Meloidogyne	*Meloidogyne incognita*, *M. arenaria*, *M. javanica*, *M. hapla*	ITS of rDNA	tomato	(Niu et al., 2011)
	M. enterolobii	5S rDNA-IGS2	tomato	(Niu et al., 2012)
	M. mali	ITS-5.8S rDNA	tomato	(Zhou et al., 2017)
	M. chitwoodi and *M. fallax*	IGS2-18S	tomato	(Zhang and Gleason, 2019)
	M. partityla	ITS-5.8S rDNA	mature pecan trees	(Waliullah et al., 2020)
Anguina	*A. wevelli*	ITS rDNA	—	(Yu et al., 2018)
	A. agrostis	ITS rDNA	—	(Yu et al., 2020)
Radopholus	*R. similis*	D2-D3 of rDNA	*Anthurium*	(Peng et al., 2012)
Ditylenchus	*D. destructor*	28S rRNA	patato	(Deng et al., 2019)
Tylenchulus	*T. semipenetrans*	ITS-rDNA	cirus orchards	(Lin et al., 2016)
	T. semipenetrans	ITS1	*citrus* rhizosphere soil	(Song et al., 2017)

xylophilus, M. incognita, *M. javanica*, and *M. arenaria* (Ju et al., 2019) (Table 3). Although RPA has been described as highly specific, it has been reported that RPA depends on the number and distribution of mismatches in sequences of closely related DNA molecules. If one or more bases are mismatched, nematode populations cannot be differentiated based on their distribution.

Coupling RPA with CRISPR (Cas) systems identifies stable differences in individual bases. Cas12a and CRISPR form ribonucleoprotein, which recognizes the protospacer adjacent motif (PAM) site on the target nucleic acid and then guides the effector Cas protein to shear the target sequence. The Cas12a enzyme can non-specifically be a shear single-stranded DNA reporter-labeled fluorophore and quencher (Chen et al., 2018). It has been concluded that RPA- CRISPR/Cas12a is more sensitive and specific than RPA alone. The PPNs *H. schachtii* (Yao et al., 2021), *H. avenae*, and *H. filipjevi* (Shao et al., 2022) have been detected using RPA-CRISPR/Cas12a technology. The combination of LAMP and CRISPR/Cas12a can also be used for pathogen detection. The use of Cas12a is a powerful method for virus detection (Broughton et al., 2020) set up a DETECTOR platform that combined RT-LAMP and CRISPR/Cas12a for SARS-CoV-2 diagnosis. In the future, this technique could also be applied to the detection of PPNs.

4 Direct detection of PPNs in the field

In order to truly implement field testing, the feasibility of field operation encompassing the entire detection process must be considered, including sample handling, the amplification process, and visualization of the results. In a previous study, isolating nematodes from a Baermann funnel or directly picking nematodes from plant root galls was time-consuming and required specialized techniques. DNA could be extracted directly from plant root nodules using the Flinders Technology Associates (FTA) technique, reducing the cost and time for diagnosis by simplifying sample storage, transport, and extraction. All of the steps of FTA-based archiving and DNA preparation are carried out at room temperature, which significantly reduces the expense and is environmentally friendly (Marek et al., 2014). FTA technology has been used for the DNA extraction of *D. dipsaci*, *H. schachtii*, and *M. hapla* (Marek et al., 2014; Peng et al., 2017). The drawback of this method is that it is limited to the extraction of pathogenic DNA from plant tissues and cannot be utilized for the extraction of DNA from soil or other media. Commercial kits for direct extraction of nematode soil DNA have now been developed and used successfully in several laboratories. The use of these kits also saves the time consumed by nematode isolation and the cost of instruments. Using only a small amount of DNA in this template, the target nematode can be detected. Soil DNA, including that from *Pratylenchus neglectus*, *P. thornei*, *M. incognita, R. similis*, and *H. schachtii*, was extracted using soil kits for the successful detection of these nematodes (Yan et al., 2008; Hu et al., 2011; Min et al., 2011; Peng et al., 2012; Jiang et al., 2021; Yao et al., 2021). Although this method has several advantages such as time-saving, simplicity, and efficiency, the soil kit can extract no more than 10 g of soil at a time. The uneven distribution of nematodes makes it difficult to extract DNA containing the target nematodes. This problem might be solved by repeating the assay multiple times to improve the detection rate for nematodes. In the amplification stage, using RPA and LAMP techniques or these two methods combined with CRISPR/Cas12a allows DNA amplification in 15-60 min without thermal cycling and expensive instruments (i.e., PCR instruments or fluorescence PCR instruments) compared to conventional PCR. It offers the possibility of field application for PPNs detection. The results of a combination of LFD technology and these methods are visible to the naked eye. RPA combined with the CRISPR/Cas12 assay has been applied to the detection of the PPN *H. schachtii* in the field (Yao et al., 2021), *H. avenae, and H. filipjevi* (Shao et al., 2022). Therefore, the combination of the FTA technique, the kit method for soil sample extraction, and a combination of LFD technology and RPA/LAMP-CRISPR/Cas12 can fully and truly realize the field detection of nematodes.

5 The remote sensing method for PPNs

Remote sensing is a method of observing and acquiring information about the properties of the studied entity without physically coming in contact with it (Kundu et al., 2022). The method could determine the

TABLE 3 Information about reported studies of RPA in nematodes.

Nematode species	Target	Time (min)	Temp (°C)	Sensitivity	References
M. enterolobii	IGS rRNA	20	37	1/10 of a second-stage juvenile(J2)	(Subbotin, 2019)
M. javanica	SCAR marker	40	39	1 pg purified genomic DNA, or 0.01 adult female, or 0.1 J2	(Chi et al., 2020)
M. hapla	IGS rRNA	20	39	1/100 of a J2 and 1/1000 of a female	(Subbotin and Burbridge, 2021)
M. enterolobii, *M. incognita*, *M. javanica* and *M. arenaria*	SCAR marker	20	38	10^{-2}, 10^{-2}, 10^{-1}, and 10^{-1} dilutions of DNA from a single J2	(Ju et al., 2019)
H. schachtii	RAPD marker	15-60	37	10^{-4} single cysts and single females, 4^{-3} single second-stage juveniles, and a 0.001 ng genomic DNA	(Yao et al., 2021)
H. avenae and H. filipjevi	SCAR marker	15	35	10^{-4} single second-stage juvenile (J2), 10^{-5} single cyst, and 0.001 ng of genomic DNA	(Shao et al., 2022)
B. xylophilus	ITS2	25	37	308 ± 51 of *B. xylophilus* per 10 g of pinewood	

presence of a nematode species by the change of symptoms in the above-ground parts of a plant. It avoids damage to the host and saves time and cost of diagnosis. Remote sensing is a fast, non-invasive, and highly effective process of acquiring information that has a wide coverage. Various spectroscopic and imaging approaches have been performed for the detection of PPNs, such as visible, multiband, infrared, and fluorescence spectroscopy, fluorescence imaging, multispectral and hyperspectral imaging, thermography, and nuclear magnetic resonance spectroscopy. Norman and Fritz (1965) were the first to use infrared sensors for pre-sign detection of *R. similis* in citrus trees. Subsequently, *R. reniformis* was detected by Heald et al. (1972) using airborne infrared imaging methods in cotton fields. Heath et al. (2000) predicted the amount of the nematodes *G. rostochiensis* and *G. pallida* on potatoes based on non-destructive hyperspectral measurements with a combination of GIS and RS technologies. Remote sensing coupled with GIS technologies was employed to identify and quantify an *H. glycines* population (Nutter et al., 2002). Three data preprocessing approaches were tested to evaluate their suitability for detecting *H. schachtii* and *R. solanii* (Hillnhutter et al., 2012). Pine wood nematode disease was discovered by Pan et al. (2014) based on hyperspectral remote sensing technology. Three methods, visible light imaging, thermometry and spectroscopy, were compared for their ability to detect *H. schachtii* in two sugar beet varieties (Joalland et al., 2017). Currently, remote sensing techniques have accuracy issues, as some nematodes are misdiagnosed due to similar symptoms and a lack of sufficient survey data for nematode surveillance modeling.

6 Machine learning for PPNs identification

Machine Learning or Artificial intelligence (AI) is a novel technology for nematode identification and quantitation based on image analysis (Bogale et al., 2020). It is an effective method for processing a large number of samples and identifying unique and minute items such as nematodes eggs and cysts in a complex background (Akintayo et al., 2018). Biological image datasets for multiple genera of PPNs were established and used to identify them based on the deep convolutional neural networks (CNNs) method (Lu et al., 2021). A convolutional CNNs model for identification of nematodes in soybean crop was developed by Abade et al. (2022).AI or Deep learning combined with hyperspectral image analysis is more popular because of the advantages this assay presents over direct soil methods (Arjoune et al., 2022). A combination of infrared spectra analysis and AI assay was used to detect rootknot nematode *M. enterorlobii* at the early stage of infection (San-Blas et al., 2020). AI, a relatively new technology, is gradually being applied to the field of PPNs detection. Though the technique could overcome the drawbacks of reduced specialist and subjective judgment, the generation of sufficient data may become a bottleneck in the development of AI.

7 Conclusion and future perspectives

In this article, we reviewed various existing methods for the detection and diagnosis of PPNs, such as morphological and biochemical methods, traditional PCR, isothermal amplification technologies, and remote sensing techniques. Practically, no single method or technique exists for diagnosing PPNs. Each approach has its strengths and weaknesses, therefore, we concluded the characteristics of each method (Table 4). Morphology-based classification forms the foundation of taxonomy, but morphological and morphometric characters are subtle and subjective, which may lead to inaccurate identification of a species (Floyd et al., 2002; Chitwood, 2003). In the future, the Protein-based approach play an important role in studies of species identification. However, the complexity of protein expression patterns and the ease of degradation of extracted proteins may affect the accuracy of the assessment; this restriction is the major challenge in the use of this technique. PCR molecular marker technologies have been

TABLE 4 Comparison of different plant nematode detection methods.

Category	Technology	Advantages	Disadvantages	Site	References
Morphology	Morphological methods	Intuitive, low cost	Difficult to judge accurately; complex to operate and requires specialized technicians	In the lab	(Oliveira et al., 2011)
Biochemical Methods	Isozymes	It can reflect phylogenetic relationships; High sensitivity	Mainly used only for root-knot nematodes; Time-consuming		(Dickson et al., 1970)
	Mass spectral analyses	fast, reliable, high sensitivity	Time- consuming, requires specialized skills		(Rivero et al., 2022)
PCR Methods	DNA barcoding	Accuracy	Time-consuming		(Hebert et al., 2003)
	Droplet digital PCR	High sensitivity and low amount of template DNA	Expensive reagents and instruments		(Rougemont et al., 2004)
	Gene chip technology	Fast, accuracy	Expensive equipment, immature technology		(Fodor, 1997)
	RFLPs	Reliable and reproducible	Complex operations, requiring large amounts of DNA		Blok and Powers, 2009
	RAPD	Generates a large amount of information			

(Continued)

TABLE 4 Continued

Category	Technology	Advantages	Disadvantages	Site	References
			Lacks repeatability, requires strict experimental reaction		(Feng et al., 2005)
	SCAR	High sensitivity and specificity	Time-consuming		(Chen et al., 2011)
	RT-qPCR	Sensitive, reliable	Time- consuming, equipment relatively expensive		(Berry et al., 2008)
	ddPCR	High sensitivity, Simple, convenient	Expensive instruments		Chen et al., 2022)
Isothermal Amplification Technology	LAMP	Low cost, simple operation, low equipment demand	False-positive results	Outdoors and in the field	(Ahuja and Somvanshi, 2021)
	RPA	Fast, high sensitivity and specificity, Low cost, simple operation, low equipment demand, visualization of results	False-positive results; Required to design specific primers, probes, and gRNA		(Babu et al., 2018)
	LRPA-CRISPR/ Cas12a				
Spectral techniques	Remote sensing systems	Fast, large-area detection, dynamic monitoring	Requires technical personnel expertise, difficult to capture detailed changes		(Tao et al., 2020)
Machine Learning	Artificial intelligence	fast, accurate and eliminate human errors	Lack of professional classification experts and a sufficient number of databases	In the lab	(Almalki, 2022)

widely used for PPNs detection, which compensate for the lack of morphological identification. The representative PCR, ddPCR, and qPCR technologies use dynamics of denaturation that drive replication events in control, and show excellent testing capability (Agüero et al., 2003; Mika et al., 2020; Wang et al., 2020). However, the requirements for expensive equipment and lack of trained scientist lead to their restriction for use in the laboratory and field detection. The isothermal amplification method is suitable for field testing because it does not require a device for temperature loop control (Niemz et al., 2011). The isothermal amplification technique takes much less time and cost than conventional PCR amplification. Among isothermal amplification techniques, LAMP-LFD and RPA-LFD are quickly evolving in the field of identification, because of their obvious specificity, efficiency, and visualization (Figure 1). The previously

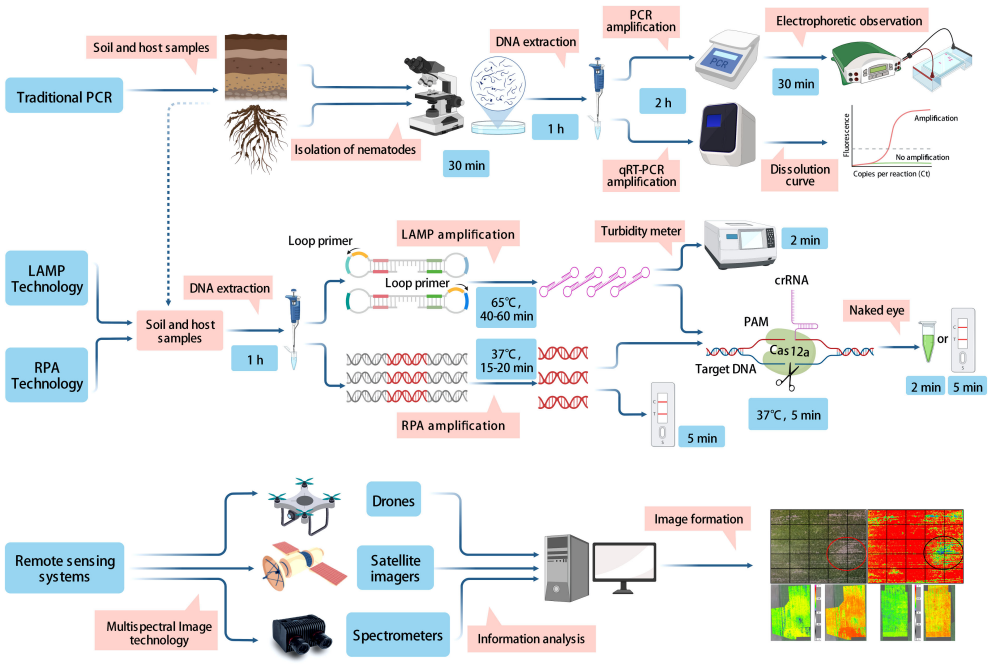

FIGURE 1
Demonstration of the principles and working processes involved in traditional PCR methods, isothermal amplification techniques, and remote sensing techniques.

mentioned techniques are only useful for identifying small-scale samples, but remote sensing techniques could be quickly applied to detect large infected areas in the field employing various instruments such as drones, spectrometers, and satellite imagers. Remote sensing technology has contributed greatly to the prediction of damage caused by PPNs in the field.

In the field, rapid and accurate early diagnosis of PPNs is essential to control nematode damage. PPNs mainly damage the root tissues of plants, symptoms on aboveground parts are often not apparent, and are difficult to differentiate with the naked eye unless the damage is particularly serious. At the early stage of a nematode infection, no obvious changes are evident in the aboveground parts of the plant. However, hyperspectral methods can find significant differences in the leaf area index, absorptivity, photosynthetically active radiation, or canopy depression. This may be due to changes in the chlorophyll content of the above-ground parts of the plant, causing a change in the spectrum of the host plant (Din et al., 2017). Thus, the first use of remote sensing technology would be a prediction of the presence of the location of nematode infestation in the field. While remote sensing techniques face the problem that many nematode symptoms (i.e., wavelength, lutein, and chlorophyll, etc.) are similar, it is difficult to capture these changes in detail, leading to misjudgment. To solve this problem, RPA/LAMP-LFD or RPA/LAMP-CRISPR/Cas and other detection methods can be used to accurately survey the samples in a potential occurrence area. Time and economic losses caused by the blind application and ineffective use of nematicide can be avoided. It is noteworthy that in the field environment, every step from sampling and nucleic acid extraction to obtaining test results is exposed to the risk of contamination. Therefore, the integration of sample pretreatment, target identification and signal acquisition into a single device to establish an integrated nucleic acid detection system is a major development trend for future pathogenic nematode detection.

Author contributions

Conceptualization, HP, DP, and EL; Article framework, L-aK, WH, and CL; software, HS and PZ; Literature collection, HS, CL, and PZ; writing—original draft preparation, HS and PZ; writing—review and editing, HP and EL; project administration, DP; funding support, HP. All authors contributed to the article and approved the submitted version.

Funding

This research was supported by the National Key R&D Program of China (2021YFD1400100), the National Natural Science Foundation of China (31972247), the Norwegian Ministry of Foreign Affairs (SINOGRAIN II, CHN-17/0019), the Open Fund of Key Laboratory of Integrated Pest Management on Crop in Northwestern Oasis, Ministry of Agriculture and Rural Affairs (KFJJ202101), and the Science and Technology Innovation Project of the Chinese Academy of Agricultural Sciences (ASTIP-2016-IPP-15).

Acknowledgments

The authors are truly grateful to Dr. Sulaiman Abdulsalam of the Ahmadu Bello University for English editing of the manuscript.

Conflict of interest

The authors declare that the research was conducted in the absence of any commercial or financial relationships that could be construed as a potential conflict of interest.

Publisher's note

References

Abade, A., Porto, L., Ferreira, P., and Vidal, F. (2022). NemaNet : A convolutional neural network model for identification of soybean nematodes. *Biosyst. Eng.* 213, 39–62. doi: 10.1016/j.biosystemseng.2021.11.016

Agüero, M., Fernández, J., Romero, L., Sánchez Mascaraque, C., Arias, M., and Sánchez-Vizcaíno, J. M. (2003). Highly sensitive PCR assay for routine diagnosis of African swine fever virus in clinical samples. *J. Clin. Microbiol.* 41, 4431–4434. doi: 10.1128/jcm.41.9.4431-4434.2003

Ahmed, H. A., Macleod, E. T., Hide, G., Welburn, S. C., and Picozzi, K. (2011). The best practice for preparation of samples from FTA®cards for diagnosis of blood borne infections using African trypanosomes as a model system. *Parasit. Vectors* 4, 68. doi: 10.1186/1756-3305-4-68

Ahmed, M., Sapp, M., Prior, T., Karssen, G., and Back, M. (2015). Nematode taxonomy: from morphology to metabarcoding. *Soil Discussions* 2, 1175–1220. doi: 10.5194/soild-2-1175-2015

Ahuja, A. (2020). Daignosis of plant parasitic nematodes using loop mediated isothermal amplification (LAMP): A review. *Crop Prot.* 147, 105459. doi: 10.1016/j.cropro.2020.105459

Ahuja, A., and Somvanshi, V. S. (2021). Diagnosis of plant-parasitic nematodes using loop-mediated isothermal amplification (LAMP). *A Rev. Crop Prot.* 147, 105459. doi: 10.1016/j.cropro.2020.105459

Aikawa, T., Kanzaki, N., and Maehara, N. (2013). ITS-RFLP pattern of bursaphelenchus xylophilus (Nematoda: Aphelenchoididae) does not reflect nematode virulence. *J. For. Res.* 18, 384–388. doi: 10.1007/s10310-012-0354-1

Akintayo, A., Tylka, G. L., Singh, A. K., Ganapathysubramanian, B., Singh, A., and Sarkar, S. (2018). A deep learning framework to discern and count microscopic nematode eggs. *Sci. Rep.* 8, 9145. doi: 10.1038/s41598-018-27272-w

Almalki, W. (2022). Advances in nematode identification: A journey from fundamentals to evolutionary aspects. *Diversity* 14, 536. doi: 10.3390/d14070536

Angeletti, S. (2017). Matrix assisted laser desorption time of flight mass spectrometry (MALDI-TOF MS) in clinical microbiology. *J. Microbiol. Methods* 138, 20–29. doi: 10.1016/j.mimet.2016.09.003

Arjoune, Y., Sugunaraj, N., Peri, S., Nair, S. V., Skurdal, A., Ranganathan, P., et al. (2022). Soybean cyst nematode detection and management: a review. *Plant Methods* 18, 110. doi: 10.1186/s13007-022-00933-8

Babu, B., Ochoa-Corona, F. M., and Paret, M. L. (2018). Recombinase polymerase amplification applied to plant virus detection and potential implications. *Analytical Biochem.* 546, 72–77. doi: 10.1016/j.ab.2018.01.021

Baidoo, R., Yan, G. P., Nelson, B., Skantar, A. M., and Chen, S. Y. (2017). Use of chemical flocculation and nested PCR for heterodera glycines detection in DNA extracts from field soils with low population densities. *Plant Dis.* 101, 1153–1161. doi: 10.1094/pdis-08-16-1163-re

Baklawa, M., Niere, B., Heuer, H., and Massoud, S. (2015). Characterisation of cereal cyst nematodes in Egypt based on morphometrics. *RFLP rDNA-ITS Sequence Analyses Nematol.* 17, 103–115. doi: 10.1163/15685411-00002855

Berry, S. D., Fargette, M., Spaull, V. W., Morand, S., and Cadet, P. (2008). Detection and quantification of root-knot nematode (Meloidogyne javanica), lesion nematode (Pratylenchus zeae) and dagger nematode (Xiphinema elongatum) parasites of sugarcane using real-time PCR. *Mol. Cell Probes* 22, 168–176. doi: 10.1016/j.mcp.2008.01.003

Bizzini, A., Durussel, C., Bille, J., Greub, G., and Prod'hom, G. (2010). Performance of matrix-assisted laser desorption ionization-time of flight mass spectrometry for identification of bacterial strains routinely isolated in a clinical microbiology laboratory. *J. Clin. Microbiol.* 48, 1549–1554. doi: 10.1128/jcm.01794-09

Blaxter, M. L., De Ley, P., Garey, J. R., Liu, L. X., Scheldeman, P., Vierstraete, A., et al. (1998). A molecular evolutionary framework for the phylum Nematoda. *Nature* 392, 71–75. doi: 10.1038/32160

Blok, V., and Powers, T. (2009). Biochemical and Molecular Identification. *Root-knot Nematodes*. 3, 21–32. doi: 10.1079/9781845934927.0098

Bogale, M., Baniya, A., and Digennaro, P. (2020). Nematode identification techniques and recent advances. *Plants-Basel* 9, 1260. doi: 10.3390/plants9101260

Broughton, J. P., Deng, X., Yu, G., Fasching, C. L., Servellita, V., Singh, J., et al. (2020). CRISPR-Cas12-based detection of SARS-CoV-2. *Nat. Biotechnol.* 38, 870–874. doi: 10.1038/s41587-020-0513-4

Brown, W. M. (1981). Mechanisms of evolution in animal mitochondrial DNA. *Ann. N Y Acad. Sci.* 361, 119–134. doi: 10.1111/j.1749-6632.1981.tb46515.x

Carneiro, R., Lima, F., and Correa, V. (2017). Methods and tools currently used for the identification of plant parasitic nematodes. *Nematology* 6, 45–60. doi: 10.5772/intechopen.69403

Carneiro, R., Santos, M., Almeida, M., Mota, F., Gomes, A., and Tigano, M. (2008). Diversity of meloidogyne arenaria using morphological, cytological and molecular approaches. *Nematology* 10, 819–834. doi: 10.1163/156854108786161526

Carneiro, R., Tigano, M., Randig, O., Almeida, M. R. ., and Sarah, J. L. . (2004). Identification and genetic diversity of meloidogyne spp. (Tylenchida: Meloidogynidae) on coffee from Brazil, central America and Hawaii. *Nematology* 6, 287–298. doi: 10.1163/1568541041217942

Carta, L. K., and Li, S. (2018). Improved 18S small subunit rDNA primers for problematic nematode amplification. *J. Nematol* 50, 533–542. doi: 10.21307/jofnem-2018-051

Carta, L. K., and Li, S. (2019). PCR amplification of a long rDNA segment with one primer pair in agriculturally important nematodes. *J. Nematol.* 51, 1–8. doi: 10.21307/jofnem-2019-026

Caswell-Chen, E. P., Williamson, V. M., and Wu, F. F. (1992). Random amplified polymorphic DNA analysis of heterodera cruciferae and h. schachtii populations. *J. Nematol* 24, 343–351. https://www.ncbi.nlm.nih.gov/pmc/articles/PMC2619296/

Cenis, J. L. (1993). Identification of four major meloidogyne spp. by random amplified polymorphic DNA (RAPD-PCR). phytopathology. *Phytopathology* 83, 76–80. doi: 10.1094/phyto-83-76

Chen, Y., Long, H. B., Feng, T. Z., Pei, Y. L., Sun, Y. F., and Zhang, X. C. (2022). Development of a novel Primer–TaqMan probe set for diagnosis and quantification of meloidogyne enterolobii in soil using qPCR and droplet digital PCR assays. *Int. J. Mol. Sci.* 23, 11185. doi: 10.3390/ijms231911185

Chen, F. M., Negi, S., and Ye, J. R. (2011). A SCAR molecular marker to distinguish bursaphelenchus mucronatus from the pinewood nematode, b. xylophilus. *For. Pathol.* 41, 376–381. doi: 10.1111/j.1439-0329.2010.00693.x

Chen, J. S., Ma, E., Harrington, L. B., Da Costa, M., Tian, X., Palefsky, J. M., et al. (2018). CRISPR-Cas12a target binding unleashes indiscriminate single-stranded DNase activity. *Science* 360, 436–439. doi: 10.1126/science.aar6245

Chitwood, D. J. (2003). Research on plant-parasitic nematode biology conducted by the united states department of agriculture-agricultural research service. *Pest Manag Sci.* 59, 748–753. doi: 10.1002/ps.684

Chi, Y. K., Zhao, W., Ye, M. D., Ali, F., Wang, T., and Qi, R. D. (2020). Evaluation of recombinase polymerase amplification assay for detecting meloidogyne javanica. *Plant Dis.* 104, 801–807. doi: 10.1094/pdis-07-19-1473-re

Chizhov, V., Butorina, N., and Subbotin, S. (2012). Entomoparasitic nematodes of the genus skarbilovinema: S. laumondi and s. lyoni (Nematoda: Tylenchida), parasites of the flies of the family syrphidae (Diptera), with phylogeny of the suborder hexatylina. *Russian J. Nematol.* 20, 141–155. doi: 10.1111/j.1744-7410.2012.00275.x

Chizhov, V. N., Chumakova, O. A., Subbotin, S. A., and Baldwin, J. G. (2006). Morphological and molecular characterization of foliar nematodes of the genus aphelenchoides: A. fragariae and a. ritzemabosi (Nematoda: Aphelenchoididae) from the main botanical garden of the Russian academy of sciences, Moscow. *Russian J. Nematol.* 14, 179–184. doi: 10.1016/j.dsr2.2007.12.007

Curran, J. M., Baillie, D. L., and Webster, J. M. J. P. (1985). Use of genomic DNA restriction fragment length differences to identify nematode species. *Parasitology* 90, 137–144. doi: 10.1017/S0031182000049088

Curran, J., Driver, F., Ballard, J. W. O., and Milner, R. J. (1994). Phylogeny of metarhizium: analysis of ribosomal DNA sequence data. *Mycological Res.* 98, 547–552. doi: 10.1016/S0953-7562(09)80478-4

Curran, J., Mcclure, M. A., and Webster, J. M. (1986). Genotypic differentiation of meloidogyne populations by detection of restriction fragment length difference in total DNA. *J. Nematol* 18, 83–86. https://eurekamag.com/research/001/375/001375845.php

Currie, V., Hold, G., Pryde, S., Rehbein, H., Quinteiro, J., Rey-Méndez, M., et al. (2000). Use of restriction fragment length polymorphism to distinguish between salmon species. *J. Agric. Food Chem.* 48, 2184–2188. doi: 10.1021/jf991213e

Decraemer, W., and Hunt, D. J. (2006). *Structure and classification* (Wallingford, UK; Cambridge, MA, USA: CABI), 3–32.

Deng, M. H., Zhong, L. Y., Kamolnetr, O., Limpanont, Y., and Lv, Z. Y. (2019). Detection of helminths by loop-mediated isothermal amplification assay: a review of updated technology and future outlook. *Infect. Dis. Poverty* 8, 20–29. doi: 10.1186/s40249-019-0530-z

Dickson, D. W., Sasser, J. N., and Huisingh, D. M. (1970). Comparative disc-electrophoretic protein analyses of selected meloidogyne, ditylenchus, heterodera and aphelenchus spp. *J. Nematol.* 2, 286–293. doi: 10.1080/09505431.2011.605921

Ding, W. C., Chen, J., Shi, Y. H., Lu, X. J., and Li, M. Y. (2010). Rapid and sensitive detection of infectious spleen and kidney necrosis virus by loop-mediated isothermal amplification combined with a lateral flow dipstick. *Arch. Virol.* 155, 385–389. doi: 10.1007/s00705-010-0593-4

Din, M., Zheng, W., Rashid, M., Wang, S., and Shi, Z. (2017). Evaluating hyperspectral vegetation indices for leaf area index estimation of oryza sativa l. at diverse phenological stages. *Front. Plant Sci.* 8. doi: 10.3389/fpls.2017.00820

Esbenshade, P. R., and Triantaphyllou, A. C. (1985). Use of enzyme phenotypes for identification of meloidogyne species. *J. Nematol* 17, 6–20. http://europepmc.org/backend/ptpmcrender.fcgi?accid=PMC2618420&blobtype=pdf

Esbenshade, P. R., and Triantaphyllou, A. C. (1990). Isozyme phenotypes for the identification of meloidogyne species. *J. Nematol* 22, 10–15. https://www.ncbi.nlm.nih.gov/pmc/articles/PMC2619005/

Espy, M. J., Uhl, J. R., Sloan, L. M., Buckwalter, S. P., Jones, M. F., Vetter, E. A., et al. (2006). Real-time PCR in clinical microbiology: applications for routine laboratory testing. *Clin. Microbiol. Rev.* 19, 165–256. doi: 10.1128/cmr.19.1.165-256.2006

Feng, M. C., Jian, R. Y., and Jian, T. (2005). A study on detection technique of bursaphelenchus xylophilus and b. mucronatus by RAPD. *J. Nanjing Forestry Univ.* 4, 25–28. doi: 10.1360/biodiv.050121

Feng, M. C., Negi, S., and Ye, J. R. (2011). A SCAR molecular marker to distinguish bursaphelenchus mucronatus from the pinewood nematode, b. xylophilus. *For. Pathol.* 41, 13–18. doi: 10.1111/j.1439-0329.2010.00693.x

Ferris, V. R., Ferris, J. M., and Faghihi, J. (1993). Variation in spacer ribosomal DNA in some cyst-forming species of plant parasitic nematodes. *Fundam. Appl. Nematol.* 16, 177–184. https://horizon.documentation.ird.fr/exl-doc/pleins_textes/fan/40289.pdf

Floyd, R., Abebe, E., Papert, A., and Blaxter, M. (2002). Molecular barcodes for soil nematode identification. *Mol. Ecol.* 11, 839–850. doi: 10.1046/j.1365-294x.2002.01485.x

Floyd, R. M., Rogers, A. D., Lambshead, P. J. D., and Smith, C. R. (2005). Nematode-specific PCR primers for the 18S small subunit rRNA gene. *Mol. Ecol. Notes* 5, 611–612. doi: 10.1111/j.1471-8286.2005.01009.x

Fodor, S. P. A. (1997). DNA Sequencing - massively parallel genomics. *Science* 277, 393–398. doi: 10.1126/science.277.5324.393

Fullaondo, A., Barrena, E., Viribay, M., Barrena, I., Salazar, A., and Ritter, E. (1999). Identification of potato cyst nematode species Globodera rostochiensis and G. pallida by PCR using specific primer combinations. *Nematology* 1, 157–163. doi: 10.1163/156854199508126

Gootenberg, J. S., Abudayyeh, O. O., Lee, J. W., Essletzbichler, P., Dy, A. J., Joung, J., et al. (2017). Nucleic acid detection with CRISPR-Cas13a/C2c2. *Science* 356, 438–442. doi: 10.1126/science.aam9321

Goto, K., Sato, E., and Toyota, K. (2009). A novel detection method for the soybean cyst nematode heterodera glycines ichinohe using soil compaction and real-time PCR. *Japanese J. Nematol.* 39, 1–7. doi: 10.3725/jjn.39.1

Green, M., Rott, M., Leal, I., Humble, L., and Allen, E. (2019). Application of a real-time PCR method for the detection of pine wood nematode, bursaphelenchus xylophilus, in wood samples from lodgepole pine. *Nematol. Int. J. Fundam. Appl. nematological Res.* 9, 351–362. doi: 10.1163/156854107781352098

Hassan, T., Martinelli, H. T., and Pr, P. (2015). Impact of phytonematode on agriculture economy. *Bio. age. phytonematodes.* chapter1, 3–4. doi: 10.1079/9781780643755.0000

Heald, C. M., Thames, W. H., and Wiegand, C. L. (1972). Detection of totylenchulus reniformis infestations by aerial infrared photography. *J. Nematol* 4, 298–300. https://www.ncbi.nlm.nih.gov/pmc/articles/PMC2619957/

Heath, W. L., Haydock, P. P. J., Wilcox, A. C., and Evans, K. (2000). The potential use of spectral reflectance from the potato crop for remote sensing of infection by potato cyst nematodes. *Aspects Appl. Biol.* 60, 185–188. https://eurekamag.com/research/003/592/003592696.php

Hebert, P. D., Cywinska, A., Ball, S. L., and Dewaard, J. R. (2003). Biological identifications through DNA barcodes. *Proc. Biol. Sci.* 270, 313–321. doi: 10.1098/rspb.2002.2218

He, X. F., Das, P., Peng, H., Ding, Z., He, W. T., Huang, W. K., et al. (2013). Loop-mediated isothermal amplification assay for rapid diagnosis of meloidogyne enterolobii directly. *Chin. Agric. Sci.* 46, 534–544. doi: 10.1016/j.plantsci.2022.111376

Hillnhutter, C., Mahlein, A. K., Sikora, R. A., and Oerke, E. C. (2012). Use of imaging spectroscopy to discriminate symptoms caused by heterodera schachtii and rhizoctonia solani on sugar beet. *Precis. Agric.* 13, 17–32. doi: 10.1007/s11119-011-9237-2

Holterman, M., van der Wurff, A., Van Den Elsen, S., Van Megen, H., Bongers, T., Holovachov, O., et al. (2006). Phylum-wide analysis of SSU rDNA reveals deep phylogenetic relationships among nematodes and accelerated evolution toward crown clades. *Mol. Biol. Evol.* 23, 1792–1800. doi: 10.1093/molbev/msl044

Hu, M. X., Zhuo, K., and Liao, J. L. (2011). Multiplex PCR for the simultaneous identification and detection of meloidogyne incognita, m. enterolobii and m. javanica using DNA extracted directly from individual galls. *Phytopathology* 101, 1270–1277. doi: 10.1094/phyto-04-11-0095

Ide, T., Kanzaki, N., Giraldo, P. P. P., and Giblin-Davis, R. M. (2017). Loop-mediated isothermal amplification (LAMP) for detection of the red ring nematode, bursaphelenchus cocophilus. *Nematology* 19, 559–565. doi: 10.1163/15685411-00003069

Jarcho, J. (2001). Restriction fragment length polymorphism analysis. *Curr. Protoc. Hum. Genet.* Chapter 2, Unit 2.7. 1–15. doi: 10.1002/0471142905.hg0207s01

Jiang, C., Zhang, Y. D., Yao, K., Abdulsalam, S., Li, G. K., Gao, H. F., et al. (2021). Development of a species-specific SCAR-PCR assay for direct detection of sugar beet cyst nematode (Heterodera schachtii) from infected roots and soil samples. *Life-Basel* 11, 1358. doi: 10.3390/life11121358

Jian, J. Z., Huang, W. K., Kong, L. A., Jian, H., Abdulsalam, S., Peng, D. L., et al. (2022). Molecular diagnosis and direct quantification of cereal cyst nematode (Heterodera filipjevi) from field soil using TaqMan real-time PCR1. *J. Integr. Agriculture*. doi: 10.1016/j.jia.2022.09.016

Joalland, S., Screpanti, C., Liebisch, F., Varella, H. V., Gaume, A., and Walter, A. (2017). Comparison of visible imaging, thermography and spectrometry methods to evaluate the effect of heterodera schachtii inoculation on sugar beets. *Plant Methods* 13, 73. doi: 10.1186/s13007-017-0223-1

Ju, Y., Lin, Y., Yang, G., Wu, H., and Pan, Y. (2019). Development of recombinase polymerase amplification assay for rapid detection of meloidogyne incognita, m. javanica, m. arenaria and m. enterolobii. *Eur. J. Plant Pathol.* 155, 1155–1163. doi: 10.1007/s10658-019-01844-6

Kanetani, S., Kikuchi, T., Akiba, M., Nakamura, K., Ikegame, H., and Tetsuka, K. (2011). Detection of bursaphelenchus xylophilus from old discs of dead pinus armandii var. amamiana trees using a new detection kit. *For. Pathol.* 41, 387–391. doi: 10.1111/j.1439-0329.2010.00695.x

Kang, J. S., Kim, A. Y., Han, H. R., Moon, Y. S., and Koh, Y. H. (2015). Development of two alternative loop-mediated isothermal amplification tools for detecting pathogenic pine wood nematodes. *For. Pathol.* 45, 127–133. doi: 10.1111/efp.12147

Keçici, A., Bozbuğa, R., Öcal, A., Yüksel, E., Özer, G., Yildiz, Ş., et al. (2022). Diversity and identification of plant-parasitic nematodes in wheat-growing ecosystems. *Microorganisms* 10, 1534. doi: 10.3390/microorganisms10081534

Kiatpathomchai, W., Jaroenram, W., Arunrut, N., Jitrapakdee, S., and Flegel, T. W. (2008). Shrimp taura syndrome virus detection by reverse transcription loop-mediated isothermal amplification combined with a lateral flow dipstick. *J. Virol. Methods* 153, 214–217. doi: 10.1016/j.jviromet.2008.06.025

Kiewnick, S., Frey, J. E., and Braun-Kiewnick, A. (2015). Development and validation of LNA-based quantitative real-time PCR assays for detection and identification of the root-knot nematode meloidogyne enterolobii in complex DNA backgrounds. *Phytopathology* 105, 1245–1249. doi: 10.1094/phyto-12-14-0364-r

Kikuchi, T., Aikawa, T., Oeda, Y., Karim, N., and Kanzaki, N. (2009). A rapid and precise diagnostic method for detecting the pinewood nematode bursaphelenchus xylophilus by loop-mediated isothermal amplification. *Phytopathology* 99, 1365–1369. doi: 10.1094/phyto-99-12-1365

Kundu, A., Chakraborty, R., and Sarkar, S. (2022). Remote sensing in nematode detection and forecasting. *Agriculture & Food : e-Newsletter* 4, 74–77. doi: 10.1117/12.614376

Lecouls, A. C., Rubio-Cabetas, M. J., Minot, J. C., Voisin, R., Bonnet, A., Salesses, G., et al. (1999). RAPD and SCAR markers linked to the Ma1 root-knot nematode resistance gene in myrobalan plum (Prunus cerasifera ehr.). *Theor. Appl. Genet.* 99, 328–335. doi: 10.1007/s001220051240

Li, H., Bai, R., Zhao, Z., Tao, L., Ma, M., Ji, Z., et al. (2018). Application of droplet digital PCR to detect the pathogens of infectious diseases. *Biosci. Rep.* 38, BSR20181170. doi: 10.1042/BSR20181170

Li, Y., Lawrence, G. W., Lu, S. E., Balbalian, C., and Klink, V. P. (2014). Quantitative field testing heterodera glycines from metagenomic DNA samples isolated directly from soil under agronomic production. *PloS One* 9, e89887. doi: 10.1371/journal.pone.0089887

Li, M., Li, H., Ding, X., Wang, L., Wang, X., and Chen, F. (2022). The detection of pine wilt disease: A literature review. *Int. J. Mol. Sci.* 23, 10797. doi: 10.3390/ijms231810797

Lin, B., Wang, H., Zhuo, K., and Liao, J. (2016). Loop-mediated isothermal amplification for the detection of tylenchulus semipenetrans in soil. *Plant Dis.* 100, 877–883. doi: 10.1094/pdis-07-15-0801-re

Lobato, I. M., and O'sullivan, C. K. (2018). Recombinase polymerase amplification: Basics, applications and recent advances. *Trends Analyt Chem.* 98, 19–35. doi: 10.1016/j.trac.2017.10.015

Lopez-Nicora, H. D., Craig, J. P., Gao, X. B., Lambert, K. N., and Niblack, T. L. (2012). Evaluation of cultivar resistance to soybean cyst nematode with a quantitative polymerase chain reaction assay. *Plant Dis.* 96, 1556–1563. doi: 10.1094/pdis-12-11-1083-re

Lu, X., Wang, Y., Fung, S., and Xue, Q. (2021). A Biological Image Dataset for Nematode Recognition. *I-Nema*. 4, 1–13. doi: 10.48550/arXiv.2103.08335

Madani, M., Subbotin, S. A., and Moens, M. (2005). Quantitative detection of the potato cyst nematode, globodera pallida, and the beet cyst nematode, heterodera schachtii, using real-time PCR with SYBR green I dye. *Mol. Cell. Probes* 19, 81–86. doi: 10.1016/j.mcp.2004.09.006

Mahmoudi, N., Pakina, E. N., Limantceva, L. A., Ivanov, A.V.J.R.J.O.A., and Industries, A. (2020). Diagnosis of potato rot nematode ditylenchus destructor using PCR-RFLP. *Plant Prot.* 3, 353–362. doi: 10.22363/2312-797X-2020-15-4-353-362

Marek, M., Zouhar, M., Douda, O., Maňasová, M., and Ryšánek, P. (2014). Exploitation of FTA cartridges for the sampling, long-term storage, and DNA-based analyses of plant-parasitic nematodes. *Phytopathology* 104, 306–312. doi: 10.1094/phyto-03-13-0067-r

Mika, T., Maghnouj, A., Klein-Scory, S., Ladigan-Badura, S., Baraniskin, A., Thomson, J., et al. (2020). Digital-droplet PCR for quantification of CD19-directed CAR T-cells. *Front. Mol. Biosci.* 7. doi: 10.3389/fmolb.2020.00084

Min, Y. Y., Toyota, K., Goto, K., Sato, E., Mizuguchi, S., Abe, N., et al. (2011). Development of a direct quantitative detection method for meloidogyne incognita in sandy soils and its application to sweet potato cultivated fields in tokushima prefecture, Japan. *Nematology* 13, 95–102. doi: 10.1163/138855410x504916

Mori, Y., Kitao, M., Tomita, N., and Notomi, T. (2004). Real-time turbidimetry of LAMP reaction for quantifying template DNA. *J. Biochem. Biophys. Methods* 59, 145–157. doi: 10.1016/j.jbbm.2003.12.005

Mori, Y., Nagamine, K., Tomita, N., and Notomi, T. (2001). Detection of loop-mediated isothermal amplification reaction by turbidity derived from magnesium pyrophosphate formation. *Biochem. Biophys. Res. Commun.* 289, 150–154. doi: 10.1006/bbrc.2001.5921

Muniz, M., Campos, V., Castagnone-Sereno, P., Castro, J., Almeida, M., and Carneiro, R. (2008). Diversity of meloidogyne exigua (Tylenchida: Meloidogynidae) populations from coffee and rubber tree. *Nematology* 10, 897–910. doi: 10.1163/156854108786161418

Nicol, J. M., Turner, S. J., Coyne, D. L., Nijs, L. D., Hockland, S., and Maafi, Z. T. (2011). "Current nematode threats to world agriculture," in *Genomics and molecular genetics of plant-nematode interactions*. Eds. J. Jones, G. Gheysen and C. Fenoll (Dordrecht: Springer Netherlands), 21–43.

Niemz, A., Ferguson, T. M., and Boyle, D. S. (2011). Point-of-care nucleic acid testing for infectious diseases. *Trends Biotechnol.* 29, 240–250. doi: 10.1016/j.tibtech.2011.01.007

Niu, J. H., Guo, Q. X., Jian, H., Chen, C. L., Yang, D., Liu, Q., et al. (2011). Rapid detection of meloidogyne spp. by LAMP assay in soil and roots. *Crop Prot.* 30, 1063–1069. doi: 10.1016/j.cropro.2011.03.028

Niu, J. H., Jian, H., Guo, Q. X., Chen, C. L., Wang, X. Y., Liu, Q., et al. (2012). Evaluation of loop-mediated isothermal amplification (LAMP) assays based on 5S rDNA-IGS2 regions for detecting meloidogyne enterolobii. *Plant Pathol.* 61, 809–819. doi: 10.1111/j.1365-3059.2011.02562.x

Norman, G. G., and Fritz, N. L. (1965). Infrared photography as an indicator of disease and decline in citrus trees. *Proc. Fla. State Horticult. Soc.* 12, 31–41. https://www.adobe.com/creativecloud/photography/discover/infrared-photography.html Powers and Sandall 1988: URL:https://www.ncbi.nlm.nih.gov/pmc/articles/PMC2618847/

Notomi, T., Okayama, H., Masubuchi, H., Yonekawa, T., Watanabe, K., Amino, N., et al. (2000). Loop-mediated isothermal amplification of DNA. *Nucleic Acids Res.* 28, E63. doi: 10.1093/nar/28.12.e63

Nunn, G. B. (1992). *Nematode Molecular Evolution*. Ph.D. Thesis. University of Nottingham, Nottingham, UK. Available at: https://ethos.bl.uk/OrderDetails.do?uin=uk.bl.ethos.334855

Nutter, F. W., Tylka, G. L., Guan, J., Moreira, A. J., Marett, C. C., Rosburg, T. R., et al. (2002). Use of remote sensing to detect soybean cyst nematode-induced plant stress. *J. Nematol* 34, 222–231. doi: 10.1016/S0022-2011(02)00111-8

Oliveira, C., Monteiroi, A., and Blok, V. (2011). Morphological and molecular diagnostics for plant-parasitic nematodes: Working together to get the identification done. *Trop. Plant Pathol.* 36, 65–76. doi: 10.1590/S1982-56762011000200001

Ou, S. Q., Peng, D. L., Liu, X. M., Li, Y., and Moens, M. (2008a). Identification of heterodera glycines using PCR with sequence characterised amplified region (SCAR) primers. *Nematology* 10, 397–403. doi: 10.1163/156854108783900212

Ou, S. Q., Peng, D. L., and Yu, L. L. (2008b). Restriction fragment length polymorphism and sequences analysis of rDNA-ITS region of cereal cyst nematode(Heterodera avenae) on wheat from zhengzhou. *Acta Phytopathologica Sin.* 4, 407–413. doi: 10.13926/j.cnki.apps.2008.04.008

Palomares-Rius, J. E., Cantalapiedra-Navarrete, C., Archidona-Yuste, A., Subbotin, S. A., and Castillo, P. (2017). The utility of mtDNA and rDNA for barcoding and phylogeny of plant-parasitic nematodes from longidoridae (Nematoda, enoplea). *Sci. Rep.* 7, 10905. doi: 10.1038/s41598-017-11085-4

Pan, J., Ju, Y., Zhang, H., and Wang, X. (2014). Detection of bursaphelenchus xylophilus infection in pinus massoniana from hyperspectral data. *Nematology* 16, 1197–1207. doi: 10.1163/15685411-00002846

Peng, H., Long, H., Huang, W., Liu, J., Cui, J., Kong, L., et al. (2017). Rapid, simple and direct detection of meloidogyne hapla from infected root galls using loop-mediated isothermal amplification combined with FTA technology. *Sci. Rep.* 7, 44853. doi: 10.1038/srep44853

Peng, H., Peng, D. L., Hu, X. Q., He, X. F., Wang, Q., Huang, W. K., et al. (2012). Loop-mediated isothermal amplification for rapid and precise detection of the burrowing nematode, radopholus similis, directly from diseased plant tissues. *Nematology* 14, 977–986. doi: 10.1163/156854112x638415

Perera, M. R., Vanstone, V. A., and Jones, M. G. K. (2005). A novel approach to identify plant parasitic nematodes using matrix-assisted laser desorption/ionization time-of-flight mass spectrometry. *Rapid Commun. Mass Spectrometry* 19, 1454–1460. doi: 10.1002/rcm.1943

Piepenburg, O., Williams, C. H., Stemple, D. L., and Armes, N. A. (2006). DNA Detection using recombination proteins. *PloS Biol.* 4, e204. doi: 10.1371/journal.pbio.0040204

Powers, T. O., and Sandall, L. J. (1988). Estimation of genetic divergence in meloidogyne mitochondrial DNA. *J. Nematol* 20, 505–511.

Qi, X. L., Peng, D., Peng, H., Long, H., Huang, W., and He, W. T. (2012). Rapid molecular diagnosis based on SCAR marker system for cereal cyst nematode. *Sci. Agric. Sin.* 45, 4388–4395. doi: 10.3864/j.issn.0578-1752.2012.21.007

Randig, O., Bongiovanni, M., Carneiro, R. M. D. G., and Castagnone-Sereno, P. (2002). Genetic diversity of root-knot nematodes from Brazil and development of SCAR markers specific for the coffee-damaging species. *Genome* 45 5, 862–870. doi: 10.1111/ppa.12108

Rani, A., Donovan, N., and Mantri, N. (2019). Review: The future of plant pathogen diagnostics in a nursery production system. *Biosens Bioelectron* 145, 111631. doi: 10.1016/j.bios.2019.111631

Rashidifard, M., Marais, M., Daneel, M. S., Mienie, C. M. S., and Fourie, H. (2019). Molecular characterisation of meloidogyne enterolobii and other meloidogyne spp. from south Africa. *Trop. Plant Pathol.* 44, 213–224. doi: 10.1007/s40858-019-00281-4

Rivero, J., Zurita, A., Cutillas, C., and Callejon, R. (2022). The use of MALDI-TOF MS as a diagnostic tool for adult trichuris species. *Front. Veterinary Sci.* 9. doi: 10.3389/fvets.2022.867919

Rougemont, M., Van Saanen, M., Sahli, R., Hinrikson, H. P., Bille, J., and Jaton, K. (2004). Detection of four plasmodium species in blood from humans by 18S rRNA gene subunit-based and species-specific real-time PCR assays. *J. Clin. Microbiol.* 42, 5636–5643. doi: 10.1128/jcm.42.12.5636-5643.2004

Sabate del Rio, J., Magrina Lobato, I., Mayboroda, O., Katakis, I., and O'sullivan, C. K. (2017). Enhanced solid-phase recombinase polymerase amplification and electrochemical detection. *Analytical Bioanalytical Chem.* 409, 3261–3269. doi: 10.1007/s00216-017-0269-y

San-Blas, E., Paba, G., Cubillan, N., Portillo, E., Casassa-Padrón, A., González-González, C., et al. (2020). The use of infrared spectroscopy and machine learning tools for detection of meloidogyne infestations. *Plant Pathol.* 69, 1589–1600. doi: 10.1111/ppa.13246

Sandrin, T. R., Goldstein, J. E., and Schumaker, S. (2013). MALDI TOF MS profiling of bacteria at the strain level: a review. *Mass Spectrom Rev.* 32, 188–217. doi: 10.1002/mas.21359

Sato, E., Min, Y. Y., Shirakashi, T., Wada, S., and Toyota, K. (2007). Detection of the root-lesion nematode, Pratylenchus penetrans (Cobb), in a nematode community using real-time PCR. *Nematological Research* 37, 87–92. doi: 10.3725/jjn.37.87

Seng, P., Drancourt, M., Gouriet, F., La Scola, B., Fournier, P. E., Rolain, J. M., et al. (2009). Ongoing revolution in bacteriology: routine identification of bacteria by matrix-assisted laser desorption ionization time-of-flight mass spectrometry. *Clin. Infect. Dis.* 49, 543–551. doi: 10.1086/600885

Shao, H., Jian, J., Peng, D., Yao, K., Abdulsalam, S., Huang, W., et al. (2022). Recombinase polymerase amplification coupled with CRISPR-Cas12a technology for rapid and highly sensitive detection of heterodera avenae and heterodera filipjevi. *Plant Dis.* doi: 10.1094/pdis-02-22-0386-re

Sikder, M. M., Vestergård, M., Sapkota, R., Kyndt, T., and Nicolaisen, M. (2020). *A novel metabarcoding strategy for studying nematode communities* (Cold Spring Harbor Laboratory).

Sjöholm, M. I., Dillner, J., and Carlson, J. (2008). Multiplex detection of human herpesviruses from archival specimens by using matrix-assisted laser desorption ionization-time of flight mass spectrometry. *J. Clin. Microbiol.* 46, 540–545. doi: 10.1128/jcm.01565-07

Smith, C. J., and Osborn, A. M. (2009). Advantages and limitations of quantitative PCR (Q-PCR)-based approaches in microbial ecology. *FEMS Microbiol. Ecol.* 67, 6–20. doi: 10.1111/j.1574-6941.2008.00629.x

Song, Z. Q., Cheng, J. E., Cheng, F. X., Zhang, D. Y., and Liu, Y. (2017). Development and evaluation of loop-mediated isothermal amplification assay for rapid detection of tylenchulus semipenetrans using DNA extracted from soil. *Plant Pathol. J.* 33, 184–192. doi: 10.5423/ppj.Oa.10.2016.0224

Stanton, J., Hugall, A. F., and Moritz, C. C. (1997). Nucleotide polymorphisms and an improved PCR-based mtDNA diagnostic for parthenogenetic root-knot nematodes (Meloidogyne spp.). *Fundam. Appl. Nematol.* 20, 261–268. https://horizon.documentation.ird.fr/exl-doc/pleins_textes/fan/010011563.pdf

Subbotin, S. A. (2019). Recombinase polymerase amplification assay for rapid detection of the root-knot nematode meloidogyne enterolobii. *Nematology* 21, 243–251. doi: 10.1163/15685411-00003210

Subbotin, S. A., and Burbridge, J. (2021). Sensitive, accurate and rapid detection of the northern root-knot nematode, meloidogyne hapla, using recombinase polymerase amplification assays. *Plants-Basel* 10, 336. doi: 10.3390/plants10020336

Subbotin, S., Franco, J., Knoetze, R., Roubtsova, T., Bostock, R., Cid, I., et al. (2019). DNA Barcoding, phylogeny and phylogeography of the cyst nematode species from the genus globodera (Tylenchida: Heteroderidae). *Nematology* 22, 1–29. doi: 10.1163/15685411-00003305

Sykes, P. J., Neoh, S. H., Brisco, M. J., Hughes, E., Condon, J., and Morley, A. A. (1992). Quantitation of targets for PCR by use of limiting dilution. *Biotechniques* 13, 444–449. https://pubmed.ncbi.nlm.nih.gov/1389177/

Szalanski, A. L., Sui, D. D., Harris, T. S., and Powers, T. O. (1997). Identification of cyst nematodes of agronomic and regulatory concern with PCR-RFLP of ITS1. *J. Nematol.* 29, 255–267. doi: 10.1006/jipa.1997.4682

Taberlet, P., Coissac, E., Pompanon, F., Brochmann, C., and Willerslev, E. (2012). Towards next-generation biodiversity assessment using DNA metabarcoding. *Mol. Ecol.* 21, 2045–2050. doi: 10.1111/j.1365-294X.2012.05470.x

Tao, H., Li, C., Cheng, C., Jiang, L., and Hu, H. (2020). Progress in remote sensing monitoring for pine wilt disease induced tree mortality: a review. *For. Res.* 3, 172–183. doi: 10.13275/j.cnki.lykxyj.2020

Toumi, F., Waeyenberge, L., Viaene, N., Dababat, A., Nicol, J. M., Ogbonnaya, F., et al. (2013). Development of two species-specific primer sets to detect the cereal cyst nematodes heterodera avenae and heterodera filipjevi. *Eur. J. Plant Pathol.* 136, 613–624. doi: 10.1007/s10658-013-0192-9

Vallejo, D., Rojas, D. A., Martinez, J. A., Marchant, S., Holguin, C. M., and Pérez, O. Y. (2021). Occurrence and molecular characterization of cyst nematode species (Globodera spp.) associated with potato crops in Colombia. *PloS One* 16, e0241256. doi: 10.1371/journal.pone.0241256

Vega-Rúa, A., Pagès, N., Fontaine, A., Nuccio, C., Hery, L., Goindin, D., et al. (2018). Improvement of mosquito identification by MALDI-TOF MS biotyping using protein signatures from two body parts. *Parasit. Vectors* 11, 574. doi: 10.1186/s13071-018-3157-1

Vrain, T. C. (1993). Restriction fragment length polymorphism separates species of the xiphinema americanum group. *J. Nematol* 25, 361–364. doi: 10.1006/jipa.1993.1100

Vrain, T. C., Wakarchuk, D. A., Lévesque, A., and Hamilton, R. I. (1992). Intraspecific rDNA restriction fragment length polymorphism in the xiphinema americanum group. *Fundam. Appl. Nematol.* 15, 563–573. doi: 10.1159/000156634

Waite, I. S., O'donnell, A. G., Harrison, A., Davies, J. T., Colvan, S. R., Ekschmitt, K., et al. (2003). Design and evaluation of nematode 18S rDNA primers for PCR and denaturing gradient gel electrophoresis (DGGE) of soil community DNA. *Soil Biol. Biochem.* 35, 1165–1173. doi: 10.1016/s0038-0717(03)00177-9

Waliullah, S., Bell, J., Jagdale, G., Stackhouse, T., Hajihassani, A., Brenneman, T., et al. (2020). Rapid detection of pecan root-knot nematode, meloidogyne partityla, in laboratory and field conditions using loop-mediated isothermal amplification. *PloS One* 15, e0228123. doi: 10.1371/journal.pone.0228123

Wang, X., Wang, L., Wang, Y., Huang, Y., Ding, Z., Zhou, J., et al. (2015). Identification and genetic analysis of the pinewood nematode bursaphelenchus xylophilus from pinus yunnanensis. *For. Pathol.* 45, 388–399. doi: 10.1111/efp.12181

Wang, X., Xiong, E., Tian, T., Cheng, M., Lin, W., Wang, H., et al. (2020). Clustered regularly interspaced short palindromic Repeats/Cas9-mediated lateral flow nucleic acid assay. *ACS Nano* 14, 2497–2508. doi: 10.1021/acsnano.0c00022

Wendt, K. R., Vrain, T. C., and Webster, J. M. (1993). Separation of three species of ditylenchus and some host races of d. dipsaci by restriction fragment length polymorphism. *J. Nematol* 25, 555–563. https://www.ncbi.nlm.nih.gov/pmc/articles/PMC2619421/

Williams, J., Kubelik, A. R., Rafalski, J. A., and Tingey, S. V. (1991). Genetic analysis with RAPD markers. *More Gene Manipulations Fungi* 81, 431–439. doi: 10.1016/B978-0-12-088642-5.50026-0

Wishart, J., Phillips, M. S., and Blok, V. C. (2002). Ribosomal intergenic spacer: A polymerase chain reaction diagnostic for meloidogyne chitwoodi, m. fallax and m. hapla. *Phytopathology* 92, 884–892. doi: 10.1094/phyto.2002.92.8.884

Yan, G., Smiley, R. W., Okubara, P. A., Skantar, A., Easley, S. A., Sheedy, J. G., et al. (2008). Detection and discrimination of pratylenchus neglectus and p. thornei in DNA extracts from soil. *Plant Dis.* 92, 1480–1487. doi: 10.1094/pdis-92-11-1480

Yao, K., Peng, D., Jiang, C., Zhao, W., Li, G., Huang, W., et al. (2021). Rapid and visual detection of heterodera schachtii using recombinase polymerase amplification combined with Cas12a-mediated technology. *Int. J. Mol. Sci.* 22, 12577. doi: 10.3390/ijms222212577

Yssouf, A., Almeras, L., Raoult, D., and Parola, P. (2016). Emerging tools for identification of arthropod vectors. *Future Microbiol.* 11, 549–566. doi: 10.2217/fmb.16.5

Yu, L. Z., Song, S. Y., Yu, C., Jiao, B. B., Tian, Y. M., and Li, Y. J. (2020). Rapid detection of anguina agrostis by loop-mediated isothermal amplification. *Eur. J. Plant Pathol.* 156, 819–825. doi: 10.1007/s10658-020-01932-y

Yu, L. Z., Song, S. Y., Yu, C., Qi, L. J., Yu, Z. X., Jiao, B. B., et al. (2018). A loop mediated isothermal amplification (LAMP) assay for rapid and reliable detection of anguina wevelli, a grass parasitic nematode. *Eur. J. Plant Pathol.* 150, 725–734. doi: 10.1007/s10658-017-1320-8

Zhang, Z. Q. (2013). Animal biodiversity: An update of classification and diversity in 2013. *Zootaxa* 3703, 5–11. doi: 10.11646/zootaxa.3703.1.3

Zhang, L., and Gleason, C. (2019). Loop-mediated isothermal amplification for the diagnostic detection of meloidogyne chitwoodi and m. fallax. *Plant Dis.* 103, 12–18. doi: 10.1094/pdis-01-18-0093-re

Zheng, J. W., Subbotin, S. A., He, S. S., Gu, J. F., and Moens, M. (2003). Molecular characterisation of some Asian isolates of bursaphelenchus xylophilus and b. mucronatus using PCR-RFLPs and sequences of ribosomal DNA. *Russian J. Nematol.* 11, 17–22. doi: 10.1051/rnd:2003010

Zheng, J.-W., Subbotin, S., Waeyenberge, L., and Moens, M. (2000). Molecular characterisation of Chinese heterodera glycines and h. avenae populations based on RFLPs and sequences of rDNA-ITS regions. *Russian J. Nematol.* 8, 109–113. doi: 10.1071/RD99037

Zhou, Q. J., Cai, Y., Gu, J. F., Wang, X., and Chen, J. (2017). Rapid and sensitive detection of meloidogyne mali by loop-mediated isothermal amplification combined with a lateral flow dipstick. *Eur. J. Plant Pathol.* 148, 755–769. doi: 10.1007/s10658-016-1130-4

Zijlstra, C., Donkers-Venne, D., and Fargette, M. (2000). Identification of meloidogyne incognita, m-javanica and m-arenaria using sequence characterised amplified region (SCAR) based PCR assays. *Nematology* 2, 847–853. doi: 10.1163/156854100750112798

Zijlstra, C., Lever, A. M. L., Uenk, B. J., and Silfhout, C.H.V.J.P. (1995). Differences between ITS regions of isolates of the root-knot nematodes meloidogyne hapla and m. chitwoodi. *Phytopathology* 85, 1231–1237. https://research.wur.nl/en/publications/differences-between-its-regions-of-isolates-of-the-root-knot-nema

frontiers | Frontiers in Plant Science

TYPE Original Research
PUBLISHED 26 January 2023
DOI 10.3389/fpls.2022.1089562

OPEN ACCESS

EDITED BY
Rahul Kumar Tiwari,
Indian Council of Agricultural Research (ICAR), India

REVIEWED BY
Ahmed H. El-Sappah,
Zagazig University, Egypt
Taimoor Hassan Farooq,
A Joint Unit of Bangor University and Central South University of Forestry and Technology, China

*CORRESPONDENCE
Zoia Arshad Awan
zoia.arshadawan@gmail.com

SPECIALTY SECTION
This article was submitted to Plant Pathogen Interactions, a section of the journal Frontiers in Plant Science

RECEIVED 04 November 2022
ACCEPTED 12 December 2022
PUBLISHED 26 January 2023

CITATION
Awan ZA, Shoaib A, Schenk PM, Ahmad A, Alansi S and Paray BA (2023) Antifungal potential of volatiles produced by *Bacillus subtilis* BS-01 against *Alternaria solani* in *Solanum lycopersicum*.
Front. Plant Sci. 13:1089562.
doi: 10.3389/fpls.2022.1089562

Antifungal potential of volatiles produced by *Bacillus subtilis* BS-01 against *Alternaria solani* in *Solanum lycopersicum*

Zoia Arshad Awan[1]*, Amna Shoaib[1], Peer M. Schenk[2], Ajaz Ahmad[3], Saleh Alansi[4] and Bilal Ahamad Paray[5]

[1]Faculty of Agricultural Sciences, University of the Punjab, Lahore, Pakistan, [2]Plant-Microbe Interactions Laboratory, School of Agriculture and Food Sciences, University of Queensland, Brisbane, QLD, Australia, [3]Department of Clinical Pharmacy, College of Pharmacy, King Saud University, Riyadh, Saudi Arabia, [4]Botany and Microbiology Department, College of Science, King Saud University, Riyadh, Saudi Arabia, [5]Zoology Department, College of Sciences, King Saud University, Riyadh, Saudi Arabia

Bacterial biocontrol agent/s (BCAs) against plant diseases are eco-friendly and sustainable options for profitable agricultural crop production. Specific beneficial strains of *Bacillus subtilis* are effective in controlling many fungal diseases including Alternaria blight caused by a notorious pathogen "*Alternaria solani*". In the present study, the biocontrol attributes of a newfangled strain of *B. subtilis* (BS-01) have been investigated and its bioactive compounds were also identified against *A. solani*. The volatile organic compounds (VOCs) produced by BS-01 in organic solvents viz., *n*-hexane, dichloromethane, and ethyl acetate were extracted and their antifungal efficacy has evaluated against *A. solani.* Also, the preventive and curative biocontrol method to reduce the fungal load of *A. solani* was estimated by both foliar and seed applications on infected tomato (Solanum lycopersicum) plants as determined by quantitative PCR assays. Growth chamber bioassay revealed that both foliar and seed application of BS-01 on tomato plants previously or subsequently infected by *A. solani* significantly reduced the pathogen load on inoculated tomato foliage. Results showed that antifungal bioassays with various concentrations (10-100 mg mL^{-1}) of extracted metabolites produced by BS-01 in ethyl acetate fraction showed the highest inhibition in fungal biomass (extracellular metabolites: 69-98% and intracellular metabolites: 48-85%) followed by *n*-hexane (extracellular metabolites: 63-88% and intracellular metabolites: 35-62%) and dichloromethane (extracellular metabolites: 41-74% and intracellular metabolites: 42-70%), respectively. The extracted volatile compounds of BS-01 were identified *via* GC-MS analysis and were found in great proportions in the organic fractions as major potent antifungal constituents including triphenylphosphine oxide; pyrrolo[1,2-a] pyrazine-1,4-dione, hexahydro-3-(2-methylpropyl); pyrrolo[1,2-a] pyrazine-1,4-dione, hexahydro-3-(phenylmethyl); *n*-hexadecanoic acid; *n*-tridecan-1-ol; octadecane;

octadecanoic acid; eicosane and dodecyl acrylate. Separate or mixture of these bioactive VOCs had the potential to mitigate the tomato early blight disease severity in the field that would act as a sustainable plant protection strategy to generate profitable tomato production.

KEYWORDS

biological agent, GC-MS, secondary metabolites, pathogen load, qPCR

1 Introduction

Biological control of plant diseases using bacterial-based biocontrol agents is considered a safer and more sustainable alternative over synthetic pesticides (Daranas et al., 2019). Many microbial biopesticides can also act as biofertilizers that contribute to nutrient cycling, enhance soil fertility, and improve crop yields (Olanrewaju et al., 2017). Multiple mechanisms have been identified for BCAs, including hyperparasitism, competition with plant pathogens (e.g. *via* the production of siderophores), priming leading to induced systemic resistance, and direct antimicrobial actions such as inactivation of pathogen enzymes, production of antibiotics, lytic enzymes (cellulase, chitinase, and proteases) or toxins (Oliva et al., 2017; Khanna et al., 2019a). For example, numerous species of *Bacillus*, *Streptomyces* and *Pseudomonas* have been identified as plant-growth-promoting bacteria (PGPRs) and biocontrol agents (BCAs) against early blight (EB) (Moreira et al., 2014; Manimaran et al., 2017; Wang et al., 2018; Khanna et al., 2019b).

The genus *Bacillus* has a unique ability to replicate promptly and exhibit broad-spectrum antibiotic activity (Shafi et al., 2017; Syed-Ab-Rahman et al., 2018; Shoaib et al., 2019). Biopesticides formulated from various strains of *Bacillus* such as *B. subtilis*, *B. sphaericus* and *B. thuringiensis* have a positive effect on plant growth by inducing systematic acquired resistance (SAR) in the host and inhibiting disease-causing pathogens (Lastochkina et al., 2019; Rashid et al., 2022). Such novel beneficial biological agents including *Bacillus* and *Paenibacillus* species are reported to improve the nutritional values of staple crops and could be used as bio-inoculants (Hussain et al., 2020; Ilyas et al., 2022). Amongst various species of *Bacillus*, *Bacillus subtilis* is widely distributed and one of the most attractive bio-agent, which is easy to isolate and culture (Zhang et al., 2016). *B. subtilis* is widely used to control agricultural diseases due to its good antimicrobial activity in the soil and strong adaptability and (Chandrasekaran et al., 2016). *B. subtilis* has been known to produce antimycotic enzymes viz., chitinase, cellulose and beta-1,3 glucanase by degrading fungal structural polymers (Yánez-Mendizábal et al., 2011). It is also considered one of the most widely used and well-studied biocontrol organisms, and 4-5% of its genome is responsible for the synthesis of antibiotics including lipopeptides, Iturin, surfactin and fengycin that contribute to the antifungal potential, for example, lipopeptides have shown low environmental toxicity and high biodegradability characteristics (Guo et al., 2014). Hence, such antibiotics are eco-friendly and environmentally sustainable as compared to chemical pesticides (More et al., 2014). Therefore, *B. subtilis* has been affirmed safe by the US Food and Drug Administration in the food processing industries (Mnif and Ghribi, 2015). Nowadays, numerous *B. subtilis*-based commercial products such as AvoGreen, Bio Yield, BioSafe and Ecoshot, etc., are available to manage many fungal diseases (Lastochkina et al., 2019; Hashem et al., 2019). Besides, *B. subtilis* strains also accelerate phosphate solubilization, nitrogen uptake, siderophore and phytohormone for better plant growth and development (Gouda et al., 2018);. Likewise, its antifungal potential against a broad range of phytopathogens has been confirmed *in vitro* and *in vivo* (greenhouse and field) studies (Hadimani and Kulkarni, 2016; Shoaib et al., 2019; Awan and Shoaib, 2019). The tolerance and resilience against plant disease are primarily related to genetics, several of the traits are required for a number of the mechanisms for biocontrol in for the synthesis of polyamines, the production of siderophores, and the synthesis of antimicrobial peptides and antibiotics which are directly involved in plant defense as structural components (e.g. thickness of cell walls) and metabolic regulators (e.g. antioxidants, phytoalexins and flavonoids Where, practical implementation of *B. subtilis* strain/s to manage tomato early blight may wean off dependence on agricultural chemicals against notorious pathogen *A. solani* (Köhl et al., 2019).

The present study aimed to isolate, identify and characterize a new strain of *Bacillus subtilis* (BS-01). Extracted volatiles from extra- and intra-cellular metabolites of BS-01 will be examined for antifungal impact and identified using GC-MS analysis. The capability of reducing Alternaria pathogen load on pathogen-inoculated tomato foliage also will be estimated by employing BS-01 (*in vivo* trial). Employing BS-01 as an alternative approach is likely to lead to a more rational and sustainable choice of disease management for promoting plant growth.

2 Material & methods

2.1 Isolation and cultivation of microbial strains

a. ***Isolation of pathogen:*** *A. solani* a pathogen of tomato early blight pathogen (FCBP 1401; MF539619) was re-isolated from infected tomato leaves showing the characteristic disease symptoms of EB following the protocol of Shoaib et al., 2019. For *in vitro* and *in vivo* bioassays the conidial suspension was prepared and used for further study (Awan et al., 2018).

b. ***Isolation of biocontrol agent:*** A beneficial strain of *Bacillus subtilis* was isolated from the rhizospheric soil of a chickpea field in the experimental area of the mother institute University of the Punjab, Lahore, Pakistan. For the microbial cultivation, about 1 g of soil samples were serially diluted 10-folds in phosphate-buffered saline (PBS, 0.05 M, pH 7.4) and 100 µL of soil suspensions were plated on Luria-Bertani agar (LB) (1% tryptone, 1% NaCl 1%, 0.5% yeast extract 0.5% with pH 7.5). After incubation of 24 h at 37°C, single colonies were picked and maintained as pure cultures on LBA plates and the pure culture of *B. subtilis* (Genebank accession LC425129.1) was maintained in LB with 20% glycerol for long-term storage at -80°C.

2.2 Evaluation of *B. subtilis* (BS-01) to reduce the pathogen load

A pot assay was conducted in a growth chamber to assess the biocontrol efficacy of *B. subtilis* in reducing fungal load by preventive (pre-infection) and curative (post-infection) methods (Syed-Ab-Rahman et al., 2019). The experiment has been repeated thrice, comprised of six treatments (T1-T6) and arranged in a completely randomized design with five replications (N=5) of each treatment. The treatments (T_1-T_6) of pot bioassays were described in Table 1. Where, T_1: -ve control (healthy tomato plants without any treatment and inoculation), T_2: +ve control (plants inoculated with AS only), T_3 & T_4: pre-infection treatments and T_5 & T_6 were post-infection treatments.

A suspension of BS-01 was prepared by harvesting bacterial cells from a one-day-old bacterial culture in ice-cold 0.1M PBS (pH 6.8). Tomato seeds were surface-sterilized with 1% bleach for 2 min followed by washing in 70% (v/v) ethanol for 5 min and rinsing three times with distilled water. Before seed sowing, dried sterilized tomato seeds were soaked in 0.05 M phosphate-buffered saline (PBS; pH: 6.8) for all treatments, but tomato seeds for treatment T_3 were soaked in BS-01 suspension ($OD595_{nm}$ = 0.8) [prepared by harvesting bacterial cells (BS-01) from a 24-hours old culture in ice-cold 0.05 M phosphate-buffered saline (PBS, pH: 6.8)] for 30 min as a pre-infection treatment (preventive measure against EB). Tomato seeds (1 seed pot^{-1}) were sown in pots (3.15"height × 3.15" width) and incubated in a growth chamber (16 hours daylight at 28°C and 8 hours a night at 20°C). After twenty days, tomato plants of all treatments were inoculated with 1-2 mL of conidial suspension (2.0×10^4 conidia mL^{-1}) through a hand sprayer. But, plants in treatment T_4 were treated with 1-2 mL of BS-01 suspension ($OD595_{nm}$ = 0.8) a day before pathogen inoculation (*A. solani*) as a pre-infection treatment, while plants in treatment T_5 were treated with 1-2 mL of BS-01 suspension ($OD595_{nm}$ = 0.8) a day after pathogen inoculation (*A. solani*) as a post-infection treatment. In treatment T_6, the root surrounding soil (rhizosphere soil) of plants was supplemented with BS-01 suspension ($OD595_{nm}$ = 0.8) a day after pathogen inoculation. All the pots were placed in trays which were filled with distilled water to maintain soil moisture (40-50%). The plants were harvested after 15 days of pathogen/bacterial inoculation (30-days old plant) and the reduction in fungal load of *A. solani* due to different inoculation methods was quantified by real-time quantitative PCR (qPCR) (Awan et al., 2022).

TABLE 1 *In vivo* experimental design to check the control efficacy of *B. subtilis* (BS-01) against *Alternaria solani*.

Treatments	Description
T1	Healthy tomato plants without any treatment and inoculation, sprayed with distilled water only (-ve control)
T2	Tomato plants inoculated with the *A. solani* only (+ve control)
T3	Tomato seeds treated with BS-01 (*B. subtilis*) before sowing (pre-infection treatment)
T4	Tomato foliage treated with BS-01 (*B. subtilis*), followed by inoculation with *A. solani* after 24 hours (pre-infection treatment)
T5	Tomato foliage was first inoculated with *A. solani*, followed by being treated with BS-01 (*B. subtilis*) after 24 hours (post-infection treatment)
T6	Tomato foliage was first inoculated with *A. solani*, and after 24 hours, rhizospheric soil supplemented with BS-01 (*B. subtilis*) (post-infection treatment)

2.2.1 DNA extraction of tomato leaves

DNA of the tomato leaves from the above treatments was isolated 2 weeks after pathogen/bacterial inoculation. A modified CTAB (cetyltrimethyl ammonium bromide) protocol was used for DNA extraction from 0.25 g of leaf sample ground in liquid nitrogen and mixed with 600 µL of 2% CTAB buffer (2 g CTAB, 10 mL of 1 M Tris-HCl, 4 mL of 0.5 M EDTA, 28 mL of 5 M NaCl, 2 mL of beta-mercaptoethanol and 56 mL of autoclaved distilled water) in a pre-cooled Eppendorf tube. After incubation (60°C 1 h) and centrifugation (13,000 rpm for 10 min), the resulting supernatant was mixed with chloroform and isoamyl alcohol (24:1). The topmost aqueous phase was separated and successively mixed with 50 µL of 3 M sodium acetate and 500 µL of absolute ethanol (100%), incubated (-20°C 1 h) and centrifuged (13,000 rpm for 20 min) for the precipitation of DNA. The DNA pellet was washed thrice with 300 µL ethanol (70% v/v) and the dried pellet was re-suspended in TE buffer (Tris-EDTA buffer [0.2 mL of 0.5 M EDTA and 1 mL of 1 M Tris-HCl pH 8.0] to preserve it at -20°C (Syed-Ab-Rahman et al., 2018). The extracted genomic DNA was quantified and adjusted to 20 ng μL^{-1} for qPCR amplification using a Thermo Scientific NanoDrop apparatus.

2.2.2 Real-time quantitative PCR

For pathogen quantification, a set of *Alternaria solani*-specific primers for cytochrome *b* As_Cytb_F (5′-TCA GGA ACT CTG TGG CGT ATC-3′) and As_Cytb_R (5′-TCA GAT GAA AGG GAG GGA GGA C-3′) and another set of primers for a tomato house-keeping gene *ACTIN* Act_F (5′-GGC AGG ATT TGC TGG TGA TGA TGC T-3′) and Act_R (5′-ATA CGC ATC CTT CTG TCC CAT TCC GA-3′) were used.

For qPCR, 10 µL of the reaction mixture contained 5 µL SYBR green, 0.7 µL of each primer (10 µM), and 3.6 µL of extracted DNA (20 ng mL^{-1}). Quantitative PCR (qPCR) was performed using a CFX96 Touch™ Real-Time PCR detection system (Life Science Research, Bio-Rad). Thermal cycling conditions were set as follows: initial denaturation for 2 min at 95°C, followed by 5 s at 95°C and 10 s at 60°C for 45 cycles, and a final extension step at 60°C and 95°C for 5 s. Results were analyzed by the inbuilt software (CFX Manager™ software) connected to the CFX96 Touch™ Real-Time PCR detection system.

2.3 Identification and characterization of BS-01

Based on the previously reported studies (Shoaib et al., 2019; Awan and Shoaib, 2019 and Awan et al., 2022), this strain (BS-01) has antifungal potential against early blight pathogen. Thus, further identification and characterization of BS-01 were done in this study. *B. subtilis* (BS-01) was identified through standard protocols of phenotypic, biochemical and 16S rDNA gene sequencing. Phenotypic characterization was done by assessing the morphology of the colony and cell growth. Biochemical characterization was assessed by employing standard protocols and biochemical kit (Microgen biochemical identification kit) for Gram staining, oxidase activity, catalase activity, nitrate reduction, hydrolysis of gelatin, utilization of citrate, catalysis of malonate, production of acid from sugars (i.e., glucose, sucrose, lactose, arabinose, rhamnose, or raffinose) and production of alcohol sugars.

For 16S rDNA gene amplification, the chromosomal DNA was isolated using a bacterial DNA extraction kit (Genomic DNA mini kit, Thermo Fisher Scientific, USA) following the manufacturer's instructions. Amplification by PCR was performed using universal primers 27f (5'AGAGTTT GATCCTGGCTCAG-3') and 1492r (5'-TACGGTTACCTT GTTACGACT-3') (Hadi, 2013). PCR amplification was carried out with a program as follows: initial denaturation at 94°C for 6 min, followed by 60 s at 94°C, 60 s at 56°C and 60 s at 72°C for 30 cycles and final extension for 10 min at 72°C. The amplified PCR product was purified using a GeneJET Gel Extraction Kit (Thermo Fisher Scientific) and sent for sequencing to Macrogen (South Korea). The obtained sequences were searched for homology with sequenced genes from the National Center for Biotechnology Information (NCBI) database. The DNAMAN bioinformatics tool was used to construct a phylogenetic tree sequence alignment of bacterial DNA.

2.4 Extraction and fractionation of bacterial metabolites

B. subtilis (BS-01) is used to extract the VOCs in the extracellular metabolites and intracellular cellular metabolites, separately in three different organic solvents of varying polarity viz., *n*-hexane, dichloromethane and ethyl acetate at the Plant-Microbe Interactions Laboratory, University of Queensland, Australia.

2.4.1 Extracellular metabolites

The primary culture of *B. subtilis* was prepared in 20 mL of LB broth and kept in a shaking incubator at 30°C, 150 rpm for 24 h. The resulting starter culture was inoculated into 500 mL of LB broth supplemented with 5 g tryptone, 5 g NaCl and 2.5 g yeast extract in 500 mL of distilled water using 2000 mL Erlenmeyer flasks incubated at 30°C with 120 rpm shaking. After 72 h of incubation, the cell-free culture (supernatant) was obtained by centrifugation at 14,000 rpm for 20 min. This cell-free culture medium was allowed to concentrate (four times reduced) in the oven at 40°C for 48 h. The resulting metabolite concentrate was sequentially extracted with double volume (500 mL) of *n*-hexane, dichloromethane and ethyl acetate,

respectively. Primarily, concentrated culture (250 mL) and expected organic solvent (500 mL) was thoroughly homogenized by shaking at 150 rpm for 30 min and allowed to stand for 6-8 hours in a separating funnel (1000 mL). After getting a clear separation, the expected organic layer was separated very carefully and dried in a 1000 mL round bottle flask on a rotary evaporator at 40°C to finally collect a slimy mass of crude metabolites by following the protocol of Syed-Ab-Rahman et al. (2018).

2.4.2 Intracellular metabolites

For the extraction of intracellular metabolites, the secondary culture of *B. subtilis* was prepared from a primary culture as mentioned above. The bacterial cells were harvested at the exponential growth phase ($OD595_{nm}$ = 0.5) after 24 h (30°C) followed by centrifugation (14,000 rpm at 4°C) for 20 min (Meyer et al., 2010). The cell pellet was separated by discarding the cell-free culture and then washed with autoclaved distilled water to remove the excess culture medium. The bacterial pellet was weighed (2 g) and suspended in 30 mL of ice-cold 0.1 M PBS (pH 6.8). BS-01 cells in PBS were lysed for 50 min at 4°C through a cell disruptor (SONICS Vibra-Cell™ Ultrasonic Liquid Processors), which was programmed with successive disruption for 10 s followed by a pause for 10 s with 40% amplitude. This cell lysate (30 mL) expected organic solvent (500 mL) i.e., *n*-hexane, dichloromethane, and ethyl acetate were used to extract intracellular metabolites as described above (Syed-Ab-Rahman et al., 2018).

Extraction and fractionation of VOCs from BS-01 extra- and intracellular metabolites were sequentially done according to the polarity of three organic solvents, first with *n*-hexane followed by dichloromethane then followed by ethyl acetate.

2.5 Preparation of stock and testing concentrations

The concentrated extracts of both extra- and intracellular metabolites in three different organic solvents were used to prepare a stock concentration solution. A test stock concentration of 100 mg mL^{-1} was prepared by dissolving 1 mg of each extracted metabolite (slimy mass) in 1 mL of the respective organic solvent (*n*-hexane, dichloromethane and ethyl acetate) in separate glass sample vials (1.5 mL). Different concentrations of each extracted fraction were prepared from the stock solution (100 mg mL^{-1}) by diluting serially with respective organic solvents to make final concentrations (10, 20, 40, 60, 80 and 100 mg mL^{-1}).

2.5.1 Antifungal bioassays with organic fractions

The organic fractions (*n*-hexane, dichloromethane, and ethyl acetate) of VOCs extracted from extra- and intracellular bacterial metabolites were assessed for their antifungal activity against *A. solani*. The antifungal activity of the fractions was tested using broth micro-dilution techniques in 96-well microtitre plates. For the bioassay, a microplate (96-well) was filled with 200 µL of malt extract broth (2% ME). Each well was supplemented with 10 µL of different concentrations (10, 20, 40, 60, 80 and 100 mg mL^{-1}) of the desired fraction and the same well was inoculated with 10 µL of a conidial suspension (1.0×10^3 conidia mL^{-1}). Microplate wells were filled with 2% ME broth (200 µL), supplemented with 10 µL of relevant pure organic solvent (*n*-hexane, dichloromethane and ethyl acetate) and 10 µL of a conidial suspension, served as a negative control treatment (0 mg mL-1: without extracted organic fraction).

For the positive control treatment, wells were filled with 2% ME broth and inoculated with 10 µL of conidial suspension of *A. solani*, only. *In vitro* antifungal bioassay was tested thrice) arranged in a completely randomized design with five replications (N=5) for each treatment. After incubation for 48 h at 28°C, the harvested fungal biomass was dried and weighed. Percentage inhibition in fungal biomass was calculated over the positive control using the following formula (Shoaib et al., 2019).

$$\text{Percent inhibition (\%)} = \frac{\text{Control} - \text{Treatment}}{\text{Control}} \times 100$$

2.5.2 Gas chromatography–mass spectrometry (GC-MS) analysis

The organic fractions of both extra- and intracellular metabolites were carried out in a GC-MS system (Shimadzu Corporation, Kyoto, Japan) for analysis. The flow rate of carrier gas (helium) was set at 17.5 mL min^{-1} at a constant linear velocity of 42.7 cm s^{-1} with a split ratio of 1:10. The injector temperature and initial oven temperature were kept at 320°C and 100°C, respectively. The temperature gradient of 100-340°C (10°C min^{-1}) and isothermal at 100°C (for 1 min) were programmed in the oven. The mass spectrometer was operated with an ion source temperature of 250°C and an interface temperature of 340°C. The analysis was performed in a full-scan mode with a mass range of 42-500 m/z and the run time was completed in 30 min (Syed-Ab-Rahman et al., 2018). For data processing, GC-MS Postrun analysis software was employed. The constituents of peaks were finally recognized after comparing them with available data in the NIST-14 mass spectrum library (National Institute of Standards and Technology, USA).

2.6 Statistical analyses

Significant differences ($p \leq 0.05$) in plant disease resistance assays were determined by Student's t-test. The relative performance of the data recorded from *in vitro* bioassays was compared after getting significant results in the analysis of

variance (ANOVA) and their means were compared using Fisher's protected least significant difference test (LSD) at $p \leq 0.05$ using Statistix 8.1.

3 Results

3.1 Evaluation of *B. subtilis* to control early blight in tomato

Preventive and curative effects of BS-01 application to control tomato early blight were evaluated by quantifying pathogen load in tomato foliage using a set of *A. solani*-specific primers "cytochrome *b*". The fungal load (0.283 pg) was highest in the positive control. It was assessed that both preventive and curative measures for the earl blight disease control in tomatoes significantly reduce the pathogen load by 85-90% as compared to the positive control (Figure 1). Notably, preventative measure (foliar or seed application with BS-01 before pathogen inoculation exhibited slightly more effective in reducing pathogen load as compared to curative measure (effect foliar or soil application with BS-01 following pathogen inoculation). Therefore, a significantly lowest fungal load by 90% (0.028 pg) was observed in a preventive method when plants were provided with a foliar application of BS-01 treatment before pathogen inoculation (T4) as compared to positive control plants.

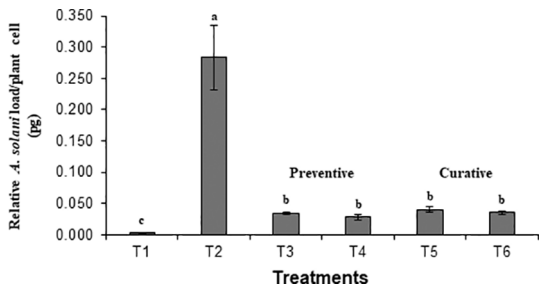

FIGURE 1
Effect of *Bacillus subtilis* (BS-01) on the relative fungal load of *Alternaria solani* (AS) in tomato foliage using qPCR after 7 days of pathogen inoculation. Values with different letters show a significant difference ($p \leq 0.05$) mean value of five biological replicates (N=5) as determined by the LSD test. Error bars indicate the standard errors of the mean of replicates (N=5). Note. T_1: -ve control (healthy tomato plants without any treatment and inoculation of AS), T_2: +ve control (plants inoculated with AS only), T_3: Tomato seeds treated with BS-01 (*B. subtilis*) before sowing, T_4: Tomato foliage treated with BS-01 one day before AS inoculation; T_5: Tomato foliage treated with BS-01 one day after AS inoculation; T_6: tomato rhizosphere soil supplemented with BS-01 one day after AS inoculation.

3.2 Characterization of *Bacillus subtilis* BS-01

BS-01 was identified as *Bacillus subtilis* based on the morphological, biochemical and molecular data. It is a gram-positive, facultatively anaerobic and endospore-forming bacterium. Colonies on Luria-Bertani agar medium were medium-sized, white to creamy, dry, flat, and round with smooth margins. The bacterial cells were motile, rod-shaped, and occurred as small clusters and short chains. They displayed a positive reaction to catalase, oxidase, citrate, gelatin hydrolysis, malonate catalysis and the ability to ferment simple sugars (glucose and sucrose) as well as sugar alcohols (inositol, sorbitol, and adonitol) for acid production, but were negative for arabinose, rhamnose and raffinose (Table 2).

16S rDNA sequences of BS-01 were aligned and identified after blasting the sequence reads against the National Center for Biotechnology Information (NCBI) nucleotide database. A sequence of BS-01 was deposited in the NCBI GenBank database with the accession number LC425129.1. The alignment results showed that the strain BS-01 was closely related to the following *Bacillus subtilis* strains i.e., SXAU-B (MK875169.1), R37 (MK696406.1), YJ73 (KY652934.1), VITSGK1 (MK817557.1), L31 (KY652944.1), C16 (MH141058.1), Q3B1 (MK774698.1), 99SS2 (MK713722.1), A1b79 (MK737184.1) and 94SS1 (MK713700.1) with the highest similar identity 99.9–100% query cover. Finally, a phylogenetic tree was constructed using Clustal X analysis of MEGA7 (Figure 2).

3.3 Antifungal activity of extracellular and intracellular metabolites

Different concentrations of ethyl acetate, *n*-hexane and dichloromethane and fractions of extracellular metabolites significantly ($p \leq 0.05$) decreased fungal biomass by 69–98%, 63–88% and 41–74%, respectively, over positive control (2.42 mg) (Table 3; Figure 3). Likewise, different concentrations (10, 20, 40, 60, 80 and 100 mg mL^{-1}) of the ethyl acetate, dichloromethane and *n*-hexane fractions of intracellular metabolites showed significant ($p \leq 0.05$) reductions in fungal biomass by 48–85%, 42–70% and 35–62%, respectively, concerning the positive control (2.42 mg) (Table 4; Figure 4).

3.3.1 GC-MS analysis of Extracellular metabolites

B. subtilis (LC425129.1.) provided an abundant source of biocidal compounds. All three fractions from extracellular metabolites were analyzed through GC-MS for the identification of the potential antifungal compounds. Based on peak area (%), these compounds were categorized into four groups i.e., most abundant, moderately abundant, less abundant and least abundant.

TABLE 2 Morphological and biochemical reactions of *Bacillus subtilis* (BS-01).

Cultural characters		Cell morphology	
Colony	White to creamy white, dry, flat, round with smooth margins	Shape	Rod
		Motile	+
Optimum temperature	30-37 °C	Gram type	+
		Endospore	+
Reactions		Reactions	
Catalase	+	Sorbitol	–
Oxidase	+	Adnonitol	–
Citrate	+	Arabinose	+
Gelatin hydrolysis	+	Raffinose	+
Malonate	+	Rhamnose	+
Inositol	–	Sucrose	+
		Lactose	–

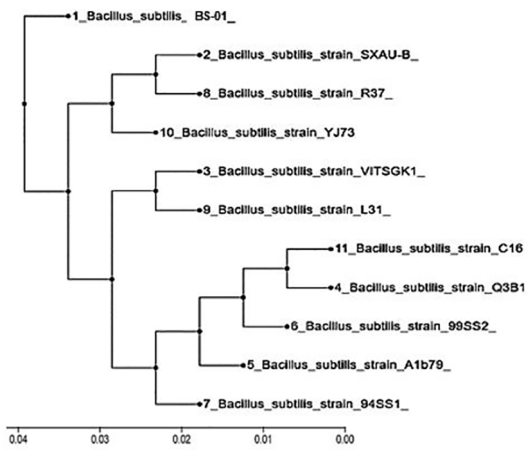

FIGURE 2
Phylogenetic tree constructed based on the 16S rDNA gene for *Bacillus subtilis* (BS-01) and ten other strains obtained from the NCBI database.

a) *n*-Hexane fraction: The GC-MS chromatogram analysis of the *n*-hexane fraction of bacterial extracellular metabolite specified eleven peaks (Supplementary Figure S1; Table 5). The most abundant compound was triphenylphosphine oxide (41.40%) followed by dodecyl acrylate (8.60%) as a moderately abundant compound. Five compounds [2-methyleicosane (3.0%); octacosane (3.0%); hexatriacontane (2.90%); *n*-hexadecanoic acid (2.40%); tetratetracontane (2.10%)] were found as less abundant compounds. The remaining four compounds viz., pyrrolo[1,2-a] pyrazine-1,4-dione, hexahydro-3-(2-methylpropyl)- (2.0%); 7-hexyleicosane (1.90%); heptacosane (1.40%) and E-15-heptadecenal (1.5%) were the least abundant compounds in the *n*-hexane fraction. The structures of these compounds are shown in Figure 5.

b) Dichloromethane fraction: GC-MS analysis revealed the occurrence of six compounds in the dichloromethane fraction of extracellular metabolites of BS-01 (Supplementary Figure S2; Table 6). Two compounds viz., pyrrolo[1,2-a] pyrazine-1,4-dione, hexahydro-3-(2-methylpropyl) and pyrrolo[1,2-a] pyrazine-1,4-dione, hexahydro-3-(phenylmethyl)- were categorized as the most abundant, exhibiting the highest proportion of 28.20% and 27.20%, respectively. Ergotaman-3',6',18-trione, 9,10-dihydro-12'-hydroxy-2'-methyl-5'-(phenylmethyl)-, (5'.alpha.,10.alpha.) was a moderately abundant compound (4.20%). Two compounds, including 3, 6-bis(2-methylpropyl)-2,5-piperazinedione (3.0%) and N-acetyl-3-methyl-1,4-diazabicyclo [4.3.0] nonan-2,5-dione (2.90%), were among the less abundant compounds and tryptophan (0.5%) occurred as the least abundant compound. The structures of these compounds are depicted in Figure 6.

c) Ethyl acetate fraction: According to the GC-MS analysis, 13 bioactive compounds were identified in the ethyl acetate fraction of extracellular metabolites (Supplementary Figure S3; Table 7). Two compounds were documented as the most abundant [*n*-hexadecanoic acid (10.10%) and octadecane (7.10%)], while three compounds were moderately abundant [dodecyl acrylate (5.90%); eicosane (5.60%) and octadecanoic acid (5.60%)]. Tetracosane (4.78%) followed by benzeneacetic acid (3.60%) and di-*n*-octyl phthalate (2.40%) were less abundant compounds. Hexadecane (1.4%); decanedioic acid, bis(2-ethylhexyl) ester (1.20%); 2-phenoxyethanol (1.0%); E-15-heptadecenal (1.0%) and hexacosane (0.70%) were the least abundant compounds. The structures of these compounds are presented in Figure 7.

TABLE 3 Effect of different fractional concentrations of extracellular metabolites of *Bacillus subtilis* (BS-01) on the growth of *Alternaria solani* (AS).

Concentrations(mg mL^{-1})	Fungal biomass (mg)		
	n-Hexane	Dichloromethane	Ethyl acetate
+ve control (AS)	2.42 ± 0.133^{a}	2.42 ± 0.133^{a}	2.42 ± 0.146^{a}
-ve control	2.23 ± 0.124^{a}	1.89 ± 0.114^{ab}	2.38 ± 0.167^{a}
10 mg mL^{-1}	1.79 ± 0.099^{b}	1.81 ± 0.109^{b}	1.62 ± 0.120^{b}
20 mg mL^{-1}	1.21 ± 0.061^{c}	1.67 ± 0.117^{bc}	0.99 ± 0.085^{c}
40 mg mL^{-1}	0.89 ± 0.048^{d}	1.42 ± 0.093^{c}	0.74 ± 0.077^{d}
60 mg mL^{-1}	0.38 ± 0.021^{e}	1.11 ± 0.061^{d}	0.26 ± 0.046^{e}
80 mg mL^{-1}	0.32 ± 0.019^{e}	0.89 ± 0.054^{de}	0.20 ± 0.04^{e}
100 mg mL^{-1}	0.28 ± 0.016^{e}	0.64 ± 0.035^{e}	0.04 ± 0.03^{f}

Values with different superscript letters show a significant difference ($p \leq 0.05$) in mean value of replicates (N=5) of each treatment as determined by LSD test. ± value indicates the standard error mean of replicates (N=5).
+ve control: with inoculation of *A. solani* (AS) only; -ve control: without inoculation of *A. solani* (AS) and applied organic solvent only.

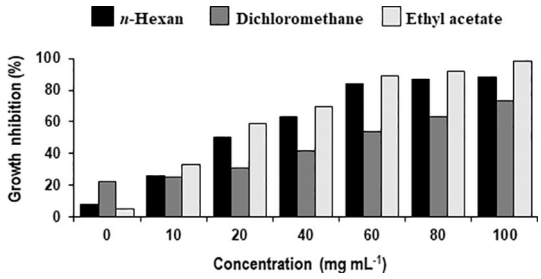

FIGURE 3
Percentage decrease in biomass of *Alternaria solani* due to different fractional concentrations of extracellular metabolites of *Bacillus subtilis* (BS-01).

3.3.2 GC-MS analysis of Intracellular metabolites

The identification of the potential antifungal compounds exhibited in all three fractions from intracellular metabolites of BS-01 were analyzed through GC-MS as mentioned above.

a) *n*-Hexane fraction: The GC-MS chromatogram revealed 16 peaks from the *n*-hexane fraction of intracellular metabolites of BS-01 (Supplementary Figure S4; Table 8). The chromatogram revealed the occurrence of octaethylene glycol monododecyl ether (1.95%); pentaethylene glycol monododecyl ether (1.90%) and hexaethylene glycol monododecyl ether (1.77%) at the highest frequency (most abundant). However, four other compounds viz., di-*n*-octyl phthalate (1.35%); heptaethylene glycol monododecyl ether (1.07%); *n*-hexadecanoic acid (1.04%) and propionic acid, 3-iodo-, octadecyl ester (1.04%) were observed in lower amounts (moderately abundant). Four compounds viz., 5-(2-methylpropyl)-nonane; octadecanoic acid; heneicosane and tetraethylene glycol monododecyl ether, displayed as less abundant compounds, while the remaining five compounds [octadecane; 1,2-benzenedicarboxylic acid, bis(2-methylpropyl) ester; hexadecane; 2,4-di-terta-butylphenol and 2,5-di-terta-butyl-1,4-benzoquinone exhibited less than 0.5% abundance and ranked as least abundant. The structures of these compounds are displayed in Figure 8.

b) Dichloromethane fraction: The GC-MS analysis of the dichloromethane fraction of intracellular metabolites of BS-01 detected eight compounds (Supplementary Figure S5; Table 9). Only one compound was noticed as the most abundant compound [phthalic acid, butyl undecyl ester (1.07%)]. Trans-geranylgeraniol (0.67%) and heneicosane (0.63%) were among the moderately abundant compounds, while pyrrolo[1,2-a] pyrazine-1,4-dione, hexahydro-3-(2-methylpropyl)- (0.55%); 1-octadecene (0.55%) and 2-methyl-1-hexadecanol (0.45%) were found as less abundant compounds. Pentaethylene glycol monododecyl ether and disooctyl phthalate were detected in a similar proportion and classified as the least abundant compounds (0.34%). The structures of these compounds are presented in Figure 9.

c) Ethyl acetate fraction: The GC-MS analysis of ethyl acetate fraction of intracellular metabolite resulted in the identification of 14 compounds (Supplementary Figure S6; Table 10). The most abundant compounds identified were *n*-hexadecanoic acid (7.73%) and *n*-tridecan-1-ol (6.15%). Moderately abundant compounds were octadecanoic acid (5.04%) and cyclopentane, 3-hexyl-1,1-dimethyl- (4.13%). Whilst, bis(2-ethylhexyl) phthalate (2.15%); nonadecane (1.97%); 1,1'-biphenyl, 2,2',5,5'-tetramethyl- (1.46%); 3,4-dimethylbenzophenone (1.03%) and heneicosane (1.01%) were

TABLE 4 Effect of different fractional concentrations of intracellular metabolites of *Bacillus subtilis* (BS-01) on the growth of *Alternaria solani* (AS).

Concentrations (mg mL^{-1})	Fungal biomass (mg)		
	n-Hexane	Dichloromethane	Ethyl acetate
+ve control (AS)	2.42 ± 0.133^{a}	2.42 ± 0.133^{a}	2.42 ± 0.146^{a}
0 mg mL^{-1} (-ve control)	2.23 ± 0.124^{a}	1.89 ± 0.114^{ab}	2.38 ± 0.167^{a}
10 mg mL^{-1}	1.79 ± 0.099^{b}	1.81 ± 0.109^{b}	1.62 ± 0.120^{b}
20 mg mL^{-1}	0.99 ± 0.061^{c}	1.67 ± 0.117^{bc}	1.21 ± 0.085^{bc}
40 mg mL^{-1}	0.74 ± 0.048^{d}	1.42 ± 0.093^{c}	0.89 ± 0.077^{c}
60 mg mL^{-1}	0.38 ± 0.021^{e}	1.11 ± 0.061^{d}	0.26 ± 0.046^{d}
80 mg mL^{-1}	0.32 ± 0.019^{e}	0.89 ± 0.054^{de}	0.20 ± 0.04^{d}
100 mg mL^{-1}	0.28 ± 0.016^{e}	0.64 ± 0.035^{e}	0.04 ± 0.03^{e}

Values with different superscript letters show a significant difference ($p \leq 0.05$) in mean value of replicates (N=3) of each treatment as determined by LSD test. ± value indicates the standard error mean of replicates (N=3).
+ve control: with inoculation of *A. solani* (AS) only; -ve control: without inoculation of *A. solani* (AS) and applied organic solvent only.

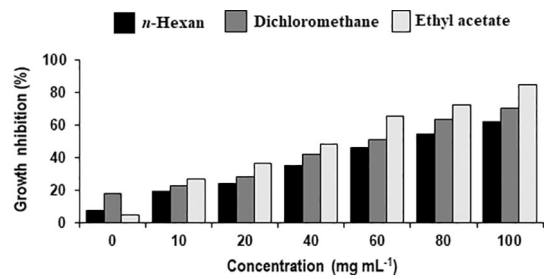

FIGURE 4
Percentage decrease in biomass of *Alternaria solani* due to different fractional concentrations of intracellular metabolites of *Bacillus subtilis* (BS-01).

ranked as less abundant compounds. In addition, the remaining compounds [benzenepropanoic acid 3,5-bis(1,1-dimethylethyl)-4-hydroxy-, octadecyl ester; trans-geranylgeraniol; decanedioic acid, bis(2-ethylhexyl) ester; 9-octadecenamide, (Z)- and propanoic acid, decyl ester] were present in the range of 0.99–0.35%. The structures of these compounds are displayed in Figure 10.

4 Discussion

A bacterial strain named "BS-01" was characterized to divulge its identity due to its clear antifungal effect against *A. solani* and its 16rDNA sequence displayed >99.5% homology with the *Bacillus subtilis*. Our results indicated that strain BS-01 is closely related to numerous species by exhibiting high similarities (≥ 99%). Several strains of *B. subtilis* and some other species of the genus are often

TABLE 5 Bioactive compounds identified from *n*-hexane fraction of extracellular metabolites of *Bacillus subtilis* (BS-01) through GC-MS analysis.

Sr. No.	Compounds	Molecular Formula	Molecular weight (g/mol)	Retention time (min)	Peakarea (%)
1	E-15-Heptadecenal	$C_{17}H_{32}O$	252	12.30	1.5
2	Pyrrolo[1,2-a] pyrazine-1,4-dione, hexahydro-3-(2-methylpropyl)-	$C_{11}H_{18}N_2O_2$	154	13.82	2.0
3	*n*-Hexadecanoic acid	C16H32O2	256	14.01	2.4
4	Dodecyl acrylate	C15H28O2	240	17.07	8.6
5	7-Hexyleicosane	$C_{26}H_{54}$	366	17.92	1.9
6	Tetratetracontane	C44H90	619	18.72	2.1
7	Triphenylphosphine oxide	C18H15OP	278	19.22	41.4

(Continued)

TABLE 5 Continued

Sr. No.	Compounds	Molecular Formula	Molecular weight (g/mol)	Retention time (min)	Peakarea (%)
8	2-Methyleicosane	C21H44	296	19.49	3.0
9	Octacosane	C28H58	394	20.95	3.0
10	Hexatriacontane	C36H74	507	22.30	2.9
11	Heptacosane	C27H56	380	23.57	1.7

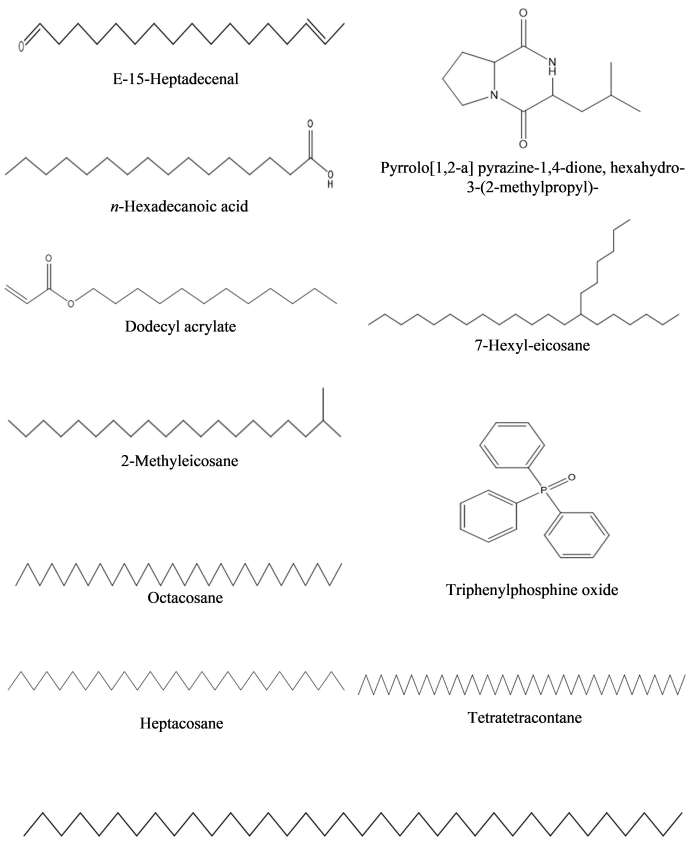

FIGURE 5
Structures of compounds identified from n-hexane fraction of extracellular metabolites of *Bacillus subtilis* (BS-01) through GC-MS analysis.

found as colonizers of the internal tissues of plants and promote plant growth even under stress (Han et al., 2015; Abbas et al. (2014)). To assess the impact of preventive and curative treatments of *B. subtilis* (BS-01) on the pathogen load in *A. solani*-infected tomato plants, BS-01 was applied before or after the pathogen's inoculation. The tomato plants or seeds inoculated with BS-01 before infection of *A. solani* (preventive) exhibited a significantly lower pathogen load as compared to the BS-01 application on plants or in soil, after pathogen challenge (curative). This observation corresponds to results found by El-Sheikh et al. (2002), who stated that protective treatments with antagonistic *Bacillus* spp. were more effective than curative treatments to control *Phytophthora infestans* in potato crops. Ongena et al. (2005) also suggested that pre-treatment of BS-01 not only produces bioactive compounds but also sensitized tomato plants to subsequently reduce a pathogen infestation. Plant protection as conferred by bacteria (*B. subtilis*) used in this study could result from the induction of systemic resistance which enhances biological control over tomato early blight through direct antagonisms (Khanna et al., 2019b; Awan et al.,

10.3389/fpls.2022.1089562

TABLE 6 Bioactive compounds identified from dichloromethane fraction of extracellular metabolites of *Bacillus subtilis* (BS-01) through GC-MS analysis.

Sr. No.	Compounds	Molecular Formula	Molecular weight (g/mol)	Retention time (min)	Peak area (%)
1	N-acetyl-3-methyl-1,4-diazabicyclo [4.3.0] nonan-2,5-dione,	$C_{10}H_{14}N_2O_3$	210	11.60	2.9
2	Pyrrolo[1,2-a] pyrazine-1,4-dione, hexahydro-3-(2-methylpropyl)-	$C_{11}H_{18}N_2O_2$	210	14.03	28.2
3	2,5-Piperazinedione, 3,6-bis(2-methylpropyl)-	$C_{12}H_{22}N_2O_2$	226	14.07	3.0
4	Ergotaman-3',6',18-trione, 9,10-dihydro-12'-hydroxy-2'-Methyl-5'-(phenylmethyl)-, (5'.alpha.,10.alpha.)-	$C_{33}H_{37}N_5O_5$	583	17.72	4.2
5	Pyrrolo[1,2-a] pyrazine-1,4-dione, hexahydro-3-(phenylmethyl)-	$C_{14}H_{16}N_2O_2$	244	18.11	27.2
6	Tryptophan	$C_{11}H_{12}N_2O_2$	204	23.54	0.5

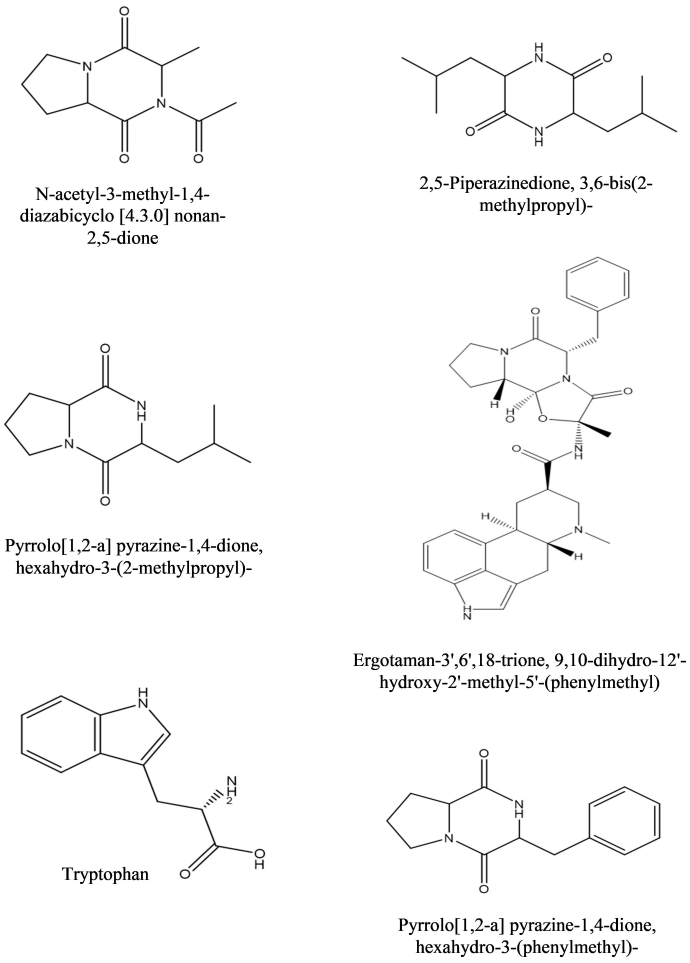

FIGURE 6
Structures of compounds identified from the dichloromethane fraction of extracellular metabolites of *Bacillus subtilis* (BS-01) through GC-MS analysis.

TABLE 7 Bioactive compounds identified from ethyl acetate fraction of extracellular metabolites of *Bacillus subtilis* (BS-01) through GC-MS analysis.

Sr. No.	Compounds	Molecular Formula	Molecular weight (g/mol)	Retention time (min)	Peakarea (%)
1	2-Phenoxyethanol	C8H10O2	138	5.59	1.0
2	Benzeneacetic acid	C8H8O2	136	5.95	3.6
3	Hexadecane	C16H34	226	7.73	1.4
4	Eicosane	C20H42	282	10.12	5.6
5	Dodecyl acrylate	C15H28O2	240	11.21	5.9
6	E-15-Heptadecenal	C17H32O	252	12.29	1.0
7	Octadecane	C18H38	254	12.37	7.1
8	n-Hexadecanoic acid	C16H32O2	256	14.06	10.1
9	Tetracosane	C24H50	338	14.38	4.78
10	Octadecanoic acid	C18H36O2	284	15.93	5.6
11	Di-n-octyl phthalate	C24H38O4	390	19.17	2.4
12	Hexacosane	C26H54	366	19.48	0.7
13	Decanedioic acid, bis(2-ethylhexyl) ester	C26H50O4	426	21.03	1.2

2022). The antifungal activity of this strain BS-01 against *A. solan* has been tested in a previous study (Shoaib et al., 2019). In another work, Awan et al. (2022) also studied tomato early blight is significantly managed with the application of a biocontrol agent namely *Bacillus subtilis* (BS-01) along with plant nutrients in the field.

In addition, the current study investigated the antifungal assays with the various concentrations (10-100 mg mL^{-1}) of extra- and intracellular bacterial metabolites of BS-01 extracted in organic solvents (*n*-hexane, dichloromethane, and ethyl acetate) revealed that higher concentrations (>40 mg mL^{-1}) of different fractions showed a noticeable antifungal effect against *A. solani* (Farhana et al., 2014). Results of our GC-MS analyses also showed an abundance of compounds of antifungal origin in all three organic fractions of both extra- and intracellular metabolites. The ethyl acetate fraction from both extra- and intracellular metabolites showed a strong inhibition in fungal biomass (69–98% and 48–85%) followed by *n*-hexane (63–88% and 35–62%) and dichloromethane (41–74% and 42–70%), respectively, indicating that the percentage of the bioactive compounds in the ethyl acetate fraction after each step of purification has increased. Therefore, it exhibited antifungal activity at a lower concentration than those for the other fractions (Al-Saraireh et al., 2015). Former studies on *Bacillus* metabolites extracted in organic solvents revealed that ethyl acetate and chloroform fractions of *Bacillus* strains hold greater antifungal potential due to chemical multiplicity (peptide, polyketide, lipopeptide, phospholipid, and others) (Numan et al., 2022).

The extracellular fraction of ethyl acetate, *n*-hexane and dichloromethane displayed the presence of 13, 11 and 6 biocidal compounds, respectively. However, the most abundant compound identified in the ethyl acetate fraction of extracellular metabolite was *n*-hexadecanoic acid (10.10%) and octadecane (7.10%) followed by three moderately abundant compounds viz., dodecyl acrylate, eicosane and octadecanoic acid in the range of 5.6–5.9%. Such compounds were also identified by Bharose and Gajera (2018) from a crude extract of *Bacillus* and *Pseudomonas* metabolites. *n*-hexadecanoic acid (fatty acid) is a potential antifungal, antibacterial, antioxidant, anticancer, nematicide and pesticide compound which has been isolated from many medicinal plants (Umaiyambigai et al., 2017) and metabolites of *B. subtilis* strain HD16b. Octadecane (alkane) identified from volatile organic compounds of *Bacillus pumilu* displayed the strongest inhibition against *Penicillium italicum* (Morita et al., 2019). Eicosane (an alkane) has antioxidant, antimicrobial and antifungal properties (Theng and Korpenwar, 2015) and has been used against target spots in tobacco leaf caused by *Rhizoctonia solani* (Ahsan et al., 2017). Likewise, octadecanoic acid (ethyl ester) isolated with other compounds from *Bacillus atrophaeus* strain showed the potential to manage *Verticillium* wilt (Mohamad et al., 2018). Another important compound i.e. tetracosane (alkane) was recorded as less abundant (4.78%) in the ethyl acetate fraction, however, it is also used as an antibacterial, antifungal and anticancer compound. Ni et al. (2018) documented a strong inhibitory effect of *Bacillus atrophaeus* against *Botrytis cinerea* and suggested the presence of tetracosane with other compounds (octadecanoic acid, hexadecane, 2-methyl- and eicosane, etc.) in their dichloromethane fraction of bacterial metabolites.

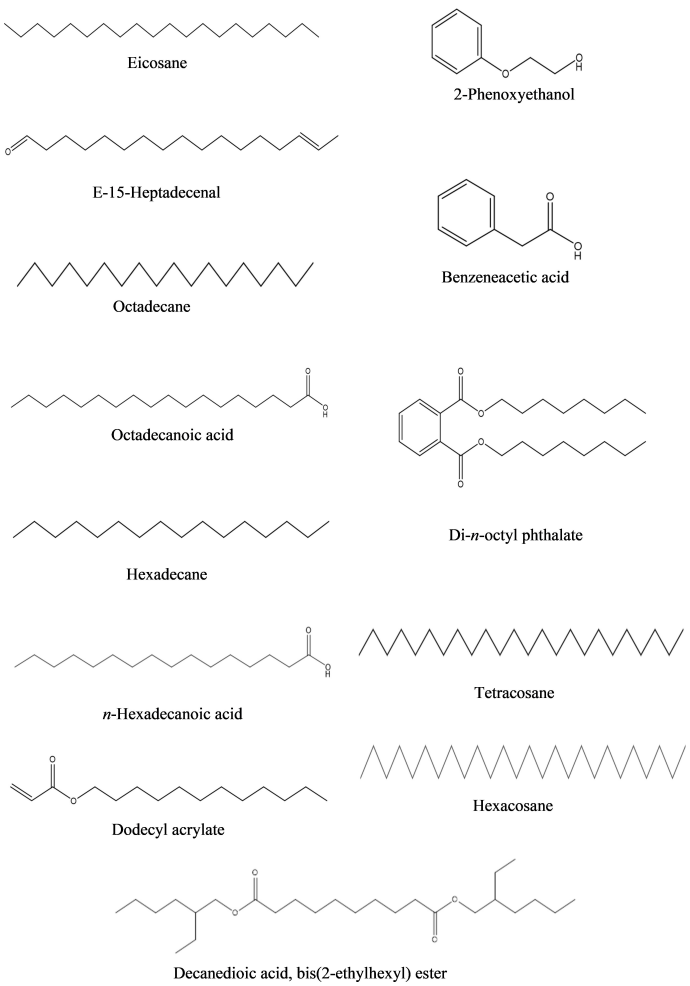

FIGURE 7
Structures of compounds identified from ethyl acetate fraction of extracellular metabolites of *Bacillus subtilis* (BS-01) through GC-MS analysis.

TABLE 8 Bioactive compounds identified from *n*-hexane fraction of intracellular metabolites of *Bacillus subtilis* (BS-01) through GC-MS analysis.

Sr. No.	Compounds	Molecular Formula	Molecular weight (g/mol)	Retention time (min)	Peak area (%)
1	Octadecanoic acid	$C_{40}H_{80}O_2$	593	27.2	0.96
2	Heptaethylene glycol monododecyl ether	$C_{26}H_{54}O_8$	494	25.7	1.07
3	Hexaethylene glycol monododecyl ether	$C_{24}H_{50}O_7$	450	25.0	1.77
4	Octaethylene glycol monododecyl ether	$C_{28}H_{58}O_9$	538	22.3	1.95
5	Pentaethylene glycol monododecyl ether	$C_{22}H_{46}O_6$	406	21.6	1.9
6	Heneicosane	$C_{21}H_{44}$	296	17.9	0.59
7	Di-*n*-octyl phthalate	$C_{24}H_{38}O_4$	390	19.1	1.35
8	Tetraethylene glycol monododecyl ether	$C_{20}H_{42}O_5$	362	18.3	0.66

(Continued)

TABLE 8 Continued

Sr. No.	Compounds	Molecular Formula	Molecular weight (g/mol)	Retention time (min)	Peak area (%)
9	Propionic acid, 3-iodo-, octadecyl ester	$C_{21}H_{41}IO_2$	452	17.0	1.04
10	Octadecane	$C_{18}H_{38}$	254	14.4	0.43
11	*n*-Hexadecanoic acid	$C_{16}H_{32}O_2$	256	13.9	1.04
12	1,2-Benzenedicarboxylic acid, bis(2-methylpropyl) ester	$C_{16}H_{22}O_4$	278	13.1	0.13
13	Hexadecane	$C_{16}H_{34}$	226	10.1	0.06
14	2,4-Di-tert-butylphenol	$C_{14}H_{22}O$	206	9.1	0.02
15	2,5-Di-tert-butyl-1,4-benzoquinone	$C_{14}H_{20}O_2$	220	8.7	0.02
16	5-(2-Methylpropyl)-nonane	$C_{13}H_{28}$	184	6.2	0.96

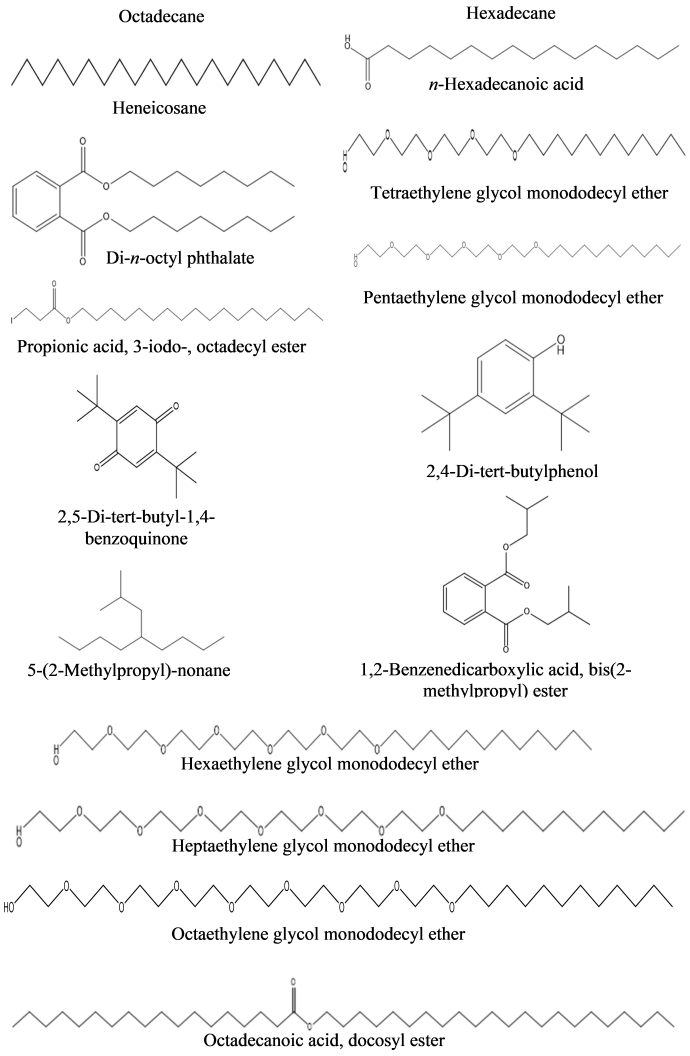

FIGURE 8
Structures of compounds identified from the n-hexane fraction of intracellular metabolites of *Bacillus subtilis* (BS-01) through GC-MS analysis.

10.3389/fpls.2022.1089562

TABLE 9 Bioactive compounds identified from dichloromethane fraction of intracellular metabolites of *Bacillus subtilis* (BS-01) through GC-MS analysis.

Sr. No.	Compounds	Molecular Formula	Molecular weight (g/mol)	Retention time (min)	Peak area (%)
1	Trans-geranylgeraniol	$C_{20}H_{34}O$	290	24.8	0.67
2	Heneicosane	$C_{21}H_{44}$	296	19.4	0.62
3	Pentaethylene glycol monododecyl ether	$C_{22}H_{46}O_6$	406	19.7	0.34
4	Diisooctyl phthalate	$C_{24}H_{38}O_4$	390	19.1	0.34
5	Pyrrolo[1,2-a] pyrazine-1,4-dione, hexahydro-3-(2-methylpropyl)-	$C_{11}H_{18}N_2O_2$	210	13.8	0.55
6	Phthalic acid, butyl undecyl ester	$C_{23}H_{36}O_4$	376	13.1	1.07
7	2-Methyl-1-hexadecanol	$C_{17}H_{36}O$	256	11.7	0.45
8	1-Octadecene	$C_{18}H_{36}$	252	11.5	0.55

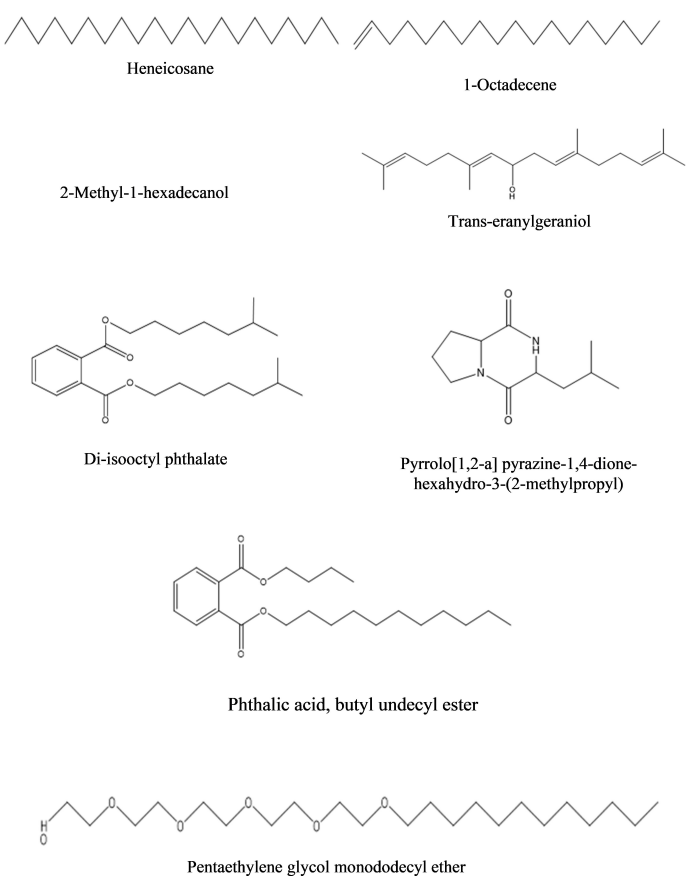

FIGURE 9
Structures of compounds identified from the dichloromethane fraction of intracellular metabolites of *Bacillus subtilis* (BS-01) through GC-MS analysis.

TABLE 10 Bioactive compounds identified from ethyl acetate fraction of intracellular metabolites of *Bacillus subtilis* (BS-01) through GC-MS analysis.

Sr. No.	Compounds	Molecular Formula	Molecular weight (g/mol)	Retention time (min)	Peak area (%)
1	Benzenepropanoic acid, 3,5-bis(1,1-dimethylethyl)-4-hydroxy-, octadecyl ester	$C_{35}H_{62}O_3$	530	26.1	0.98
2	Trans-geranylgeraniol	$C_{20}H_{34}O$	290	24.8	0.46
3	Decanedioic acid, bis(2-ethylhexyl) ester	$C_{26}H_{50}O_4$	426	20.9	0.77
4	Bis(2-ethylhexyl) phthalate	$C_{24}H_{38}O_4$	390	19.1	2.15
5	9-Octadecenamide, (Z)-	$C_{18}H_{35}NO$	281	17.6	0.37
6	Propanoic acid, decyl ester	$C_{13}H_{26}O_2$	214	17.1	0.35
7	Heneicosane	$C_{21}H_{44}$	296	16.2	1.01
8	Octadecanoic acid	$C_{18}H_{36}O_2$	284	15.9	5.04
9	Nonadecane	$C_{19}H_{40}$	268	14.3	1.97
10	*n*-Hexadecanoic acid	$C_{16}H_{32}O_2$	256	14.0	7.73
11	3,4-Dimethylbenzophenone	$C_{15}H_{14}O$	210	13.5	1.03
12	Cyclopentane, 3-hexyl-1,1-dimethyl-	$C_{13}H_{26}$	182	11.9	4.13
13	1,1'-Biphenyl, 2,2',5,5'-tetramethyl-	$C_{34}H_{36}$	444	11.5	1.46
14	*n*-Tridecan-1-ol	$C_{13}H_{28}O$	200	11.2	6.15

In the *n*-hexane fraction of extracellular metabolites of BS-01, triphenylphosphine oxide (TPPO: 41.40%) was detected as the most abundant compound followed by dodecyl acrylate (8.60%) as a moderately abundant compound. TPPO is a popular organophosphorus compound, which has been extensively employed as a ligand for many metals and the resulting compounds indicated strong antimicrobial activities (Karakus et al., 2014; Faiz et al., 2016). TPPO exhibited potential antifungal activities due to mitochondrial dysfunction in *Candida albicans* as TPP^+-conjugates can bypass active expulsion by efflux pumps and accumulate in the fungal mitochondria to exert fungicidal activity (Chang et al., 2018). Dodecyl acrylate (ester), isolated from secondary metabolites of *Streptomyces werraens* has also shown antifungal potential against *Fusarium oxysporum* (Singh and Wahla, 2018). Bharose and Gajera (2018) reported that dodecyl acrylate extracted from *B. subtilis* has strong antioxidant and antifungal effects against the aflatoxin-producing fungus *Aspergillus flavus*.

The most abundant compound detected from the dichloromethane fraction of extracellular metabolites was pyrrolo [1,2-a] pyrazine-1,4-dione, hexahydro-3-(2-methylpropyl) (28.20%) and a moderately abundant compound was pyrrolo[1,2-a] pyrazine-1,4-dione, hexahydro-3-(phenylmethyl)- (27.20%). Likewise, both of these organic compounds have been reported as possible antifungal compounds from *Bacillus* and *Streptomyces* species (Manimaran et al., 2017). Kiran et al. (2018) and Tangjitjaroenkun (2018) reported that pyrrolo[1,2-a] pyrazine-1,4-dione, hexahydro-3-(2-methylpropyl)- is a strong antioxidant agent isolated from *Bacillus* and *Streptomyces* spp., exhibiting antimicrobial and antifungal activity against various pathogenic bacteria (*Staphylococcus aureus, Enterobacter cloacae, Klebsiella pneumoniae*, and *Bacillus subtilis*) and fungi (*Pyricularia oryzae*).

However, GC-MS profiles of intracellular metabolites of ethyl acetate, dichloromethane and *n*-hexane fractions exhibited the occurrence of 14, 8 and 16 bioactive compounds, respectively. In the ethyl acetate fraction, *n*-hexadecanoic acid (7.73%) and *n*-tridecan-1-ol (6.15%) were the most abundant, while octadecanoic acid (5.04%) was among the moderately abundant compounds. *n*-tridecan-1-ol (alkane) is used in the production of detergents and surfactants, cosmetics, foods, industrial solvents as an effective antimicrobial compound (Garaniya and Bapodra, 2014). Ojinnaka et al. (2016) detected octadecanoic acid from the crude extracts of *Buchholzia coriacea* and showed its bioactivity against several fungi and bacteria.

In the dichloromethane fraction of intracellular metabolites from BS-01, the most abundant compounds were phthalic acid, butyl undecyl ester (1.07%), while trans-geranylgeraniol (0.67%) and heneicosane (0.63%) were among the moderately abundant compounds. Phthalic acid (dicarboxylic acid) is a benzoic acid derivative and is known for its antimycotic potential. Lago et al. (2004) documented fungitoxic activity of benzoic acid derivatives isolated from P*iper* species against phytopathogenic fungi i.e. *Cladosporium cladosporioides* and *Cladosporium sphaerospermum*. Trans-geranylgeraniol is present in medicinal

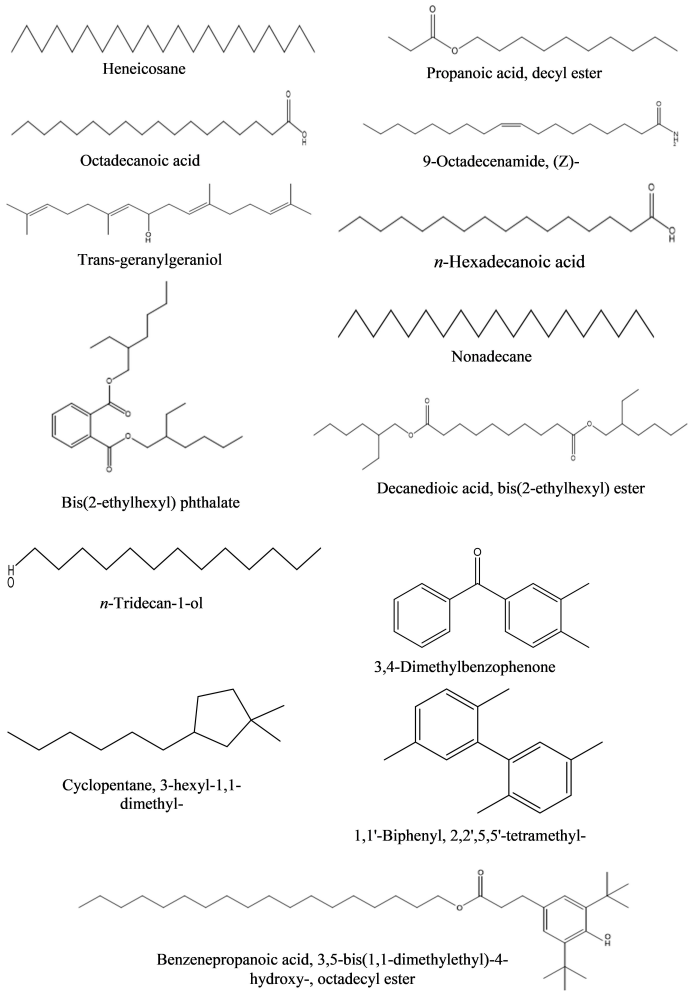

FIGURE 10
Structures of compounds identified from the ethyl acetate fraction of intracellular metabolites of *Bacillus subtilis* (BS-01) through GC-MS analysis.

plants (*Bauhinia variegata* and *Garcinia cambogia*) and exhibited pharmaceutical value.

The *n*-hexane fraction of intracellular metabolites contained octaethylene glycol monododecyl ether (1.95%); pentaethylene glycol monododecyl ether (1.90%) and hexaethylene glycol monododecyl ether (1.77%) as the most abundant compounds. These alcoholic compounds have been reported to show variable antimicrobial activity. For example, octaethylene glycol monododecyl ether acts as detergent and displayed antimicrobial potential (Nardello-Rataj and Leclercq, 2014); pentaethylene glycol monododecyl ether is a surfactant used to reduce the development of powdery mildew on cucumber plants (Yu et al., 2009), and hexaethylene glycol monododecyl ether is also a surfactant and reportedly acts as anti-microbial and antifungal compound (Angarska et al., 2015). Nardello-Rataj and Leclercq (2016) also revealed that a mixture of two surfactants viz, octaethylene glycol monododecyl ether and didecyldimethylammonium chloride, showed a high synergistic effect against enveloped viruses. Our results indicated that biocidal compounds identified in the present study from different fractions of extra- and intracellular metabolites of BS-01 belonging to long chains of alkanes, fatty acids, esters, and alkyl polyglycol ethers, which might have significant antifungal properties against *A. solani* as confirmed *in vitro* antifungal assays.

5 Conclusion

Controlling fungal growth (*A. solani*) and early blight severity in tomato plants by employing the biocontrol agent

Bacillus subtilis (BS-01) is a safe, effective and sustainable approach in contrast to synthetic pesticides. The strain was identified and characterized based on 16S rDNA sequence analysis. Our results indicated that *Bacillus subtilis* (BS-01) produces potent bioactive VOCs extracted from extra- and intra-cellular metabolites which are effective in inhibiting the growth of *Alternaria solani*. Afterward, the active constituents (VOCs) of this strain (BS-01) which could have a potential antifungal impact were identified by GC–MS. Besides, it was studied that preventive measure to control the pathogenic attack is more sound to reduce the pathogenic load on tomato foliage than a curative measure against tomato early blight. The current results suggest that the application of *B. subtilis* as a potential biocontrol agent not only enables the production of bioactive compounds but may suppress *A. solani*-associated diseases and could potentially be applied in multiple horticultural crops.

Data availability statement

The datasets presented in this study can be found in online repositories. The names of the repository/repositories and accession number(s) can be found in the article/Supplementary Material.

Author contributions

ZAA prepared the draft. All the authors mentioned in the manuscript have made a substantial, direct, and intellectual contribution to the work and have approved it for publication.

Acknowledgments

The authors extend their appreciation to the Deputyship for Research & Innovation, Ministry of Education in Saudi Arabia for funding this research work through project number IFKSURG-2-418.

Conflict of interest

The authors declare that the research was conducted in the absence of any commercial or financial relationships that could be construed as a potential conflict of interest.

Publisher's note

All claims expressed in this article are solely those of the authors and do not necessarily represent those of their affiliated organizations, or those of the publisher, the editors and the reviewers. Any product that may be evaluated in this article, or claim that may be made by its manufacturer, is not guaranteed or endorsed by the publisher.

Supplementary material

The Supplementary Material for this article can be found online at: https://www.frontiersin.org/articles/10.3389/fpls.2022.1089562/full#supplementary-material

References

Abbas, M. T., Hamza, M. A., Youssef, H. H., Youssef, G. H., Fayez, M., Monib, M., et al. (2014). Bio-preparates support the productivity of potato plants grown under desert farming conditions of north Sinai: Five years of field trials. *J. Advan. Res.* 5 (1), 41–48. doi: 10.1016/j.jare.2012.11.004

Ahsan, T., Chen, J., Zhao, X., Irfan, M., and Wu, Y. (2017). Extraction and identification of bioactive compounds (eicosane and dibutyl phthalate) produced by *Streptomyces* strain KX852460 for the biological control of *Rhizoctonia solani* AG-3 strain KX852461 to control target spot disease in tobacco leaf. *AMB Express* 7 (1), 1–9. doi: 10.1186/s13568-017-0351-z

Al-Saraireh, H., Al-Zereini, W. A., and Tarawneh, K. A. (2015). Antimicrobial activity of secondary metabolites from a soil *Bacillus* sp. 7B1 isolated from south Al-karak, jordan. Jordan. *J. Biol. Sci.* 8, 127–132. doi: 10.12816/0027558

Angarska, J. K., Ivanova, D. S., and Manev, E. D. (2015). Drainage of foam films stabilized by nonionic, ionic surfactants and their mixtures. colloids surfaces a physicochem. *Eng. Asp.* 481, 87–99. doi: 10.1016/j.colsurfa.2015.04.043

Awan, Z. A., Shoaib, A., and Khan, K. A.. (2018). Variations in total phenolics and antioxidant enzymes cause phenotypic variability and differential resistant response in tomato genotypes against early blight disease. *Sci. Hortic.* 239, 216–223. doi: 10.1016/j.scienta.2018.05.044

Awan, Z. A., and Shoaib, A. (2019). Combating early blight infection by employing *Bacillus subtilis* in combination with plant fertilizers. *Curr. Plant Biol.* 20, 100125. doi: 10.1016/j.cpb.2019.100125

Awan, Z. A., Shoaib, A., Iftikhar, M. S., Jan, B. L., and Ahmad, P. (2022). Combining biocontrol agent with plant nutrients for integrated control of tomato early blight through the modulation of physio-chemical attributes and key antioxidants. *Front. Microbiol.* 13. doi: 10.3389/fmicb.2022.807699

Bharose, A., and Gajera, H. (2018). Antifungal activity and metabolites study of bacillus strain against aflatoxin producing aspergillus. *J. Appl. Microbiol. Biochem.* 2 (8), 1–8. doi: 10.21767/2576-1412.100024

Chandrasekaran, M., and Chun, S. C. (2016). Expression of PR-protein genes and induction of defense-related enzymes by Bacillus subtilis CBR05 in tomato (Solanum lycopersicum) plants challenged with Erwinia carotovora subsp. carotovora. *Biosci. Biotech. and Biochem.* 80, 2277–2283.

Chang, W., Liu, J., Zhang, M., Shi, H., Zheng, S., Jin, X., et al. (2018). Efflux pump-mediated resistance to antifungal compounds can be prevented by conjugation with triphenylphosphonium cation. *Nat. Commun.* 9, 5102. doi: 10.1038/s41467-018-07633-9

Daranas, N., Roselló, G., Cabrefiga, J., Donati, I., Francés, J., Badosa, E., et al. (2019). Biological control of bacterial plant diseases with lactobacillus plantarum strains selected for their broad-spectrum activity. *Ann. Appl. Biol.* 174, 92–105. doi: 10.1111/aab.12476

Faiz, Y., Zhao, W., Feng, J., Sun, C., He, H., and Zhu, J. (2016). Occurrence of triphenylphosphine oxide and other organophosphorus compounds in indoor air and settled dust of an institute building. *Build. Environ.* 106, 196–204. doi: 10.1016/j.buildenv.2016.06.022

Farhana, S., Ab, S., Sijam, K., and Omar, D. (2014). Chemical composition of piper sarmentosum extracts and antibacterial activity against the plant pathogenic bacteria *Pseudomonas fuscovaginae* and *Xanthomonas oryzae* pv . oryzae. *J. Plant Dis. Prot.* 121, 237–242. doi: 10.1007/BF03356518

Garaniya, N., and Bapodra, A. (2014). Ethno botanical and phytophrmacological potential of abrus precatorius l.: A review. *Asian Pac. J. Trop. Biomed.* 4, S27–S34. doi: 10.12980/APJTB.4.2014C1069

Gouda, S., Kerry, R. G., Das, G., Paramithiotis, S., Shin, H. S., and Patra, J. K. (2018). Revitalization of plant growth promoting rhizobacteria for sustainable development in agriculture. *Microbiol. Res.* doi: 10.1016/j.micres.2017.08.016

Guo, Q., Dong, W., Li, S., Lu, X., Wang, P., Zhang, X., et al. (2014). Fengycin produced by *Bacillus subtilis* NCD-2 plays a major role in biocontrol of cotton seedling damping-off disease. *Microbiol. Res.* 169, 533–540. doi: 10.1016/j.micres.2013.12.001

Hadi, A.. (2013). A critical appraisal of Grice's cooperative principle. *Open J Mod. Ling.* 3, 69–72. doi: 10.4236/ojml.2013.31008

Han, Q., Wu, F., Wang, X., Qi, H., Shi, L., Ren, A., et al. (2015). The bacterial lipopeptide iturins induce *Verticillium dahliae* cell death by affecting fungal signalling pathways and mediate plant defence responses involved in pathogen-associated molecular pattern-triggered immunity. *Environ. Microbiol.* 17, 1166–1188. doi: 10.1111/1462-2920.12538

Hashem, A., Tabassum, B., and Fathi Abd_Allah, E. (2019). *Bacillus subtilis*: A plant-growth promoting rhizobacterium that also impacts biotic stress. *Saudi J. Biol. Sci.* 26, 1219-1297. doi: 10.1016/j.sjbs.2019.05.004

Hadimani, B. R., and Kulkarni, S. (2016). Bioefficacy of B diseases of tomato Bacillus subtilis against foliar fungal diseases of tomato. *Int. J. Appl. Pure Sci. Agric.* 3(2), 220–27.

Hussain, A., Ahmad, M., Nafees, M., Iqbal, Z., Luqman, M., Jamil, M., et al. (2020). Plant-growth-promoting bacillus and *Paenibacillus* species improve the nutritional status of *Triticum aestivum* l. *PloS One* 15 (12), e0241130. doi: 10.1371/journal.pone.0241130

Ilyas, N., Akhtar, N., Yasmin, H., Sahreen, S., Hasnain, Z., Kaushik, P., et al. (2022). Efficacy of citric acid chelate and bacillus sp. in amelioration of cadmium and chromium toxicity in wheat. *Chemosphere* 290, 133342. doi: 10.1016/j.chemosphere.2021.133342

Karakus, M., Ikiz, Y., Kaya, H. I., and Simsek, O. (2014). Synthesis, characterization, electrospinning and antibacterial studies on triphenylphosphine-dithiphosphonates Copper(I) and Silver(I) complexes. *Chem. Cent. J.* doi: 10.1186/1752-153X-8-18

Khanna, K., Jamwal, V. L., Kohli, S. K., Gandhi, S. G., Ohri, P., Bhardwaj, R., et al. (2019b). Role of plant growth promoting bacteria (PGPRs) as biocontrol agents of meloidogyne incognita through improved plant defense of *Lycopersicon esculentum*. *Plant Soil* 436 (1), 25–345. doi: 10.1007/s11104-019-03932-2

Khanna, K., Jamwal, V. L., Sharma, A., Gandhi, S. G., Ohri, P., Bhardwaj, R., et al. (2019a). Supplementation with plant growth promoting rhizobacteria (PGPR) alleviates cadmium toxicity in *Solanum lycopersicum* by modulating the expression of secondary metabolites. *Chemosphere* 230, 628–639. doi: 10.1016/j.chemosphere.2019.05.072

Kiran, G. S., Priyadharsini, S., Sajayan, A., Ravindran, A., and Selvin, J. (2018). An antibiotic agent pyrrolo[1,2-: A] pyrazine-1,4-dione,hexahydro isolated from a marine bacteria *Bacillus tequilensis* MSI45 effectively controls multi-drug resistant *Staphylococcus aureus*. *RSC Adv.* 8, 17837–17846. doi: 10.1039/c8ra00820e

Köhl, J., Kolnaar, R., and Ravensberg, W. J. (2019). Mode of action of microbial biological control agents against plant diseases: Relevance beyond efficacy. *Front. Plant Sci.* 10. doi: 10.3389/fpls.2019.00845

Lago, J. H. G., Ramos, C. S., Casanova, D. C. C., Morandim, A. D. A., Bergamo, D. C. B., Cavalheiro, A. J., et al. (2004). Benzoic acid derivatives from piper species and their fungitoxic activity against cladosporium cladosporioides and c. sphaerospermum. *J. Nat. Prod.* doi: 10.1021/np030530j

Lastochkina, O., Seifikalhor, M., Aliniaeifard, S., and Baymiev, A. (2019). Bacillus spp.: Efficient biotic strategy to control postharvest diseases of fruits and vegetables. *Plants* 8, 1–24. doi: 10.3390/plants8040097

Manimaran, M., Gopal, J. V., and Kannabiran, K. (2017). Antibacterial activity of *Streptomyces* sp. VITMK1 isolated from mangrove soil of pichavaram, Tamil nadu, India. *Proc. Natl. Acad. Sci. India Sect. B Biol. Sci.* 87, 499–506. doi: 10.1007/s40011-015-0619-5

Meyer, H., Liebeke, M., and Lalk, M. (2010). A protocol for the investigation of the intracellular staphylococcus aureus metabolome. *Anal. Biochem.* 401, 250–259. doi: 10.1016/j.ab.2010.03.003

Mnif, I., and Ghribi, D. (2015). Lipopeptides biosurfactants: Mean classes and new insights for industrial, biomedical, and environmental applications. *Biopolymers* 104, 129–147. doi: 10.1002/bip.22630

Mohamad, O. A. A., Li, L., Ma, J.-B., Hatab, S., Xu, L., Guo, J.-W., et al. (2018). Evaluation of the antimicrobial activity of endophytic bacterial populations from Chinese traditional medicinal plant licorice and characterization of the bioactive secondary metabolites produced by *Bacillus atrophaeus* against *Verticillium dahliae*. *Front. Microbiol.* 9. doi: 10.3389/fmicb.2018.00924

Moreira, R. R., Nesi, C. N., and May De Mio, L. L. (2014). *Bacillus* spp. and *Pseudomonas* putida as inhibitors of the *Colletotrichum acutatum* group and potential to control *Glomerella* leaf spot. *Biol. Control* 72, 30–37. doi: 10.1016/j.biocontrol.2014.02.001

More, T. T., Yadav, J. S. S., Yan, S., Tyagi, R. D., and Surampalli, R. Y. (2014). Extracellular polymeric substances of bacteria and their potential environmental applications. *J. Environ. Manage* 144, 1–25. doi: 10.1016/j.jenvman.2014.05.010

Morita, T., Tanaka, I., Ryuda, N., Ikari, M., Ueno, D., and Someya, T. (2019). Antifungal spectrum characterization and identification of strong volatile organic compounds produced by *Bacillus pumilus* TM-r. *Heliyon* 5, e01817. doi: 10.1016/j.heliyon.2019.e01817

Nardello-Rataj, V., and Leclercq, L. (2014). Encapsulation of biocides by cyclodextrins: toward synergistic effects against pathogens. *Beilstein J. Org. Chem.* 10, 2603–2622. doi: 10.3762/bjoc.10.273

Nardello-Rataj, V., and Leclercq, L. (2016). Aqueous solutions of didecyldimethylammonium chloride and octaethylene glycol monododecyl ether: Toward synergistic formulations against enveloped viruses. *Int. J. Pharm.* 511, 550–559. doi: 10.1016/j.ijpharm.2016.07.045

Ni, M., Wu, Q., Wang, J., Liu, W. C., Ren, J. H., Zhang, D. P., et al. (2018). Identification and comprehensive evaluation of a novel biocontrol agent *Bacillus atrophaeus* JZB120050. *J. Environ. Sci. Heal. Part B* 53, 777–785. doi: 10.1080/03601234.2018.1505072

Numan, M., Shah, M., Asaf, S., Ur Rehman, N., and Al-Harrasi, A.. (2022). Bioactive compounds from endophytic bacteria bacillus subtilis strain EP1 with their antibacterial activities. *Metabolites* 12 (12), 1228. doi: 10.3390/metabo12121228

Ojinnaka, C. M., Nwachukwu, K. I., and Ezediokpu, M. N. (2016). The chemical constituents and bioactivity of the seed (Fruit) extracts of *Buchholzia coriacea engler* (Capparaceae). J. *Appl. Sci. Environ. Manage.* 19, 795. doi: 10.4314/jasem.v19i4.29

Olanrewaju, O. S., Glick, B. R., and Babalola, O. O. (2017). Mechanisms of action of plant growth promoting bacteria. *World J. Microbiol. Biotechnol.* 33, 197. doi: 10.1007/s11274-017-2364-9

Oliva, J., Messal, M., Wendt, L., and Elfstrand, M. (2017). Quantitative interactions between the biocontrol fungus *Phlebiopsis gigantea*, the forest pathogen *Heterobasidion annosum* and the fungal community inhabiting Norway spruce stumps. *For. Ecol. Manage.* 402, 253–264. doi: 10.1016/j.foreco.2017.07.046

Ongena, M., Duby, F., Jourdan, E., Beaudry, T., Jadin, V., Dommes, J., et al. (2005). *Bacillus subtilis* M4 decreases plant susceptibility towards fungal pathogens by increasing host resistance associated with differential gene expression. *Appl. Microbiol. Biotechnol.* 67, 692–698. doi: 10.1007/s00253-004-1741-0

Rashid, U., Yasmin, H., Hassan, M. N., Naz, R., Nosheen, A., Sajjad, M., et al. (2022). Drought-tolerant *Bacillus megaterium* isolated from semi-arid conditions induces systemic tolerance of wheat under drought conditions. *Plant Cell Rep.* 41 (3), 549–569. doi: 10.1007/s00299-020-02640-x

Shafi, J., Tian, H., and Ji, M. (2017). Bacillus species as versatile weapons for plant pathogens: a review. *Biotechnol. Equip.* 31, 446–459. doi: 10.1080/13102818.2017.1286950

Shoaib, A., Awan, Z. A., and Khan, K. A. (2019). Intervention of antagonistic bacteria as a potential inducer of disease resistance in tomato to mitigate early blight. *Sci. Hortic.* 252, 20–28. doi: 10.1016/j.scienta.2019.02.073

Singh, T., and Wahla, V. (2018). GC-MS analysis of antifungal compounds derived from soil actinobacteria. *Int. Res. J. Phar.* 9, 81–84. doi: 10.7897/2230-8407.09232

Syed-Ab-Rahman, S. F., Carvalhais, L. C., Chua, E., Xiao, Y., Wass, T. J., and Schenk, P. M. (2018). Identification of soil bacterial isolates suppressing different *Phytophthora* spp. and promoting plant growth. *Front. Plant Sci.* 9. doi: 10.3389/fpls.2018.01502

Syed-Ab-Rahman, S. F., Xiao, Y., Carvalhais, L. C., Ferguson, B. J., and Schenk, P. M. (2019). Suppression of *Phytophthora capsici* infection and promotion of tomato growth by soil bacteria. *Rhizosphere* 9, 72–75. doi: 10.1016/j.rhisph.2018.11.007

Tangjitjaroenkun, J. (2018). Evaluation of antioxidant, antibacterial, and gas chromatography-mass spectrometry analysis of ethyl acetate extract of *Streptomyces omiyaensis* SCH2. Asian. *J. Pharm. Clin. Res.* 11, 271. doi: 10.22159/ajpcr.2018.v11i7.25692

Theng, B., and Korpenwar, A. N. (2015). Phytochemical analysis of ethanol extract of *Ampelocissus latifolia* (Roxb.) *Planch tuberous* root using UV-VIS, FTIR and GC-MS. *Int. J. Pharm. Sci. Res.* 6 (9), 3936–3942. doi: 10.13040/IJPSR.0975-8232.6(9).3936-42

Umaiyambigai, D., Saravanakumar, K., and Adaikala Raj, G. (2017). Phytochemical profile and antifungal activity of leaves methanol extract

from the *Psydrax dicoccos* (Gaertn) teys. & binn. rubiaceae family. *Int. J. Pharmacol. Phytochem. Ethnomed.* 7, 53–61. doi: 10.18052/www.scipress.com/IJPPE.7.53

Wang, X. Q., Zhao, D. L., Shen, L. L., Jing, C. L., and Zhang, C. S. (2018). "Application and mechanisms of bacillus subtilis," in *Biological control of plant disease*. Ed. V. S. Meena (Singapore: Springer Singapore), 225–250. doi: 10.1007/978-981-10-8402-7

Yánez-Mendizábal, V., Usall, J., Viñas, I., Casals, C., Marín, S., Solsona, C., et al. (2011). Potential of a new strain of *Bacillus subtilis* CPA-8 to control the major postharvest diseases of fruit. *Biocontrol Sci. Technol.* 21, 409–426. doi: 10.1080/09583157.2010.541554

Yu, J.-H., Choi, G.-J., Lim, H.-K., and Kim, H.-T. (2009). Surfactants effective to the control of cucumber powdery mildew. *J. Appl. Biol. Chem.* 52, 195–199. doi: 10.3839/jabc.2009.033

Zhang, B., Li, X. L., Fu, J., Li, N., Wang, Z., Tang, Y. J., et al. (2016). Production of acetoin through simultaneous utilization of glucose, xylose, and arabinose by engineered *Bacillus subtilis*. *PloS One* 11, e0159298. doi: 10.1371/journal.pone.0159298

frontiers | Frontiers in Plant Science

TYPE Original Research
PUBLISHED 03 March 2023
DOI 10.3389/fpls.2023.1088544

OPEN ACCESS

EDITED BY
Ravinder Kumar,
Central Potato Research Institute (ICAR), India

REVIEWED BY
Susheel Kumar Sharma,
Indian Agricultural Research Institute (ICAR), India
Xu Junfeng,
Zhejiang Academy of Agricultural Sciences, China

*CORRESPONDENCE
Yongjiang Zhang
zhangyjpvi@yeah.net
Zaifeng Fan
fanzf@cau.edu.cn

SPECIALTY SECTION
This article was submitted to Plant Pathogen Interactions, a section of the journal Frontiers in Plant Science

RECEIVED 03 November 2022
ACCEPTED 20 February 2023
PUBLISHED 03 March 2023

CITATION
Lei R, Kuang R, Peng X, Jiao Z, Zhao Z, Cong H, Fan Z and Zhang Y (2023) Portable rapid detection of maize chlorotic mottle virus using RT-RAA/CRISPR-Cas12a based lateral flow assay.
Front. Plant Sci. 14:1088544.
doi: 10.3389/fpls.2023.1088544

Portable rapid detection of maize chlorotic mottle virus using RT-RAA/CRISPR-Cas12a based lateral flow assay

Rong Lei[1], Ruirui Kuang[1,2], Xuanzi Peng[1], Zhiyuan Jiao[2], Zhenxing Zhao[1], Haolong Cong[1], Zaifeng Fan[2]* and Yongjiang Zhang[1]*

[1]Institute of Plant Inspection and Quarantine, Chinese Academy of Inspection and Quarantine, Beijing, China, [2]State Key Laboratory of Agro-biotechnology and MARA Key Laboratory of Surveillance and Management for Plant Quarantine Pests, College of Plant Protection, China Agricultural University, Beijing, China

Introduction: Maize lethal necrosis seriously threatens maize production worldwide, which was caused by coinfection by maize chlorotic mottle virus (MCMV) and a potyvirid. To effectively control maize lethal necrosis, it is vital to develop a rapid, sensitive, and specific detection method for the early diagnosis of MCMV in host plant tissues.

Methods: We established a rapid detection procedure by combining the one-step reverse-transcription recombinase-aided amplification (one-step RT-RAA) and CRISPR/Cas12a-based lateral flow assay in one tube (one-tube one-step RT-RAA/CRISPR-Cas12a), which can be implemented on a portable metal incubator at 37~42°C. Furthermore, the crude extract of total RNA from plant materials using alkaline-PEG buffer can be directly used as the template for one-step RT-RAA.

Results: The developed one-tube one-step RT-RAA/CRISPR-Cas12a lateral flow assay can detect as low as 2.5 copies of the coat protein (CP) gene of MCMV and 0.96 pg of the total RNA extracted from MCMV infected maize leaves. Furthermore, the MCMV infected maize leaves at 5 dpi having no obvious symptoms was detected as weak positive.

Discussion: The crude extraction method of total RNA from plant materials required no complicated device, and all the procedures could be implemented at room temperature and on a portable metal incubator, costing a total time of about 1h. The one-step RT-RAA reagents and CRISPR/Cas12a reagents can be lyophilized for easy storage and transportation of reagents, which makes this method more feasible for the filed detection. This method presents rapidness, robustness and on-site features in detecting viral RNA, and is a promising tool for the field application in minimally equipped laboratories.

KEYWORDS

MCMV, Cas12a, RT-RAA, one-tube, lateral flow assay

Introduction

Maize (*Zea mays* L.) is one of the most important cereal crops in the world. In 2011, a large outbreak of maize lethal necrosis disease (MLND) occurred in the Southern Rift Valley of Kenya (Wangai et al., 2012), caused up to 100% losses in maize yield, and affected the income of farmers (Redinbaugh and Pratt, 2009; Pratt et al., 2017). MLND is caused by a mixed infection of maize chlorotic mottle virus (MCMV) and a virus of the family *Potyviridae*, such as sugarcane mosaic virus (SCMV) or maize dwarf mosaic virus (MDMV). MCMV was first identified in Peru in 1971 (Castillo and Hebert, 1974), and found in Kansas/Nebraska, Argentina/Thailand, Mexico (Aguilera et al., 2019), Hawaii (Jiang et al., 1992), China (Xie et al., 2011; Wu et al., 2013), Kenya (Kusia et al., 2015), Rwanda (Adams et al., 2014), Ethiopia (Mahuku et al., 2015), Taiwan, China (Deng et al., 2014), Ecuador (Quito-Avila et al., 2016), Spain (Achon et al., 2017) and other countries/regions (Lukanda et al., 2014; Pratt et al., 2017). Since SCMV is worldwide distributed (Redinbaugh and Pratt, 2009), MCMV is the emerging critical virus driving MLND expansion. Therefore, rapid and sensitive detection of MCMV is pivotal to effective control and management of the disease.

MCMV is only member of the genus *Macblomovirus* in the family *Tombusviridae*, which is readily transmissible to its natural host maize by mechanical damage, beetles or thrips (Nault et al., 1978) and seeds (Jiang et al., 1992). Present detection methods for MCMV include enzyme-linked immunosorbent assay (ELISA) (Uyemoto, 1980; Wu et al., 2013; Fentahun et al., 2017), immuno-fluorescence (Nault et al., 1979), surface plasmon resonance-based biosensor (Zeng et al., 2013), RT-PCR (Kiarie et al., 2020), quantitative TaqMan RT-PCR (Zhang et al., 2011; Zhang et al., 2016; Bernardo et al., 2021), the next generation sequencing (Adams et al., 2013), reverse transcription loop-mediated isothermal amplification (RT-LAMP) (Liu et al., 2016; Chen et al., 2017), reverse transcription recombinase polymerase amplification (RT-RPA) (Jiao et al., 2019; Gao et al., 2021) and reverse transcription recombinase-aided amplification/Cas12a (RT-RAA/Cas12a)-based visual detection (Duan et al., 2022). The immunological assay, *e.g.* ELISA and immune-fluorescence, relies on the quality and specificity of the antibodies (Bernardo et al., 2021). Quantitative RT-PCR requires an expensive thermal cycler with fluorescence detector. RT-LAMP requires a relatively high isothermal temperature (60 ~ 65°C), which requires high-capacity battery in portable field test. RPA requires relative low temperature (37 ~ 42°C), proceeds fast to produce exponential amplification of nucleic acid in the presence of two primers (Lei et al., 2019; Li et al., 2019a).

CRISPR (Clustered Regularly Interspaced Short Palindromic Repeats) based diagnostic system has been used to detect various nucleic acids (Kellner et al., 2019; Fapohunda et al., 2022). CRISPR-associated proteins (Cas) cleave foreign nucleic acids under the guidance of crRNA (East-Seletsky et al., 2016). Cas12a, an RNA-guided DNA endonuclease, exhibits its non-specific cleavage of single stranded DNA (ssDNA) after recognizing target dsDNA (Chen et al., 2018; Swarts and Jinek, 2019). Combining the cleavage effect of Cas12a with isothermal amplification created versatile rapid and specific platform, such as DETECTR (DNA Endonuclease Targeted CRISPR Trans Reporter) with fluorescence readout (Chen et al., 2018), Cas12VDet (Cas12a-based Visual Detection) in a one-pot reaction (Wang et al., 2019), lateral flow strips for visual readout (Gootenberg et al., 2017; Myhrvold et al., 2018), colorimetric detection with AuNPs-DNA probe (Li et al., 2019b; Jiao et al., 2020; Yuan et al., 2020). Importantly, these CRISPR-based diagnostic tests without complex apparatus can offer analytical sensitivities better than or comparable to real-time PCR technique, thus are suitable for field diagnosis application. Recently a visual detection of MCMV based on two-step RT-RAA and Cas12a technique using a blue light as the excitation light has been reported (Duan et al., 2022). However, the cDNA preparation, step-by-step experimental operation and visual observation based on fluorescence are not suitable for the purpose of field detection.

In this study, we integrated one-step RT-RAA with Cas12a-based lateral flow assay in one tube to develop a rapid detection method for MCMV with high specificity and sensitivity. By adopting a fast RNA exaction method free of device at room temperature, the developed one-tube one-step RT-RAA/Cas12a method can be used to detect MCMV in plant samples. Furthermore, the RT-RAA and Cas12a reagents can be lyophilized for easy storage and transportation (Lei et al., 2022), making this portable and sensitive detection strategy more suitable for plant virus in field.

Materials and methods

Virus sources, virus inoculation and RNA extraction

The sources of MCMV and SCMV were kept in our laboratory. Both viruses were propagated on maize inbred line B73 and cv. Nongda 108 plants, which were grown in a growth chamber (28 °C 16h light and 22°C 8h night cycles) for virus propagation. The first true leaves of one-week-old maize seedlings were rub-inoculated with the homogenized MCMV- and SCMV- infected maize leaf tissues in 0.01 M phosphate buffer [0.01 M KH_2PO_4: 0.01 M Na_2HPO_4 = 49: 51 (v/v), pH 7.0] at a ratio of 1:10 (g/mL). The systemically infected leaves were harvested at about 10 days post inoculation (dpi). The total RNA of cucumber mosaic virus (CMV), tobacco mosaic virus (TMV), tomato ringspot virus virus (TRSV), tomato black ring virus (TBRV) were stored in our laboratory.

Extraction of total RNA from maize leaf tissue (~100 mg) was performed using *EasyPure*® RNA Purification Kit (TransGen, Beijing, China) according to the manufacturer's instructions. The extracted nucleic acid was dissolved in 50 µL nuclease-free water and stored at -80°C prior to testing. Total RNA was quantified using a BioTek Epoch spectrophotometer (BioTek, Vermont, USA).

The crude extracts of total RNA from plant materials was extracted with modified alkaline polyethylene glycol (PEG) extraction method (Chomczynski and Rymaszewski, 2006; Huang et al., 2013; Silva et al., 2018). In brief, the fresh leaf samples (about ϕ 8 mm size) were punched with the lids of 1.5 mL tubes, crushed with quartz sands using a plastic pestle, immersed in 100 µL of

freshly prepared alkaline-PEG buffer [6% PEG 200 (Solarbio, Beijing, China) with 20 mM NaOH] (Huang et al., 2013; Silva et al., 2018), and incubated at room temperature for 4 min. The plant extract supernatants were tested immediately or kept on ice until further use.

RT-RAA primers, fluorescent probe and crRNA design

RT-RAA primers and real time fluorescent probe were designed from the conserved coat protein region of MCMV following multiple sequence alignment of the available virus sequences in the GenBank database (Figure 1). The primers and probe were BLASTed against the GenBank to exclude other plant viruses, including SCMV, cucumber mosaic virus (CMV), tobacco mosaic virus (TMV), tomato ringspot virus (TRSV), tomato black ring virus (TBRV). The forward primer MCMV-F (30 nt) and reverse primer (33 nt) (Table 1) produced target amplicons of 116 bp. The real-time fluorescent probe consists of an oligonucleotide with homology to the target amplicon that contains a dSpacer which replaces a nucleotide in the target sequence flanked by a dT-FAM (fluorophore) and corresponding dT-BHQ1 (quencher). In addition, C3-spacer as a blocker was labelled at the 3'-end to prevent polymerase extension from the 3'-terminus. When the target amplicon was produced, this fluorescent probe is cleaved by the *E.* coli exonuclease III at the abasic site to separate the fluorophore "FAM" from the quencher "BHQ1" and generate an extensible 3'-OH group for polymerization, thus generating fluorescent signals. All primers and probe were synthesized by Sangon Biotech (Shanghai, China).

The crRNA was designed to recognize a site specific to MCMV genome and to be homologous to a region within the amplicon between the RT-RAA primer pair binding sequences. The Cas12a/crRNAs recognize a 20-bp target sequence adjacent to a PAM site (TTTN or NAAA) site and were designed from the highly conserved region of each virus as found in the GenBank (NCBI). There was one PAM site (GAAA) in the RT-RAA amplicons of MCMV, whose reverse complement sequence is TTTC, so the corresponding reverse and complementary sequence was reversely transcribed as the DNA template for crRNA. The DNA template for crRNA was further checked its specificity by BLAST against the GenBank. The DNA sequences and modifications are outlined in Table 1. Fluorescent quencher reporter (FQ reporter: FAM-TTATT-BHQ1), lateral flow assay reporter (LF reporter: FAM-T_{20}-biotin) and crRNA were synthesized by General BioL. (Anhui, China).

One-step RT-RAA reaction of viral RNA

The real-time fluorescent detection of the viral RNA was performed with fluorescent RT-RAA kits according to the instructions of the RT-RAA fluorescent kit (Cat No. F00R01, Jiangsu Qitian Gene Biotechnology Co., Ltd., Jiangsu, China). Briefly, a master mix containing 25.0 μL of supplied rehydration buffer, 10.0 μL of DNase/RNase-free deionized water (Cat. No. RT121, Tiangen, Beijing, China), 2.4 μL of forward primer (10 μM), 2.4 μL of reverse primer (10 μM), and 2.5 μL of magnesium acetate (280 mM) was added to a RT-RAA pellet to dissolved the enzyme. And 2 μL of extracted RNA was added and mixed. Next, 2.5 μL of magnesium acetate (280 mM) was added on the tube lid, which was

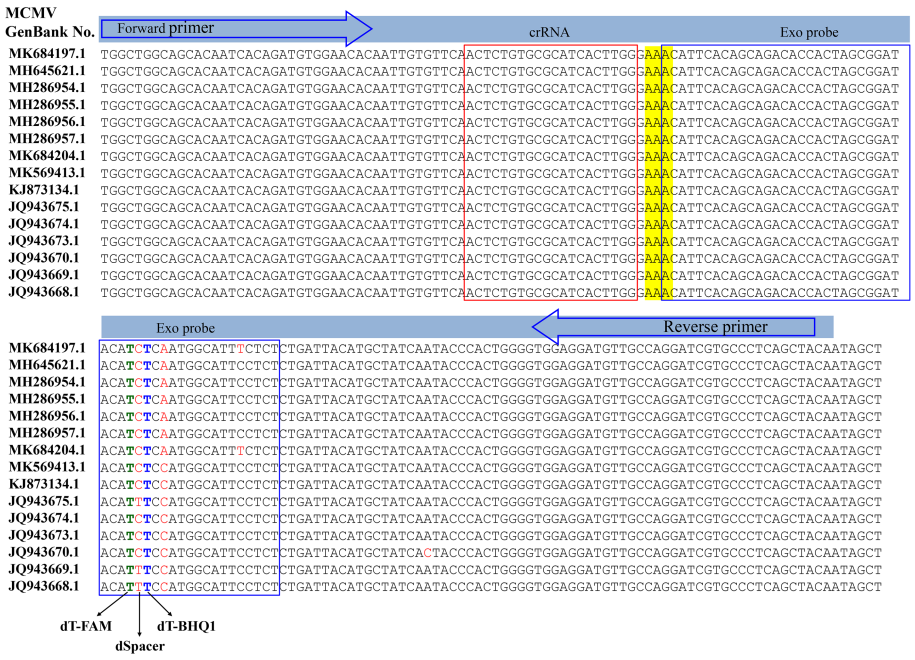

FIGURE 1
Design of the primer set and crRNA in the coat protein gene of MCMV.

TABLE 1 Oligonucleotide sequences used in this study.

Oligonucleotide	Sequences (5′-3′)	Ref.
MCMV-F	TGGCTGGCAGCACAATCACAGATGTGGAACA	This study
MCMV-R	CTATTGTAG CTGAGGGCAC GATCCTGGCA ACAT	
MCMV-exoP	ACATTCACAGCAGACACCACTAGCGGATACA/iFAMdT//idSpace//iBHQ1dT/CMATGGCATTTCTCT-C3 spacer	
MCMV-crRNA	UAAUUUCUACUCUUGUAGAUCCAAGUGAUGCGCACAGAGU	
FQ reporter	FAM/TTATT/BHQ1	
LF reporter (5 nt)	FAM/TTATT/biotin	
LF reporter (20 nt)	FAM/TTTTTTTTTTTTTTTTTTTT/biotin (FAM/T_{20}/biotin)	
MCMV-PF1	5'-TTATGGCGACCCTACCTTCAAT-3'	(Zhang et al., 2016)
MCMV-PR1	5'-ACCACCGTCATCTTCCGTTC-3'	
MCMV-probe	FAM-CACGCATTTTGGAAGCTGTGGTGGC-BHQ1	

mixed with the RT-RAA reaction buffer with centrifugation. The Eppendorf tubes were put in a LightCycler 480 (Roche, USA) to record the emitted fluorescence signals. The excited and emitted wavelength are 488/520 nm, respectively. RNA extracted from healthy maize leaves and DNase/RNase-free deionized water were included as the negative control alongside tested samples.

The pre-amplification of the viral RNA for CRISPR/Cas12a detection was performed with RT-RAA kits according to the instructions of the RT-RAA basic kit (Cat. No. B00R00, Jiangsu Qitian Gene Biotechnology Co., Ltd., Jiangsu, China) with modifications. Briefly, a master mix containing 25.0 μL of supplied rehydration buffer, 10.0 μL of DNase/RNase-free deionized water (Cat. No. RT121, Tiangen, Beijing, China), 2.4 μL of forward primer (10 μM), 2.4 μL of reverse primer (10 μM), and 2.5 μL of magnesium acetate (280 mM) was added to a RT-RAA pellet to dissolved the enzyme. A reconstituted RT-RAA reaction aliquot of 9.0 μL was transferred to new PCR tubes, then 2 μL of extracted RNA was added to each reaction, and mixed by carefully pipetting up and down. The reactions were incubated at 39°C on a self-developed thermal block for 15-30 min. RNA extracted from healthy maize leaves and DNase/RNase-free deionized water were included as the negative control alongside tested samples.

CRISPR/Cas12a based detection for one-step RT-RAA amplicons

The Cas12a-mediated fluorescent detection contained 1×NEBuffer 3.1 (Cat. No. B7203, New England Biolabs, Ipswich, MA, USA), 0.1 μM of EnGenLba Cas12a (Cat. No. M0653T, New England Biolabs, Ipswich, MA, USA), 0.12 μM of crRNA, 0.1 μM FQ reporter, 8U of RNase inhibitor (Cat. No. NG209, Tiangen, Beijing, China), 2.0 mM DTT (Cat. No. 43816, Sigma Aldrich, St. Louis, MO, USA) and 1 μL RT-RAA amplicons in 20 μL reaction volume. The reaction was performed at 37 °C in a LightCycler 480 (Roche, USA) to record the emitted fluorescence signals. The excited and emitted wavelength are 488/520 nm, respectively.

The Cas12a-mediated lateral flow assay contained 1×NEBuffer3.1 (New England Biolabs, Ipswich, MA, USA), 0.1 μM of EnGenLba Cas12a (New England Biolabs, Ipswich, MA, USA), 0.12 μM of crRNA, 1.0 μM LF reporter, 8U of RNase inhibitor (Tiangen, Beijing, China), 2.0 mM DTT (Sigma Aldrich, St. Louis, MO, USA) and 1 μL RT-RAA amplicons in 20 μL reaction volume. The reaction was performed at 37 °C in an incubator for 30 min and the products were detected with lateral flow strips (Cat. No. JY0301, Tiosbio Biotechnology Co, Ltd., Beijing, China).

One-tube one-step RT-RAA/Cas12a based lateral flow detection

A master mix containing 25.0 μL of supplied rehydration buffer, 6.0 μL of nuclease free water, 4.0 μL LF reporter (10 μM), 2.4 μL of forward primer (10 μM), 2.4 μL of reverse primer (10 μM) was added to an RT-RAA pellet to dissolve the enzyme, followed by the addition of 2.5 μL of magnesium acetate (280 mM), then 9 μL of the reconstituted RT-RAA reaction buffer was distributed to the bottom of a new PCR tube. Meanwhile, the Cas12a reaction buffer containing 7.5 μL NEBuffer 3.1 (10×), 2.5 μL EnGenLba Cas12a (5 μM), 2.5 μL DTT (0.1 M), 2.5 μL RNase inhibitor (40U) and 5.0 μL crRNA (5 μM) was distributed into 4 μL aliquots, which was added on the PCR tube lid. If a larger number of reactions are needed, the master mix volume and pellets are scaled up accordingly. One microliter RNA sample was added into the bottom of the PCR tube, mixed by carefully pipetting up and down, then the PCR tubes were gently closed and put on an incubator at 37°C for 20 min. Subsequently, the CRISPR reagents pre-placed on the PCR tube lid were mixed with the RPA reaction buffer by inverting and centrifuging the tube, and incubated at 37°C for another 20 min. When the FQ reporter was used, the PCR tubes were put in a portable fluorimeter or real-time PCR instrument. When the LF reporter was used, the PCR tubes were put in an incubator and lateral flow strip was directly inserted into the reaction buffer after 85 μL water was added.

Evaluation of sensitivity for fluorescent RT-RAA assay and RT-RAA/Cas12a based detection

Ten-fold serial dilutions of total RNA (96.0 ng/μL) and plasmid genomic DNA containing the MCMV coat protein gene (2.5×10^7 copies) were used to evaluate the detection sensitivity of the real-time fluorescent RT-RAA assay and one-tube one-step RT-RAA/CRISPR-Cas12a detection in triplicate. The previously reported primers (MCMV-PF1/MCMV-PR1) and TaqMan probe (MCMV-Probe) (Table 1) of the TaqMan real-time RT-PCR method (Zhang et al., 2016) was employed as a control. The TaqMan real-time RT-PCR amplification was performed in a 20.0 μL of reaction volume containing 10 μL of 2×*PerfectStart*™ Probe One-Step qPCR SuperMix (Cat. AQ221, TransGen, Beijing, China), 0.4 μL of *TransScript*®II Probe One-step RT/RI Enzyme Mix (Cat. AQ221, TransGen, Beijing, China), 0.4 μL of MCMV-PF1 (10 μM), 0.4 μL of MCMV-PR1 (10 μM), 1 μL of MCMV-probe (1 μM), 6.8 μL of RNase-free and 1.0 μL of RNA, were run on a LightCycler 480 (Roche, USA).

Detection of MCMV in maize leaves

MCMV inoculated maize leaves were harvested at 5, 7 and 12 dpi, and the fresh maize leaves were punched with the lids of 1.5 mL tubes, and the crude extracts of total RNA from plant materials were prepared using freshly prepared alkaline-PEG buffer. One microliter of the supernatant was detected using this one-tube one-step RT-RAA/Cas12a assay. Three biological repeats were tested for each sample at different dpi.

Results

Strategy for portable detection of plant virus

As illustrated in Figure 2, this Cas12a-based one-tube plant viral RNA detection platform using lateral flow strips integrates (A) RNA extraction, (B) RT-RAA pre-amplification of plant viral RNA, (C) sequence-specific recognition of amplicons and non-specific cleavage of LF reporters by Cas12a/crRNA, and (D) visual detection of cleaved product from LF reporter. Both RT-RAA amplification reaction buffer and Cas12a/crRNA buffer were loaded into the same tube before the reaction started, and the Cas12a/crRNA buffer was mixed with RT-RAA pre-amplification reaction buffer by shaking operation after the RT-RAA finished. When the Cas12a reaction ended, water was added into the tube to dilute the reaction buffer, and a lateral flow strip was inserted to detect the cleaved products of LF reporters. As shown in Figure 2C, the cleavage ability of CRISPR/Cas12 complex is activated when the crRNA specifically complements with the target DNA amplicons, and the LF reporters modified with both FAM- and biotin-group was cleaved to produce molecules with free FAM- or biotin-group. When the lateral flow strip contacts with the diluted Cas12a reaction buffer, the FAM-group in the buffer conjugates with the anti-FITC antibody on the surface of AuNPs immobilized at the conjugation pad. For negative sample, the LF reporter is intact, and the FAM-AuNPs conjugates have biotin-group, which would be captured by the streptavidin immobilized on the control area to form the control band. For positive sample, the FAM-AuNPs conjugate passes through the control area due to the lack of biotin group, arriving at the test area to form positive band (Figure 2D). Therefore, for the negative sample, only control band

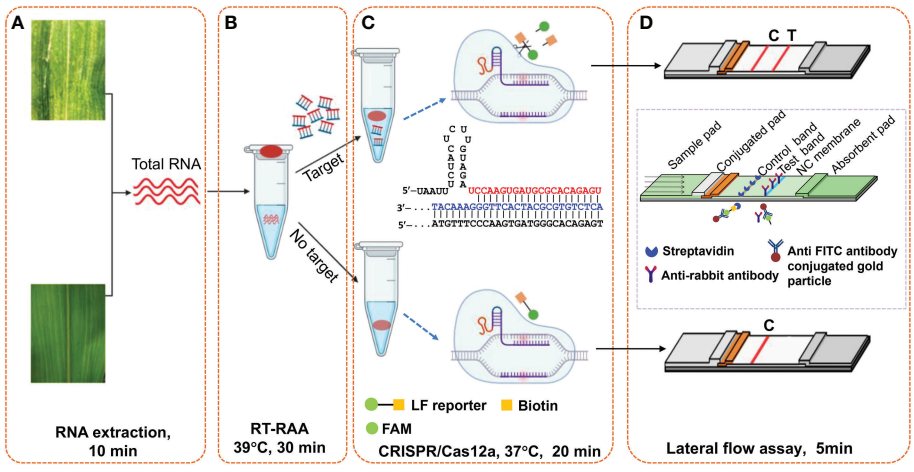

FIGURE 2
Schematic illustration of Cas12a-based one-tube plant viral RNA detection platform. **(A)** Total RNA extraction from plant tissue, **(B)** RT-RAA pre-amplification, **(C)** Cas12a/crRNA cleavage assay, and **(D)** visual readout of lateral flow strips. Total RNA was extracted from plant tissues with extraction kits or PEG-NaOH reagents. Cas12a/crRNA reagent mixture containing crRNA, cas12a enzyme and reaction buffer were added on the tube lid, which was shaken down to mix with the RT-RAA reaction buffer after the RT-RAA pre-amplification, followed by further incubation at 37°C for another 20 min. The lateral flow strips assay is complete in 5 min, and the bands can be immediately visually observed.

appears, while both test band and control band appear for the positive control, or only test band for the strong positive control. The whole experiment including both RT-RAA and Cas12a reaction can be performed on a home-made portable incubator between 37~42°C. By employing the fast plant RNA extraction procedure, the total time from sample preparation to results readout is about 1 h.

Specific detection of MCMV

The specificity of RT-RAA primers was first evaluated using the real-time fluorescent RT-RAA assay. As shown in Figure 1, the forward and reverse primers covered the conserved sequences of all the MCMV strains, while the sequences after the "dSpacer" group have one or two different bases. The real-time fluorescence signals showed that only RNA extracted from MCMV infected maize leaves produced obvious fluorescence intensity, but no intense fluorescence intensity was produced by the total RNA extracted from SCMV- infected maize leaves, healthy maize leaves and other plant virus infected plant leaves, which demonstrated that the RT-RAA primers are specific for MCMV (Figure 3A).

The specificity of RT-RAA primers and crRNA for RT-RAA/CRISPR-Cas12a detection were tested with the CRISPR-Cas12a based fluorescent detection and lateral flow assay. The results showed that other plant viruses, such as SCMV, CMV, TMV, TRV, TBRV produced very low fluorescence signals (Figure 3B), while MCMV produced strong fluorescence signals, indicating that the primers and crRNA have good specificity for MCMV. The lateral flow strips results demonstrated that only MCMV showed up on the test band, which was consistent with that of fluorescent detection (Figure 3C).

Optimization of Cas12a/crRNA-mediated lateral flow assay of MCMV RNA

In this study, we tested 5 nt and 20 nt ssDNA modified with FAM- and biotin-group with different concentration to check the effect of LF reporter on the control and test bands. The results showed that 100 nM LF reporter (20 nt) in the final detection buffer is enough to avoid the false positive phenomenon (Figure 4A). To optimize the CRISPR/Cas12 reaction time, the lateral flow strips results were compared using MCMV RNA (positive control) and DNase/RNase-free deionized water (negative control) as the template for RT-RAA. The results showed that MCMV RNA as the template could generate obvious test bands with 10 min CRISPR/Cas12a reaction time, while negative control produced no test bands (Figure 4B). Although the intensity of test band became darker with the increased CRISPR reaction time, long reaction time may generate non-specific products, and is not favorable for rapid detection. Therefore, 20-30 min is selected as the subsequent Cas12a/crRNA reaction time.

One-tube one-step RT-RAA/CRISPR-Cas12a lateral flow strip detection

To make this method feasible for the field detection, we adopted a one-tube strategy to avoid the step-by-step (two-step) experimental operation. In this strategy, one-step RT-RAA reagents and CRISPR-Cas12a reagents were put in one tube before the addition of sample RNA, so no lid opening was required during the experiment. To compare the detection efficiency of two-step and one-tube operation, three levels of MCMV RNA were tested using two-step way (10 µL RT-RAA reaction buffer was mixed with 10 µL CRISPR reaction buffer and 2 µL RT-RAA reaction buffer was mixed with 18 µL CRISPR reaction buffer) and one-tube way. There is no big difference amongst the three ways when high amount of MCMV RNA (9.6 ng and 9.6×10^{-3} ng) was used (Figure 5). When lower MCMV RNA was detected, the one-step operation generated the highest fluorescence signal, while the two-step (2 µL RT-RAA buffer was mixed with 18 µL CRISPR buffer) produced the lowest. Therefore, one-tube operation is a good alternative for the combined one-step RT-RAA with CRISPR-Cas12a detection system.

Sensitivity assessment of the real-time fluorescent RT-RAA

The results showed that the real-time fluorescent RT-RAA assay could detect the total RNA down to 10^{-6} dilution of total RNA (9.6×

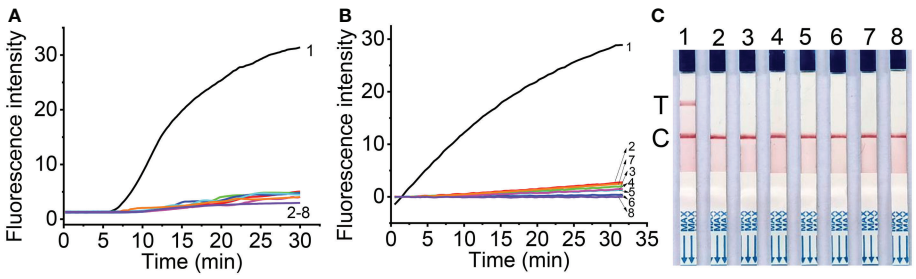

FIGURE 3
Specificity of real-time fluorescent RT-RAA **(A)**, Cas12a mediated fluorescent detection **(B)** and lateral flow assay **(C)** of RT-RAA pre-amplification products from total RNA. 1, Maize chlorotic mottle virus (MCMV); 2, Sugarcane mosaic virus (SCMV); 3, Cucumber mosaic virus (CMV); 4, Tobacco mosaic virus (TMV); 5, Tomato ringspot virus (TRSV); 6, Tomato black ring virus (TBRV); 7, healthy maize leaves; 8, DNase/RNase-free deionized water.

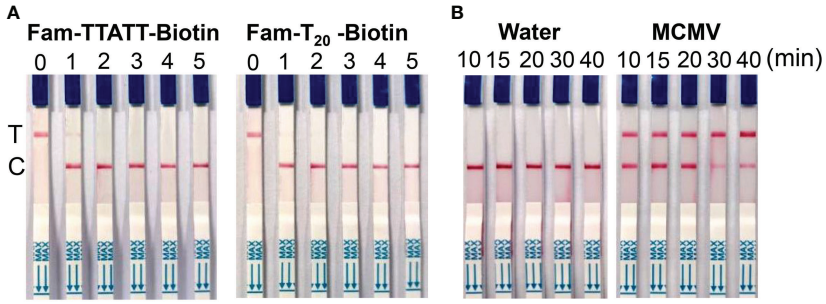

FIGURE 4
(A) Optimization of LF reporter concentration for lateral flow strips detection. 0, 0 nM; 1, 50 nM; 2, 100 nM; 3, 200 nM; 4, 500 nM; 5, 1 μM in the final detection buffer; **(B)** Optimization of CRISPR/Cas12a reaction time.

10^{-5}ng), whose weak fluorescence signal could be detected (Figure 6A). Since the RNA was exponentially amplified by the RAA technique, the onset time of amplification was plotted against the log concentration of the total RNA. The highest RNA concentration (96.0 ng) and the lowest RNA concentration (9.6×10^{-5} ng) were excluded out of the linear range, and the concentration range from 9.6 ng to 9.6×10^{-4} ng was linearly fitted with a R^2 value of 0.963 (Figure 6B).

Aa comparison, the TaqMan real-time RT-PCR detection results showed that although the total RNA down to 10^{-8} dilution of (9.6×10^{-7}ng) generated fluorescence signal (Figure 6C), the Ct value of the 3 replicas is 40, 37.59 and 38.37, respectively. The 10^{-7} dilution of total RNA (9.6×10^{-6}ng) generated fluorescence signal, and the Ct value of the 3 replicas 32.99, 35.29 and 34.94, respectively. The 10^{-6} dilution of total RNA (9.6×10^{-5}ng) generated fluorescence signal, and the Ct value of the 3 replicas 30.69, 30.8 and 30.55, respectively. Since Ct value of 35 was regarded as the critical value, the linearity was evaluated using the total RNA from 9.6 ng to 9.6×10^{-5} ng, and the Ct value was fitted against Log (total RNA) with a R^2 value of 0.98 (Figure 6D).

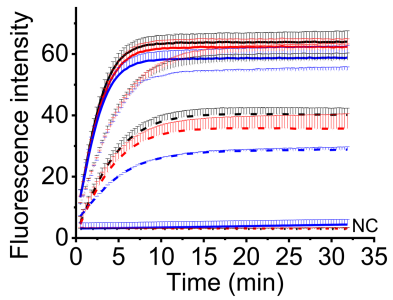

FIGURE 5
The real-time fluorescent intensity of different RT-RAA/CRISPR-Cas12a operation for different MCMV RNA amount. Black line, one-step operation; red line, two-step operation (10 μL RT-RAA buffer/10 μL CRISPR buffer); blue line, two-step operation (2 μL RT-RAA buffer/18 μL CRISPR buffer). Solid lines indicate the 9.6 ng total RNA; short dot lines indicate 9.6×10^{-3} ng total RNA; short dash dot lines indicate 9.6×10^{-4} ng total RNA. DNase/RNase-free deionized water was used as the negative control (NC).

Sensitivity assessment of one-tube one-step RT-RAA/CRISPR-Cas12a detection

The sensitivity of one-tube one-step RT-RAA/Cas12a detection for MCMV was evaluated using the ten-fold serially diluted RNA as the template. The results showed that 10^{-6} dilution of total RNA (96 fg) can be detected using the fluorescent detection (Figure 7A), and 10^{-5} dilution of total RNA (0.96 pg) can be obviously detected using the lateral flow assay (Figure 7B). Since one-step RT-RAA/Cas12a involved exponential amplification and enzyme/nucleic acid reaction, there is no good mathematic mode to explain the relation between the fluorescence signal and RNA concentration. To determine the absolute sensitivity, plasmid genomic DNA containing MCMV coat protein gene ranging from 2.5 to 2.5×10^7 DNA copies were tested. Both the fluorescent detection and lateral flow assay could detect as low as 2.5 copies (Figures 7C, D).

Detection of MCMV in maize leaves

To check the feasibility of the developed one-tube one-step RT-RAA/Cas12a lateral flow assay, MCMV were tested in inoculated maize leaves at different days post-inoculation (dpi). The crude extracts of total RNA from MCMV inoculated maize leaves produced obvious fluorescence signals, whose intensity increased with longer infection time from 5 to 12 days (Figure 8A), while there was no fluorescence signal resulted from the mock inoculated maize leaves (Figure 8A, Line Mock 1-3). Accordingly, the one-tube one-step RT-RAA/Cas12a based lateral flow assay showed that no test band was detected from the crude extracts of total RNA from mock inoculated healthy maize leaves, but the MCMV inoculated maize leaves at 5 dpi was detected as weak positive (Figure 8B). Results of both fluorescent detection and lateral flow assay demonstrated that the amount of MCMV in maize leaves increased with the longer infection time, indicating that this one-tube one-step RT-RAA/CRISPR-Cas12a can be used to detect the field plant sample.

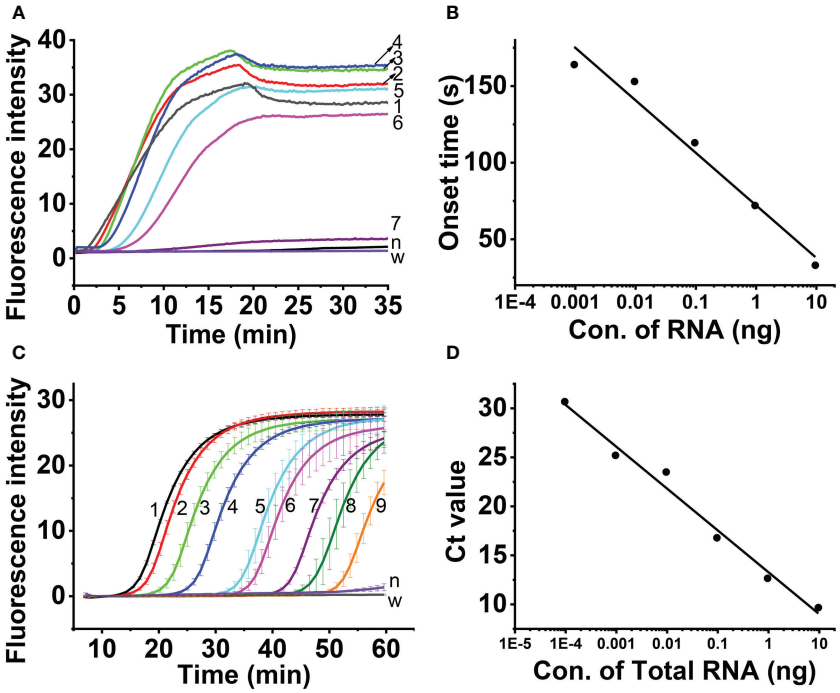

FIGURE 6
Sensitivity assessment of real-time one-step RT-RAA **(A, B)** and TaqMan real time RT-PCR **(C, D)**, Lines 1 ~ 8 indicated the amount of total RNA. 1, 96 ng; 2, 9.6 ng; 3, 0.96 ng; 4, 96 pg; 5, 9.6 pg; 6, 0.96 pg; 7, 96 fg; 8, 9.6 fg; 9, 0.96 fg; n, healthy maize plant; w, water.

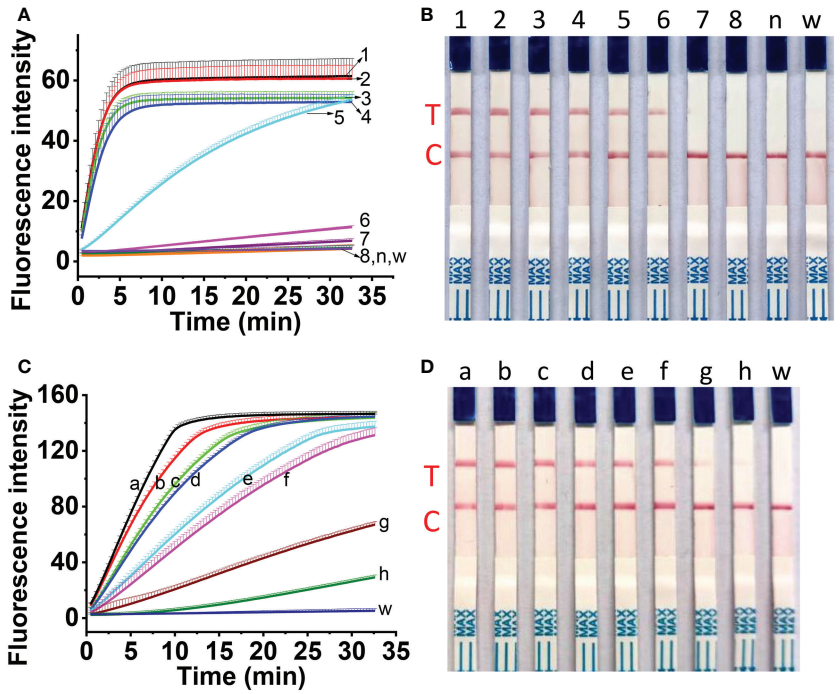

FIGURE 7
Sensitivity assessment of one-tube one-step RT-RAA/Cas12a-based detection for 10-fold diluted total RNA **(A, B)** and for 10-fold diluted plasmid DNA containing coat protein gene **(C, D)**. **(A, B)** No.1 ~ 8 indicated the amount of total RNA. 1, 96 ng; 2, 9.6 ng; 3, 0.96 ng; 4, 96 pg; 5, 9.6 pg; 6, 0.96 pg; 7, 96 fg; 8, 9.6 fg; n, RNA from healthy maize leaves; w, water. **(C, D)** a ~ h indicated the copies of plasmid containing the coat protein gene of MCMV. a, 2.5 × 10^7 copies; b, 2.5x10^6 copies; c, 2.5x10^5 copies; d, 2.5x10^4 copies; e, 2.5x10^3 copies; f, 2.5x10^2 copies; g, 2.5x10^1 copies; h, 2.5 copies; w, water.

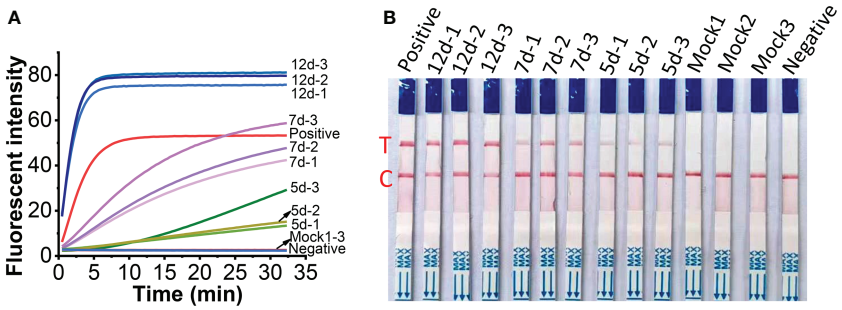

FIGURE 8
Detection of crude extracts of total RNA from MCMV inoculated maize leaves at different day post inoculation (dpi). **(A)**, one-tube one-step RT-RAA/Cas12a fluorescent detection; **(B)**, one-tube one-step RT-RAA/Cas12a lateral flow assay. Mock1~3, the mock inoculated maize leaves; 5d-1~5d-2, the MCMV inoculated maize leaves at 5 dpi; 7d-1~7d~3, the MCMV inoculated maize leaves at 7 dpi; 12d-1~12d-3, the MCMV inoculated maize leaves at 12 dpi.

Discussion

The positive-sense RNA genome of MCMV (4437 nucleotides) encodes six proteins, i.e. P32 (32 kDa protein), RNA dependent RNA polymerase (P50 and P111), P31 (31 kDa protein), P7 (7 kDa protein), and coat protein (25 kDa) (Nutter et al., 1989; Stenger and French, 2008; Scheets, 2016). Coat protein gene is the most used target for MCMV detection (Zhang et al., 2011; Chen et al., 2017; Jiao et al., 2019; Duan et al., 2022). The P32 gene (Gene ID: 26522936) was also used to detect MCMV (Zhang et al., 2016). Integral coat protein is indispensable for the cell-to-cell movement of MCMV virions in plants (Scheets, 2016). Therefore, the conserved sequences of coat protein region are ideal targets for the detection of MCMV. In this study, the RT-RAA primers were designed based on the coat protein genes of MCMV isolates whose sequences are available in the GenBank database. The primers cover the most conserved sequences of all the isolates as possible. Except of the primers for RT-RAA, the crRNA design has played an essential role in the sensitivity of Cas12-based pathogen detection (Roy and Kirchner, 2000; Chen et al., 2018). It is critical to establish a single crRNA strategy that monitors most MCMV strains *via* the Cas12a-based detection. The recognition of dsDNA by Cas12a requires the target DNA strands to contain the protospacer adjacent motif (PAM) sequence of TTTN or AAAN (Chen et al., 2018; Gootenberg et al., 2018; Yan et al., 2019; Karvelis et al., 2020). There was one PAM site (GAAA) in the RT-RAA amplicons of MCMV, whose reverse complement sequence is TTTC, so the corresponding reverse and complmentary sequence was reversely transcribed as the DNA template for crRNA. The further check of the specifity by BLAST against GenBank showed that the DNA template for crRNA was specific to MCMV coat protein gene.

Developing a portable and rapid detection approach is a practical requirement for the monitoring of MCMV in farmland. Since gel electrophoresis is unsuitable for diagnosis of plant pathogen in the field (Jiao et al., 2019; Gao et al., 2021), we turned our attention to the lateral flow assay, one of the most convenient portable field detection techniques, which have been widely used for pathogen detection (Corstjens et al., 2001; Mao et al., 2009; Wang et al., 2020). Although a number of laboratory and commercial assays are available for detection of MCMV in maize plant, the rapid and accurate detection applicable for field detection was still limited. LAMP is an isothermal nucleic acid amplification technique, but it requires four primers, complex primer design and a reaction temperature as high as 63°C, which is difficult to achieve in remote field. Recombinase-aided amplification (RAA) or Recombinase polymerization amplification (RPA) adopts three key proteins, i.e. recombinase, recombinase loading factor and single-stranded binding protein in reaction buffer, and run between 37~42°C (Li et al., 2019a). As we know, almost all the applications of RPA or RAA for MCMV RNA detection adopted two-step operation, that is, total RNA was firstly transcribed to cDNA, then the cDNA was amplified in RPA or RAA reaction system and detected by electrophoresis (Jiao et al., 2019; Gao et al., 2021), or by Cas12a based visual detection (Duan et al., 2022). The synthesis of cDNA needs additional time from 30 min to 60 min at a temperature between 37°C and 42°C. To save the time and simplify the experimental operation, we adopted the one-step RT-RAA procedure which includes the reverse transcriptase and RAA enzymes in one reaction buffer, thus the reverse transcription and amplification could carry out simultaneously. Furthermore, to reduce the reliance on equipment, simplify the operations and avoid contamination, we established a one-tube one-step RT-RAA/Cas12a lateral flow assay for MCMV in maize, requiring minimum equipment, such as pipettes, reagent tubes, a portable thermal block, and lateral flow strips. The feasibility of one-pot detection including RPA and CRISPR-Cas12a reaction has been assessed in our previous work (Lei et al., 2022), the results (Figures 5, 8) demonstrated that one-tube one-step RAA/CRISPR-Cas12a was also applicable for MCMV RNA detection. As we showed in our previous work (Lei et al., 2022), all the equipment can be integrated into a portable suitcase. The proposed method has great potential to enable on-site field assay of plant virus outside of laboratory.

Reporter concentration and Cas12a/crRNA cleavage reaction time affected the results of lateral flow strips, such as the intensity of test/control bands and the false positive results. It has been reported that low concentration of LF reporter easily result in false positive

test band, thus decrease the detection limit (Lu et al., 2020). Sequences of 5 nt (Gootenberg et al., 2018), 6 nt (Kellner et al., 2019), or 12 nt (Bai et al., 2019) between FAM and biotin group of LF reporter have been used. In this study, we tried FAM-TTATT-biotin (5 nt) and FAM-T20-biotin (20 nt) as the ssDNA reporter of combined RT-RAA amplification and Cas12a-based detection, and found that 100 nM LF reporter (20 nt) in the final detection buffer is enough to avoid the false positive phenomena, but LF reporter with shorter sequences (5 nt) needed higher concentration (1 μM) in the final detection buffer to avoid the false positive band (Lu et al., 2020). It is important to reduce the cost of experiments, thus LF reporter (20 nt) with lower concentration is a good choice.

Several detection methods have been summarized in Table 2. The detection sensitivity of ELISA is dependent on the quality of antibody, and requires long incubation time (normally overnight), which is unsuitable for the rapid detection of MCMV (Uyemoto, 1980; Bernardo et al., 2021). Although RT-qPCR provides high detection sensitivity, and is the widely recognized gold standard method to detect pathogen, it requires thermos cycling and complex instrument (Zhang et al., 2011; Bernardo et al., 2021). LAMP, in spite of one of the widely used isothermal amplification techniques, requires high temperatures up to 65˚C (Chen et al., 2017), which is not well compatible with field detection requirements. In contrast, both RT-RAA and Cas12a detection systems run around 37˚C, take less time, and are more practicable for the application in rapid on-site detection. In the developed one-tube one-step RT-RAA/Cas12a lateral flow assay, the RT-RAA enzymes, dNTPs, primers, reporters, and $MgAc_2$ were lyophilized and pre-stored in the bottom of a PCR tube, while

TABLE 2 Comparison of different detection methods for MCMV.

Method	Main instrument	Detection	Detection type	LOD	Characteristics	References
ELISA	ELISA instrument	UV spectrum	Coat Protein	0.1 μg/mL	~18h, requiring antibody	(Uyemoto, 1980)
			Coat Protein	100 pg virion protein		(Bernardo et al., 2021)
TAS-ELISA	ELISA instrument			1: 327680 (w/v, g/ml)	~21~31h, requiring antibody	(Wu et al., 2013)
RT-PCR	PCR thermocycler	Electrophoresis	Total RNA	161.4 fg	~3h, High specificity, requiring complex instruments	(Zhang et al., 2016)
	PCR thermocycler		cDNA	23.0 pg		(Jiao et al., 2019)
	PCR thermocycler		Viral RNA	10 fg		(Bernardo et al., 2021)
One-step RT-qPCR (TaqMan)	Real-time PCR	Real-time fluorescence	Total RNA	4 fg/μL total RNA (Ct value of 36.2)	~1.5h, High sensitivity, requiring complex instruments	(Zhang et al., 2011)
		Real-time fluorescence	Total RNA	1.61 fg		(Zhang et al., 2016)
		Real-time fluorescence	Viral RNA	10 fg		(Bernardo et al., 2021)
One-step RT-qPCR (SYBR Green)	Real-time PCR instrument	Real-time fluorescence	Total RNA	7.86 fg	~1.5h, High sensitivity, requiring complex instruments	(Zhang et al., 2016)
One-step RT-LAMP	60-65˚C	Electrophoresis or SYBR Green I visualization	Total RNA	2.5 pg	~1h, High specificity	(Chen et al., 2017)
RT-RPA	38˚C, water bath	Electrophoresis	cDNA	2.3 pg	~2h, High specificity	(Jiao et al., 2019)
RT-RAA/CRISPR-Cas12a visual detection	37-39 ˚C	Fluorescence visualization	cDNA	20 pg total RNA	~1.5h, Rapid, Portability, Qualitative testing	(Duan et al., 2022)
One-step RT-qPCR (TaqMan)	Real-time PCR	Real-time fluorescence	Total RNA	96 fg total RNA	~1h, High sensitivity, requiring complex instruments	This study
One-step RT-RAA/Cas12a LFD	37 ˚C, Incubator	Latera flow strips	Total RNA; Plasmid DNA containing CP gene	96 fg total RNA; 2.5 copies	<1h, High specificity and sensitivity, rapidness, portability, qualitative testing	This study
One-step RT-qRAA	39 ˚C	Real-time fluorescence	Total RNA	0.96 pg total RNA	~0.5h, High specificity, rapidness, quantification	This study

Cas12a protein, crRNA, RNase inhibitor were lyophilized inside the tube lid. The total RNA extracted from maize leaves with possible infection of MCMV can be directly added to the lyophilized RT-RAA reagents, so the operation and transportation of reagents can be greatly simplified. The lateral flow assay has the advantages of visualization, portability, and simple operation (Broughton et al., 2020). The developed platform showed great potential in rapid field detection of MCMV in infected maize plants in farmland.

Conclusion

In this study, a rapid and sensitive detection method based on RT-RAA/CRISPR/Cas12a system was developed for the diagnosis of maize chlorotic mottle virus (MCMV), which is responsible for a severe maize lethal necrosis disease. The limit of detection was 2.5 copies MCMV coat protein genes, and 0.96 pg of the total RNA extracted from MCMV-infected maize leaves. The developed one-tube one-step RT-RAA and CRISPR-Cas12a lateral flow assay can detect MCMV infected maize leaves at early infection time using crude extracts of total RNA from virus infected plant materials, which meets the requirement of real sample detection. The one-step RT-RAA reagents and CRISPR/Cas12a reagents can be lyophilized for easy storage and transportation of reagents, which makes this method more feasible for the filed detection. All the pipettes, reagent tubes, thermal blocks and extraction reagents are portable, which is applicable for field diagnosis of plant viral diseases.

Data availability statement

The original contributions presented in the study are included in the article/supplementary material. Further inquiries can be directed to the corresponding authors.

Author contributions

RL, RRK, and YJZ designed, conceived and performed the experiments. RL, HLC and XZP wrote the manuscript. ZYJ, ZXZ and ZFF validated the experiments. All authors contributed to the article and approved the submitted version.

Funding

This work was supported by National Key Research and Development Program of China (No. 2021YFD1400100, 2021YFD1400103), Basic Scientific Research Foundation of Chinese Academy of Inspection and Quarantine (2022JK20), and China Agricultural Research System of MOF and MARA (CARS-02).

Conflict of interest

The authors declare that the research was conducted in the absence of any commercial or financial relationships that could be construed as a potential conflict of interest.

Publisher's note

All claims expressed in this article are solely those of the authors and do not necessarily represent those of their affiliated organizations, or those of the publisher, the editors and the reviewers. Any product that may be evaluated in this article, or claim that may be made by its manufacturer, is not guaranteed or endorsed by the publisher.

References

Achon, M. A., Serrano, L., Clemente-Orta, G., and Sossai, S. (2017). First report of maize chlorotic mottle virus on a perennial host, sorghum halepense, and maize in Spain. *Plant Dis.* 101, 393–393. doi: 10.1094/pdis-09-16-1261-pdn

Adams, I. P., Harju, V. A., Hodges, T., Hany, U., Skelton, A., Rai, S., et al. (2014). First report of maize lethal necrosis disease in Rwanda. *New Dis. Rep.* 29, 22–22. doi: 10.5197/j.2044-0588.2014.029.022

Adams, I. P., Miano, D. W., Kinyua, Z. M., Wangai, A., Kimani, E., Phiri, N., et al. (2013). Use of next-generation sequencing for the identification and characterization of maize chlorotic mottle virus and sugarcane mosaic virus causing maize lethal necrosis in Kenya. *Plant Pathol.* 62, 741–749. doi: 10.1111/j.1365-3059.2012.02690.x

Aguilera, S., Rodriguez-Escobar, J. G., Romero-Gonzalez, V. N., Osorio-Acosta, F., Lopez-Romero, G., and Silva-Rosales, L. (2019). Identification and abundance of six viruses and a spiroplasma in single and mixed infections in maize fields in veracruz, Mexico. *Rev. Bio Cienc.* 6, e419. doi: 10.15741/revbio.06.e419

Bai, J., Lin, H. S., Li, H. J., Zhou, Y., Liu, J. S., Zhong, G. R., et al. (2019). Cas12a-based on-site and rapid nucleic acid detection of African swine fever. *Front. Microbiol.* 10. doi: 10.3389/fmicb.2019.02830

Bernardo, P., Frey, T. S., Barriball, K., Paul, P. A., Willie, K., Mezzalama, M., et al. (2021). Detection of diverse maize chlorotic mottle virus isolates in maize seed. *Plant Dis.* 105, 1596–1601. doi: 10.1094/pdis-07-20-1446-sr

Broughton, J. P., Deng, X. D., Yu, G. X., Fasching, C. L., Servellita, V., Singh, J., et al. (2020). CRISPR-Cas12-based detection of SARS-CoV-2. *Nat. Biotechnol.* 38, 870–874. doi: 10.1038/s41587-020-0513-4

Castillo, J., and Hebert, T. T. (1974). A new virus disease of maize in Peru. *Fitopatologia.* 9, 79–84.

Chen, J. S., Ma, E. B., Harrington, L. B., Da Costa, M., Tian, X. R., Palefsky, J. M., et al. (2018). CRISPR-Cas12a target binding unleashes indiscriminate single-stranded DNase activity. *Science.* 360, 436–439. doi: 10.1126/science.aar6245

Chen, L., Jiao, Z. Y., Liu, D. M., Liu, X. L., Xia, Z. H., Deng, C. L., et al. (2017). One-step reverse transcription loop-mediated isothermal amplification for the detection of maize chlorotic mottle virus in maize. *J. Virol. Methods* 240, 49–53. doi: 10.1016/j.jviromet.2016.11.012

Chomczynski, P., and Rymaszewski, M. (2006). Alkaline polyethylene glycol-based method for direct PCR from bacteria, eukaryotic tissue samples, and whole blood. *Biotechniques.* 40, 454–458. doi: 10.2144/000112149

Corstjens, P., Zuiderwijk, M., Brink, A., Li, S., Feindt, H., Neidbala, R. S., et al. (2001). Use of up-converting phosphor reporters in lateral-flow assays to detect specific nucleic acid sequences: A rapid, sensitive DNA test to identify human papillomavirus type 16 infection. *Clin. Chem.* 47, 1885–1893. doi: 10.1093/clinchem/47.10.1885

Deng, T. C., Chou, C. M., Chen, C. T., Tsai, C. H., and Lin, F. C. (2014). First report of maize chlorotic mottle virus on sweet corn in Taiwan. *Plant Dis.* 98, 1748–1748. doi: 10.1094/pdis-06-14-0568-pdn

Duan, X. Y., Ma, W. D., Jiao, Z. Y., Tian, Y. Y., Ismail, R. G., Zhou, T., et al. (2022). Reverse transcription–recombinase–aided amplification and CRISPR/Cas12a–based visual detection of maize chlorotic mottle virus. *Phytopathol. Res.* 4, 23. doi: 10.1186/s42483-022-00128-y

East-Seletsky, A., O'Connell, M. R., Knight, S. C., Burstein, D., Cate, J. H. D., Tjian, R., et al. (2016). Two distinct RNase activities of CRISPR-C2c2 enable guide-RNA processing and RNA detection. *Nature.* 538, 270–273. doi: 10.1038/nature19802

Fapohunda, F. O., Qiao, S., Pan, Y., Wang, H. Y., Liu, Y., Chen, Q. S., et al. (2022). CRISPR cas system: A strategic approach in detection of nucleic acids. *Microbiol. Res.* 259, 127000. doi: 10.1016/j.micres.2022.127000

Fentahun, M., Feyissa, T., Abraham, A., and Kwak, H. R. (2017). Detection and characterization of maize chlorotic mottle virus and sugarcanemosaic virus associated with maize lethal necrosis disease in Ethiopia: an emerging threat to maize production in the region. *Eur. J. Plant Pathol.* 149, 1011–1017. doi: 10.1007/s10658-017-1229-2

Gao, X. R., Chen, Y., Luo, X. C., Du, Z. C., Hao, K. Q., An, M. N., et al. (2021). Recombinase polymerase amplification assay for simultaneous detection of maize chlorotic mottle virus and sugarcane mosaic virus in maize. *ACS Omega.* 6, 18008–18013. doi: 10.1021/acsomega.1c01767

Gootenberg, J. S., Abudayyeh, O. O., Kellner, M. J., Joung, J., Collins, J. J., and Zhang, F. (2018). Multiplexed and portable nucleic acid detection platform with Cas13, Cas12a, and Csm6. *Science.* 360, 439–444. doi: 10.1126/science.aaq0179

Gootenberg, J. S., Abudayyeh, O. O., Lee, J. W., Essletzbichler, P., Dy, A. J., Joung, J., et al. (2017). Nucleic acid detection with CRISPR-Cas13a/C2c2. *Science.* 356, 438–442. doi: 10.1126/science.aam9321

Huang, H., Chang, A., Churl, B. C., Lee, S.-B., and Lee, Y.-H. (2013). A rapid and simple genotyping method for various plants by direct-PCR. *Plant Breed. Biotechnol.* 1, 290–297. doi: 10.9787/pbb.2013.1.3.290

Jiang, X. Q., Meinke, L. J., Wright, R. J., Wilkinson, D. R., and Campbell, J. E. (1992). *Maize chlorotic mottle virus* in Hawaiian-grown maize: vector relations, host range and associated viruses. *Crop Prot.* 11, 248–254. doi: 10.1016/0261-2194(92)90045-7

Jiao, Y. B., Jiang, J. Y., An, M. N., Xia, Z. H., and Wu, Y. H. (2019). Recombinase polymerase amplification assay for rapid detection of maize chlorotic mottle virus in maize. *Arch. Virol.* 164, 2581–2584. doi: 10.1007/s00705-019-04361-3

Jiao, J., Kong, K., Han, J., Song, S., Bai, T., Song, C., et al. (2020). Field detection of multiple RNA viruses/viroids in apple using a CRISPR/Cas12a-based visual assay. *Plant Biotechnol. J.* 19, 394–405. doi: 10.1111/pbi.13474

Karvelis, T., Bigelyte, G., Young, J. K., Hou, Z. L., Zedaveinyte, R., Budre, K., et al. (2020). PAM recognition by miniature CRISPR-Cas12f nucleases triggers programmable double-stranded DNA target cleavage. *Nucleic Acids Res.* 48, 5016–5023. doi: 10.1093/nar/gkaa208

Kellner, M. J., Koob, J. G., Gootenberg, J. S., Abudayyeh, O. O., and Zhang, F. (2019). SHERLOCK: nucleic acid detection with CRISPR nucleases. *Nat. Protoc.* 14, 2986–3012. doi: 10.1038/s41596-019-0210-2

Kiarie, S., Nyasani, J. O., Gohole, L. S., Maniania, N. K., and Subramanian, S. (2020). Impact of Fungal Endophyte Colonization of Maize (Zea mays L.) on Induced Resistance to Thrips- and Aphid-Transmitted Viruses. *Plants-Basel.* 9. doi: 10.3390/plants9040416

Kusia, E. S., Subramanian, S., Nyasani, J. O., Khamis, F., Villinger, J., Ateka, E. M., et al. (2015). First report of lethal necrosis disease associated with Co-infection of finger millet with maize chlorotic mottle virus and sugarcane mosaic virus in Kenya. *Plant Dis.* 99, 899–900. doi: 10.1094/pdis-10-14-1048-pdn

Lei, R., Kong, J., Qiu, Y. H., Chen, N. Z., Zhu, S. F., Wang, X. Y., et al. (2019). Rapid detection of the pathogenic fungi causing blackleg of brassica napus using a portable real-time fluorescence detector. *Food Chem.* 288, 57–67. doi: 10.1016/j.foodchem.2019.02.089

Lei, R., Li, Y., Li, L. M., Wang, J. Y., Cui, Z. H., Ju, R., et al. (2022). A CRISPR/Cas12a-based portable platform for rapid detection of leptosphaeria maculans in brassica crops. *Front. Plant Sci.* 13. doi: 10.3389/fpls.2022.976510

Li, J., Macdonald, J., and von Stetten, F. (2019a). Review: a comprehensive summary of a decade development of the recombinase polymerase amplification. *Analyst.* 144, 31–67. doi: 10.1039/c8an01621f

Li, Y. Y., Mansour, H., Wang, T., Poojari, S., and Li, F. (2019b). Naked-eye detection of grapevine red-blotch viral infection using a plasmonic CRISPR Cas12a assay. *Anal. Chem.* 91, 11510–11513. doi: 10.1021/acs.analchem.9b03545

Liu, Z. M., Xia, X. Y., Yang, C. Y., and Huang, J. Y. (2016). Colorimetric detection of maize chlorotic mottle virus by reverse transcription loop-mediated isothermal amplification (RT-LAMP) with hydroxynapthol blue dye. *RSC. Adv.* 6, 73–78. doi: 10.1039/c5ra20789d

Lu, S. H., Li, F., Chen, Q. B., Wu, J., Duan, J. Y., Lei, X. L., et al. (2020). Rapid detection of African swine fever virus using Cas12a-based portable paper diagnostics. *Cell Discovery* 6, 18. doi: 10.1038/s41421-020-0151-5

Lukanda, M., Owati, A., Ogunsanya, P., Valimunzigha, K., Katsongo, K., Ndemere, H., et al. (2014). First report of maize chlorotic mottle virus infecting maize in the democratic republic of the Congo. *Plant Dis.* 98, 1448–1449. doi: 10.1094/pdis-05-14-0484-pdn

Mahuku, G., Wangai, A., Sadessa, K., Teklewold, A., Wegary, D., Ayalneh, D., et al. (2015). First report of maize chlorotic mottle virus and maize lethal necrosis on maize in Ethiopia. *Plant Dis.* 99, 1870–1870. doi: 10.1094/pdis-04-15-0373-pdn

Mao, X., Ma, Y. Q., Zhang, A. G., Zhang, L. R., Zeng, L. W., and Liu, G. D. (2009). Disposable nucleic acid biosensors based on gold nanoparticle probes and lateral flow strip. *Anal. Chem.* 81, 1660–1668. doi: 10.1021/ac8024653

Myhrvold, C., Freije, C. A., Gootenberg, J. S., Abudayyeh, O. O., Metsky, H. C., Durbin, A. F., et al. (2018). Field-deployable viral diagnostics using CRISPR-Cas13. *Science.* 360, 444–448. doi: 10.1126/science.aas8836

Nault, L. R., Gordon, D. T., Gingery, R. E., Bradfute, O. E., and Castilloloayza, J. (1979). Identification of maize viruses and mollicutes and their potential insect vectors in Peru. *Phytopathology.* 69, 824–828. doi: 10.1094/Phyto-69-824

Nault, L. R., Styer, W. E., Coffey, M. E., Gordon, D. T., Negi, L. S., and Niblett, C. L. (1978). Transmission of maize chlorotic mottle virus by chrysomelid beetles. *Phytopathology.* 68, 1071–1074. doi: 10.1094/Phyto-68-1071

Nutter, R. C., Scheets, K., Panganiban, L. C., and Lommel, S. A. (1989). The complete nucleotidesequence of the maize chlorotic mottle virus genomeE. *Nucleic Acids Res.* 17, 3163–3177. doi: 10.1093/nar/17.8.3163

Pratt, C. F., Constantine, K. L., and Murphy, S. T. (2017). Economic impacts of invasive alien species on African smallholder livelihoods. *Glob. Food Secur-AgricPolicy.* 14, 31–37. doi: 10.1016/j.gfs.2017.01.011

Quito-Avila, D. F., Alvarez, R. A., and Mendoza, A. A. (2016). Occurrence of maize lethal necrosis in Ecuador: a disease without boundaries? *Eur. J. Plant Pathol.* 146, 705–710. doi: 10.1007/s10658-016-0943-5

Redinbaugh, M. G., and Pratt, R. C. (2009). "Virus resistance," in *Handbook of maize: Its biology*. (New York: Springer). doi: 10.1007/978-0-387-79418-1_13

Roy, B. A., and Kirchner, J. W. (2000). Evolutionary dynamics of pathogen resistance and tolerance. *Evolution.* 54, 51–63. doi: 10.1111/j.0014-3820.2000.tb00007.x

Scheets, K. (2016). Analysis of gene functions in maize chlorotic mottle virus. *Virus Res.* 222, 71–79. doi: 10.1016/j.virusres.2016.04.024

Silva, G., Oyekanmi, J., Nkere, C. K., Bomer, M., Kumar, P. L., and Seal, S. E. (2018). Rapid detection of potyviruses from crude plant extracts. *Anal. Biochem.* 546, 17–22. doi: 10.1016/j.ab.2018.01.019

Stenger, D. C., and French, R. (2008). Complete nucleotide sequence of a maize chlorotic mottle virus isolate from Nebraska. *Arch. Virol.* 153, 995–997. doi: 10.1007/s00705-008-0069-y

Swarts, D. C., and Jinek, M. (2019). Mechanistic insights into the cis- and trans-acting DNase activities of Cas12a. *Mol. Cell.* 73, 589–600. doi: 10.1016/j.molcel.2018.11.021

Uyemoto, J. K. (1980). Detection of maize chlorotic mottle virus serotypes by enzyme-linked immunosorbent-assay. *Phytopathology.* 70, 290–292. doi: 10.1094/Phyto-70-290

Wang, B., Wang, R., Wang, D. Q., Wu, J., Li, J. X., Wang, J., et al. (2019). Cas12aVDet: A CRISPR/Cas12a-based platform for rapid and visual nucleic acid detection. *Anal. Chem.* 91, 12156–12161. doi: 10.1021/acs.analchem.9b01526

Wang, X. S., Xiong, E. H., Tian, T., Cheng, M., Lin, W., Wang, H., et al. (2020). Clustered regularly interspaced short palindromic Repeats/Cas9-mediated lateral flow nucleic acid assay. *ACS Nano.* 14, 2497–2508. doi: 10.1021/acsnano.0c00022

Wangai, A. W., Redinbaugh, M. G., Kinyua, Z. M., Miano, D. W., Leley, P. K., Kasina, M., et al. (2012). First report of maize chlorotic mottle virus and maize lethal necrosis in Kenya. *Plant Dis.* 96, 1582–1583. doi: 10.1094/pdis-06-12-0576-pdn

Wu, J. X., Wang, Q., Liu, H., Qian, Y. J., Xie, Y., and Zhou, X. P. (2013). Monoclonal antibody-based serological methods for maize chlorotic mottle virus detection in China. *J. Zhejiang. Univ-SCI. B.* 14, 555–562. doi: 10.1631/jzus.B1200275

Xie, L., Zhang, J. Z., Wang, Q. A., Meng, C. M., Hong, J. A., and Zhou, X. P. (2011). Characterization of maize chlorotic mottle virus associated with maize lethal necrosis disease in China. *J. Phytopathol.* 159, 191–193. doi: 10.1111/j.1439-0434.2010.01745.x

Yan, W. X., Hunnewell, P., Alfonse, L. E., Carte, J. M., Keston-Smith, E., Sothiselvam, S., et al. (2019). Functionally diverse type V CRISPR-cas systems. *Science.* 363, 88–91. doi: 10.1126/science.aav7271

Yuan, C. Q., Tian, T., Sun, J., Hu, M. L., Wang, X. S., Xiong, E. H., et al. (2020). Universal and naked-eye gene detection platform based on the clustered regularly interspaced short palindromic Repeats/Cas12a/13a system. *Anal. Chem.* 92, 4029–4037. doi: 10.1021/acs.analchem.9b05597

Zeng, C., Huang, X., Xu, J. M., Li, G. F., Ma, J., Ji, H. F., et al. (2013). Rapid and sensitive detection of maize chlorotic mottle virus using surface plasmon resonance-based biosensor. *Anal. Biochem.* 440, 18–22. doi: 10.1016/j.ab.2013.04.026

Zhang, L. X., Liu, Z. M., Xia, X. Y., Hu, P. L., Yu, C., and Yang, C. Y. (2016). Developent and comparison of three PCR methods for detecting maize chlorotic mottle virus. *Acta Phytophy. Sin.* 46, 507–513. doi: 10.13926/j.cnki.apps.2016.04.009

Zhang, Y. J., Zhao, W. J., Li, M. F., Chen, H. J., Zhu, S. F., and Fan, Z. F. (2011). Real-time TaqMan RT-PCR for detection of maize chlorotic mottle virus in maize seeds. *J. Virol. Methods* 171, 292–294. doi: 10.1016/j.jviromet.2010.11.002

frontiers | Frontiers in Plant Science

TYPE Original Research
PUBLISHED 09 March 2023
DOI 10.3389/fpls.2023.1151471

OPEN ACCESS

EDITED BY
Ravinder Kumar,
Central Potato Research Institute (ICAR), India

REVIEWED BY
Pierre Eke,
University of Yaounde I, Cameroon
Manoj Choudhary,
University of Florida, United States

*CORRESPONDENCE
Virendra Kumar Baranwal
vbaranwal2001@yahoo.com

SPECIALTY SECTION
This article was submitted to Plant Pathogen Interactions, a section of the journal Frontiers in Plant Science

RECEIVED 26 January 2023
ACCEPTED 21 February 2023
PUBLISHED 09 March 2023

CITATION
Kishan G, Kumar R, Sharma SK, Srivastava N, Gupta N, Kumar A and Baranwal VK (2023) Development and application of crude sap-based recombinase polymerase amplification assay for the detection and occurrence of grapevine geminivirus A in Indian grapevine cultivars.
Front. Plant Sci. 14:1151471.
doi: 10.3389/fpls.2023.1151471

Development and application of crude sap-based recombinase polymerase amplification assay for the detection and occurrence of grapevine geminivirus A in Indian grapevine cultivars

Gopi Kishan[1,2], Rakesh Kumar[1], Susheel Kumar Sharma[1], Nishant Srivastava[1], Nitika Gupta[1], Ashwini Kumar[1] and Virendra Kumar Baranwal[1*]

[1]Advanced Centre for Plant Virology, Division of Plant Pathology, ICAR-Indian Agricultural Research Institute, New Delhi, India, [2]ICAR-Indian Institute of Seed Science, Kushmaur, Mau, Uttar Pradesh, India

Geminiviruses are known to infect several fields and horticultural crops around the globe. Grapevine geminivirus A (GGVA) was reported in the United States in 2017, and since then, it has been reported in several countries. The complete genome recovered through high-throughput sequencing (HTS)-based virome analysis in Indian grapevine cultivars had all of the six open reading frames (ORFs) and a conserved nonanucleotide sequence 5′-TAATATTAC-3′ similar to all other geminiviruses. Recombinase polymerase amplification (RPA), an isothermal amplification technique, was developed for the detection of GGVA in grapevine samples employing crude sap lysed in 0.5 M NaOH solution and compared with purified DNA/cDNA as a template. One of the key advantages of this assay is that it does not require any purification or isolation of the viral DNA and can be performed in a wide range of temperatures (18°C–46°C) and periods (10–40 min), which makes it a rapid and cost-effective method for the detection of GGVA in grapevine. The developed assay has a sensitivity up to 0.1 fg μl^{-1} using crude plant sap as a template and detected GGVA in several grapevine cultivars of a major grapevine-growing area. Because of its simplicity and rapidity, it can be replicated for other DNA viruses infecting grapevine and will be a very useful technique for certification and surveillance in different grapevine-growing regions of the country.

KEYWORDS

RPA, grapevine, geminiviruses, detection, crude sap

Introduction

Grape is one of the first and important fruit crops to be cultivated by man (McGovern, 2019). Viruses are among the major biotic stressors for grapevine, and more than 80 viruses and other graft-transmissible agents like viroids have been reported so far (Fuchs, 2020). Most of these are RNA viruses that include leafroll disease-causing ampeloviruses [grapevine leafroll-associated virus 1 (GLRaV-1), GLRaV-3, GLRaV-4, and GLRaV-7], closterovirus (GLRaV-2), Shiraz disease-causing vitiviruses [grapevine virus A (GVA), grapevine virus B (GVB)], and stem pitting-associated foveavirus [grapevine rupestris stem pitting-associated virus (GRSPaV)] (Martelli, 2014).

Several DNA viruses such as grapevine red blotch-associated virus [*Grablovirus* (GRBV)] (Krenz et al., 2012; Al Rwahnih et al., 2013), grapevine vein clearing virus (*Badnavirus*) (Zhang et al., 2011; Qiu and Schoelz, 2017), grapevine Roditis leaf discoloration-associated virus (*Badnavirus*) (Maliogka et al., 2015), and grapevine geminivirus A (GGVA) (*Maldovirus*) have also been reported to infect grapevine (Al Rwahnih et al., 2017). These DNA viruses alter the development of berries and consequently negatively impact yield (Sudarshana et al., 2015; Blanco-Ulate et al., 2017). Geminiviruses are monopartite or bipartite having circular single-stranded DNA (ssDNA) genome infecting both herbaceous and woody plants. Fourteen different genera, namely, *Becurtovirus*, *Begomovirus*, *Capulavirus*, *Citlodavirus*, *Curtovirus*, *Eragrovirus*, GRBV, *Maldovirus*, *Mastrevirus*, *Mulcrilevirus*, *Opunvirus*, *Topilevirus*, *Topocuvirus*, and *Turncurtovirus*, are included in the *Geminiviridae* family (Fiallo-Olivé et al., 2021). GGVA is assigned to *Maldovirus* that also includes apple geminivirus 1 and Juncus maritimus geminivirus 1. All of the maldoviruses have a monopartite genome and contain a conserved nonanucleotide sequence (5′-TAATATTAC-3′), a characteristic feature of all of the geminiviruses (Sun et al., 2020; Fiallo-Olivé et al., 2021). GGVA was reported by Al Rwahnih et al. (2017) for the first time in 2017 from the United States during screening of two table grape accessions received from South Korea. In recent years, it has been reported in other parts of the world such as China (Fan et al., 2017; Sun et al., 2020), South Korea (Jo et al., 2017), and New Zealand (Veerakone et al., 2019). From India, its presence was reported through bioinformatic analysis of publicly available raw sequence reads of the grapevine cultivar 'Red Globe' (Sidharthan et al., 2020). GGVA contains an ssDNA genome (size of 2,903–2,907 nucleotides) having six open reading frames (ORFs) and a conserved 'TAATATTAC' sequence and is monopartite in nature (Sun et al., 2020).

Detection of grapevine viruses becomes crucial to control their spread and reduce the subsequent impact on quality and yield. Several molecular (RT-PCR, q-PCR) and next-generation sequencing (NGS)-based techniques have been employed to efficiently detect these viruses (Sidharthan et al., 2022). However, isothermal amplification-based detection assays such as recombinase polymerase amplification (RPA) and loop-mediated isothermal amplification (LAMP) are becoming popular for targeted detection due to their sensitivity, specificity, and attribute of not requiring stringent thermal cycling (Sharma et al., 2023). RPA is based on the utilization of three different enzymes, viz., a recombinase, an ssDNA-binding protein (SSB), and a strand-displacing polymerase (Piepenburg et al., 2006). RPA reactions require an isothermal temperature of 25°C–42°C and can be completed within 5–30 min depending on the concentration of nucleic acid and size of the amplicon. RPA in general has advantages over the parallel nucleic acid-based detection methods in terms of its applicability in an isothermal temperature, short reaction time, and robustness. The RPA assay has been employed to detect both DNA [*Nanoviridae* (Kapoor et al., 2017; Cao et al., 2020); *Caulimoviridae* (Kumar et al., 2018; Mohandas and Bhat, 2020); *Geminiviridae* (Londoño et al., 2016)] and RNA [*Closteroviridae* (Mekuria et al., 2014; Sharma et al., 2023); *Potyviridae* (Zhang et al., 2014; Kumar et al., 2021b); *Fimoviridae* (Babu et al., 2017); *Bromoviridae* (Srivastava et al., 2019); *Alphaflexiviridae* (Kumar et al., 2021a); *Betaflexiviridae* (Kumar et al., 2022)] viruses of several field and horticultural crops. Grapevine viruses such as GRBV (through AmplifyRP® Acceler8 assay) and GLRaV-3 (through AmplifyRP® XRT assay) have also been detected successfully using RPA-based assays (Li et al., 2017). In grapevine, purified nucleic acid has been used as a template for RPA-based detection of GRBV and GLRaV-3 (Li et al., 2017). With this background information, the present study was designed to develop a fast, robust, sensitive, and feasible detection assay that requires minimum laboratory setup and can also be operated at field level using crude sap for efficient detection of GGVA in large-scale grapevine samples and planting material.

Materials and methods

Plant sample

Virome analysis of grapevine cultivars 'Super Sonaka' and 'Anushka' (clonal selection of Thompson Seedless) was performed using robust high-throughput sequencing (HTS) coupled with bioinformatic tools. High-quality ribo-depleted RNA was used for library preparation, and sequencing was done using Illumina NovaSeq 6000 V1.5 sequencing system (Illumina, San Diego, CA, USA). Furthermore, employing *de novo* assembly and homology search based on NCBI Non Human Host Virus sequences, a multitude of viruses has been identified along with GGVA (unpublished data). These plants were maintained in the containment facility of Indian Agricultural Research Institute (IARI), New Delhi, and used for optimization of RPA. The complete genome of GGVA (2,905 nt) recovered from 'Anushka' is submitted to NCBI Gene Bank (Accession No. OQ079131 and OQ079132). The phylogenetic tree of these recovered sequences with other available world genomes of GGVA was constructed using the maximum likelihood (ML) method and Kimura 2-parameter model in MEGA11 with 1,000 bootstrap replicates. PCR-based wet-lab confirmation was done employing coat protein (CP)-based primer pair (GGVA-Fp579 5′–3′: CGCAGGTCAAGTCAGTCAGT and GGVA-Rp 579 5′–

3′: TTTTGCACCTGCATCCGAAC), amplifying the 579-bp genomic region. Symptomatic plants showing leaf yellowing and chlorosis from 'Super Sonaka', 'Anushka', and 'Manik Chaman', common table grape fruit cultivars, were tested for GGVA using already available PCR primers before using them for the RPA assay. Field samples were collected from grapevine-breeding plots (10 different cultivars) of ICAR-IARI, New Delhi, and 30 vineyards (representing five grapevine cultivars) from a major table grape production area in Anantapur district of Andhra Pradesh, India. Five plants were randomly selected from individual vineyards during sample collection from the Anantapur region and pooled to make one sample. Pooling was done to elucidate the GGVA infection status of a particular vineyard and to make the assay cost-effective. Two PCR-negative plants were used as the control for subsequent experiments conducted during the course of the study.

RNA and DNA isolation

Purified RNA and DNA were isolated from petioles and midrib regions of collected leaves of three grapevine cultivars (Super Sonaka, Anushka, and Manik Chaman), and both were used as a template for the detection of GGVA. RNA isolation was done using Spectrum™ Plant Total RNA kit (Sigma-Aldrich, St. Louis, MO, USA) with slight modifications by adding 2% polyvinylpyrrolidone to the lysis solution at the time of sample crushing. DNA extraction was carried out according to the standard cetyltrimethylammonium bromide (CTAB) method and also using DNeasy® Plant Mini Kit (QIAGEN GmbH, Hilden, Germany). Extracted RNA/DNA from each sample was eluted in 40 µl of nuclease-free water. The quantity and quality of the extracted RNA and DNA were assessed using NanoDrop One Spectrophotometer (Thermo Fisher Scientific, Waltham, MA, USA) and electrophoresis in 1% agarose gel.

Crude extract preparation

Leaf samples were processed to extract DNA for the RPA-based detection assay using different extraction buffers, viz., 0.5 M NaOH solution (Kapoor et al., 2017), phosphate buffer pH 7.4, NaOH : EDTA (1:1) (Sharma et al., 2023), and lysis buffer from DNeasy® Plant Mini Kit (QIAGEN GmbH, Hilden, Germany). In brief, 100 mg of leaf tissues from the petiole and midrib portion was ground in the extraction buffers (1:10 w/v) using sterile mortar and pestle. The crude sap was transferred to a 2-ml microcentrifuge tube and centrifuged for 3 min at 12,000 rpm. The supernatant was collected without disturbing the particulate matter formed at the bottom of the tube and transferred to a sterile 2-ml collection tube for use as a template for the RPA-based detection assay.

Primer designing

PCR-positive samples (Super Sonaka, Anushka, and Manik Chaman) for the CP genomic region-based primers (GGVA-Fp 579 and GGVA-Rp 579) were used for all subsequent RPA assays. The RPA primer pair was designed following the guidelines of the manufacturers (www.twistdx.co.uk). GGVA complete genomes recovered through HTS (OQ079131 and OQ079132) along with other available world genomes (KX517616, MZ488502, MF163262, MK690474, KX570618, KX570617, MF163264, KX950822, and NC031340) were used for primer designing (www.ncbi.nlm.nih.gov). The RPA primer pair GGVA-RPA212-Fp (CTACCTATGTATCTATGCCTCATTTGGG) and GGVA-RPA212-Rp (CCCTCCACCAGTAAACAGATCATAAAAG) was selected from the CP conserved region after aligning all of these sequences through CLUSTALW multiple alignment (Bio-Edit). The specificity of the primers was assessed by *in silico* analysis using BLASTn (http://www.ncbi.nlm.nih.govt/blast). These primers were 28 nt long and amplified amplicons of 212 bp.

Primer validation through the PCR assay

The designed primer pair was validated using a standard PCR assay. The isolated DNA and cDNA (prepared from RNA) from positive samples were used as template, and a reaction mixture of 20 µl was prepared. The PCR program of initial denaturation at 94°C for 5 min followed by 35 cycles of denaturation at 94°C for 30 s, annealing at 56°C for 40 s, extension at 72°C for 35 s, and a final extension at 72°C for 10 min was performed. The resulting PCR amplicons were separated on 1.0% agarose gel at 85 V, and a 100-bp ladder (GeneDireX®) was used for product size estimation through visualization in a gel documentation system (Bio-Rad, Gel Doc XR system) under UV light. Furthermore, the DNA products from gel slices were eluted using NucleoSpin® Gel and PCR Clean-Up Kit (Macherey-Nagel, Duren, Germany) as per manufacturer's protocol. Cloning of eluted products was done using pGEMT vector, and sequencing of the cloned products was carried out in paired-end manner at Barcode Biosciences (Bengaluru, Karnataka, India). The sequences obtained were further aligned using BLASTn to verify the virus and submitted to the NCBI database.

Recombinase polymerase amplification assay using DNA, RNA, and crude sap as template

The RPA assay was performed as per manufacturer's guidelines using TwistAmp® Basic kit (TwistAmp® Basic-TwistDx limited). In brief, a reaction mixture of 45 µl was prepared by adding forward primer: 2.4 µl (10 µmol μl^{-1}), reverse primer: 2.4 µl (10 µmol μl^{-1}), rehydration buffer: 29.5 µl, and sterile distilled water of 10.7 µl. Freeze-dried pellet was added to this mixture and mixed thoroughly. Equal volumes (22.50 µl) of this mixture were distributed into two PCR tubes, and template (DNA, RNA, and crude sap lysed in 0.5 M NaOH solution) of 1 µl was added. At the end, 1.50 µl of magnesium acetate (280 mmol) was added to start the reaction and incubated at 38°C for 30 min for amplification. For the reaction in which RNA was used as template, 1 µl of reverse transcriptase was also added. The reaction was heat-inactivated at 65°C for 10 min, and the product was loaded on 1.5% agarose gel.

Also, 5% Sodium Dodecyl Sulfate (SDS) (w/v) was added to the final mixture to observe the differences in band formation in comparison to those of the heat-inactivated one.

Comparison of incubation temperatures and time limit for efficient detection of grapevine geminivirus A (GGVA) through the RPA assay

The RPA assay was performed at different incubation temperatures of 10°C, 14°C, 18°C, 22°C, 26°C, 30°C, 34°C, 38°C, 42°C, and 46°C to ascertain the limit and the most suitable temperature to perform the reaction. The reactions were kept for 30 min at these different temperatures using crude plant extract (lysed in 0.5 M NaOH solution) from the positive sample as a template. Similarly, to know the limit and best period required for obtaining confirmative results, the RPA reaction was kept for different periods, viz., 10, 15, 20, 25, 30, 35, and 40 min at an isothermal temperature of 38°C.

Sensitivity and specificity comparison of the RPA assay with PCR

Detection limit or sensitivity comparison of RPA and conventional PCR was carried out using different templates, viz., DNA, RNA, plasmid DNA (GGVA viral insert cloned in pGEMT vector), and crude sap obtained from a GGVA-positive sample. The plant sample was found negative in the RPA, and PCR was used as healthy control. For obtaining different dilutions of templates, a 10-fold serial dilution technique was followed. In this, extracted templates having an initial concentration of 100 ng/µl were used and considered as 10^0. For DNA, 1 µl from 10^0 was taken and added to 9 µl of DNA extracted from healthy plants and serially diluted up to the strength of 10^{-10}. The same procedure was followed for other templates, and 1 µl of an aliquot from 10^0 obtained from the positive sample was added to 9 µl of the respective templates extracted from healthy plants. For plasmid DNA as template, initial stock (100 ng/µl) was considered as 10^0 from which 1 µl was taken and mixed with 90 µl of healthy crude sap in a new tube to obtain 10^{-1} and serially diluted up to the strength of 10^{-15}. In this study, 1 µl of an aliquot from all of these dilutions was used as template in their respective reaction mixtures prepared for both RPA and PCR reactions. The RPA reactions for all of the sensitivity analysis experiments were performed at an isothermal temperature of 38°C for 30 min.

To validate the specificity of RPA primers designed for the detection of GGVA through the RPA assay, different grapevine samples found to be positive for different viruses were used. For this, grapevine plants detected positive for GLRaV-3, GLRaV-4, GVA, and GVB were used. Crude plant extracts from all of these plants along with GGVA-positive and -negative plants were added to the reaction mixtures to ascertain the specificity of the GGVA RPA primers.

Application of the developed crude sap-based RPA assay for determining the occurrence of grapevine geminivirus A (GGVA) in different grapevine cultivars

Grapevine plant samples collected from different locations from Andhra Pradesh, Maharashtra, and IARI, New Delhi, were used for field validation of the RPA assay and to know the occurrence of GGVA (Supplementary Table S1). The standardized crude sap-based RPA assay was performed using all of these collected symptomatic and asymptomatic plants. The standard conventional PCR was also performed parallelly to identify any discrepancies in the detection of GGVA through these two techniques. Crude sap (lysed in 0.5 M NaOH) and DNA extracted from all of these samples were used as templates in the RPA assay and PCR, respectively.

Results

High-throughput sequencing and PCR-based confirmation of grapevine geminivirus A (GGVA)

Virome analysis of 'Super Sonaka' and 'Anushka' indicated the presence of GGVA along with the multitude of viruses (unpublished data). These positive samples along with 'Manik Chaman' and Dogridge (Figure 1A) have been validated through PCR to confirm the HTS results. During PCR, amplicons of 579 bp were observed that indicated the presence of GGVA in 'Super Sonaka', 'Anushka', and 'Manik Chaman', while Dogridge rootstock was found as healthy (Figure 1B). This amplified region was cloned in a pGEMT vector, and sequencing was carried out in a paired-end manner at Eurofins Genomics (Bengaluru, Karnataka, India). Sequences obtained showed 98%–100% identity with the corresponding CP region of HTS-recovered genome and other world genomes of GGVA.

The GGVA complete genome (2,905 bp) obtained through HTS from Anushka cultivar was further analyzed for ORF prediction through NCBI ORF Finder [ORF finder Home-NCBI (nih.gov)]. All of the six ORFs, viz., V1, CP (771 nt); V2, pre-CP (312 nt); C1, replication-associated protein (1,212 nt); C2, transcriptional activator protein (420 nt); C3, replication enhancer protein (429 nt); and C4, host activator protein (258 nt), were found in this GGVA genome along with intergenic regions (IRs) and a stem-loop structure having a conserved 9-base nucleotide sequence "TAATATTAC" similar to other geminiviruses (Figure 1C). Phylogenetic analysis of the recovered complete genomes with all other NCBI-available world genomes using CLUSTALW program of MEGA11 showed the close relationship of our genomes with all of the available Asian genomes (Figure 1D). Furthermore, there was no recombination detected in GGVA genomes as analyzed by the RDP4 package program.

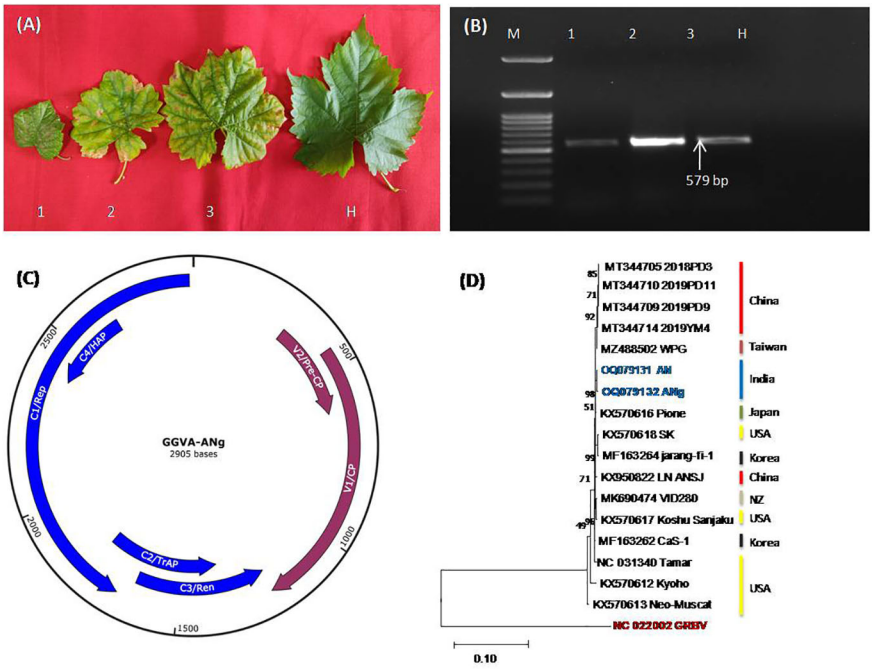

FIGURE 1
(A) Represents symptomatic leaves from three different grapevine cultivars, Super Sonaka, Anushka, and Manik Chaman (Lanes 1, 2, and 3, respectively), and an asymptomatic leaf from Dogridge (Lane H). **(B)** PCR amplicons of 579 bp obtained from amplifications of coat protein genomic region of grapevine geminivirus A (GGVA) using primer pairs of GGVA-Fp and GGVA-Rp synthesized through IDT (Integrated DNA Technologies, Inc., IA, USA). M, 100-bp DNA Ladder; 1, Super Sonaka; 2 Anushka; 3, Manik Chaman plants; H, Healthy plant (Dogridge). **(C)** Represents genomic regions of GGVA isolate ANg (Anushka-grafted plants) as predicted by SnapGene v6.2.1. V1, coat protein (CP); V2, pre-CP; C1, replication-associated protein (Rep); C2, transcriptional activator protein (TrAP); C3, replication enhancer protein (Ren); C4, host activator protein (HAP); intergenic regions (IRs) and a stem-loop structure having a conserved 9-base nucleotide sequence "TAATATTAC" similar to other geminiviruses were also present. **(D)** Phylogenetic relationship between our GGVA isolates AN and ANg with other available world isolates. Phylogenetic analysis is based on maximum likelihood method and Kimura 2-parameter model with 1,000 bootstrap replicates (MEGA11).

Validation of RPA primers through conventional PCR

GGVA-positive samples (Super Sonaka, Anushka, and Manik Chaman) confirmed through HTS and PCR were used for testing of RPA primers (GGVA-RPA212-Fp and GGVA-RPA212-Rp) designed from the CP genomic region of GGVA. *In silico* hybridization of RPA primer pairs (GGVA-RPA212-Fp and GGVA-RPA212-Rp) and previously tested primer pairs (GGVA-Fp 579 and GGVA-Rp 579) illustrated their position on the CP gene (771 bp) of GGVA (Figure 2A). These RPA primers were designed keeping in view the guideline from manufacturers of the RPA kits. Conventional PCR was performed to validate the RPA primers. Amplicons of 212 bp were amplified using cDNA (Figure 2B) and DNA (Figure 2C) extracted from GGVA-positive samples as a template. These results confirm the functionality of the designed RPA primers that will be used for all of the experiments conducted during the course of the study.

Crude sap preparation and standardization of the RPA assay

Crude extracts prepared using different buffers along the purified RNA and DNA were employed as a template for further validation of the RPA primers (GGVA-RPA212-Fp and GGVA-RPA212-Rp) using RPA reagents. Template of RNA (1 µl) coupled with reverse transcriptase (1 µl) results in amplification of the 212-bp genomic region of CP of GGVA in all of the three previously confirmed positive samples, while amplicons were not obtained in water control and healthy plants (Figure 3A). Results obtained by using different crude extracts show variation in amplification, as amplicons obtained from 0.5 M NaOH-based crude extracts were clear and bright as compared to the other three buffers (Figure 3B). However, lysis buffer from DNeasy® Plant Mini Kit-based crude plant extract did not result in any amplification. Results from DNA and crude sap (lysed in 0.5 M NaOH) were analyzed on 1.5% agarose gel with and without the addition of 5% SDS (Supplementary Figures S1A–S1D). These comparative results showed a clearer and brighter band in the case of the addition of 5% SDS at the time of product loading, whereas the bands of untreated ones were slightly faint. Keeping this in view, the results of all of the downstream processing were obtained using 0.5 M NaOH for crude plant extract preparation.

Standardization of the incubation temperature and time period for the RPA assay using crude plant extracts

Crude plant extracts obtained from GGVA-positive samples lysed in 0.5 M NaOH were used as a template to establish the best

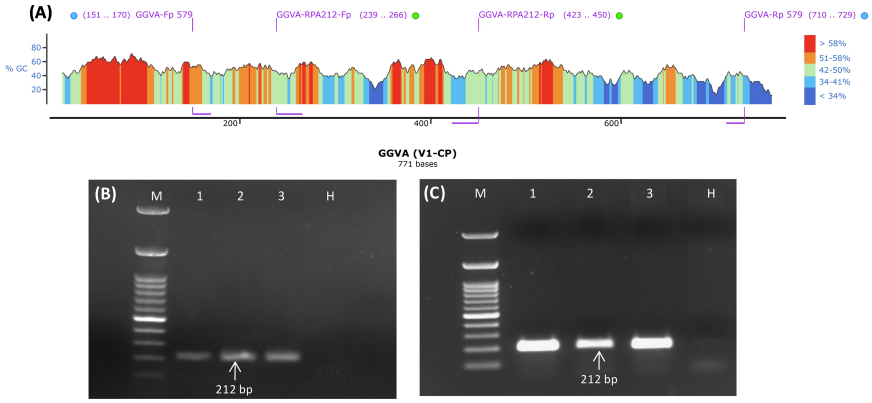

FIGURE 2
Designing and validation of PCR and RPA-based primers for the detection of GGVA from grapevine plants. **(A)** Diagrammatic illustration of position of PCR and RPA primers within the genomic region (771 bp) of V1/CP gene as visualized by SnapGene v6.2.1 (blue and green dots represent PCR and RPA-based primers, respectively). **(B)** PCR amplicons of 212 bp obtained from amplifications of coat protein genomic region of GGVA using cDNA as template and primer pair of GGVA-RPA212-Fp/Rp synthesized through IDT (Integrated DNA Technologies, Inc., IA, USA). M, 100-bp DNA Ladder; 1, Super Sonaka; 2, Anushka; 3, Manik Chaman plants; H, Healthy plant. **(C)** PCR amplicons of 212 bp obtained from amplifications of coat protein genomic region of GGVA using DNA as template and primer pair of GGVA-RPA212-Fp/Rp synthesized through IDT (Integrated DNA Technologies, Inc., IA, USA). M, 100-bp DNA Ladder; 1, Super Sonaka; 2, Anushka; 3, Manik Chaman plants; H, Healthy plant; GGVA, grapevine geminivirus A; RPA, recombinase polymerase amplification.

temperature and period to perform the RPA assay. The RPA assay using crude plant extract was performed at different temperature ranges from 10°C to 46°C at a constant period of 30 min. Results showed that temperature treatment of 26°C, 30°C, 34°C, and 38°C yielded the best amplification of the GGVA genomic region, while the band intensity of amplification was relatively lower at 18°C, 22°C, 42°C, and 46°C as visualized on 1.5% agarose gel (Figure 4A). RPA at 10°C and 14°C did not yield any amplification, as these low temperatures may have caused alterations in RPA reactions. Similarly, the RPA assay using crude plant extract was incubated for different periods of 10, 15, 20, 25, 30, 35, and 40 min while keeping an isothermal temperature of 38°C. Results indicated that the reaction starts as early as 10 min of incubation, and this can be visualized clearly on 1.5% agarose gel (Figure 4B). However, we chose to perform all of the downstream RPA assays at 38°C for 30 min of incubation, as this has been suggested to be the best by the manufacturers and also by many researchers in previous studies.

Comparative sensitivity analysis of the RPA assay with conventional PCR using different templates

Different templates, viz., DNA, RNA, cDNA (prepared from purified RNA), plasmid DNA (GGVA viral insert cloned in pGEMT vector), and crude sap (lysed in 0.5 M NaOH) obtained from positive samples, were serially diluted (10-fold) and used for the analysis of sensitivity for the detection of GGVA through the developed RPA assay and conventional PCR. PCR using isolated DNA as template gave positive amplifications up to 10^{-10} dilutions (equivalent to 0.01 fg μl^{-1}) (Figure 5A), while RPA using the same templates gave positive amplification up to 10^{-9} dilutions (equivalent to 0.1 fg μl^{-1}) (Figure 5B). Sensitivity analysis experiment using cDNA (prepared from purified RNA) (template for PCR) and RNA (template for RPA) showed positive amplification up to 10^{-10} (equivalent to 0.01 fg μl^{-1}) and 10^{-9}

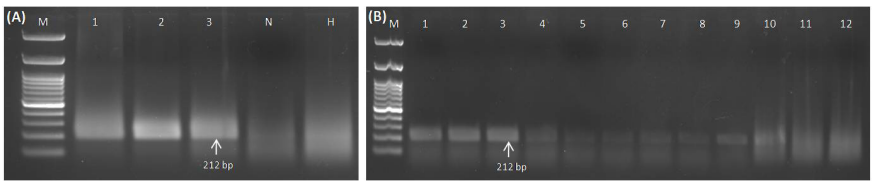

FIGURE 3
Standardization of RPA assay using RNA and crude sap (isolated from GGVA-positive and healthy grapevine plants) as templates. **(A)** Lane M, 100-bp DNA ladder; 1–3, GGVA-positive plants; N, water control; H, healthy plants. **(A)** RPA-based detection of GGVA from positive samples. Amplicons of 212 bp (primer pairs of GGVA-RPA212-Fp and GGVA-RPA212-Rp) obtained as a result of RNA as template in addition to reverse transcriptase enzyme. **(B)** Comparative analysis of performance of different extraction buffers for the preparation of the crude plant extract. M, 100-bp DNA Ladder; 1–3, 0.5 M NaOH (1:10 w/v); 4–6, phosphate buffer pH 7.4; 7–9, NaOH : EDTA (1:1); 10–12, lysis buffer from DNeasy® Plant Mini Kit (QIAGEN GmbH, Hilden, Germany). GGVA, grapevine geminivirus A; RPA, recombinase polymerase amplification.

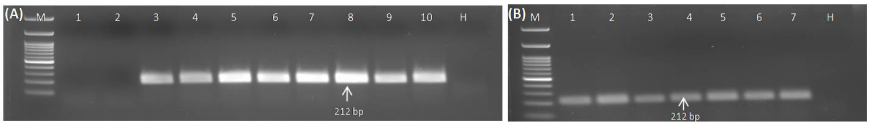

FIGURE 4
Optimization of the RPA assay to ascertain the best incubation temperature and time using crude extract (isolated from GGVA-positive and healthy grapevine plants) as templates. **(A)** RPA assay performed at different temperatures and a constant time period of 30 min. Lane M, 100-bp DNA ladder; 1, 10°C; 2, 14°C; 3, 18°C; 4, 22°C; 5, 26°C; 6, 30°C; 7, 34°C; 8, 38°C; 9, 42°C; 10, 46°C; H, healthy sample. **(B)** RPA assay performed for different time periods at an isothermal temperature of 38°C. Lane M, 100-bp DNA ladder; 1, 10 min; 2, 15 min; 3, 20 min; 4, 25 min; 5, 30 min; 6, 35 min; 7, 40 min; H, Healthy sample; GGVA, grapevine geminivirus A; RPA, recombinase polymerase amplification.

dilutions (equivalent to 1.0 fg μl^{-1}), respectively (Figures 5C, D). The RPA assay employing crude sap amplified the GGVA CP region up to 10^{-9} dilutions (equivalent to 0.1 fg μl^{-1}) (Figure 5E), while no amplification was observed in PCR reactions from the same templates (Figure 5F). PCR and RPA employing serially plasmid DNA showed positive amplification up to dilutions of 10^{-15} and 10^{-10}, respectively (Supplementary Figures S2A, S2B). These results showed that the RPA assay is at par with conventional PCR and highly efficient, rapid, and sensitive in the detection of GGVA in grapevine plants.

Specificity analysis of the RPA assay

RPA reactions employing GGVA-RPA212-Fp/Rp primer pair and crude sap obtained from GGVA-positive and -negative samples along with grapevine samples positive for other viruses, viz., GLRaV-3, GLRaV-4, GVA, and GVB, showed the amplification of GGVA-specific band of 212 bp from the positive sample, while no amplification was observed in all other samples (Supplementary Figure S3A). Although GGVA-positive samples (Super Sonaka and Anushka) were also positive for these viruses, they did not show any amplification specific to these viruses and amplified only 212-bp amplicons using GGVA CP-based RPA primer pair (GGVA-RPA212-Fp/Rp). These results showed the specificity of the developed crude sap-based RPA assay for the detection of GGVA. This was further confirmed through cloning of these GGVA-specific amplicons (both PCR and RPA products) and subsequent restriction digestion and sequencing by obtaining 212 bp of sequences having 100% similarity with corresponding CP genomic region and submitted to the NCBI database under accession no. OQ427641 (Supplementary Figure S3B). This shows that the developed RPA assay is highly specific for the amplification of GGVA and can be used for detection from field samples.

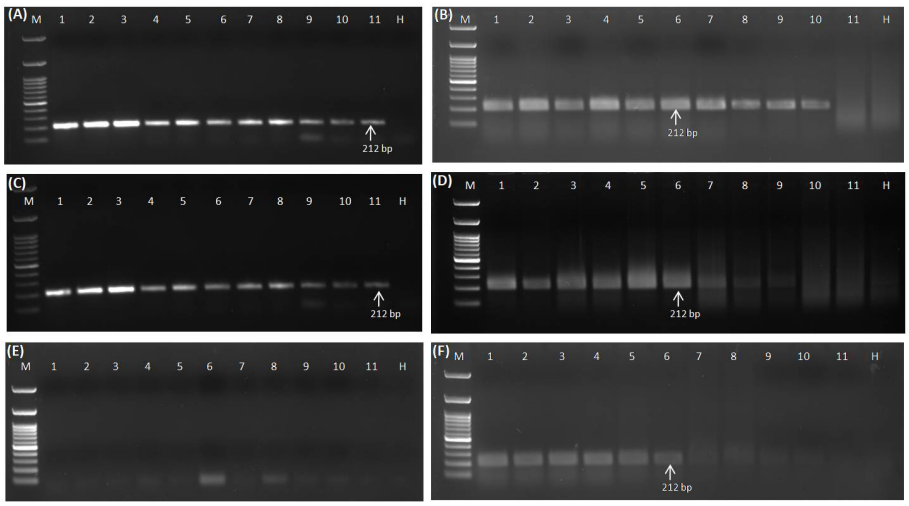

FIGURE 5
Comparative sensitivity analysis of conventional PCR **(A)** and RPA assay **(B)** to elucidate the detection limit using DNA as template isolated from GGVA-infected plant employing primer pair GGVA-212RPA-Fp/Rp in a 10-fold serial dilution. Lane M, 100-bp DNA ladder; Lane 1, Stock (100 ng); 2, 10^{-1}; 3, 10^{-2}; 4, 10^{-3}; 5, 10^{-4}; 6, 10^{-5}; 7, 10^{-6}; 8, 10^{-7}; 9, 10^{-8}; 10, 10^{-9}; 11, 10^{-10}; H, healthy. Comparative sensitivity analysis of conventional PCR **(C)** and RPA assay **(D)** to elucidate the detection limit using cDNA **(C)** and RNA **(D)** as template isolated from GGVA-infected plant employing primer pair GGVA-212RPA-Fp/Rp. In case of RNA template, 1 µl of reverse transcriptase was added in the RPA reaction mixture. Lane M, 100-bp DNA ladder; Lane 1, Stock (100 ng); 2, 10^{-1}; 3, 10^{-2}; 4, 10^{-3}; 5, 10^{-4}; 6, 10^{-5}; 7, 10^{-6}; 8, 10^{-7}; 9, 10^{-8}; 10, 10^{-9}; 11, 10^{-10}; H, healthy. Comparative sensitivity analysis of conventional PCR **(E)** and RPA assay **(F)** to elucidate the detection limit using crude plant extract (lysed in 0.5 M NaOH) as template isolated from GGVA-infected plant employing primer pair GGVA-212RPA-Fp/Rp. Lane M, 100-bp DNA ladder; Lane 1, Stock (10^{0}); 2, 10^{-1}; 3, 10^{-2}; 4, 10^{-3}; 5, 10^{-4}; 6, 10^{-5}; 7, 10^{-6}; 8, 10^{-7}; 9, 10^{-8}; 10, 10^{-9}; 11, 10^{-10}; H, healthy. All PCR reactions were performed at initial denaturation at 94°C for 5 min followed by 35 cycles of denaturation at 94°C for 30 s, annealing at 56°C for 40 s, extension at 72°C for 35 s, and a final extension at 72°C for 10 min. All of the RPA assays were performed at 38°C for 30 min followed by heat inactivation at 65°C for 10 min. GGVA, grapevine geminivirus A; RPA, recombinase polymerase amplification.

Application of the developed crude sap-based RPA assay for determining the occurrence of GGVA in different grapevine cultivars

The collected plant samples showed different levels of symptoms ranging from leaf chlorosis, reddening, yellowing, and leaf rolling to no visible symptoms. Detection of GGVA through the conventional PCR (Figure 6A) and RPA assay (Figure 6B) was performed in parallel for all of these collected samples to evaluate the discrepancies in performance. Results showed that the developed crude sap-based RPA assay is very much effective in the detection of GGVA from grapevine plants. The RPA assay gave a positive reaction for 43 samples out of 60 samples tested (72%) as compared to 39 samples in PCR (65%). Out of these 60 samples, 11 samples were asymptomatic, and three of them showed a positive reaction for GGVA in the PCR, while four showed a positive reaction in the RPA assay. This might be due to the low level of virus titer in asymptomatic plants leading to false-negative results. The remaining samples were symptomatic, and only 13 of them showed a negative reaction for GGVA in the RPA assay. These obtained results demonstrate the feasibility of the crude plant extract-based RPA assay for the detection of GGVA in field samples of grapevine. Test results showed the widespread presence of GGVA in different cultivars across major grapevine areas of India (Table 1; Supplementary Table S1).

Discussion

Grapevine is a host of a large number of RNA and DNA viruses. These viruses were detected and characterized at different timelines using different approaches, viz., ELISA, PCR, and qPCR. Some of the viruses were recently detected in India using HTS (Sidharthan et al., 2020). GGVA was reported from India in the Red Globe cultivar (Sidharthan et al., 2020), although it was not validated through lab-based molecular techniques. Screening of the large number of germplasm materials at the University of California, Davis, showed the presence of the novel GGVA virus in a diverse set of cultivars, source of propagation material that were introduced from different countries like China, Japan, South Korea, and Israel (Al Rwahnih et al., 2017). These results suggested a possible global spread of GGVA that could have escaped the detection procedures due to its novelty and inconsistent symptomatology (Al Rwahnih et al., 2017). Although studies by Sun et al. (2020) associated the leaf edge curling and dwarfism symptoms in *Nicotiana benthamiana* plant with GGVA infection, they could not succeed in establishing a similar association in grapevine plants. These results suggested the possible latent infection or mixed infection of GGVA with other grapevine-infecting viruses. Our results from HTS and bioinformatic analysis also report GGVA infection in Indian grapevine cultivars like Super Sonaka and Anushka in both symptomatic and asymptomatic plants. The complete GGVA genome recovered from Anushka cultivars has a similar genome organization as reported by Sun et al. (2020) representing all of the six ORFs, IRs, and a stem-loop structure having a conserved 9-base nucleotide sequence "TAATATTAC." The formation of a single clade in the phylogenetic tree and the absence of recombination events indicate the possible origin of this virus from Asian countries, as GGVA isolates reported from US cultivars also had a history from Asian countries only (Al Rwahnih et al., 2017).

Although geminiviruses are known to infect both herbaceous and woody plants of important horticultural crops like citrus, apple, and grapevine (Loconsole et al., 2012; Al Rwahnih et al., 2013; Liang et al., 2015; Al Rwahnih et al., 2017), their detection largely depends on molecular and recently emerging HTS-based techniques that are quite cumbersome in sample preparation and subsequent downstream processing. Once these viruses are detected and characterized, it is important to develop a simplified diagnostic assay for routine detection. In this context, RPA is the recent methodology that has gained the attention of plant pathologists given its simplicity and rapidity in the testing of field and nursery

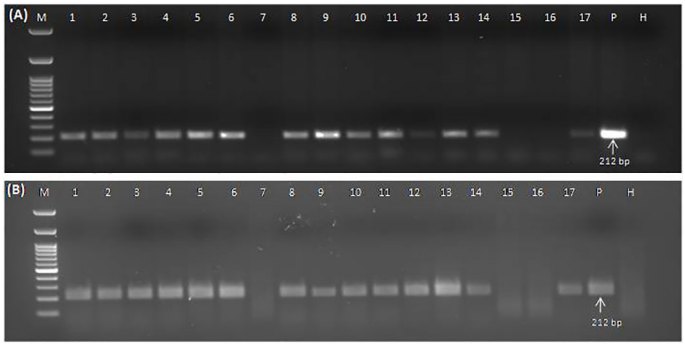

FIGURE 6
Conventional PCR **(A)** and RPA assay **(B)** to detect GGVA in different field samples using DNA **(A)** and crude plant extract lysed in 0.5 M NaOH **(B)** as template employing primer pair GGVA-212RPA-Fp/Rp. Lane M, 100-bp DNA ladder; Lane 1, Bharat Early (BE); 2, Beauty Seedless (BS1); 3, Beauty Seedless (BS2); 4, Borqui Abyad (BA); 5, Pusa Swarnika (PS1); 6, 1103P; 7, Pusa Navrang (PN1); 8, Pusa Trishar (PT1); 9, Pusa Aditi (PA1); 10, Pusa Aditi (PA2); 11, Pusa Swarnika (PS2); 12, Pusa Swarnika (PS3); 13, Pusa Trishar (PT2); 14, S04; 15, Dogridge (D1); 16, Dogridge (D2); 17, Pusa Trishar (PT3); P, positive control; H, healthy control. PCR reaction was performed at an initial denaturation at 94°C for 5 min followed by 35 cycles of denaturation at 94°C for 30 s, annealing at 56°C for 40 s, extension at 72°C for 35 s, and a final extension at 72°C for 10 min. RPA assays were performed at 38°C for 30 min followed by heat inactivation at 65°C for 10 min. GGVA, grapevine geminivirus A; RPA, recombinase polymerase amplification.

TABLE 1 Validation of the developed crude plant extract-based RPA assay for the detection of GGVA in symptomatic and asymptomatic grapevine plant leaf samples collected from different locations in India.

Sr. No.	Location	Cultivar	Total positive samples/Total samples indexed			
			Purified DNA (PCR)		Crude plant extract (RPA)	
			Symptomatic	Asymptomatic	Symptomatic	Asymptomatic
1.	IARI, New Delhi	Beauty Seedless	3/4	1/2	4/4	2/2
2.		Pusa Trishar	3/3	–	3/3	–
3.		Pusa Swarnika	3/3	–	3/3	–
4.		Pusa Aditi	2/3	–	3/3	–
5.		Pusa Navrang	–	0/2	–	0/2
6.		Bharat Early	1/1	–	1/1	–
7.		Borqui Abyad	1/1	–	1/1	–
8.		1103P	1/1	–	1/1	–
9.		S04	1/1	–	1/1	–
10.		Dogridge	0/2	–	0/2	–
11.	Solapur (Maharashtra)	Manik Chaman	1/1	–	1/1	–
12.		Super Sonaka	2/2	–	2/2	–
13.		Anushka	1/1	–	1/1	–
14.		Dogridge	–	0/3	–	0/3
15.	Anantapur (Andhra Pradesh)	Super Sonaka	6/6	–	6/6	–
16.		Manik Chaman	4/6	–	5/6	–
17.		Dilkush	5/12	2/4	5/12	2/4
18.		Red Globe	1/1	–	1/1	–
19.		Flame Seedless	1/1	–	1/1	–

GGVA, grapevine geminivirus A; RPA, recombinase polymerase amplification.

samples for different viruses infecting both field and horticultural crops (Londoño et al., 2016; Kapoor et al., 2017; Romero et al., 2019; Mohandas and Bhat, 2020). RPA coupled with lateral flow dipstick (RPA-LFD) assay was developed for rapid and robust detection of tomato yellow leaf curl virus (TYLCV), although its detection limit was quite low (5 pg μl^{-1}) and required laborious DNA extraction protocols (Zhou et al., 2022). Almost similar results were reported by Londoño et al. (2016) for TYLCV detection, and they detected this virus from crude sap itself. Banana bunchy top virus (BBTV) and piper yellow mottle virus (PYMoV) were detected through the crude leaf sap-based RPA assay, but its detection limit was up to 10^{-5} and 10^{-3} dilutions only (Kapoor et al., 2017; Mohandas and Bhat, 2020).

The developed crude sap-based RPA assay was very fast and accurate in the detection of GGVA within 30 min of reaction time, eliminating the requirement of a stringent thermal cycler. Although a LAMP-based detection assay for another ssDNA virus (GRBV) infecting grapevine has been developed by Romero et al. (2019), which required a higher temperature of 65°C, comparatively long incubation period (35 min), and four sets of primers as compared to RPA assay, which can be performed at the temperature range of 18°C–46°C with best amplification at 38°C and needed minimum laboratory setup. Although the developed RPA assay sufficiently amplified the desired amplicons at 18°C and 22°C, its band intensity was relatively lower, as this temperature is not in the most ideal temperature range for recombinase polymerase-based nucleic acid amplification. The developed RPA assay can be completed from reaction to product visualization within a total period of 50–60 min. Although this developed RPA assay requires visualization under gel electrophoresis, it can also be done through the application of probes like RT-exo-RPA (Silva et al., 2015; Srivastava et al., 2019), AmplifyRP® Acceler8™ (Mekuria et al., 2014; Li et al., 2017), and gold nanoparticle (Wang and Yang, 2019). The cost factor for probe-based RPA assays usually limits their application in the routine detection of field samples and planting materials. So keeping in view the limiting factors like the requirement of a stringent thermal cycler, costly reagents, probes, and labor, it is suggested to use crude sap-based RPA assay.

The developed crude sap-based RPA assay is more sensitive and feasible as compared to previously reported detection assays for DNA viruses (Londoño et al., 2016; Kapoor et al., 2017; Mohandas and Bhat, 2020; Zhou et al., 2022) by amplifying the target genomic region. Although the detection limit of crude sap-based RPA was 10 times less as compared to RPA using DNA as a template, this RPA

assay does not require lengthy RNA or DNA extraction protocols that are notoriously difficult and time-consuming in the case of crops like grapevine due to the presence of a large number of inhibitors. In the simplified template preparation, only NaOH solution was needed without requiring costly reagents and allows the reaction to start by direct use of this template. This was possibly due to buffering abilities of RPA reagents used and gave an edge over other reported assays that use GEB and GEB3 as extraction buffer and can be used in resource-poor laboratories (Sharma et al., 2023). The present study also reported that RNA isolated for the detection of GGVA can also be used for the RPA-based detection by adding the reverse transcriptase to it. Although the sensitivity of this RNA template-based RPA is comparatively lower (1 fg μl^{-1}) than the DNA and crude sap-based RPA assay, it can sufficiently detect GGVA from positive samples. This adds value to our study, as there is no need to isolate RNA and DNA separately for indexing grapevine-infecting RNA and DNA viruses.

The specificity of the developed RPA exists in the amplification of only GGVA-specific amplicons, although tested samples were also positive for other grapevine viruses like GLRaV-3, GLRaV-4, GVA, and GVB. These results were constant with all of the templates (RNA, DNA, and crude sap) used in RPA. This confirms that the developed crude sap-based RPA assay is very specific and robust in the detection of GGVA from infected field samples and did not give any false-positive results. Application of the developed RPA assay presented its effectiveness in the testing of large-scale samples, as 72% of samples collected from different locations were positive in crude sap-based RPA, which was higher as compared to PCR-based results (65% of samples were positive). This might be due to the higher sensitivity of the RPA assay or loss of DNA quality during lengthy extraction protocols for PCR. Furthermore, this study reported widespread occurrence of GGVA infection in Indian grapevine cultivars from different locations including farmer fields. All of these results present the feasibility of crude sap-based RPA assay in the application for large-scale surveillance and planting material certification for GGVA infection.

Conclusion

In this study, we have successfully characterized the GGVA for the first time in grapevine cultivars from India. Our results indicate the genetic closeness of Indian isolates with other world isolates and suggest that the GGVA infection is prevalent in grapevine plantations in India and may have a significant impact on grape production. Further research is needed to fully understand the impact of GGVA on grapevine growth and yield in India. The developed crude sap-based RPA assay for the detection of GGVA can efficiently detect the virus in field samples with high sensitivity and feasibility. The assay utilizes a crude plant extract and RPA enzymes to amplify and detect GGVA in grapevine samples, making it highly sensitive and specific. The assay eliminates the need for specialized equipment and purification or isolation of the viral DNA, making it a rapid and cost-effective method for the detection of GGVA. The assay has the potential to play a crucial role in the prevention of the spread of GGVA by detecting the presence of the virus in field samples and planting material. Overall, this assay is a valuable tool for the detection and management of GGVA in India and may have implications for other regions where GGVA is prevalent.

Data availability statement

The datasets presented in this study can be found in online repositories. The names of the repository/repositories and accession number(s) can be found below: NCBI GeneBank database, accession OQ079131 and OQ079132.

Author contributions

Conceptualization VB, SS. Investigation and Methodology GK, RK, NS, AK. Resources VB. Validation GK, RK, NS, AK. Writing GK. Review and Editing SS, VB, NG. All authors contributed to the article and approved the submitted version.

Acknowledgments

The authors are thankful to Head and Professor, Division of Plant Pathology, ICAR-IARI, New Delhi and Director, ICAR-IARI, New Delhi for providing facilities to carrying out the study. The authors would also like to extend their sincere appreciation to the researchers (Zainul Abdeen Khan, Damini Diksha, Pooja Thapa and Mailem Y.S.) supporting ICAR-National Professor Project and NCS-TCP Project.

Conflict of interest

The authors declare that the research was conducted in the absence of any commercial or financial relationships that could be construed as a potential conflict of interest.

Publisher's note

Supplementary material

The Supplementary Material for this article can be found online at: https://www.frontiersin.org/articles/10.3389/fpls.2023.1151471/full#supplementary-material

SUPPLEMENTARY FIGURE 1
Standardization of RPA assay using RNA, DNA and crude sap (isolated from GGVA positive and healthy grapevine plants) as templates. RPA based detection of GGVA from positive samples using DNA **(A)** and crude sap **(B)** as template and products were run on 1.5% gel without adding 5% SDS. RPA based detection of GGVA from positive samples using DNA **(C)** and crude sap **(D)** as template and products were run on 1.5% gel with addition of 5% SDS. Lane M: 100 bp DNA ladder, 1-3: GGVA positive plants, N: Water Control, H: Healthy plants.

SUPPLEMENTARY FIGURE 2
Comparative sensitivity analysis of conventional PCR **(A)** and RPA assay **(B)** to elucidate the detection limit using plasmid (with GGVA insert) employing primer pair GGVA-212RPA-Fp/Rp in a 10-fold serial dilutions. Lane M: 100 bp DNA ladder, Lane 1: Stock; 2: 10^{-1}; 3: 10^{-2}; 4: 10^{-3}; 5: 10^{-4}; 6: 10^{-5}; 7: 10^{-6}; 8: 10^{-7}; 9: 10^{-8}; 10: 10^{-9}; 11: 10^{-10}; 12: 10^{-11}; 13: 10^{-12}; 14: 10^{-13}; 15: 10^{-14}; 16: 10^{-15}.

SUPPLEMENTARY FIGURE 3
(A) Specificity analysis of crude sap-based RPA assay to elucidate the cross-reaction with other grapevine infecting viruses. Crude sap lysed in 0.5M NaOH was used as template employing primer pair GGVA-212RPA-Fp/Rp. Lane M: 100 bp DNA ladder, Lane 1: GLRaV-3 infected plant sample; 2: GLRaV-4 infected plant sample; 3: GVA infected plant sample; 4: GVB infected plant sample; 5: Negative control; H: healthy sample and P: GGVA positive sample. **(B)** Represents restriction digestion of GGVA specific amplicons (212 bp) from PCR and RPA products cloned in pGEMT vector. Lane M: 100 bp DNA ladder, Lane 1-2: cloned PCR product; 3-4: cloned RPA product and H: negative control.

SUPPLEMENTARY TABLE 1
List of samples tested for validation of developed crude sap-based RPA assay representing different cultivars and locations of India.

References

Al Rwahnih, M., Alabi, O. J., Westrick, N. M., Golino, D., and Rowhani, A. (2017). Description of a novel monopartite geminivirus and its defective subviral genome in grapevine. *Phytopathology* 107, 240–251. doi: 10.1094/PHYTO-07-16-0282-R

Al Rwahnih, M., Dave, A., Anderson, M. M., Rowhani, A., Uyemoto, J. K., and Sudarshana, M. R. (2013). Association of a DNA virus with grapevines affected by red blotch disease in California. *Phytopathology* 103, 1069–1076. doi: 10.1094/PHYTO-10-12-0253-R

Babu, B., Washburn, B. K., Miller, S. H., Poduch, K., Sarigul, T., Knox, G. W., et al. (2017). A rapid assay for detection of rose rosette virus using reverse transcription-recombinase polymerase amplification using multiple gene targets. *J. Virol. Methods* 240, 78–84. doi: 10.1016/j.jviromet.2016.11.014

Blanco-Ulate, B., Hopfer, H., Figueroa-Balderas, R., Ye, Z., Rivero, R. M., Albacete, A., et al. (2017). Red blotch disease alters grape berry development and metabolism by interfering with the transcriptional and hormonal regulation of ripening. *J. Exp. Bot.* 68, 1225–1238. doi: 10.1093/JXB/ERW506

Cao, Y., Yan, D., Wu, X., Chen, Z., Lai, Y., Lv, L., et al. (2020). Rapid and visual detection of milk vetch dwarf virus using recombinase polymerase amplification combined with lateral flow strips. *Virol. J.* 17. doi: 10.1186/s12985-020-01371-5

Fan, X. D., Zhang, Z. P., Ren, F., Hu, G. J., Li, Z. N., and Dong, Y. F. (2017). First report of grapevine geminivirus a from grapevines in China. *Plant Dis.* 101, 1333. doi: 10.1094/PDIS-01-17-0106-PDN

Fiallo-Olivé, E., Lett, J. M., Martin, D. P., Roumagnac, P., Varsani, A., Zerbini, F. M., et al. (2021). ICTV virus taxonomy profile: Geminiviridae 2021. *J. Gen. Virol.* 102. doi: 10.1099/JGV.0.001696

Fuchs, M. (2020). Grapevine viruses: a multitude of diverse species with simple but overall poorly adopted management solutions in the vineyard. *J. Plant Pathol.* 102, 643–653. doi: 10.1007/S42161-020-00579-2

Jo, Y., Choi, H., Song, M. K., Park, J. S., Lee, J. W., and Cho, W. K. (2017). First report of grapevine geminivirus a in diverse vitis species in Korea. *Plant Dis.* 102, 255. doi: 10.1094/PDIS-05-17-0771-PDN

Kapoor, R., Srivastava, N., Kumar, S., Saritha, R. K., Sharma, S. K., Jain, R. K., et al. (2017). Development of a recombinase polymerase amplification assay for the diagnosis of banana bunchy top virus in different banana cultivars. *Arch. Virol.* 162, 2791–2796. doi: 10.1007/s00705-017-3399-9

Krenz, B., Thompson, J. R., Fuchs, M., and Perry, K. L. (2012). Complete genome sequence of a new circular DNA virus from grapevine. *J. Virol.* 86, 7715–7715. doi: 10.1128/JVI.00943-12

Kumar, R., Kaundal, P., Tiwari, R. K., Siddappa, S., Kumari, H., Chandra Naga, K., et al. (2021a). Rapid and sensitive detection of potato virus X by one-step reverse transcription-recombinase polymerase amplification method in potato leaves and dormant tubers. *Mol. Cell. Probes* 58. doi: 10.1016/J.MCP.2021.101743

Kumar, R., Kaundal, P., Tiwari, R. K., Siddappa, S., Kumari, H., Lal, M. K., et al. (2022). Establishment of a one-step reverse transcription recombinase polymerase amplification assay for the detection of potato virus s. *J. Virol. Methods* 307. doi: 10.1016/J.JVIROMET.2022.114568

Kumar, R., Pant, R. P., Kapoor, S., Khar, A., and Baranwal, V. K. (2021b). Development of a reverse transcription-recombinase polymerase amplification (RT-RPA) assay for the detection of onion yellow dwarf virus (OYDV) in onion cultivars. *Indian Phytopathol.* 74, 201–207. doi: 10.1007/S42360-020-00311-1

Kumar, P. V., Sharma, S. K., Rishi, N., Ghosh, D. K., and Baranwal, V. K. (2018). An isothermal based recombinase polymerase amplification assay for rapid, sensitive and robust indexing of citrus yellow mosaic virus. *Acta Virol.* 62, 104–108. doi: 10.4149/AV_2018_113

Li, R., Fuchs, M. F., Perry, K. L., Mekuria, T., and Zhang, S. (2017). Development of a fast amplifyrp acceler8 diagnostic assay for grapevine red blotch virus. *J. Plant Pathol.* 99, 657–662. doi: 10.4454/JPP.V99I3.3952

Liang, P., Navarro, B., Zhang, Z., Wang, H., Lu, M., Xiao, H., et al. (2015). Identification and characterization of a novel geminivirus with a monopartite genome infecting apple trees. *J. Gen. Virol.* 96, 2411–2420. doi: 10.1099/VIR.0.000173

Loconsole, G., Saldarelli, P., Doddapaneni, H., Savino, V., Martelli, G. P., and Saponari, M. (2012). Identification of a single-stranded DNA virus associated with citrus chlorotic dwarf disease, a new member in the family geminiviridae. *Virology* 432, 162–172. doi: 10.1016/J.VIROL.2012.06.005

Londoño, M. A., Harmon, C. L., and Polston, J. E. (2016). Evaluation of recombinase polymerase amplification for detection of begomoviruses by plant diagnostic clinics. *Virol. J.* 13. doi: 10.1186/S12985-016-0504-8

Maliogka, V. I., Olmos, A., Pappi, P. G., Lotos, L., Efthimiou, K., Grammatikaki, G., et al. (2015). A novel grapevine badnavirus is associated with the roditis leaf discoloration disease. *Virus Res.* 203, 47–55. doi: 10.1016/J.VIRUSRES.2015.03.003

Martelli, G. P. (2014). Directory of virus and virus-like diseases of the grapevine and their agents. *J. Plant Pathol.* 96, 1–136. doi: 10.4454/JPP.V96I1SUP

McGovern, P. (2019). *Ancient wine: The search for the origins of viniculture*. (Princeton Univers. Press). doi: 10.1515/9780691198965

Mekuria, T. A., Zhang, S., and Eastwell, K. C. (2014). Rapid and sensitive detection of little cherry virus 2 using isothermal reverse transcription-recombinase polymerase amplification. *J. Virol. Methods* 205, 24–30. doi: 10.1016/j.jviromet.2014.04.015

Mohandas, A., and Bhat, A. I. (2020). Recombinase polymerase amplification assay for the detection of piper yellow mottle virus infecting black pepper. *VirusDisease* 31, 38–44. doi: 10.1007/s13337-019-00566-x

Piepenburg, O., Williams, C. H., Stemple, D. L., and Armes, N. A. (2006). DNA Detection using recombination proteins. *PloS Biol.* 4, e204. doi: 10.1371/JOURNAL.PBIO.0040204

Qiu, W., and Schoelz, J. (2017). Grapevine vein clearing virus: Diagnostics, genome, genetic diversity, and management. *Grapevine Viruses Mol. Biol. Diagn. Manage.* 315–330. doi: 10.1007/978-3-319-57706-7_15/COVER

Romero, J. L. R., Carver, G. D., Arce Johnson, P., Perry, K. L., and Thompson, J. R. (2019). A rapid, sensitive and inexpensive method for detection of grapevine red blotch virus without tissue extraction using loop-mediated isothermal amplification. *Arch. Virol.* 164, 1453–1457. doi: 10.1007/S00705-019-04207-Y/METRICS

Sharma, S. K., Pathaw, N., Wangkhem, B., Jackson, K. S., Devi, K. S., Roy, S. S., et al. (2023). Simple template-based reverse transcription-recombinase polymerase amplification assay for routine diagnosis of citrus tristeza virus. *Lett. Appl. Microbiol.* 0, 1–9. doi: 10.1093/LAMBIO/OVAC060

Sidharthan, V. K., Sevanthi, A. M., Jaiswal, S., and Baranwal, V. K. (2020). Robust virome profiling and whole genome reconstruction of viruses and viroids enabled by use of available mRNA and sRNA-seq datasets in grapevine (Vitis vinifera l.). *Front. Microbiol.* 11. doi: 10.3389/fmicb.2020.01232

Sidharthan, V. K., Sevanthi, A. M., Venkadesan, S., Diksha, D., and Baranwal, V. K. (2022). Seasonal dynamics in leaf viromes of grapevines depicting leafroll syndrome under tropical condition. *Trop. Plant Pathol.* 47, 635–645. doi: 10.1007/s40858-022-00524-x

Silva, G., Bömer, M., Nkere, C., Lava Kumar, P., and Seal, S. E. (2015). Rapid and specific detection of yam mosaic virus by reverse-transcription recombinase polymerase amplification. *J. Virol. Methods* 222, 138–144. doi: 10.1016/j.jviromet.2015.06.011

Srivastava, N., Kapoor, R., Kumar, R., Kumar, S., R.K., S., Kumar, S., et al. (2019). Rapid diagnosis of cucumber mosaic virus in banana plants using a fluorescence-based real-time isothermal reverse transcription-recombinase polymerase amplification assay. *J. Virol. Methods* 270, 52–58. doi: 10.1016/j.jviromet.2019.04.024

Sudarshana, M. R., Perry, K. L., and Fuchs, M. F. (2015). Grapevine red blotch-associated virus, an emerging threat to the grapevine industry. *Phytopathology* 105, 1026–1032. doi: 10.1094/PHYTO-12-14-0369-FI

Sun, S., Hu, Y., Jiang, G., Tian, Y., Ding, M., Yu, C., et al. (2020). Molecular characterization and genomic function of grapevine geminivirus a. *Front. Microbiol.* 112121. doi: 10.3389/FMICB.2020.555194/BIBTEX

Veerakone, S., Blouin, A. G., Barrero, R. A., Napier, K. R., MacDiarmid, R. M., and Ward, L. I. (2019). First report of grapevine geminivirus a in vitis in New Zealand. *Plant Dis.* 104, 600. doi: 10.1094/PDIS-06-19-1142-PDN

Wang, T. M., and Yang, J. T. (2019). Visual DNA diagnosis of tomato yellow leaf curl virus with integrated recombinase polymerase amplification and a gold-nanoparticle probe. *Sci. Rep.* 9. doi: 10.1038/s41598-019-51650-7

Zhang, S., Ravelonandro, M., Russell, P., McOwen, N., Briard, P., Bohannon, S., et al. (2014). Rapid diagnostic detection of plum pox virus in prunus plants by isothermal AmplifyRP® using reverse transcription-recombinase polymerase amplification. *J. Virol. Methods* 207, 114–120. doi: 10.1016/j.jviromet.2014.06.026

Zhang, Y., Singh, K., Kaur, R., and Qiu, W. (2011). Association of a novel DNA virus with the grapevine vein-clearing and vine decline syndrome. *Phytopathology* 101, 1081–1090. doi: 10.1094/PHYTO-02-11-0034

Zhou, Y., Zheng, H. Y., Jiang, D. M., Liu, M., Zhang, W., and Yan, J. Y. (2022). A rapid detection of tomato yellow leaf curl virus using recombinase polymerase amplification-lateral flow dipstick assay. *Lett. Appl. Microbiol.* 74, 640–646. doi: 10.1111/lam.13611

frontiers | Frontiers in Plant Science

TYPE Original Research
PUBLISHED 10 May 2023
DOI 10.3389/fpls.2023.1164245

OPEN ACCESS

EDITED BY
Ahmed Abdelkhalek,
City of Scientific Research and Technological Applications, Egypt

REVIEWED BY
Bita Naseri,
Agricultural Research, Education and Extension Organization (AREEO), Iran
Deepa Khare,
Bennett University, India
Said Ibrahim Behiry,
Alexandria University, Egypt

*CORRESPONDENCE
Harwinder Singh Buttar
harwinderbuttar59@gmail.com
Rahul Kumar Tiwari
rahultiwari226@gmail.com
Ravinder Kumar
chauhanravinder97@gmail.com

RECEIVED 12 February 2023
ACCEPTED 12 April 2023
PUBLISHED 10 May 2023

CITATION
Buttar HS, Singh A, Sirari A, Anupam, Kaur K, Kumar A, Lal MK, Tiwari RK and Kumar R (2023) Investigating the impact of fungicides and mungbean genotypes on the management of pod rot disease caused by *Fusarium equiseti* and *Fusarium chlamydosporum*. *Front. Plant Sci.* 14:1164245. doi: 10.3389/fpls.2023.1164245

Investigating the impact of fungicides and mungbean genotypes on the management of pod rot disease caused by *Fusarium equiseti* and *Fusarium chlamydosporum*

Harwinder Singh Buttar[1]*, Amarjit Singh[1], Asmita Sirari[2], Anupam[1], Komalpreet Kaur[3], Abhishek Kumar[4], Milan Kumar Lal[5], Rahul Kumar Tiwari[5]* and Ravinder Kumar[5]*

[1]Department of Plant Pathology, Punjab Agricultural University, Ludhiana, India, [2]Department of Plant Breeding and Genetics, Punjab Agricultural University, Ludhiana, India, [3]Department of Chemistry, Punjab Agricultural University, Ludhiana, India, [4]Department of Plant Pathology, Chaudhary Charan Singh Haryana Agricultural University, Hisar, India, [5]Department of Plant Protection; Department of Crop Physiology, Biochemistry & Postharvest Technology, Indian Council of Agricultural Research (ICAR)-Central Potato Research Institute, Shimla, Himachal Pradesh, India

Introduction: Mungbean is a vital pulse crop in India that can thrive in dry-land conditions and is grown in three seasons, with the added benefit of being used as green manure due to its ability to fix atmospheric nitrogen. Recently, pod rot disease has emerged as a serious threat to mungbean cultivation in India.

Methods: In this study, morpho-molecular identification of associated pathogens and the bio-efficacy of systemic and non-systemic fungicides as well as genotype screening was performed during the years 2019 and 2020. The pathogens associated with this disease were confirmed on the basis of morphological and molecular characterization. For the molecular characterization, the translation elongation factor 1-alpha (tef-1) gene sequences were amplified by using primers (EF1 and EF2).

Results: Under in vitro conditions, trifloxystrobin + tebuconazole 75% WG was found to be the most effective against Fusarium equiseti (ED_{50} 2.39 µg ml^{-1}) and Fusarium chlamydosporum (ED_{50} 4.23 µg ml^{-1}) causal agents of pod rot of mungbean. Under field conditions, three applications of trifloxystrobin + tebuconazole 75% WG at 0.07% as a foliar application at fortnightly intervals starting from the last week of July proved to be the most effective against pod rot disease on mungbean cultivars, i.e., ML 2056 and SML 668. To identify the potential resistance sources, 75 interspecific derivative and mutant lines of mungbean were screened for disease reaction to pod rot under natural epiphytotic conditions for the years 2019 and 2020. Genotypic differences

were observed for resistance to pod rot disease. The study revealed that among the tested genotypes, ML 2524 exhibited resistance to pod rot disease, with a disease incidence of 15.62% and disease severity of 7.69%. In addition, 41 other genotypes were found to be moderately resistant (MR) to the disease.

Conclusion: Altogether, the identified management options will offer an immediate solution to manage this disease under recent outbreak conditions and pave a path for futuristic disease management using identified resistant sources in breeding programs.

KEYWORDS

propiconazole, screening, resistance, tabuconazole, trifloxystrobin

1 Introduction

Mungbean, also known as *Moong*, or *Green gram*, is one of the most important pulse crops in India. It is a short-duration crop that can tolerate dry-land conditions and is cultivated in three different seasons, *viz*., *Kharif*, *Rabi*, and summer, and also used as green manuring as having the capacity to fix atmospheric nitrogen (Nadeem et al., 2004; Pataczek et al., 2018). India contributes the maximum production of mungbean in South Asia, which accounts for around 90% of world output (Nair et al., 2012). The potential yield of mungbean is 2.5–3.0 t per hectare with selected varieties and good management practices under Indian conditions. However, the yield of mungbean in India is still relatively low, coming in at an average of 0.5 t per hectare (Nair et al., 2019). This could be because of changing climate conditions such as temperature and carbon dioxide levels within rain-fed areas, which can lead to varying levels of biotic stress (Chakraborty et al., 2000; Sharma et al., 2007). One of the most significant factors that contribute to this biotic stress is the presence of fungal infections, which can diminish the yield of mungbean by anywhere between 40% and 60% (Kaur et al., 2011). The loss of mungbean output that is caused by fungal diseases is a big worry for both the country's farmers and the nation's overall food security. Powdery mildew, rust, and anthracnose are just a few of the many fungal diseases that are frequent in the cultivation of mungbeans and are responsible for major losses in production. *Fusarium solani* and its related species are a significant concern among the various root rot pathogens and pose a considerable threat to several legumes, such as bean, pea, chickpea, and lentil (Carvalho et al., 2015; Naseri and Hamadani 2017a, Naseri, 2019). Additionally, *Fusarium virguliforme* (formerly known as *F. solani* f. sp. *glycine*) and other related *Fusarium* species are responsible for causing sudden death syndrome, which is a major issue for soybean cultivation in many regions (Rubiales et al., 2015).

Among the sustainable management approaches, agronomic and soil management practices have been reported highly effective in managing root rot in legumes (Naseri and Hemmati, 2017b; Naseri et al., 2018). The better understanding of agronomic practices and soil factors with special emphasis on soil texture, microbial populations, date of planting, method of cultivation, preceding crop, and fertilizer application are essential in root and stem rot disease management in legumes (Naseri et al., 2018). The introduction of beneficial microorganisms in the rhizosphere has also been found effective in controlling root rot pathogens. *Trichoderma* fungal species are commonly used for biological control of *Fusarium* incited rots in legumes. For example, treatment of lentil seedlings with *Trichoderma hamatum* was found to reduce colonization of *Fusarium oxysporum* f. sp. *lentis*, whereas soil application of *Trichoderma harzianum* in common bean- and chickpea-growing areas was found to effectively reduce the infection rates of *Fusarium oxysporum* f. sp. *phaseoli* and *Fusarium oxysporum* f. sp. *ciceris*, respectively (El-Hassan et al., 2013; Carvalho et al., 2015). However, it is a consistent challenge to find a highly efficacious strain of bioagent, which can effectively manage the disease under field conditions. For a newly emerging disease, the immediate solution is to identify broad-spectrum fungicides that can minimize the consistent outbreak in the farmers' field. Parallelly, the exploitation of host plant resistance from the perspective of developing resistant varieties is the suitable long-term management strategy to manage root and stem rot diseases in legumes. During the last few years, pod rot disease caused by *Fusarium equiseti* and *Fusarium chlamydosporum* has emerged as a significant bottleneck in mungbean production (Buttar et al., 2023). The disease is characterized by pod discoloration and rotting of pods and seeds and aggravates if high rainfall occurs during maturity (Buttar et al., 2023). Since pods are the economic part of the crop, the farmers therefore have to achieve efficient control of this disease because it negatively affects the yield and subsequently their income. The disease is characterized by the rot of mungbean pods and stems, resulting in the death of infected plants. This not only reduces the yield of mungbean but also affects the quality of the beans by causing discoloration, cracking, and shriveling. Because the disease can also be transmitted through contaminated seed, it is absolutely necessary for the production of mungbeans to make use of seed that is of excellent quality and free of disease. There is a great need to prospect for the optimal approach in the management of pod rot to ensure efficient control. The application of broad-spectrum fungicides, both as a seed treatment and as a foliar spray, was the conventional strategy for disease control in mungbean production (Pandey et al., 2018). When it comes to the management of fungal infections in

mungbean, utilizing host resistance has been acknowledged as a method that is both cost-effective and environmentally beneficial (Yadav et al., 2014a). The use of disease-resistant cultivars in conjunction with other agronomic and soil management practices is the most effective method for preventing and treating fungal diseases in mungbean crops (Pandey et al., 2018). As a reliable and quickly effective method, farmers prefer resistant varieties and use synthetic chemical pesticides to control the disease. Being a recently reported problem with the potential to inflict grave losses and lack of desirable host resistance, fungicides, bioagents, and botanicals were evaluated both under *in vitro* and field conditions against the associated pathogens. Moreover, the elite germplasms derived from interspecific hybridization between mungbean and ricebean/urdbean were screened for pod rot resistance to identify the resistant genotypes for resistance breeding programs.

2 Material and methods

2.1 Confirmation of pathogens associated with a pod rot disease

2.1.1 Isolation, purification, and identification of the fungus

Mungbean pods showing symptoms of pod rot were collected from mungbean fields (untreated plots) of Punjab Agriculture University, Ludhiana, Punjab, India. Initial identification of pathogens based on cultural and morphological characteristics was done to confirm the association of *F. equiseti* and *F. chalamydosporum* with this disease. Field samples were sent to the laboratory for additional evaluation and isolation. The pods were meticulously cleaned and sliced into small bits. The components were sanitized before being placed on water agar medium for incubation under normal conditions. The cultures were then transferred to potato dextrose agar and purified using a single method of spore isolation. For further research, the pure cultures were maintained on PDA and Spezieller Nährstoffarmer Agar at 25 ± 1°C in the incubator. The cultural and morphological characters of the isolated pathogens were compared with those described previously by Leslie and Summerell (2006), Wollenweber and Reinking (1935), and Booth (1971).

2.1.2 Molecular characterization of the pathogens

The identification of the pathogens causing pod rot was also confirmed by sequencing the translation elongation factor 1-alpha (tef-1) gene sequences. The mycelial mat of isolated pathogens causing pod rot of mungbean was grown in potato dextrose broth at 25 ± 10°C for 6 days in a BOD incubator. The total genomic DNA was isolated from mycelial mats using (Doyle and Doyle, 1987) DNA extraction methods with some modifications (CTAB method for DNA extraction). The translation elongation factor 1-alpha (tef-1) gene region from genomic DNA of both the fungal pathogens from genomic DNA was amplified with EF primers (EF1 and EF2) (O'Donnell et al., 1998) in polymerase chain reaction (PCR). For molecular-based identification of the culture, the purified PCR amplicons were outsourced for sequencing to Biologia Research India Pvt. Ltd. The rDNA tef-1 sequences were edited using MEGA-X Sequence viewer software. The edited nucleotide sequences were subjected to blast in three different tools, i.e., the "nucleotide BLAST" tool of NCBI (http://blast.ncbi.nlm.nih.gov/Blast) and the Fusarium MLST tool of the MYCOBANK database (https://fusarium.mycobank.org/) for its closest homology with database available in these databases for its identification.

2.2 Test fungicides

Commercial samples of seven fungitoxicants, *viz*., copper oxychloride (Blitox 50% WP, Rallis India Limited, Mumbai), propineb (Antracol 70% WP, Bayer Crop Science Limited, Mumbai), mancozeb (Indofil 75% WP, Indofil Chemicals, Mumbai), carbendazim (Bavistin 50% WP, BASF India Ltd., Mumbai), propiconazole (Tilt 25% EC, Bayer Crop Science Limited, Mumbai), tebuconazole (Folicur 25.9% WP, Bayer Crop Science Limited, Mumbai), and trifloxystrobin + tebuconazole (Nativo 75% WG, Bayer Crop Science Limited, Mumbai), were freshly procured from the market to evaluate their efficacy under *in vitro* and field conditions against pod rot in mungbean.

2.3 *In vitro* bioassay of fungitoxicants

To assess effectiveness under lab conditions, a poisoned food assay (Nene and Thapliyal, 1993) was conducted on potato dextrose agar (PDA) medium. The three non-systemic fungitoxicants, i.e., copper oxychloride, propineb, and mancozeb, were tested at a series of concentrations, *viz*., 0, 10, 25, 50, 100, 200, and 500 µg/ml, whereas systemic fungitoxicants (propiconazole, trifloxystrobin + tebuconazole, tebuconazole, and carbendazim) were tested at concentrations 0, 5, 10, 25, 50, 75, 100, and 200 µg/ml. The needed amount of the test chemical was combined with 100 ml of sterile PDA medium, and the resulting solution was poured under aseptic conditions into Petri plates with a 90-mm diameter. Each Petri dish contained a 7-mm circular slice of actively growing fungus, and each concentration was reproduced four times. The control were the Petri dishes using PDA medium without a fungicide. The Petri dishes were incubated at a temperature of 25 1°C. When the growth in the control plate reached 90 mm, the radial growth of the pathogens was measured, and the percent inhibition in colony growth (Pi) was computed using a formula published by Vincent (1947).

2.4 Field trials

The two-season field trials for evaluation of fungicides against pod rot disease were conducted at Krishi Vigyan Kendra, Goniana Sri Muktsar Sahib, Punjab, during 2019–2020 and at the experimental field, Pulse section, Department of Plant Breeding and Genetics, Punjab Agricultural University, Ludhiana, Punjab, during 2021 in a randomized block design with three replications. The location for the experiment was selected based on the previous

10.3389/fpls.2023.1164245

history of high disease intensity in the chosen field. Cultivars 'ML 2056' and 'SML 668' for the years 2019–2020 and 'ML 2056' for the year 2021 were sown in the third week of July as per the standard agronomic practices recommended by Punjab Agricultural University (Anonymous, 2019).

Treatments details: Eight treatments (T1: copper oxychloride 50% WP at 0.3%, T2: propineb 70% WP at 0.3%, T3: mancozeb 75% WP at 0.3%, T4: carbendazim 50% WP at 0.2%, T5: propiconazole 25% EC at 0.1%, T6: tebuconazole 25.9% EC at 0.1%, T7: trifloxystrobin + tebuconazole 75% WG at 0.07%) were applied with untreated control for the years 2019–2020, and 10 treatments (T1: trifloxystrobin + tebuconazole 75% WG at 0.05%, T2: trifloxystrobin + tebuconazole 75% WG at 0.07%, T3: trifloxystrobin + tebuconazole 75% WG at 0.09%, T4: tebuconazole 25.9% EC at 0.08%, T5: tebuconazole 25.9% EC at 0.1%, T6: tebuconazole 25.9% EC at 0.3%, T7: *Trichoderma harzianum* at 1.5%, T8: *Pseudomonas fluorescens* at 1.5%, and T9: neem extract at 5%) that were applied with untreated control for the year 2021 were evaluated for management of pod rot of mungbean. Treatments were given as a foliar application of different fungicides (water volume for spray 500 l/ha using a knapsack sprayer fitted with a hollow-cone nozzle), and the untreated control was sprayed with water. Three applications were done for each treatment at an interval of 15 days starting from the last week of July. The disease incidence and severity were recorded 10 days after the last application following a 0–5 scale as described by Singh (2021). The percent disease index (PDI) was calculated as per the formulae given by Wheeler (1969). Percent incidence and percent disease control (PDC) were calculated according to the following:

$$\text{Percent incidence} = \frac{\text{Number of diseased plants}}{\text{Total no. of plants assessed}} \times 100$$

$$\text{Percent disease control} = \frac{\text{PDI in Untreated} - \text{PDI in Treatment}}{\text{PDI in Untreated}} \times 100$$

2.5 Field evaluation of mungbean genotypes for resistance against pod rot disease

Seventy-five interspecific derivative and mutant lines of mungbean (Table 1) were screened for reaction to pod rot under natural epiphytotic conditions for the years 2019 and 2020. The experiment was conducted in the Experimental area of the Pulses section, Department of Plant Breeding and Genetics, Punjab Agricultural University, Ludhiana, India. The test entries were sown on 4-m rows with a 30 × 10 cm spacing with two replications. Disease incidence and severity were recorded for each entry.

TABLE 1 Interspecific derivative and mutant lines of mungbean screened against pod rot disease.

S. no.	Germplasm	S. no.	Germplasm	S. no.	Germplasm	S. no.	Germplasm
1	MML 2539	20	MML 2575	39	SML 2063	58	ML 2482
2	MML 2543	21	MML 2577	40	SML 2064	59	ML 2483
3	MML 2544	22	MML 2578	41	SML 2065	60	ML 2498
4	MML 2545	23	MML 2579	42	SML 2066	61	ML 2500
5	MML 2546	24	SML 2048	43	SML 2067	62	ML 2506
6	MML 2549	25	SML 2049	44	SML 2068	63	ML 2507
7	MML 2550	26	SML 2050	45	SML 2069	64	ML 2524
8	MML 2551	27	SML 2051	46	SML 2070	65	ML 2525
9	MML 2560	28	SML 2052	47	SML 2071	66	ML 2566
10	MML 2561	29	SML 2053	48	SML 2073	67	ML 2567
11	MML 2562	30	SML 2054	49	SML 1839	68	ML 2568
12	MML 2563	31	SML 2055	50	SML 2015	69	ML 2569
13	MML 2565	32	SML 2056	51	SML 2016	70	ML 2576
14	MML 2568	33	SML 2057	52	ML 2423	71	MML 2566
15	MML 2570	34	SML 2058	53	ML 2459	72	MML 2567
16	MML 2571	35	SML 2059	54	ML 2460	73	MML 2569
17	MML 2572	36	SML 2060	55	ML 2479	74	MML 2576
18	MML 2573	37	SML 2061	56	ML 2480	75	MML 2580
19	MML 2574	38	SML 2062	57	ML 2481		

Percent incidence was calculated according to the following:

$$\text{Percent incidence} = \frac{\text{Number of diseased plants}}{\text{Total no of plants assessed}} \times 100$$

To record the data on pod rot disease severity, 100 pods were selected at random across the field, following a 0–5 scale (Singh, 2021).

Score	Disease description
0	Apparently healthy plant
1	0%–10% of pod infected
2	11%–25% of pod infected
3	26%–50% of pod infected
4	51%–75% of pod infected
5	>75% of pod infected

The categorization of host reaction (HI, R, MR, MS, S, and HS) was done as follows on the basis of the per cent disease index:

Disease severity (%)	Reaction
0	Highly resistant (HI)
0–10	Resistant (R)
10.1–25	Moderately resistant (MR)
25.1–45	Moderately susceptible (MS)
45.1–70	Susceptible (S)
More than 70.1	Highly susceptible (HS)

2.6 Statistical analysis

The data on percent growth inhibition under *in vitro* trials were subjected to analysis of variance (ANOVA) for factorial completely randomized design (CRD) to test the significance of the differences at a 5% probability level. ED_{50} and ED_{90} were calculated by Probit analysis using statistical software SPSS 16.0. The field data on disease incidence and disease severity was subjected to statistical analysis by Duncan's multiple-range test employing R-studio software. The phylogenetic tree for the screened mungbean genotypes was prepared by using R-studio software (RStudio Team, 2021).

3 Results

3.1 Confirmation of pathogens associated with a pod rot disease

3.1.1 Isolation, purification, and identification of the fungus

Symptomatic mungbean pods exhibiting signs of pod rot were gathered from experimental plots in the mungbean fields at Punjab Agriculture University, located in Ludhiana, Punjab, India. Two isolates of Fusarium, i.e., PR I and PR II, were collected in this experiment. The cultures of both fungi were purified by employing the hyphal tip method (Tutte, 1969). The colony morphology of the PR I isolate (Figure 1A) was initially white with floccose abundant aerial mycelium changed to beige and finally to buff after 7 days with dense distribution, entire margins, and flat elevation. The conidia were falcate with a prominent foot cell and tapered and elongated apical cells with a pronounced dorsiventral curvature. Mature conidia usually contain five to seven septa measuring 28.42–52.32 × 3.8–5.9 µm (Figure 1B). Microconidia were not formed. Chlamydospores were formed singly or in chains with brown color, thick-walled, globose, and 5–10 µm in diameter (Figure 1C). Initially, the colony morphology of the PR II isolate (Figure 2A) was off-white with dark-pink pigments. Mycelium was floccose, snow-white initially, and later turned pink with irregular margins. After 7 to 14 days, dark-pink to burgundy pigmentation was observed in the culture, giving a dark-violet to black-colored appearance to cultures below at the agar base. The conidia were thick-walled, slightly curved from the upper side, and almost straight from the lower side with foot-shaped basal cells and pointed apical cells. Smaller conidia were aseptate to septate with two septa, and the larger ones usually contained three to five septa, measuring 22.72–38.62 × 2.7–6.1 µm (Figure 2B). Microconidia were oval to ovate, measuring 5.5–18.54 × 3.2–5.1 µm, and found in the aerial mycelium as being aseptate to having two septa (Figure 2C). Chlamydospores were abundant, verrucose with pale brown color, and formed singly or in chains (Figure 2D). The pathogens associated with pod rot of mungbean were confirmed PRI as *Fusarium equiseti* and PRII as *Fusarium chlamydosporum* after comparing the morphological features with those described previously by Leslie and Summerell (2006), Wollenweber and Reinking (1935), and Booth (1971).

3.1.2 Molecular characterization of the pathogens

The pathogens were also identified by sequencing the translation elongation factor 1-alpha (tef-1) region, and nucleotide sequences were submitted to GenBank (NCBI). Results from the BLAST analysis of tef-1 sequences revealed that the PR-1 isolate was identified as *F. equiseti* (accession number: OK033107.1) based on the tef-1 gene sequence basis, whereas the PR-II isolate was identified as *F. chlamydosporum* (accession number: OK033106.1) (Buttar et al., 2023). In BLASTn search, sequences of isolate *F. equiseti* exhibited 96.49% resemblance with the sequences of *Fusarium equiseti* isolate PAK54 (https://blast.ncbi.nlm.nih.gov/Blast.cgi) and sequences of isolate *F. chlamydosporum* exhibited 97.07% resemblance with the sequences of *Fusarium chlamydosporum* strain DTO 418-C1 (https://blast.ncbi.nlm.nih.gov/Blast.cgi).

3.2 *In vitro* evaluation of non-systemic and systemic fungicides against *Fusarium equiseti* and *Fusarium chlamydosporum* causing pod rot of mungbean

All non-systemic fungitoxicants differed significantly at 10, 25, 50, 100, 200, and 500 µg ml^{-1} concentrations in terms of mean percent growth inhibition of *F. equiseti* (Table 2) and *F.*

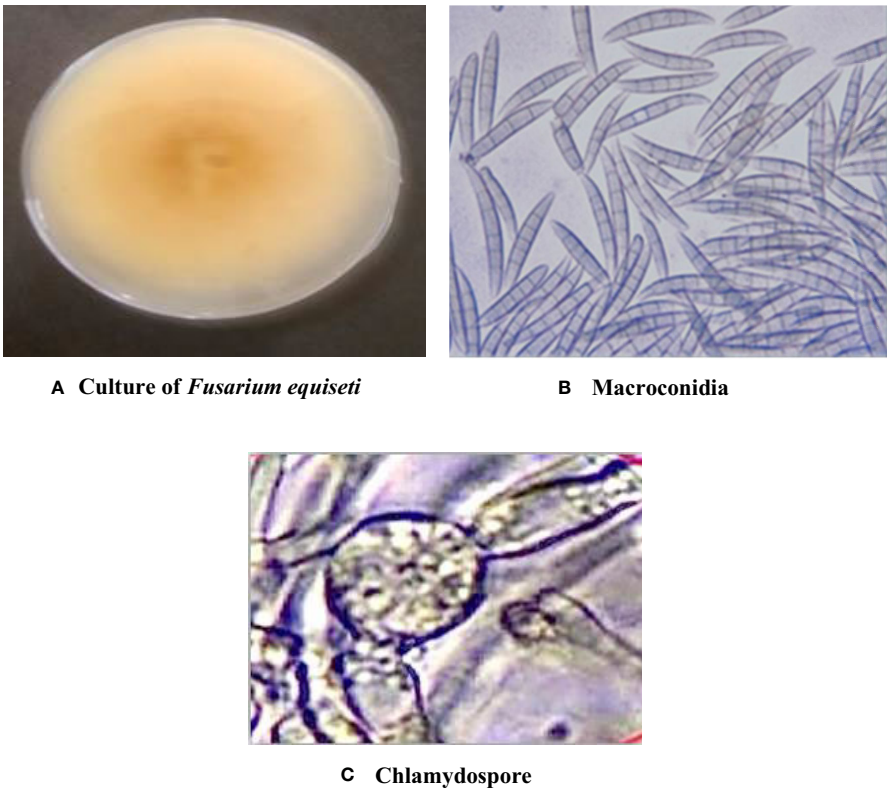

FIGURE 1
Cultural and morphological characteristics of the PR I isolate. **(A)** Colony morphology of *Fusarium equiseti*. **(B)** Macroconidia at 40× magnification. **(C)** Chlamydospores at 40X magnification.

chlamydosporum (Table 3). Among the test non-systemic fungitoxicants, propineb 70% WP was the most superior among the non-systemic fungicides against *F. equiseti* with mean percent inhibition of colony growth of 35.63% and 41.88% mean growth inhibition of *F. chlamydosporum* followed by mancozeb 75% WP with 19.36% growth inhibition of *F. equiseti* and 27.60% growth inhibition of *F. chlamydosporum*. Copper oxychloride 50% WP proved to be the least effective in inhibiting the colony growth of both fungi (Figures 3A, C).

Among the test systemic fungicides trifloxystrobin + tebuconazole 75%, WG proved to be the most effective by providing 80.30% mean percent inhibition of *F. equiseti* colony growth (Table 2) (Figure 3B) and 86.80% mean percent inhibition of *F. chlamydosporum* colony growth (Table 3) (Figure 3D), whereas the tebuconazole 25.9% EC inhibits 71.83% colony growth of *F. equiseti*, which was at par with carbendazim 50% WP with 69.42% inhibition of colony growth. The least effective fungitoxicants among the systemic fungicides against *F. equiseti* was propiconazole 25% EC as it only recorded 64.08% colony growth inhibition and carbendazim 50% WP proved to be the least effective fungitoxicant against *F. chlamydosporum* 74.20% colony growth inhibition. At the concentration of 200 µg ml^{-1}, trifloxystrobin + tebuconazole 75% WG proved to be the most effective as it completely inhibited the colony growth of *F. equiseti*, and at the concentration of 100 µg ml^{-1}, trifloxystrobin + tebuconazole 75% WG and tebuconazole 25.9% EC proved to be the most effective against *F. chlamydosporum* as these completely inhibited the colony growth.

ED_{50} and ED_{90} values of different fungicides against *F. equiseti* (Table 4) and *F. chlamydosporum* (Table 5) were calculated and found that the propineb 70% WP had the lowest ED_{50} and ED_{90} values (429.22 and 963.62 µg ml^{-1}) among the non-systemic fungicides tested against *F. equiseti* whereas mancozeb 75% WP and copper oxychloride 50% WP were less effective as the ED_{50} and ED_{90} values of these fungicides were 476.17 and 1166 µg ml^{-1} and 795.81 and 1524 µg ml^{-1}, respectively. Among the systemic fungicides, trifloxystrobin + tebuconazole 75% WG recorded the lowest (2.40 µg ml^{-1}) ED_{50} and ED_{90} (140.16 µg ml^{-1}) values. ED_{50} (31.60 µg/ml) and ED_{90} (202.58 µg ml^{-1}) values were recorded as the highest in the case of propiconazole 25% WP. ED_{50} and ED_{90} values of different fungicides against *F. chlamydosporum* are given in Table 5. Among the non-systemic fungicides tested against *F. chlamydosporum*, ED_{50} value 378.57 µg ml^{-1} was found to be the least value in the case of propineb 70% WP, whereas ED_{90} value 897.49 µg ml^{-1} was found to be the least value in the case of mancozeb 75% WP. Among the systemic fungicides, trifloxystrobin + tebuconazole 75% WG recorded the lowest (4.23 µg ml^{-1}) ED_{50} and ED_{90} (54.78 µg ml^{-1}) values. ED_{50} (18.51 µg/ml) and ED_{90} (102.59 µg ml^{-1}) values were recorded as the highest in the case of propiconazole 25% WP.

Copper oxychloride 50% WP was less effective as the ED_{50} and ED_{90} values of these fungicides were 981.69 and 1924.96 µg ml^{-1},

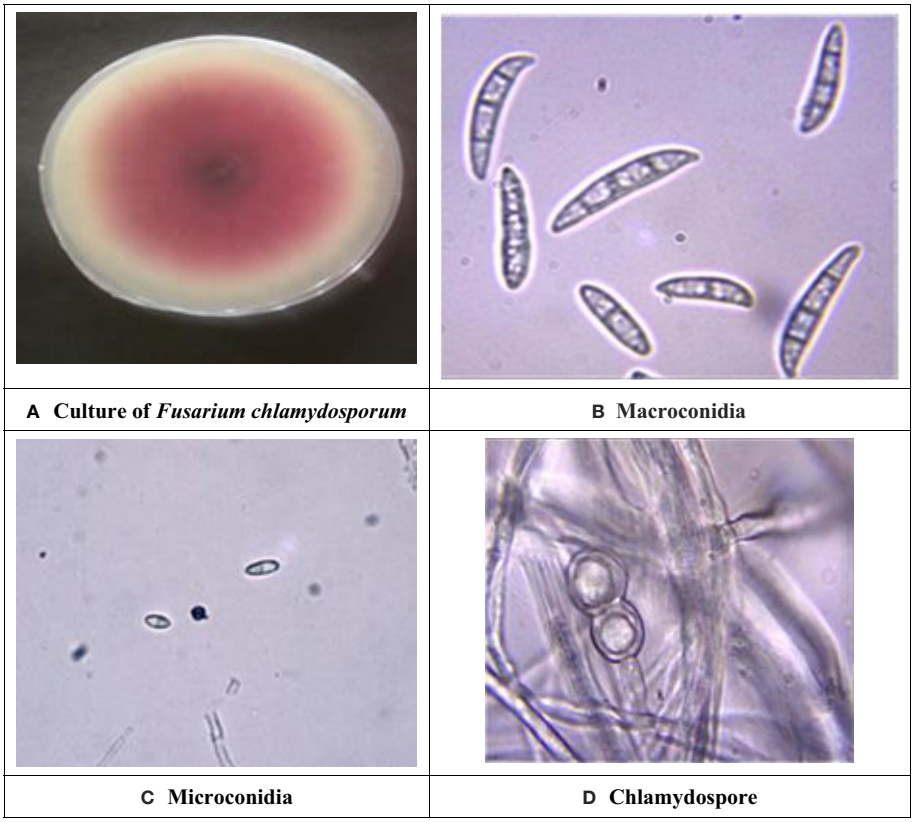

FIGURE 2
Cultural and morphological characteristics of PR II isolate. **(A)** Colony morphology of *Fusarium chlamydosporum*. **(B)** Macroconidia at 40× magnification. **(C)** Microconidia at 40× magnification. **(D)** Chlamydospores at 100× magnification.

respectively. Among the systemic fungicides, carbendazim 50% WP recorded the lowest ED_{50} (0.21 µg ml^{-1}) and ED_{90} (76.32 µg ml^{-1}) values. Propiconazole 25% EC was less effective as the ED_{50} and ED_{90} values of these fungicides were 3.64 and 247.69 µg ml^{-1}, respectively.

3.3 Field evaluation of fungicides against pod rot of mungbean

All the treatments were found to be significantly different against pod rot disease in mungbean (Table 6). The minimum severity and maximum disease control of pod rot to the tune of 8.28% and 82.16%, respectively, were observed in treatment T7, i.e., trifloxystrobin + tebuconazole (75% WG) for SML 668, whereas it was 71.94% disease control with 10.94% severity for ML 2056. It was followed by T6, i.e., tebuconazole (25% EC) application showed 13.24% severity and 71.48% disease control for SML 668 and 13.21% severity and 66.11% disease control for ML 2056 over the control. However, T4 and T5 were adjudged at par statistically. Copper oxychloride (50% WP) was found to be the least effective among the evaluated fungicides with 25.16% disease control for ML 2056 and 36.54% disease control for SML 668. Application of propineb (70% WP) showed 39.72% and 33.25% disease control for SML 668 and ML 2056, respectively, which was adjudged at par with treatment T3 (mancozeb 75% WP).

The minimum yield loss over control 16.98% was found for SML 668 when sprayed with trifloxystrobin + tebuconazole (75% WG), whereas it was 20.43% for ML 2056 in the same treatment. It was followed by 21.63% for SML 668 and 21.96% for ML 2056 in T6, i.e., tebuconazole (25% EC). Yield loss of 32.39% and 27.21% was observed in T5 for ML 2056 and SML 668, respectively, which was adjudged at par with treatment T4. Copper oxychloride (50% WP) was least effective, which showed 61.09% yield loss for ML 2056 and 50.47% yield loss for SML 668 followed by 47.61% for ML 2056 and 44.42% for SML 668 in T3, i.e., propineb (70% WP).

3.4 Field evaluation of different fungicides, bioagents, and neem extract against pod rot of mungbean during the year 2021

During the field evaluation of different fungicides against pod rot of mungbean in the years 2019–2020, trifloxystrobin + tebuconazole (75% WG) and tebuconazole (25% EC) were found to be effective against pod rot disease. Therefore, in the year 2021, these two fungicides were again evaluated against pod rot disease with different concentrations. In addition to these fungicides, two biocontrol agents, i.e., *Trichoderma harzianum* and *Pseudomonas fluorescence*, and one extract, i.e., neem extract, were also evaluated against pod rot disease of mungbean (cv. ML 2056) under field conditions. All the tested fungicides at different doses were found to

10.3389/fpls.2023.1164245

TABLE 2 *In vitro* evaluation of different fungicides against *Fusarium equiseti*.

Systematicity	Fungitoxicants	Percent growth inhibition over a check at different concentrations (µg ml^{-1})								
		5	10	25	50	75	100	200	500	Mean
Non-systemic	Copper oxychloride 50% WP	–	6.07 (14.23)	8.15 (16.39)	12.63 (20.55)	–	18.07 (25.13)	19.15 (25.93)	25.44 (30.27)	14.92 (22.08)
	Propineb 70% WP	–	25.70 (30.42)	30.63 (33.58)	31.56 (34.16)	–	35.44 (36.51)	40.52 (39.51)	49.93 (44.94)	35.63 (35.63)
	Mancozeb 75% WP	–	11.52 (19.57)	14.56 (22.21)	16.78 (24.16)	–	20.07 (26.60)	25.89 (30.56)	27.33 (31.48)	19.36 (25.76)
	Mean		14.43 (21.41)	17.78 (24.05)	2032 (26.29)		24.53 (29.41)	28.52 (31.99)	34.23 (35.56)	
Systemic	Carbendazim 50% WP	53.85 (47.19)	62.18 (52.64)	63.18 (52.63)	67.26 (55.12)	78.15 (62.10)	79.22 (63.13)	82.11 (64.99)	–	69.42 (56.75)
	Propiconazole 25% EC	49.63 (44.77)	53.59 (47.04)	61.04 (51.36)	62.41 (52.17)	71.78 (57.92)	72.85 (58.62)	77.30 (61.58)	–	64.08 (53.35)
	Tebuconazole 25.9% EC	57.30 (49.19)	62.44 (52.20)	68.81 (56.04)	72.37 (58.26)	78.81 (62.58)	79.52 (63.09)	83.51 (66.20)	–	71.83 (58.22)
	Trifloxystrobin + tebuconazole 75% WG	66.07 (54.37)	68.74 (56.01)	71.96 (58.01)	81.70 (64.69)	85.33 (67.50)	88.30 (69.98)	100.00 (89.65)	–	80.30 (65.75)
	Mean	56.71 (48.88)	61.74 (51.82)	66.25 (54.51)	70.93 (57.56)	78.51 (62.53)	79.97 (63.71)	85.73 (70.60)		

Non-systemic
CD (p=0.05)
Fungitoxicants = 1.587
Concentrations = 2.244
Fungitoxicants x Concentrations = NS

Systemic:
CD (p=0.05)
Fungitoxicants = 1.462
Concentrations = 1.934
Fungitoxicants x Concentrations =3.868

TABLE 3 *In vitro* evaluation of different fungicides against *Fusarium chlamydosporum*.

Systematicity	Fungitoxicants	Percent growth inhibition over a check at different concentrations (µg ml^{-1})								
		5	10	25	50	75	100	200	500	Mean
Non-systemic	Copper oxychloride 50% WP	–	4.81 (12.60)	7.56 (15.93)	8.52 (16.94)	–	12.07 (20.32)	13.41 (21.39)	20.22 (26.69)	11.09 (18.99)
	Propineb 70% WP	–	30.52 (33.49)	34.96 (36.22)	41.52 (40.09	–	43.96 (41.51)	51.26 (45.70)	49.11 (44.47)	41.88 (40.25)
	Mancozeb 75% WP	–	12.74 (20.75)	16.44 (23.58)	19.33 (26.05)	–	24.96 (29.92)	39.81 (39.10)	52.33 (46.32)	27.60 (30.95)
	Mean	–	16.02 (22.28)	19.65 (25.24)	23.12 (27.69)	–	27.00 (30.58)	34.83 (35.39)	40.55 (39.16)	–
Systemic	Carbendazim 50% WP	54.19 (47.38)	63.41 (52.76)	67.59 (55.29)	71.00 (57.40)	75.96 (60.62)	79.56 (63.09)	83.33 (65.88)	–	70.72 (57.49
	Propiconazole 25% EC	53.56 (47.02)	62.41 (52.16)	69.22 (56.64)	72.44 (58.32)	77.96 (62.01)	83.33 (65.88)	100.00 (89.65)	–	74.20 (61.67)
	Tebuconazole 25.9% EC	72.44 (58.32)	74.15 (59.42)	79.44 (63.06)	82.22 (65.05)	89.00 (70.60)	100.00 (89.65)	100.00 (89.65)	–	85.32 (70.82)
	Trifloxystrobin + tebuconazole 75% WG	73.78 (59.17)	75.96 (60.63)	80.22 (63.60)	88.30 (69.97)	89.37 (70.94)	100.00 (89.65)	100.00 (89.65)	–	86.80 (71.95)
	Mean	63.49 (52.98)	68.98 (56.24)	74.24 (59.65)	78.49 (62.69)	83.07 (66.04)	90.72 (77.07)	95.83 (83.70)	–	

Non-systemic
CD (p=0.05)
Fungitoxicants = 1.628
Concentrations = 2.302
Fungitoxicants x Concentrations = 3.988

Systemic:
CD (p=0.05)
Fungitoxicants = .846
Concentrations = 1.119
Fungitoxicants x Concentrations =2.239

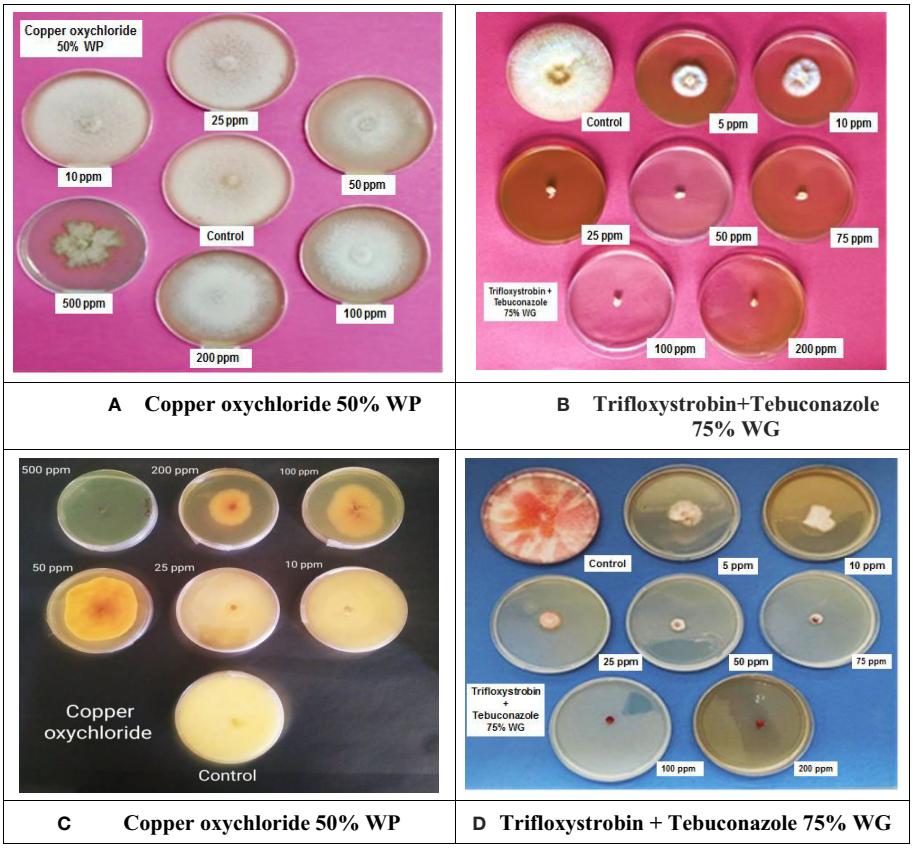

FIGURE 3
In vitro evaluation of non-systemic and systemic fungicides against *Fusarium equiseti* and *Fusarium chlamydosporum*: **(A)** Effectiveness of copper oxychloride 50% WP against *F. equiseti*. **(B)** Effectiveness of trifloxystrobin + tebuconazole 75% against *F. equiseti*. **(C)** Effectiveness of copper oxychloride 50% WP against *F. chlamydosporum*. **(D)** Effectiveness of trifloxystrobin + tebuconazole 75%against *F. chlamydosporum*.

significantly control the pod rot disease (Table 7). Among the tested fungicides, trifloxystrobin + tebuconazole (75% WG) at the rate of 0.09% was found most effective with 93.99% control of pod rot disease over control followed by trifloxystrobin + tebuconazole (75% WG) (91.48% PDC) at the rate 0.07% dose. Tebuconazole (25% EC) at the rate of 0.08% was found least effective among the fungicides with 55.78% disease control. Two biocontrol agents, i.e., *Trichoderma harzianum* at 1.5% and *Pseudomonas fluorescence* at 1.5%, were found less effective against pod rot disease with only 7.28 and 3.55 PDC, respectively, and showed the non-significant results with untreated control. Neem extract at the rate of 5% (2.90 PDC) was also found to be non-significant in pod rot disease control.

TABLE 4 ED_{50} and ED_{90} values of different fungicides against pod rot of mungbean (*Fusarium equiseti*).

Fungicides	ED values (μg ml^{-1})	
	ED_{50}	ED_{90}
Non-systemic fungicides		
Copper oxychloride 50% WP	795.81	1524
Propineb 70% WP	429.22	1166
Mancozeb 75% WP	476.17	963.62
Systemic fungicides		
Carbendazim 50% WP	16.05	189.25
Propiconazole 25% EC	31.60	202.58
Tebuconazole 25.9% EC	3.86	211.88
Trifloxystrobin + tebuconazole 75% WG	2.39	106.16

The yield of mungbean was found to be significantly changed with different fungicide treatments as compared with the untreated control, whereas the yield with biocontrol agents and neem extract was found to be statistically at par with untreated control. Minimum yield loss was supported by trifloxystrobin + tebuconazole (75% WG) (1.09%) at the rate of 0.09% dose followed by trifloxystrobin + tebuconazole (75% WG) (1.88%) at the rate 0.07% dose. While the yield loss with the treatment of trifloxystrobin + tebuconazole (75% WG) (15.22%) with 0.05% dose and tebuconazole (25% EC) (15.94%) at the rate of 0.1% were found statistically at par with each other.

3.5 Evaluations of genotypes for pod rot disease resistance

The data recorded revealed that all 75 genotypes of mungbean differed in their response to pod rot disease. These genotypes were categorized into six groups, i.e., highly resistant, resistant, moderately resistant, moderately susceptible, susceptible, and

10.3389/fpls.2023.1164245

TABLE 5 ED_{50} and ED_{90} values of different fungicides against pod rot of mungbean (*Fusarium chlamydosporum*).

Fungicides	ED values (μg ml^{-1})	
	ED_{50}	ED_{90}
Non-systemic fungicides		
Copper oxychloride 50% WP	962.02	1749.00
Propineb 70% WP	378.57	1252.00
Mancozeb 75% WP	417.39	897.49
Systemic fungicides		
Carbendazim 50% WP	11.80	184.24
Propiconazole 25% EC	18.51	102.59
Tebuconazole 25.9% EC	5.58	59.34
Trifloxystrobin + tebuconazole 75% WG	4.23	54.78

highly susceptible on the basis of disease severity (Table 8). The pod rot incidence of screened genotypes was found to be significantly different and ranged from 15.62% to 95.00% (Table 9). Of the tested genotypes, one genotype ML 2524 was found to exhibit resistant (R) reaction with 15.62% disease incidence and 7.69% disease severity. A total of 41 genotypes were found to be moderately resistant (MR) with disease incidence ranging from 23.37% to 58.39% and disease severity ranging from 11.38% to 24.91%. Twenty-four genotypes showed the moderately susceptible (MS) reaction having disease incidence of 60.52% to 85.19% and disease severity of 25.56% to 44.71% whereas nine genotypes, *viz*., MML 2543, MML 2545, MML 2551, MML 2560, MML 2563, MML 2575, ML 2566, ML 2568, and ML 2569, were found to exhibit susceptible (S) reactions with disease incidence that varied from 83.60% to 95.00% and disease.

4 Discussion

To manage root and stem rot diseases in legumes, it is essential to have a thorough understanding of agronomic practices and soil factors, including soil texture, microbial populations, planting date, cultivation method, preceding crop, fungicide requirements, and fertilizer application (Naseri and Hamadani, 2017a; Naseri et al., 2018). Moreover, the strategic application of fungicides to mitigate newly emerging plant disease has been believed to be a quick and effective control measure (Ahmad et al., 2021). It was concluded from the 2-year field trials of this study that pod rot disease in mungbean can be effectively controlled with the treatment of trifloxystrobin + tebuconazole (75% WG) and tebuconazole (25% EC) as a foliar application. Three applications at 15-day intervals starting from the last week of July countered the disease successfully. The active ingredient in each of these fungicides is tebuconazole, which is categorized as a demethylation inhibitor (DMI) fungicide. Inhibiting the cytochrome P450-dependent enzyme, DMI fungicides affect the manufacture of sterols, which are key components of fungal cell walls (Odds et al., 2003; Patón et al., 2017). Golakiya et al. (2018) reported tebuconazole + trifloxystrobin (73.50%) as the most effective among the six evaluated fungicides against Fusarium associated with the chickpea wilt. In a study conducted by Gabrekiristos and Ayana (2020), five fungicides were tested against the Fusarium wilt of hot pepper and found that Nativo SC 300 (trifloxystrobin + tebuconazole 100:200 g/l) and Twinstar 75 WG (trifloxystrobin + tebuconazole

TABLE 6 Field evaluation of different systemic and non-systemic fungicides against pod rot of mungbean during the years 2019–2020.

S. No.	Fungitoxicant	Dose (%)	ML 2056					SML 668				
			Incidence (%)	Severity (%)	PDC*	Yield (q/acre)	Yield loss (%)	Incidence (%)	Severity (%)	PDC*	Yield (q/acre)	Yield loss (%)
T1	Copper oxychloride (50% WP)	0.3	69.19^{F}	29.17^{B}	25.16	1.79^{A}	61.09	71.42^{C}	29.46^{B}	36.54	2.13^{A}	50.47
T2	Propineb (70% WP)	0.3	62.63^{E}	26.02^{B}	33.25	2.44^{B}	46.96	70.68^{C}	27.98^{B}	39.72	2.47^{B}	42.56
T3	Mancozeb (75% WP)	0.3	66.75^{F}	27.75^{B}	28.82	2.41^{B}	47.61	68.84^{C}	27.05^{B}	41.73	2.39^{B}	44.42
T4	Carbendazim (50%WP)	0.2	32.50^{C}	15.92^{A}	59.16	3.06^{C}	33.48	26.32^{B}	13.64^{A}	70.62	3.09^{C}	27.14
T5	Propiconazole (25% EC)	0.1	38.68^{D}	18.17^{A}	53.39	3.11^{C}	32.39	28.64^{B}	15.67^{A}	66.24	3.13^{C}	27.21
T6	Tebuconazole (25% EC)	0.1	27.00^{B}	13.21^{A}	66.11	3.59^{D}	21.96	24.74^{A}	13.24^{A}	71.48	3.37^{D}	21.63
T7	Trifloxystrobin + tebuconazole (75% WG)	0.07	22.57^{A}	10.94^{A}	71.94	3.66^{D}	20.43	18.36^{AB}	8.28^{A}	82.16	3.57^{D}	16.98
T8	Untreated control	–	79.37^{G}	38.98^{C}		1.66^{A}	63.91	83.28^{D}	46.42^{C}		1.51^{A}	64.88

*Percent disease control.

The values following the same letter are not significantly different according to Duncan's multiple range test.

TABLE 7 Field evaluation of different fungicides, bioagents, and neem extract against pod rot of mungbean during the year 2021.

S. no.	Fungitoxicant	Dose (%)	ML 2056				
			Incidence (%)	Severity (%)	PDC*	Yield (q/acre)	Yield loss (%)
T1	Trifloxystrobin + tebuconazole (75% WG)	0.05	17.12^{E}	8.51^{D}	75.35	3.90^{B}	15.22
T2	Trifloxystrobin + tebuconazole (75% WG)	0.07	8.18^{F}	2.94^{E}	91.48	4.51^{A}	1.88
T3	Trifloxystrobin + tebuconazole (75% WG)	0.09	6.20^{F}	2.08^{E}	93.99	4.55^{A}	1.09
T4	Tebuconazole (25% EC)	0.08	31.31^{C}	15.27^{B}	55.78	3.27^{C}	28.99
T5	Tebuconazole (25% EC)	0.1	24.88^{D}	11.98^{C}	65.33	3.87^{B}	15.94
T6	Tebuconazole (25% EC)	0.3	17.20^{E}	8.36^{D}	75.80	4.10^{AB}	10.87
T7	*Trichoderma harzianum*	1.5	76.65^{B}	32.03^{A}	7.28	1.84^{D}	60.00
T8	*Pseudomonas florescence*	1.5	79.19^{AB}	33.31^{A}	3.55	1.81^{D}	60.58
T9	Neem extract	5	80.04^{AB}	33.54^{A}	2.90	1.69^{D}	63.26
T10	Untreated control	–	82.87^{A}	34.54^{A}	0.00	1.67^{D}	63.77

*Percent disease control.
The values following the same letter are not significantly different according to Duncan's multiple range test.

50:25% w/w) fungicides have the nature of both systemic and contact action and led to 94.0% and 92.3% mycelia growth inhibition, respectively. Flint Max (tebuconazole 50% + trifloxystrobin 25%) was a very effective fungicide with an EC50 value of less than 1 ppm, at inhibiting mycelial growth of *F. proliferatum* causing bulb rot of garlic (Patón et al., 2017), and the results are consistent with earlier research on the efficacy of tebuconazole, the active ingredient in both Nativo and the fungicide evaluated in this study. Marin et al. (2013) determined that the EC50 (the concentration necessary to create 50% inhibition) and EC90 (the concentration required to produce 90% inhibition) of tebuconazole against *F. proliferatum* from wheat were 0.50 and 10.0 ppm, respectively. Ivić et al. (2011) determined the EC50 for tebuconazole to be between 0.85 and 2.57 ppm for *F. graminearum*, 0.85 and 1.58 ppm for *F. avenaceum*, and 0.22 and 0.85 ppm for *F. verticillioides*. *In vitro* testing by Jain et al. (2015) revealed that tebuconazole was effective against Fusarium associated with tomato, with IC50 values of 19.27 g ml^{-1} (the dose necessary to achieve 50% inhibition). DMI fungicides, such as tebuconazole, have been demonstrated to be more effective against Fusarium species than other fungicides. Based on EC50 and EC90 values, the triazole chemical group, which includes prothioconazole, cyproconazole, and tebuconazole, is more effective against Fusarium spp. than strobilurin fungicides (such as azoxystrobin and kresoxim-methyl) (Patron et al., 2016). Fusarium species are sensitive to fungicides belonging to the DMI group, such as tebuconazole, but innately resistant to complex III respiration inhibitors (QoI) such as trifloxystrobin, according to Dubos et al. (2011); Dubos et al. (2013) and Pasquali et al. (2013). Given these data, it appears that tebuconazole is responsible for the inhibitory effects seen in this investigation.

Prior to this study, there were no reports of sources of high pod rot disease resistance. The evaluation of mungbean germplasm for resistance to the pod rot pathogen allowed us to find one highly

TABLE 8 Reaction(s) of mungbean genotypes against pod rot disease.

S. no.	Disease severity (%)	Reaction	Genotypes
1	0	Highly resistant	–
2	0–10	Resistant	ML 2524
3	10.1–25	Moderately resistant	MML 2561, MML 2571, SML 2048, SML 2050, SML 2051, SML 2052, SML 2053, SML 2054, SML 2055, SML 2059, SML 2060, SML 2062, SML 2063, SML 2065, SML 2066, SML 2067, SML 2068, SML 2069, SML 2070, SML 2071, SML 2073, SML 1839, SML 2015, SML 2016, ML 2423, ML 2459, ML 2460, ML 2479, ML 2480, ML 2481, ML 2482, ML 2483, ML 2498, ML 2500, ML 2506, ML 2507, ML 2525, MML 2566, MML 2567, MML 2569, MML 2580
4	25.1–45	Moderately susceptible	MML 2539, MML 2544, MML 2546, MML 2549, MML 2550, MML 2562, MML 2565, MML 2568, MML 2570, MML 2572, MML 2573, MML 2574, MML 2577, MML 2578, MML 2579, SML 2049, SML 2056, SML 2057, SML 2058, SML 2061, SML 2064, ML 2567, ML 2576, MML 2576
5	45.1–70	Susceptible	MML 2543, MML 2545, MML 2551, MML 2560, MML 2563, MML 2575, ML 2566, ML 2568, ML 2569
6	More than 70.1	Highly susceptible	–

10.3389/fpls.2023.1164245

TABLE 9 Screening of mungbean interspecific derivates and mutant genotypes against pod rot disease.

S. no.	Genotypes	Incidence (%)		Pooled mean (%)	Severity (%)		Pooled mean (%)	Reaction
		2019	2020		2019	2020		
1	MML 2539	87.73	74.76	81.25	43.30	31.55	37.43	MS
2	MML 2543	80.73	86.46	83.60	40.55	49.68	45.12	S
3	MML 2544	76.05	67.48	71.76	38.80	28.05	33.43	MS
4	MML 2545	94.60	83.85	89.23	57.33	47.65	52.49	S
5	MML 2546	83.81	67.57	75.69	41.70	28.69	35.20	MS
6	MML 2549	91.22	73.48	82.35	51.09	30.93	41.01	MS
7	MML 2550	96.88	72.18	84.53	54.26	30.33	42.30	MS
8	MML 2551	100.00	87.43	93.72	55.56	43.44	49.50	S
9	MML 2560	79.35	97.83	88.59	42.02	54.80	48.41	S
10	MML 2561	51.40	40.00	45.70	22.38	18.52	20.45	MR
11	MML 2562	89.38	79.63	84.50	47.45	41.62	44.54	MS
12	MML 2563	88.32	83.41	85.86	49.95	42.43	46.19	S
13	MML 2565	95.45	72.81	84.13	59.12	30.29	44.71	MS
14	MML 2568	91.18	66.86	79.02	51.37	28.36	39.87	MS
15	MML 2570	91.25	68.46	79.86	50.70	28.86	39.78	MS
16	MML 2571	43.26	51.94	47.60	19.50	22.09	20.80	MR
17	MML 2572	85.29	67.71	76.50	47.93	28.22	38.08	MS
18	MML 2573	82.45	57.54	70.00	41.71	24.43	33.07	MS
19	MML 2574	60.91	66.03	63.47	32.82	27.28	30.05	MS
20	MML 2575	87.87	82.82	85.34	49.26	40.96	45.11	S
21	MML 2577	77.42	80.95	79.18	39.37	42.59	40.98	MS
22	MML 2578	66.28	74.54	70.41	36.17	31.44	33.81	MS
23	MML 2579	75.59	78.41	77.00	38.90	32.72	35.81	MS
24	SML 2048	60.33	54.26	57.30	25.67	23.80	24.73	MR
25	SML 2049	66.48	58.48	62.48	33.69	24.58	29.14	MS
26	SML 2050	51.64	51.41	51.53	22.20	22.45	22.32	MR
27	SML 2051	61.13	51.45	56.29	25.98	22.13	24.05	MR
28	SML 2052	56.25	39.51	47.88	23.78	18.01	20.89	MR
29	SML 2053	65.13	51.30	58.21	27.44	22.24	24.84	MR
30	SML 2054	57.81	44.79	51.30	24.22	19.14	21.68	MR
31	SML 2055	52.88	51.03	51.96	22.49	22.40	22.44	MR
32	SML 2056	82.33	70.99	76.66	40.13	30.33	35.23	MS
33	SML 2057	74.71	58.00	66.36	40.20	25.00	32.60	MS
34	SML 2058	61.77	59.28	60.52	26.11	25.01	25.56	MS
35	SML 2059	56.86	53.68	55.27	24.39	21.13	22.76	MR
36	SML 2060	48.29	46.41	47.35	20.97	20.08	20.53	MR
37	SML 2061	69.54	59.48	64.51	28.79	25.00	26.90	MS
38	SML 2062	48.48	50.82	49.65	21.22	22.29	21.75	MR

(Continued)

10.3389/fpls.2023.1164245

TABLE 9 Continued

S. no.	Genotypes	Incidence (%)		Pooled mean (%)	Severity (%)		Pooled mean (%)	Reaction
		2019	2020		2019	2020		
39	SML 2063	55.13	59.35	57.24	24.06	25.75	24.91	MR
40	SML 2064	75.71	47.87	61.79	39.06	20.70	29.88	MS
41	SML 2065	67.20	47.82	57.51	28.14	20.88	24.51	MR
42	SML 2066	52.27	52.03	52.15	22.98	22.52	22.75	MR
43	SML 2067	44.73	42.52	43.63	19.67	19.35	19.51	MR
44	SML 2068	40.53	44.12	42.33	18.40	18.93	18.67	MR
45	SML 2069	37.81	44.47	41.14	18.62	19.46	19.04	MR
46	SML 2070	20.10	26.64	23.37	9.80	12.96	11.38	MR
47	SML 2071	41.25	25.19	33.22	18.83	12.33	15.58	MR
48	SML 2073	40.57	31.64	36.10	18.60	15.68	17.14	MR
49	SML 1839	55.00	53.85	54.42	23.81	23.01	23.41	MR
50	SML 2015	58.14	46.81	52.47	24.85	20.00	22.42	MR
51	SML 2016	62.22	51.85	57.04	25.71	22.45	24.08	MR
52	ML 2423	50.00	45.71	47.86	21.37	19.88	20.62	MR
53	ML 2459	44.74	50.00	47.37	19.71	21.93	20.82	MR
54	ML 2460	42.86	27.27	35.06	18.71	13.37	16.04	MR
55	ML 2479	43.94	41.03	42.48	19.10	17.53	18.32	MR
56	ML 2480	22.64	40.48	31.56	11.10	17.91	14.50	MR
57	ML 2481	40.35	36.36	38.36	17.93	17.91	17.92	MR
58	ML 2482	43.94	40.00	41.97	19.02	19.14	19.08	MR
59	ML 2483	40.30	50.00	45.15	17.91	21.37	19.64	MR
60	ML 2498	46.34	55.77	51.06	19.97	24.25	22.11	MR
61	ML 2500	34.43	30.23	32.33	16.47	14.53	15.50	MR
62	ML 2506	43.14	58.33	50.74	18.84	25.47	22.16	MR
63	ML 2507	42.31	37.14	39.73	18.08	17.77	17.93	MR
64	ML 2524	7.55	23.68	15.62	3.77	11.61	7.69	R
65	ML 2525	24.14	25.71	24.93	11.89	12.79	12.34	MR
66	ML 2566	88.24	85.00	86.62	53.80	50.30	52.05	S
67	ML 2567	70.37	100.00	85.19	28.96	59.88	44.42	MS
68	ML 2568	90.00	100.00	95.00	50.85	56.50	53.67	S
69	ML 2569	80.65	85.19	82.92	45.05	49.53	47.29	S
70	ML 2576	70.45	87.10	78.78	29.85	55.83	42.84	MS
71	MML 2566	37.50	44.00	40.75	18.38	19.30	18.84	MR
72	MML 2567	35.59	46.88	41.23	17.03	20.20	18.62	MR
73	MML 2569	53.85	40.00	46.92	23.51	19.05	21.28	MR
74	MML 2576	100.00	63.33	81.67	54.35	26.39	40.37	MS
75	MML 2580	64.15	52.63	58.39	26.62	23.19	24.90	MR

resistant genotype and 41 moderately resistant genotypes. In contrast to susceptible genotypes, these lines exhibited only moderate resistance, as evidenced by reduced symptoms and slower disease progression. Breeding programs may be able to increase the resistance levels of already existing cultivars with advantageous agronomic qualities by incorporating the resistance levels discovered in this study. This knowledge of resistance sources is advantageous for selecting germplasm for such programs (Larsen and Porter, 2010).

5 Conclusion

Mungbean is an important pulse crop that is widely grown for food, green manuring, and intercropping. It is of high economic importance due to its various uses and benefits. However, mungbean crops are susceptible to pod rot disease, which can cause significant yield losses if not managed properly. Pod rot disease can develop quickly under favorable weather conditions, especially in fields with a long history of mungbean cultivation, typically over 4–5 years. This disease can be devastating to crops and cause significant economic losses for farmers, and hence, chemical control and resistant varieties are valuable options for managing this devastating problem effectively. In conclusion, the management options identified in this study provide an effective means of managing pod rot disease in mungbean crops during recent outbreaks. Moreover, the identification of resistant sources through breeding programs can offer a sustainable long-term solution for managing the disease. Therefore, implementing these management options can provide an immediate solution to control the disease and pave the way for future disease management efforts.

Data availability statement

The datasets presented in this study can be found in online repositories. The names of the repository/repositories and accession number(s) can be found in the article/supplementary material.

Author contributions

HB, AmS: conceptualization, methodology, investigation, writing—original draft preparation. AsS, A, KK: methodology, software, visualization. RT, RK: reviewing and editing. AK, ML: supervision, project administration. All authors contributed to the article and approved the submitted version.

Acknowledgments

We would like to thank the Head of Department, Plant Pathology, Punjab Agricultural University, Ludhiana, for providing the necessary facilities.

Conflict of interest

The authors declare that the research was conducted in the absence of any commercial or financial relationships that could be construed as a potential conflict of interest.

Publisher's note

References

Ahmad, S., Yousaf, M., Anjum, R., Raza, W., Ali, Y., and Rehman, M. A. (2021). Evaluation of fungicides against *Fusarium oxysporum* f. sp. *lycopersici* the cause of fusarium wilt of tomato. *J. Pl. Environ.* 3 (2), 125–135. doi: 10.33687/jpe.003.02.3909

Anonymous (2019). *Package of practices for vegetable crops* (Ludhiana, Punjab: Punjab Agricultural University).

Booth, C. (1971). *The genus fusarium* (Kew Surrey, England: Commonwealth Mycological Institute), 14–233.

Buttar, H. S., Singh, A., Sirari, A., and Sharma, S. (2023). Pod rot of mungbean in Punjab, India: First record of association of *Fusarium equiseti and Fusarium chlamydosporum*. *Crop Prot.* 168, 106230. doi: 10.1016/j.cropro.2023.106230

Carvalho, D. D. C., de Mello, S. C. M., Martins, I., and Lobon, M. (2015). Biological control of fusarium wilt on common beans by in-furrow application of *Trichoderma harzianum*. trop. *Plant Pathol.* 40, 375–381. doi: 10.1007/s40858-015-0057-1

Chakraborty, S., Tiedemann, A. V., and Teng, P. S. (2000). Climate change: potential impact on plant diseases. *Environ. Pollut.* 108, 317–326. doi: 10.1016/S0269-7491(99)00210-9

Doyle, J. J., and Doyle, J. L. (1987). A rapid DNA isolation procedure for small amounts of fresh leaf tissue. *Phytochem. Bull.* 19, 11–15.

Dubos, T., Pasquali, M., Pogoda, F., Casanova, A., and Hoffmann, L. (2013). Differences between the succinate dehydrogenase sequences of isopyrazam sensitive *Zymoseptoria tritici* and insensitive *Fusarium graminearum* strains. *Pestic Biochem. Physio.* 105 (1), 28–35. doi: 10.1016/j.pestbp.2012.11.004

Dubos, T., Pasquali, M., Pogoda, F., Hoffmann, L., and Beyer, M. (2011). Evidence for natural resistance towards trifloxystrobin in *Fusarium graminearum*. *Eur. J. Plant Pathol.* 130, 239–248. doi: 10.1007/s10658-011-9749-7

El-Hassan, S. A., Gowen, S. R., and Pembroke, B. (2013). Use of trichoderma hamatum for biocontrol of lentil vascular wilt disease: efficacy, mechanisms of interaction and future prospects. *J. Plant Prot. Res.* 53, 12–26. doi: 10.2478/jppr-2013-0002

Gabrekiristos, E., and Ayana, G. (2020). *In Vitro* Evaluation of some fungicides against *Fusarium oxysporum* the causal of wilt disease of hot pepper *(Capsicum annum* l.) in Ethiopia. *Adv. Crop Sci. Tech* 8, 443. doi: 10.35248/2329-8863.20.8.443

Golakiya, B. B., Bhimani, M. D., and Akbar, L. F. (2018). Efficacy of different fungicides for the management of chickpea wilt *(Fusarium oxysporum* f. sp. *ciceri*). *Int. J. Chem. Stud.* 6 (2), 199–205. doi: 10.13140/RG.2.2.32521.88160

Ivić, D., Sever, Z., and Kuzmanovska, B. (2011). *In vitro* Sensitivity of *Fusarium graminearum*, f. avenaceum and *F. verticillioides* to carbendazim, tebuconazole,

flutriafol, metconazole and prochloraz. *Pestic Fitomed* 26 (1), 35–42. doi: 10.2298/PIF1101035I

Jain, S., Singh, A., Kaur, Y., and Sekhon, P. S. (2015). Comparative performance of tomato seed treatments against major soil-borne fungi inciting damping-off disease and their effect on seedling vigour. *Pl. Dis. Res.* 30 (2), 117–122.

Kaur, L., Singh, P., and Sirari, A. (2011). Biplot analysis for locating multiple disease resistant diversity in mungbean germplasm. *Dis. Res.* 26, 55–60.

Larsen, R. C., and Porter, L. D. (2010). Identification of noval sources of resistance to pea enation mosaic virus in chickpea germplasm. *Plant Pathol.* 59, 42–47. doi: 10.1111/j.1365-3059.2009.02198.x

Leslie, J. F., and Summerell, B. A. (2006). *The fusarium laboratory manual* (USA: Blackwell Publishing), 22–25.

Marin, P., de-Ory, A., Cruz, A., Magan, N., and González-Jaen, M. T. (2013). Potential effects of environmental conditions on the efficiency of the antifungal tebuconazole controlling *Fusarium verticillioides* and *Fusarium proliferatum* growth rate and fumonisin biosynthesis. *Int. J. Food Microbiol.* 165 (3), 251–258. doi: 10.1016/j.ijfoodmicro.2013.05.022

Nadeem, M. A., Ahmad, R., and Ahmad, M. S. (2004). Effect of seed inoculation and different fertilizer levels on the growth and yield of mungbean *(Vigna radiata* l.). *J. Agron.* 3, 40–42. doi: 10.3923/ja.2004.40.42

Nair, M. R., Pandey, A. K., War, A., Hanumantharao, B., Shwe, T., Alam, A. K. M. M., et al. (2019). Biotic and abiotic constraints in mungbean production-progress in genetic improvement. *Front. Plant Sci.* 10, 1340. doi: 10.3389/fpls.2019.01340

Nair, R. M., Schalfleitner, R., Kenyon, L., Srinivasan, R., Easdown, W., and Ebert, A. (2012). Genetic improvement of mungbean. *Sabrao J. Breed Gen.* 44, 177–190.

Naseri, B. (2019). Legume root rot control through soil management for sustainable agriculture. *Sustain. Manage. Soil Environ.*, 217–258. doi: 10.1007/978-981-13-8832-3_7

Naseri, B., and Hamadani, S. A. (2017a). Characteristic agro-ecological features of soil populations of bean root rot pathogens. *Rhizosphere* 3, 203–208. doi: 10.1016/j.rhisph.2017.05.005

Naseri, B., and Hemmati, R. (2017b). Bean root rot management: recommendations based on an integrated approach for plant disease control. *Rhizosphere* 4, 48–53. doi: 10.1016/j.rhisph.2017.07.001;

Naseri, B., Veisi, M., and Khaledi, N. (2018). Towards a better understanding of agronomic and soil basis for possible charcoal root rot control and production improvement in bean. *Arch. Phytopathol. Plant Prot.* 51 (7-8), 349–358.

Nene, Y. L., and Thapliyal, P. N. (1993). *Fungicides in plant disease control* (New Delhi, India: Oxford and IBH publishing Co. Pvt. Ltd.), 531.

Odds, F. C., Brown, A. J. P., and Gow, N. A. R. (2003). Antifungal agents: mechanisms of action. *Trends Microbiol.* 11, 272–279. doi: 10.1016/S0966-842X(03)00117-3

O'Donnell, K., Kistler, H. C., Cigelnik, E., and Ploetz, R. C. (1998). Multiple evolutionary origins of the fungus causing Panama disease of banana: concordant evidence from nuclear and mitochondrial gene genealogies. *Proc. Natl. Acad. Sci.* 95, 2044–2049. doi: 10.1073/pnas.95.5.2044

Pandey, A. K., Burlakoti, R. R., Kenyon, L., and Nair, R. M. (2018). Perspectives and challenges for sustainable management of fungal diseases of mungbean *[Vigna radiata* (L.) r. wilczek var. *radiata]*: a review. *Front. Environ. Sci.* 6, 53. doi: 10.3389/fenvs.2018.00053

Pasquali, M., Spanu, F., Scherm, B., Balmas, V., Hoffmann, L., Hammond-Kosack, K. E., et al. (2013). FcStuA from *Fusarium culmorum* controls wheat foot and root rot in a toxin dispensable manner. *PloS One* 8 (2), e57429. doi: 10.1371/journal.pone.0057429

Pataczek, L., Zahir, Z. A., Ahmad, M., Rani, S., Nair, R., Schafleitner, R., et al. (2018). Beans with benefits–the role of mungbean *(Vigna radiata)* in a changing environment. *Am. J. Pl Sci.* 9, 1577–1600. doi: 10.4236/ajps.2018.97115

Patón, L. G., Marrero, M., and Llamas, D. P. (2017). *In vitro* And field efficacy of three fungicides against fusarium bulb rot of garlic. *Eur. J. Plant Pathol.* 148 (2), 321–328. doi: 10.1007/s10658-016-1091-7

RStudio Team. (2021). *RStudio: Integrated Development for R.* RStudio, PBC, Boston, MA. Available at: http://www.rstudio.com/.

Rubiales, D., Fondevilla, S., Chen, W., Gentzbittel, L., Higgins, T. J., Castillejo, M. A., et al. (2015). Achievements and challenges in legume breeding for pest and disease resistance. *Crit. Rev. Plant Sci.* 34 (1-3), 195–236. doi: 10.1080/07352689.2014.898445

Sharma, R., Duveiller, E., and Ortiz-Ferrara, G. (2007). Progress and challenge towards reducing wheat spot blotch threat in the Eastern gangetic plains of south Asia: is climate change already taking its toll? *Field Crops Res.* 103, 109–118. doi: 10.1016/j.fcr.2007.05.004

Singh, H. (2021). *Etiology and management of pod rot of mungbean [Vigna radiata l.) wilczek]* (Ludhiana: Dissertation, Punjab Agricultural University).

Tutte, J. (1969). *Plant pathological methods. fungi and bacteria* Vol. 229 (U.S.A: Burgess publishing company).

Vincent, J. M. (1947). Distortion of fungal hyphae in the presence of certain inhibitors. *Nature* 159, 850. doi: 10.1038/159850b0

Wheeler, B. E. (1969). *An introduction to plant diseases* (London, UK: John Wiley and Sons Ltd.).

Wollenweber, H. W., and Reinking, O. A. (1935). *Die fusarien, ihre beschreibung, schadwirkung und bekimpfung* (Berlin: Paul Parey).

Yadav, D. L., Jaisani, P., and Pandey, R. N. (2014a). Identification of sources of resistant in mungbean genotypes and influence of fungicidal application to powdery mildew epidemics. *Int. J. Curr. Microbiol. Appl. Sci.* 3, 513–519.

frontiers | Frontiers in Plant Science

TYPE Original Research
PUBLISHED 06 June 2023
DOI 10.3389/fpls.2023.1129714

OPEN ACCESS

EDITED BY
Youxiong Que,
Fujian Agriculture and Forestry University, China

REVIEWED BY
Malkhan Singh Gurjar,
Indian Agricultural Research Institute (ICAR), India
Hira Kamal,
National Institute for Biotechnology and Genetic Engineering, Pakistan

*CORRESPONDENCE
Rahul Kumar Tiwari
rahul.tiwari@icar.gov.in
Milan Kumar Lal
milan2925@gmail.com
Ravinder Kumar
chauhanravinder97@gmail.com

RECEIVED 22 December 2022
ACCEPTED 08 May 2023
PUBLISHED 06 June 2023

CITATION
Lal P, Tiwari RK, Kumar A, Altaf MA, Alsahli AA, Lal MK and Kumar R (2023) Bibliometric analysis of real-time PCR-based pathogen detection in plant protection research: a comprehensive study. *Front. Plant Sci.* 14:1129714. doi: 10.3389/fpls.2023.1129714

Bibliometric analysis of real-time PCR-based pathogen detection in plant protection research: a comprehensive study

Priyanka Lal[1], Rahul Kumar Tiwari[2*], Awadhesh Kumar[3], Muhammad Ahsan Altaf[4], Abdulaziz Abdullah Alsahli[5], Milan Kumar Lal[2*] and Ravinder Kumar[2*]

[1]Department of Agricultural Economics and Extension, School of Agriculture, Lovely Professional University, Phagwara, India, [2]ICAR-Central Potato Research Institute, Shimla, Himachal Pradesh, India, [3]ICAR-National Rice Research Institute, Cuttack, Odisha, India, [4]School of Horticulture, Hainan University, Haikou, China, [5]Botany and Microbiology Department, Faculty of Science, King Saud University, Riyadh, Saudi Arabia

Introduction: The discovery of RT-PCR-based pathogen detection and gene expression analysis has had a transformative impact on the field of plant protection. This study aims to analyze the global research conducted between 2001 and 2021, focusing on the utilization of RT-PCR techniques for diagnostic assays and gene expression level studies. By retrieving data from the 'Dimensions' database and employing bibliometric visualization software, this analysis provides insights into the major publishing journals, institutions involved, leading journals, influential authors, most cited articles, and common keywords.

Methods: The 'Dimensions' database was utilized to retrieve relevant literature on RT-PCR-based pathogen detection. Fourteen distinct search queries were employed, and the resulting dataset was analyzed for trends in scholarly publications over time. The bibliometric visualization software facilitated the identification of major publishing journals, institutions, leading journals, influential authors, most cited articles, and common keywords. The study's search query was based on the conjunction 'AND', ensuring a comprehensive analysis of the literature.

Results: The analysis revealed a significant increase in the number of scholarly publications on RT-PCR-based pathogen detection over the years, indicating a growing interest and investment in research within the field. This finding emphasizes the importance of ongoing investigation and development, highlighting the potential for further advancements in knowledge and understanding. In terms of publishing journals, Plos One emerged as the leading journal, closely followed by BMC Genomics and Phytopathology. Among the highly cited journals were the European Journal of Plant Pathology, BMC Genomics, and Fungal Genetics and Biology. The publications with the highest number of citations and publications were associated with the United Nations and China. Furthermore, a network visualization map of co-authorship analysis provided intriguing insights into the collaborative nature of

the research. Out of 2,636 authors analyzed, 50 surpassed the level threshold, suggesting active collaboration among researchers in the field.

Discussion: Overall, this bibliometric analysis demonstrates that the research on RT-PCR-based pathogen detection is thriving. However, there is a need for further strengthening using modern diagnostic tools and promoting collaboration among well-equipped laboratories. The findings underscore the significance of RT-PCR-based pathogen detection in plant protection and highlight the potential for continued advancements in this field. Continued research and collaboration are vital for enhancing knowledge, developing innovative diagnostic tools, and effectively protecting plants from pathogens.

KEYWORDS

diagnostic, fungi, bibliometric, on-site detection, infection, PCR

1 Introduction

The technology to visualize polymerase-chain-reaction (PCR) products in real time in an ongoing reaction has revolutionized the field of plant pathogen diagnostics (Donoso and Valenzuela, 2018). During the last two decades, the utilization of real-time PCR techniques has dramatically increased and has been extensively popularized among various stakeholders in plant and animal sciences (Buja et al., 2021). Real-time PCR differs from conventional PCR in that the amplified PCR product is measured at every cycle of the PCR process. In actuality, a fluorochrome included within the freshly generated PCR result emits light that is captured by a video camera (Kralik and Ricchi, 2017). Real-time PCR thus enables the amplification to be followed in real time during the exponential phase of the run, enabling precise estimation of the starting material amount. In contrast to end-point PCR methods, the result is not dependent on the reaction's saturation plateau, which results in erroneous quantification (Kainz, 2000). Real-time PCR has a variety of advantages over other well-known laboratory procedures, making it the method of choice for several sorts of research. It enables the quick, accurate, and extremely sensitive detection of a specific nucleic acid target as compared with other currently available approaches (Kumar et al., 2017; Kumar et al., 2021). Additionally, it allows for the initial target's absolute quantification. Real-time PCR's dependability has never been questioned to this point. Additionally, real-time amplification recording saves time and effort by avoiding the need to collect samples at various stages of the PCR experiment. Additionally, some machines can handle queuing plates for up to 24 h straight while processing 384-well plates (Gachon et al., 2004), which may be an advantage for high-throughput research or if quick sample processing is needed (Kumar Tiwari et al., 2019; Kumar et al., 2020; Kumar et al., 2022).

When just a tiny percentage of the sample contains the mutation, real-time PCR provides for quantitative genotyping, detection of single-nucleotide polymorphisms, allelic discrimination, and genetic variations (Zhou et al., 2001; Morlan et al., 2009). The limitations of traditional PCR methods for live systems have become apparent, and there is an increasing need for more advanced techniques. As a result, the use of multiplex PCR methods has become increasingly important in recent years. These techniques involve the use of coupled probes and primers, which are targeted to specific sequences that are relevant to plant/microbe relationships. This approach enables the simultaneous amplification of multiple target sequences in a single reaction, allowing for the efficient and accurate detection of multiple organisms or gene variants. Overall, the use of multiplex PCR methods represents an important advance in the study of live systems and has the potential to provide valuable insights into the dynamics of plant/microbe interactions (Elnifro et al., 2000; Palka-Santini et al., 2009). The development of bioscience over the past century has aided in a thorough understanding of information pertaining to the network of diverse gene modules that interact and carry out integrated cellular function in a coordinated but somewhat isolated manner, or the molecular mechanism of phenotypic expression of genotype (Costanzo et al., 2019). Our understanding of the intricate connections between enzymes, signaling molecules, and numerous small molecules remains incomplete, and a considerable portion of the genome's functionality remains a mystery. To comprehensively understand how metabolism is regulated, we need to gain more insight into gene expression, DNA recognition by proteins, transcription factors, and the mechanisms of action of various drugs and small molecules. Such knowledge is crucial for developing effective strategies to manipulate metabolic processes to improve human health and combat diseases. As research continues in these areas, we can expect to uncover new insights into the complex networks governing cellular metabolism (Bai et al., 2013). The link between ecologically influenced or disease-related phenotypes and cellular expression patterns has been extensively studied using gene expression profiles. In-depth knowledge of the biology of plant/microbe interactions, particularly concerning the ecology, etiology, and epidemiology of plant pathogenic microorganisms, is being provided by PCR-based detection technologies using species-specific primers (Hariharan and Prasannath, 2021).

Since the earliest study by Böhm et al. (1999), the number of real-time PCR tests designed to measure the extent of plant infection by a pathogen has increased (Böhm et al., 1999). The majority of them rely on two distinct plant and pathogen DNA sequences being relatively quantified. Compared with conventional protocols based on symptom recording or conidiophore or colony counts, they are quicker, more precise, and more sensitive. Most importantly, they can be applied to almost all pathosystems. Due to these factors, they are frequently utilized for both practical and field-based disease diagnosis (Liu et al., 2019). These assays have been extensively used in the field of plant pathology due to their high sensitivity, specificity, and rapid detection capabilities. They are particularly useful for detecting low-level infections and for identifying new or emerging pathogens that can cause devastating crop losses. The application of real-time PCR-based assays has revolutionized the diagnosis and management of plant diseases, enabling growers to respond to outbreaks and implement effective control measures quickly (Mirmajlessi et al., 2015; Londoño et al., 2016; Tiwari et al., 2020a; Tiwari et al., 2020b). Furthermore, real-time quantitative PCR has emerged as the preferred technology for determining food adulteration or contamination. Compared with ELISA, PCR tests are simpler to create because they do not need to be developed with particular antibodies. Because DNA is more thermo-stable than proteins, PCR tests offer greater sensitivity and are more suited for the detection of undesirable dietary constituents in highly processed foods. For instance, a real-time PCR test of cereal genes can be used to control the absence of gluten in infant food (Sandberg et al., 2003). Real-time quantitative PCR has also been demonstrated to be an excellent method for detecting adulteration of durum wheat pasta with common wheat (*Triticum aestivum*) (Terzi et al., 2003).

The validation of data produced from microarray investigations is one of the fastest-growing uses of real-time PCR (Deepak et al., 2007). The validity of microarray experiments can occasionally be put into question. Cross-hybridization between cDNA representatives of gene family members on cDNA-based chips may produce inaccurate results since plants exhibit a large number of multigene families (Palka-Santini et al., 2009). However, compared with real-time PCR, which is frequently restricted to fewer genes, microarray assays can analyze thousands of genes in a single step. Because real-time PCR devices can detect only a finite number of fluorophores and light spectra, only a few genes can be detected in a single multiplex PCR run. Real-time PCR necessitates the construction of individual oligonucleotides for each gene to be analyzed. Consequently, a common approach is to identify a small number of potentially relevant genes using microarray tests and then to confirm those candidates using real-time RT-PCR analysis (Kumar et al., 2020).

Through a quantitative examination of patterns in the body of scientific literature, bibliometrics enables the identification of new trends and knowledge structures in the research subject (Fan et al., 2020; Lin et al., 2020; Akintunde et al., 2021; Dmytriw et al., 2021). Based on published studies on statistical data on plant pathogen detection, one may comprehend the general global picture, including the number of such studies, the level of research capability in various nations, the major research institutions, the top journals publishing such studies, and other factors (Tang et al., 2022). To develop a comprehensive scientific research strategy, it is crucial to understand the current state of research, key areas of focus, and significant gaps in knowledge. In this context, a bibliometric analysis can provide an accurate, validated, and systematic overview of developments in plant-based pathogen detection technologies. This analysis can help identify the most recent detection techniques and their efficacy and pinpoint research boundaries, topic trends, and innovative collaborations between scientists at various universities. By conducting this analysis, we can gain insights into the current state of research in this area, identify knowledge gaps, and develop strategies to address them. Overall, bibliometric analysis is a powerful tool for understanding the research landscape, which is essential for developing a focused and effective scientific research strategy.

2 Material and methods

We acquired pertinent "Dimensions" data for the study using several search engines. Dimensions offer a diverse database of research outcomes. The platform enables stakeholders to get data and construct concepts simply. Researchers are now using bibliometric methods to track and analyze the impact of the pandemic on various scientific disciplines and to identify emerging research areas related to COVID-19. This approach has helped to inform public health policies and guide research priorities in the fight against the pandemic. Overall, the COVID-19 crisis has highlighted the importance of real-time bibliometric studies in providing timely and relevant insights into the rapidly evolving research landscape (Hook et al., 2021). Dimensions enables scholars to search full-text data for various years and scholarly works like pre-prints, articles, chapters, conferences, monographs, and edited books. This expanded data collection for examination opens up new research opportunities. Machine learning techniques have become increasingly popular in constructing links between items in large datasets, enabling researchers to identify patterns and relationships that would be difficult to detect manually. Per-object categorizations and person and institution disambiguation provide further context, improving the accuracy and reliability of results. These tools allow researchers to extract valuable insights from complex datasets, revealing hidden connections and trends that may have been overlooked in traditional analysis methods, ultimately enabling more informed decisions based on data-driven insights. The detailed flow chart of the steps followed in the study is depicted in Figure 1.

2.1 Database selection and search query

In this investigation, the Dimensions database provides details on the authors' names, title of the article, author's affiliation, etc., making it appropriate for bibliometric research. The data extracted possess numerous analytical functions, including citation and subject analysis. There were no restrictions on language, and the data extracted were in English as the search query required an English title and abstract, allowing researchers to authenticate the substance of non-English documents by title/abstract content. A correct search

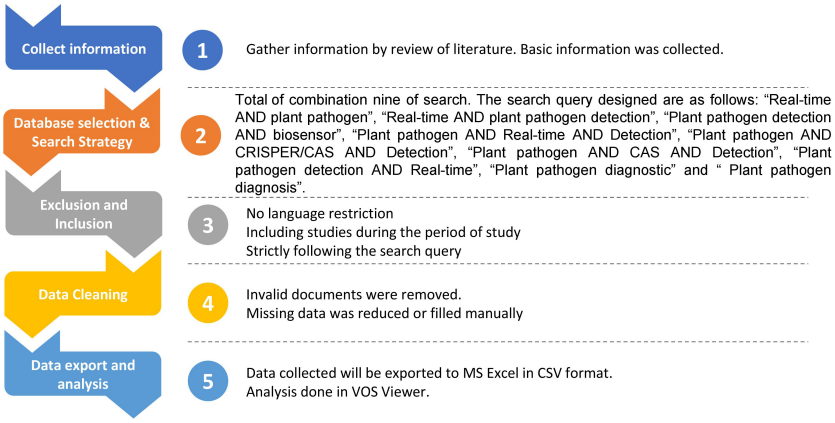

FIGURE 1
Flow chart of bibliometric analysis.

query is an essential component of a bibliometric study in order to obtain high-quality and dependable findings. To form the query, the initial idea was formed after reading scientific papers and identifying research gaps. The study's search query was based on the conjunction "AND." A total of 14 combinations of search queries were used in order to arrive at the final data. The search queries designed are as follows: "Real-time AND plant pathogen," "Real-time PCR and plant pathogen detection," "Cycle threshold AND plant pathogen," "RT-RPA and plant pathogen," "Lateral Flow devices AND plant pathogen," "LAMP-based detection," "Real-time AND plant pathogen detection," "Plant pathogen detection AND biosensor," "Plant pathogen AND Real-time AND Detection," "Plant pathogen AND CRISPER/CAS AND Detection," "Plant pathogen AND CAS AND Detection," "Plant pathogen detection AND Real-time," "Plant pathogen diagnostic," and "Plant pathogen diagnosis." Later the data derived were merged.

2.2 Document exclusion and inclusion

The data were extracted strictly according to the search query because any departure could result in erroneous results. The Dimensions database provides articles in several categories such as articles, books, notes, and pre-prints. We included only research articles and left out the rest of the categories. The study period was limited to the last 20 years (2001–2022). The data were collected in a single day to eliminate ambiguity in the results caused by the daily addition of documents. Because the search query was in English, all of the documents were in the English literature.

2.3 Data extraction and analysis

The data were obtained in the form of an MS Excel file in CSV format for further research. The Excel software was used for tabular analysis, and the VOSviewer software was used for map visualization (van Eck and Waltman, 2011). The citation value can be utilized for analysis in order to assess the scientific contribution and influence of publications. The "connection strength" metric derived from visualization maps was used to assess international research collaboration among participating countries. The strength of any two countries' connections is a measure of the degree of their scientific collaboration. The strength of the link varies according to the thickness of the connecting wires between countries. The more the research collaborations, the greater the importance of link strength, or the thickness of the connecting wire.

3 Results and discussion

The data were analyzed, and the following estimates were made. Various forms of analysis were performed, including citation analysis and authorship analysis. Table 1 shows the results of a citation analysis performed to understand the influence of publication sources better. *Plos One* published the most papers and received the most citations during the research period, followed by *BMC Genomics* and *Phytopathology*. However, a similar pattern was not observed when calculating citations per paper. The *European Journal of Plant Pathology* received the most CPP citations, followed by *BMC Genomics* and *Fungal Genetics and Biology*.

Following data collection, it was analyzed in the VOSviewer, leading us to a list of journals that produced most of the articles throughout the study period. The VOSviewer analysis yielded a total of 28 top journals that met the limitation of a minimum of five documents. Figure 1 depicts a visual representation of the citation analysis.

The analysis found that the articles published during the study period on the real-time detection of pathogens in plants were published in journals like *Plos One*, *Plant Disease*, and *Frontiers in Plant Science* with 29, 24, and 19 documents, respectively. In addition, our selection contained a wide variety of journals. The larger the bubble, the higher the impact of that particular source. It can be seen from Figure 2 that there is a strong connection between the *Plos One* and *Plant Disease* journals. This depicts the publishing behavior of the researchers on the study theme.

TABLE 1 Top 20 sources where the documents were published during the study period.

Source	Documents	Citations	Citations per paper
Plos One	29	1,188	40.97
BMC Genomics	15	707	47.13
Phytopathology	7	692	98.86
European Journal of Plant Pathology	15	466	31.07
Plant Disease	24	425	17.71
Molecular Plant-Microbe Interactions	10	422	42.20
Applied and Environmental Microbiology	9	382	42.44
Canadian Journal of Plant Pathology	8	337	42.13
Journal of Microbiological Methods	10	329	32.90
Planta	11	328	29.82
Molecular Plant Pathology	8	305	38.13
Fungal Genetics and Biology	6	265	44.17
Frontiers in Plant Science	19	234	12.32
Plant Physiology and Biochemistry	5	201	40.20
Frontiers in Microbiology	8	199	24.88
BMC Plant Biology	8	195	24.38
Plant Pathology	5	170	34.00
Fungal Biology	6	160	26.67

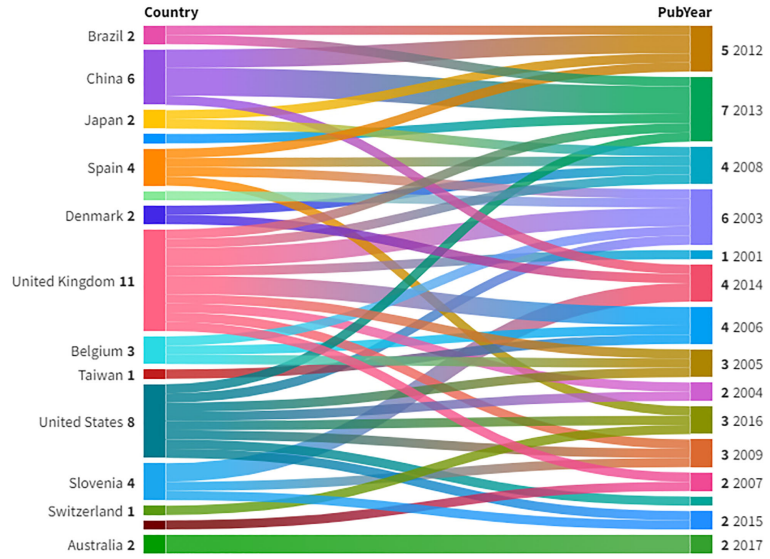

FIGURE 2
Network map for citation sources.

3.1 Intellectual structure

The intellectual structure is typically based on the interest of the researcher in a particular topic (Marsilio et al., 2011). In the case of pathogen detection, either the countries with the same pathogen attack collaborate or the countries with possible invasion of foreign virus do. In this paper, we tried to map the intellectual structure of scholars and the concerned countries. Figure 3 shows a Sankey diagram for the most productive countries and the publication year of the same. The diagram is the representation of how the items are

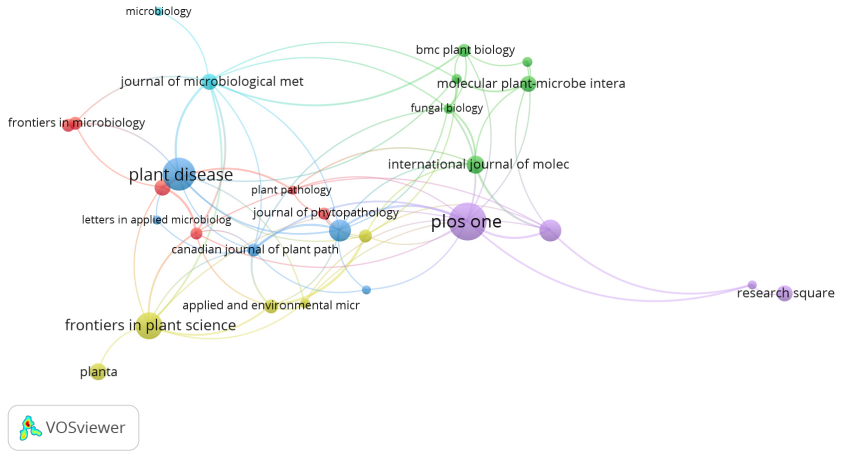

FIGURE 3
Sankey Graph between countries and publication year. Source: VOSviewer.

distributed, and the thickness of the link shows the volume of the flow. Figure 3 shows the top countries with the highest citations and the year in which they published the articles.

3.2 Analysis of co-authorship among countries

The normalized citation value of each country's published documents can be used to compare the scientific impact of publications from different countries (Bornmann and Wohlrabe, 2019). The concept of normalized citation value has been derived from the network visualization maps generated by VOSviewer. In these maps, the size of each node representing a particular country corresponds to its normalized citation value, which is essentially a measure of the impact and quality of its research output. The larger the size of a country's node in the normalized citation visualization map, the higher its research output's scientific significance. Therefore, this metric provides a valuable means of assessing the relative performance of countries in terms of research impact and productivity based on their normalized citation values.

The data were analyzed in VOSviewer by keeping some constraints such as a minimum number of documents of 5. There was no minimum number of citations kept in this analysis. It was found that out of 56 countries, only 26 meet the threshold. There were six clusters found in the analysis and each cluster had a dominating country in terms of citations. The United Nations and China had publications that had the highest number of citations and publications. The clusters were a group of countries that collaborated with each other. The top 10 countries with the highest number of citations were visualized using a world map, as shown in Figure 4. It clearly shows that the countries of interest were among the top 10 cited countries. In Figure 5, the line connecting two independent bubbles indicates a relationship in each source of highly referenced documents (van Eck and Waltman, 2011). The complexity represents the significant interconnectedness of the countries, and the differences in the color of the bubbles represent differences in temporal pattern (Zhu et al., 2009).

3.4 Co-authorship authors

Collaboration has been found to have a generally beneficial effect on citation impact in almost all subject domains and at all levels of aggregation (Moed et al., 1991; Narin et al., 1991). Bibliometrics shows the authors that collaborate with each other as it shows the scientific engagement and relationship between teams and organizations. Such analysis of co-authorship among authors was done using the software and is presented in Figure 6. Co-authorship is a valuable tool that enables us to identify, measure, and illustrate the links between individual contributors to a particular piece of research. Through co-authorship, we can gain insight into the extent of collaboration between researchers and track the development of their collaborative relationships over time. Co-authorship can also measure the quality and impact of scientific output, as it indicates the degree to which research is being conducted in partnership with other experts in the field. Overall, co-authorship is a vital tool that helps to foster collaboration and teamwork and is an important element in the production of high-quality scientific output.

In the analysis, we kept the threshold as 100 citations and five documents per author. It was found that out of 2,636 authors, only 50 meet the threshold. There was total of six clusters found in the analysis. Co-authorship occurs when two authors collaborate on a study. It is one of the most prominent and well-documented types of scientific co-operation. Almost every feature of scientific collaboration networks can be accurately tracked by examining co-authorship networks using bibliometric methodologies (Glänzel and Schubert, 2006). These co-operation networks (co-authorship) indicate research teams as well as characteristics that influence collaboration impact or production. The limitation here emphasizes that older papers have more citations than younger documents, which reduces the likelihood of fresh publications being examined

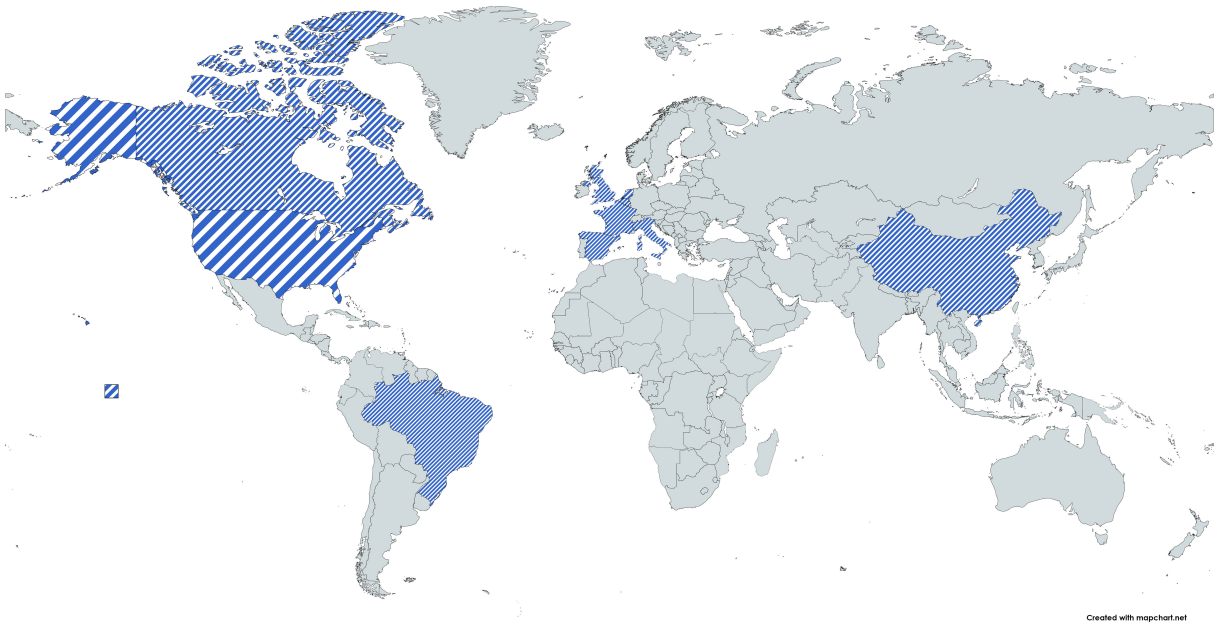

FIGURE 4
World map of top 10 countries with highest citations.

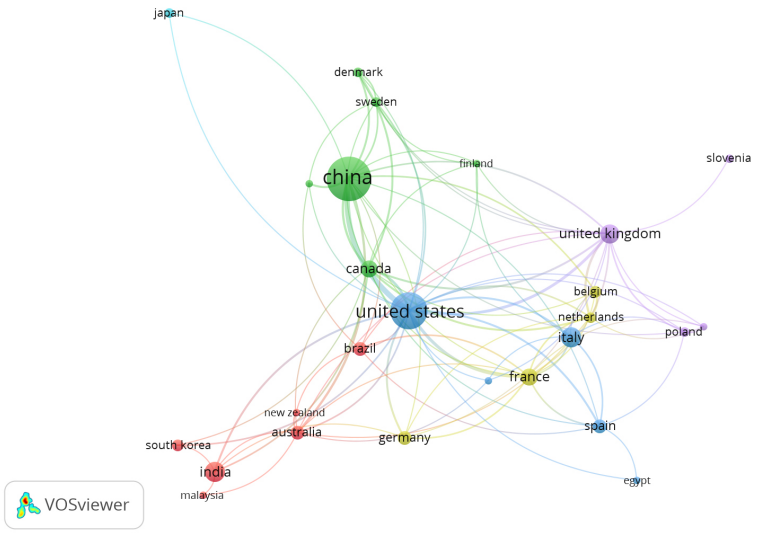

FIGURE 5
Network Visualization map for Co-authorship countries. Source: VOSviewer.

and affects the order of the top writers in the list (Luther and Tiberius, 2020; Wu et al., 2021).

We discovered the co-authorship network approach to be the best and most dependable method to adopt in our research methodology based on our research requirements. Interdisciplinary collaboration, on the other hand, has been found to improve research outputs. According to the study, co-authors are two authors who collaborate on research and have the most concrete and well-documented kind of research interaction (Glänzel and Schubert, 2006). Almost any component of scientific collaboration networks can be reliably studied by examining co-"author" networks using bibliometric techniques. These co-authorship co-operation networks demonstrate the impact of co-authorship, research teams, and collaborative output.

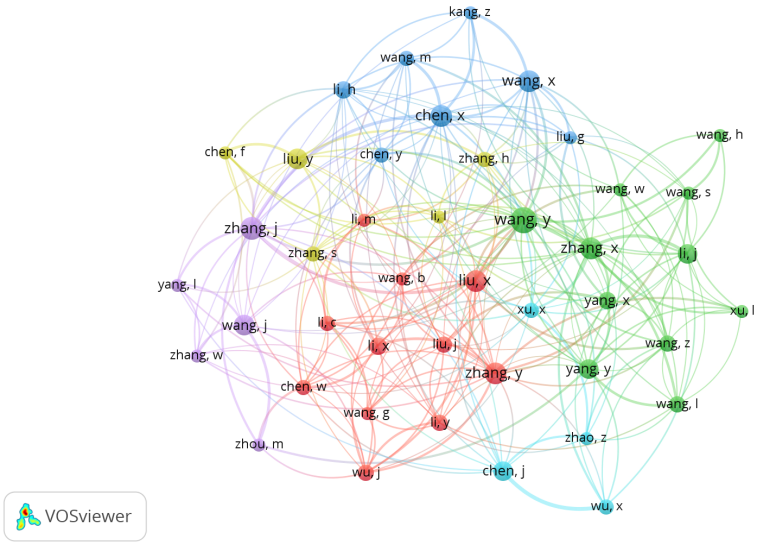

FIGURE 6
Network visualization map of Co-authorship authors. Source: VOSviewer.

3.5 Co-citation source analysis

According to Rousseau (1994), the three major uses of co-citation are, namely, qualitative and quantitative appraisal of scientists, publications, and scientific institutions; modeling of the historical development of science and technology; and information search and retrieval. In other words, using journal relationships, citation analysis can be used to define disciplines and emerging specialties, as well as to determine the transdisciplinary or multidisciplinary nature of research programs and initiatives. The cited documents are linked together by the process of co-citation, which is analogous to the similarity metrics of word co-occurrence. To display the diversity of documents and communities in the systems thinking literature, document co-citation networks were created. Co-citation analysis of sources of publications was done, and it was found that out of 2,115 sources, 216 meet the threshold. A total of four clusters were found in the analysis.

From Figure 7, we can conclude that among the clusters, the highest number of citations and publications was found for the journals *Phytopathology*, *Plant Physiology*, *Plos One*, etc. These are the journals that cover the topic of real-time PCR technique of detection of plant pathogens.

By this co-citation network, we see how multiple sources recognize a common set and theme of documents (Braam et al.,

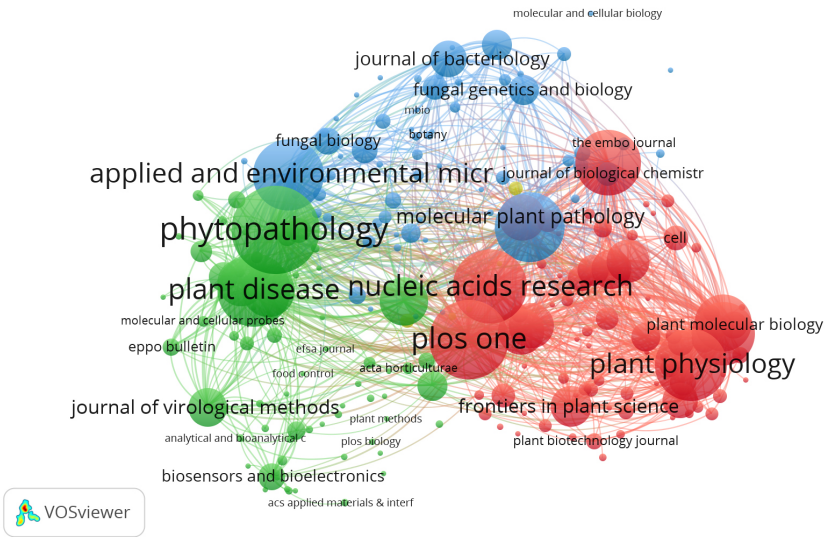

FIGURE 7
Co-citation analysis of sources. Source: VOSviewer.

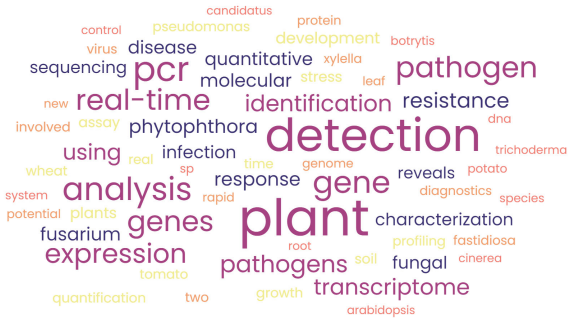

FIGURE 8
Word cloud of frequently used keywords.

1991). Therefore, future work would benefit from analysis of both cited and citing works to understand what ideas, findings, or experiments are being communicated and the meaning attributed to the co-cited documents. In addition, a survey of leading sources or analyzing keywords may reveal deeper patterns underlying co-citations (Small, 1977).

3.6 Keyword analysis

Keyword analysis gives us an insight into the words that the authors feel is important in their papers. In this analysis, we conducted keyword analysis based on the words of the title chosen by the researchers in their manuscript. The reason behind this is that the Dimensions data retrieved do not particularly allow us to conduct keyword analysis. There are few advantages of using keyword analysis as it gives an idea about trending research topics. The analysis will also reveal the direction of research in the theme of study. The results of keyword analysis are presented as a word cloud in Figure 8.

The keyword analysis results clearly indicate that the studies focused on detection in plants only as "plant" was found to be the most highlighted word in the figure. It is to be noted that the other highlighted texts were "gene," "*Fusarium*," "*Phytophthora*," "transcriptome," etc., which depict the direction of trends in the research of nucleic acid–based pathogen detection.

4 Conclusion

This bibliometric analysis clearly depicted that articles on RT-PCR-based pathogen detection are consistently increasing. The exponential increase in publications related to the detection technique can be attributed to its versatility and usefulness in screening a large number of germplasms of horticultural and field crops. Additionally, the technique has been used extensively in functional validation studies of transcriptomic data, contributing to its widespread adoption and popularity in the field. A comprehensive analysis of articles indexed in the "Dimensions" database from 2001 to 2021 revealed that the United States and China were the top countries in terms of the number of publications related to this detection technique. This suggests that both countries have made significant contributions to the development and advancement of the technique and are leaders in the field. The findings of this analysis provide valuable insights into the global research landscape and highlight the importance of continued research and innovation in this area. The top journals were primarily *Plos One*, followed by *BMC Genomics* and *Phytopathology*. The most cited journal was the *European Journal of Plant Pathology*. From a future perspective, the multi-institutional and multidisciplinary relationship between different countries requires further strengthening. The changing pest and pathogen dynamics and rapid advancement of novel isothermally based detection tools will affect the crucial role of RT-PCR in plant disease diagnostics. This is an ongoing process, and with the advent of new software and the involvement of a more exhaustive database, the study can be further strengthened.

Availability of data and materials

The datasets generated and analyzed in the current study are available in this manuscript.

Data availability statement

The original contributions presented in the study are included in the article/supplementary material. Further inquiries can be directed to the corresponding authors.

Author contributions

PL, ML, and RT: conceptualization, methodology, investigation, writing—original draft preparation. RK, MA, AAA, and AK: reviewing, analysis editing. All authors contributed to the article and approved the submitted version.

Acknowledgments

The authors would like to extend their sincere appreciation to the Researchers Supporting Project Number (RSP2023R236), King Saud University, Riyadh, Saudi Arabia.

Conflict of interest

The authors declare that the research was conducted in the absence of any commercial or financial relationships that could be construed as a potential conflict of interest.

Publisher's note

References

Akintunde, T. Y., Musa, T. H., Musa, H. H., Musa, I. H., Chen, S., Ibrahim, E., et al. (2021). Bibliometric analysis of global scientific literature on effects of COVID-19 pandemic on mental health. *Asian J. Psychiatr.* 63, 102753. doi: 10.1016/j.ajp.2021.102753

Bai, J. P. F., Alekseyenko, A. V., Statnikov, A., Wang, I. M., and Wong, P. H. (2013). Strategic applications of gene expression: from drug Discovery/Development to bedside. *AAPS J.* 15, 427. doi: 10.1208/S12248-012-9447-1

Böhm, J., Hahn, A., Schubert, R., Bahnweg, G., Adler, N., Nechwatal, J., et al. (1999). Real-time quantitative PCR: DNA determination in isolated spores of the mycorrhizal fungus glomus mosseae and monitoring of phytophthora infestans and phytophthora citricola in their respective host plants. *J. Phytopathol.* 147, 409–416. doi: 10.1111/J.1439-0434.1999.TB03842.X

Bornmann, L., and Wohlrabe, K. (2019). Normalisation of citation impact in economics. *Scientometrics* 120, 841–884. doi: 10.1007/S11192-019-03140-W

Braam, R. F., Moed, H. F., and Raan Van, A. F. J. (1991). Mapping of science by combined Co-citation and word analysis . I . structural aspects. *J. Am. Soc Inf. Sci.* 42, 233–251. doi: 10.1002/(SICI)1097-4571(199105)42:4<233::AID-ASI1>3.0.CO;2-I

Buja, I., Sabella, E., Monteduro, A. G., Chiriacò, M. S., De Bellis, L., Luvisi, A., et al. (2021). Advances in plant disease detection and monitoring: from traditional assays to in-field diagnostics. *Sensors* 21, 2129. doi: 10.3390/S21062129

Costanzo, M., Kuzmin, E., van Leeuwen, J., Mair, B., Moffat, J., Boone, C., et al. (2019). Global genetic networks and the genotype to phenotype relationship. *Cell* 177, 85. doi: 10.1016/J.CELL.2019.01.033

Deepak, S., Kottapalli, K., Rakwal, R., Oros, G., Rangappa, K., Iwahashi, H., et al. (2007). Real-time PCR: revolutionizing detection and expression analysis of genes. *Curr. Genomics* 8, 234. doi: 10.2174/138920207781386960

Dmytriw, A. A., Hui, N., Singh, T., Nguyen, D., Omid-Fard, N., Phan, K., et al. (2021). Bibliometric evaluation of systematic review and meta analyses published in the top 5 "high-impact" radiology journals. *Clin. Imaging* 71, 52–62. doi: 10.1016/j.clinimag.2020.11.008

Donoso, A., and Valenzuela, S. (2018). In-field molecular diagnosis of plant pathogens: recent trends and future perspectives. *Plant Pathol.* 67, 1451–1461. doi: 10.1111/PPA.12859

Elnifro, E. M., Ashshi, A. M., Cooper, R. J., and Klapper, P. E. (2000). Multiplex PCR: optimization and application in diagnostic virology. *Clin. Microbiol. Rev.* 13, 559. doi: 10.1128/CMR.13.4.559-570.2000

Fan, J., Gao, Y., Zhao, N., Dai, R., Zhang, H., Feng, X., et al. (2020). Bibliometric analysis on COVID-19: a comparison of research between English and Chinese studies. *Front. Public Heal.* 8. doi: 10.3389/FPUBH.2020.00477/FULL

Gachon, C., Mingam, A., and Charrier, B. (2004). Real-time PCR: what relevance to plant studies? *J. Exp. Bot.* 55, 1445–1454. doi: 10.1093/JXB/ERH181

Glänzel, W., and Schubert, A. (2006). Analysing scientific networks through Co-authorship. *Handb. Quant. Sci. Technol. Res.*, 257–276. doi: 10.1007/1-4020-2755-9_12

Hariharan, G., and Prasannath, K. (2021). Recent advances in molecular diagnostics of fungal plant pathogens: a mini review. *Front. Cell. Infect. Microbiol.* 10. doi: 10.3389/FCIMB.2020.600234/BIBTEX

Hook, D. W., Porter, S. J., Draux, H., and Herzog, C. T. (2021). Real-time bibliometrics: dimensions as a resource for analyzing aspects of COVID-19. *Front. Res. Metrics Anal.* 5. doi: 10.3389/FRMA.2020.595299

Kainz, P. (2000). The PCR plateau phase - towards an understanding of its limitations. *Biochim. Biophys. Acta - Gene Struct. Expr.* 1494, 23–27. doi: 10.1016/S0167-4781(00)00200-1

Kralik, P., and Ricchi, M. (2017). A basic guide to real time PCR in microbial diagnostics: definitions, parameters, and everything. *Front. Microbiol.* 8. doi: 10.3389/FMICB.2017.00108/FULL

Kumar, R., Jeevalatha, A., Baswaraj, R., Kumar, R., Sharma, S., and Nagesh, M. (2017). A multiplex RT-PCR assay for simultaneous detection of five viruses in potato. *Journal of Plant Pathology*, 37-45. doi: 10.4454/jpp.v99i1.3824

Kumar, R., Kaundal, P., Arjunan, J., Sharma, S., and Chakrabarti, S. K. (2020). Development of a visual detection method for potato virus s by reverse transcription loop-mediated isothermal amplification. *3 Biotech.* 10, 1–8. doi: 10.1007/S13205-020-02214-4

Kumar, R., Kaundal, P., Tiwari, R. K., Siddappa, S., Kumari, H., Chandra Naga, K., et al. (2021). Rapid and sensitive detection of potato virus X by one-step reverse transcription-recombinase polymerase amplification method in potato leaves and dormant tubers. *Mol. Cell. Probes* 58, 101743. doi: 10.1016/j.mcp.2021.101743

Kumar, R., Kaundal, P., Tiwari, R. K., Siddappa, S., Kumari, H., Lal, M. K., et al. (2022). Establishment of a one-step reverse transcription recombinase polymerase amplification assay for the detection of potato virus s. *J. Virol. Methods* 307, 114568. doi: 10.1016/J.JVIROMET.2022.114568

Kumar Tiwari, R., Kumar, R., Kaundal, P., Sharma, S., and Chakrabarti, S. (2019). Potato viruses and their diagnostic techniques: an overview. *J. Pharmacogn. Phytochem.* 8, 1932–1944.

Lin, M., Chen, Y., and Chen, R. (2020). Bibliometric analysis on Pythagorean fuzzy sets during 2013–2020. *Int. J. Intell. Comput. Cybern.* 14, 104–121. doi: 10.1108/IJICC-06-2020-0067/FULL/HTML

Liu, H., Wu, W., Tan, J., Li, Y., Mi, W., Jiang, L., et al. (2019). Development and evaluation of a one-step reverse transcription loop-mediated isothermal amplification for detection of citrus leaf blotch virus. *J. Virol. Methods* 270, 150–152. doi: 10.1016/j.jviromet.2019.05.009

Londoño, M. A., Harmon, C. L., and Polston, J. E. (2016). Evaluation of recombinase polymerase amplification for detection of begomoviruses by plant diagnostic clinics. *Virol. J.* 13, 1–9. doi: 10.1186/s12985-016-0504-8

Luther, L., and Tiberius, V. (2020). User experience (UX) in business , management , and Psychology: a bibliometric mapping of the current state of research. *Multimodal Technol. Interact.* 4, 18. doi: 10.3390/mti4020018

Marsilio, M., Cappellaro, G., and Cuccurullo, C. (2011). The intellectual structure of research into PPPS: a bibliometric analysis. *Public Manage. Rev.* 13, 763–782. doi: 10.1080/14719037.2010.539112

Mirmajlessi, S. M., Loit, E., Mänd, M., and Mansouripour, S. M. (2015). Real-time PCR applied to study on plant pathogens: potential applications in diagnosis - a review. *Plant Prot. Sci.* 51 (2015), 177–190. doi: 10.17221/104/2014-PPS

Moed, H., Bruin, R., Nederhof, A., and Scientometrics, R. T. (1991). International scientific co-operation and awareness within the European community: problems and perspectives. *akjournals.com* 21, 291–311. doi: 10.1007/BF02093972

Morlan, J., Baker, J., and Sinicropi, D. (2009). Mutation detection by real-time PCR: a simple, robust and highly selective method. *PloS One* 4, e4584. doi: 10.1371/JOURNAL.PONE.0004584

Narin, F., Stevens, K., and Whitlow, E. S. (1991). Scientific co-operation in Europe and the citation of multinationally authored papers. *Scientometrics* 21, 313–323. doi: 10.1007/BF02093973

Palka-Santini, M., Cleven, B. E., Eichinger, L., Krönke, M., and Krut, O. (2009). Large Scale multiplex PCR improves pathogen detection by DNA microarrays. *BMC Microbiol.* 9 (1), 1–12. doi: 10.1186/1471-2180-9-1

Rousseau, R. (1994). Documentation note: the number of authors per article in library and information science can often be described by a simple probability distribution. *J. Doc.* 50, 134–141. doi: 10.1108/EB026928/FULL/HTML

Sandberg, M., Lundberg, L., Ferm, M., and Malmheden Yman, I. (2003). Real time PCR for the detection and discrimination of cereal contamination in gluten free food. *European Food Research and Technology* 217, 344–349. doi: 10.1007/s00217-003-0758-4

Small, H. G. (1977). A Co-citation model of a scientific Specialty: a longitudinal study of. *Soc Stud. Sci.* 7, 139–166. doi: 10.1177/030631277700700202

Tang, Y., He, G., He, Y., and He, T. (2022). Plant resistance to fungal pathogens: bibliometric analysis and visualization. *Toxics* 10 (10), 624. doi: 10.3390/TOXICS10100624

Terzi, V., Malnati, M., Barbanera, M., and Stanca, A. M. (2003) *Development of analytical systems based on real-time PCR for triticum species-specific detection and quantitation of bread wheat contamination in semolina and* (Elsevier). Available at: https://www.sciencedirect.com/science/article/pii/S0733521002001388 (Accessed December 21, 2022).

Tiwari, R. K., Kumar, R., Sharma, S., Naga, K. C., Subhash, S., and Sagar, V. (2020a). Continuous and emerging challenges of silver scurf disease in potato. *Int. J. Pest Manage* 68 (1), 89-101. doi: 10.1080/09670874.2020.1795302

Tiwari, R. K., Kumar, R., Sharma, S., Sagar, V., Aggarwal, R., Naga, K. C., et al. (2020b). Potato dry rot disease: current status, pathogenomics and management. *3 Biotech.* 10, 1–18. doi: 10.1007/s13205-020-02496-8

van Eck, N. J., and Waltman, L. (2011) *Text mining and visualization using VOSviewer*. Available at: http://arxiv.org/abs/1109.2058 (Accessed December 21, 2022).

Wu, H., Tong, L., Wang, Y., Yan, H., and Sun, Z. (2021). Bibliometric analysis of global research trends on ultrasound Microbubble: a quickly developing. *Front. Pharmacol.* 12. doi: 10.3389/fphar.2021.646626

Zhou, G. H., Kamahori, M., Okano, K., Chuan, G., Harada, K., and Kambara, H. (2001). Quantitative detection of single nucleotide polymorphisms for a pooled sample by a bioluminometric assay coupled with modified primer extension reactions (BAMPER). *Nucleic Acids Res.* 29, e93. doi: 10.1093/NAR/29.19.E93

Zhu, S., Takigawa, I., Zeng, J., and Mamitsuka, H. (2009). Field independent probabilistic model for clustering multi-field documents. *Inf. Process. Manage.* 45, 555–570. doi: 10.1016/j.ipm.2009.03.005

frontiers | Frontiers in Plant Science

TYPE Original Research
PUBLISHED 06 June 2023
DOI 10.3389/fpls.2023.1185337

OPEN ACCESS

EDITED BY
Prem Lal Kashyap,
Indian Institute of Wheat and Barley Research (ICAR), India

REVIEWED BY
Dalia Gamil Aseel,
Arid Lands Cultivation Research Institute (ALCRI), Egypt
Evans N. Nyaboga,
University of Nairobi, Kenya
Sapna Langyan,
Indian Council of Agricultural Research (ICAR), India
Susheel Kumar Sharma,
Indian Agricultural Research Institute (ICAR), India

*CORRESPONDENCE
Ravinder Kumar
chauhanravinder97@gmail.com
Rahul Kumar Tiwari
rahultiwari226@gmail.com
Milan Kumar Lal
milan2925@gmail.com

RECEIVED 13 March 2023
ACCEPTED 02 May 2023
PUBLISHED 06 June 2023

CITATION
Chauhan P, Mehta N, Chauhan RS, Kumar A, Singh H, Lal MK, Tiwari RK and Kumar R (2023) Utilization of primary and secondary biochemical compounds in cotton as diagnostic markers for measuring resistance to cotton leaf curl virus. *Front. Plant Sci.* 14:1185337. doi: 10.3389/fpls.2023.1185337

Utilization of primary and secondary biochemical compounds in cotton as diagnostic markers for measuring resistance to cotton leaf curl virus

Prashant Chauhan[1], Naresh Mehta[2], R. S. Chauhan[3], Abhishek Kumar[2], Harbinder Singh[2], Milan Kumar Lal[4]*, Rahul Kumar Tiwari[5]* and Ravinder Kumar[5]*

[1]College of Agriculture, Chaudhary Charan Singh (CCS) Haryana Agricultural University, Hisar, India, [2]Department of Plant Pathology, Chaudhary Charan Singh (CCS) Haryana Agricultural University, Hisar, India, [3]Krishi Vigyan Kendra, Chaudhary Charan Singh (CCS) Haryana Agricultural University, Hisar, India, [4]Department of Crop Physiology, Biochemistry & Postharvest Technology, Indian Council of Agricultural Research (ICAR)-Central Potato Research Institute, Shimla, Himachal Pradesh, India, [5]Department of Plant Protection, Indian Council of Agricultural Research (ICAR)-Central Potato Research Institute, Himachal Pradesh, India

Introduction: Cotton (*Gossypium hirsutum* L.) is one of the most important staple fibrous crops cultivated in India and globally. However, its production and quality are greatly hampered by cotton leaf curl disease (CLCuD) caused by cotton leaf curl virus (CLCuV). Therefore, the aim of the present study was to investigate the biochemical mechanisms associated with CLCuD resistance in contrasting cotton genotypes.

Methods: Four commercial cotton varieties with susceptible (HS 6 and RCH-134 BG-II) and resistant (HS 1236 and Bunty) responses were used to analyze the role of primary (sugar, protein, and chlorophyll) and secondary (gossypol, phenol, and tannin) biochemical compounds produced by the plants against infection by CLCuV. The resistant cultivars with increased activity of protein, phenol, and tannin exhibited biochemical barriers against CLCuV infection, imparting resistance in cotton cultivars.

Results: Reducing sugar in the healthy plants of the susceptible Bt cultivar RCH 134 BG-II exhibited the highest value of 1.67 mg/g at 90 days. In contrast, the lowest value of 0.07 mg g^{-1} was observed at 60 DAS in the highly diseased plants of the susceptible hybrid HS 6. Higher phenol content (0.70 mg g^{-1}) was observed at 90 DAS in resistant cultivars, whereas highly susceptible plants exhibited the least phenol (0.25 mg g^{-1}) at 90 DAS. The lowest protein activity was observed at 120 DAS in susceptible cultivars HS 6 (9.4 mg g^{-1}) followed by RCH 134 BG-II (10.5 mg g^{-1}). However, other biochemical compounds, including chlorophyll, sugar, and gossypol, did not show a significant role in resistance

against CLCuV. The disease progression analysis in susceptible cultivars revealed non-significant differences between the two susceptible varieties.

Discussion: Nevertheless, these compounds are virtually associated with the basic physiological and metabolic mechanisms of cotton plants. Among the primary biochemical compounds, only protein activity was proposed as the first line of defense in cotton against CLCuV. The secondary level of defense line in resistance showed the activity of secondary biochemical compounds phenol and tannins, which displayed a significant increase in their levels while imparting resistance against CLCuV in cotton.

KEYWORDS

cotton, cotton leaf curl virus, biochemical, CLCuD, resistance

1 Introduction

Cotton (*Gossypium hirsutum*) is a staple fibrous crop cultivated in the sub-tropical and seasonally dry regions of the northern and southern hemispheres. India is the largest producer of cotton on the global map, contributing to 23% of its production (Barwale, 2016; Anonymous, 2019). However, global cotton production has shown a decline of approximately 2% in 2018 due to biotic and abiotic stresses. Nevertheless, an overall 6% yield growth of cotton can help achieve the global demand for cotton by 2028 (Anonymous, 2019). Cotton leaf curl disease (CLCuD) caused by cotton leaf curl virus (CLCuV) is one of the most devastating and prominent diseases of cotton in the Indian subcontinent (Farooq et al., 2011; Monga, 2014; Qadir et al., 2019). The virus is a begomivirus of the family Geminiviridae and is closely associated with satellite molecules (beta satellite and alpha satellite). It is transmitted by whitefly (*Bemisiatabaci* Gem.) through circulative persistent transmission in plants (Sharma and Rishi, 2003; Kumar et al., 2021). CLCuV poses a significant threat to cotton production around the world, causing substantial yield loss and economic harm. The CLCuV is transmitted by whiteflies and causes crinkled, misshapen, and discolored leaves in infected cotton plants, severely reducing their growth and output. This virus poses a significant challenge in cotton-growing regions, especially in major cotton-producing nations like Pakistan, India, and China. Widespread crop damage caused by CLCuV has resulted in significant economic losses for farmers and the cotton sector (Farooq et al., 2011; Monga, 2014; Qadir et al., 2019). To combat the problem, various techniques have been developed, such as adopting virus-resistant cotton types, implementing integrated pest management practices to control whitefly populations, and creating fast diagnostic tools to detect the virus early. Despite these efforts, CLCuV remains a chronic concern, and its control is still a priority in global cotton production.

The acquisition of the virus by whiteflies may vary due to biochemical and genetic differences in whitefly races with their host (Yang et al., 2011). Additionally, the compositional differences in host saps could affect the behavior and growth of the insects (Gupta et al., 2010). Understanding the biochemical responses of different varieties can enhance the management of CLCuD and its vector, the whitefly. Plants rely heavily on biochemical compounds to defend against numerous biotic stress factors, such as diseases and insect pests (Iqbal et al., 2021). Sugars and phenols provide the plant with energy and also act as signaling molecules to activate defense responses (Lal et al., 2022; Kumar et al., 2023). In response to pathogen attacks, plants produce secondary metabolites such as antifungal and antibacterial phytoalexins. Pathogenesis-related (PR) proteins and other proteins are involved in cell defense, cell wall reinforcement, and acquired systemic resistance. Insects feed on chlorophyll because it is necessary for photosynthesis and a food source for plants. The degradation of chlorophyll can produce harmful by-products, which can discourage feeding. Phenols are essential components of lignin and suberin, which reinforce plant cell walls and inhibit disease penetration. Gossypol, which is present in cotton plants, is poisonous to numerous insect pests and functions as a defense mechanism. Tannins are astringent secondary metabolites with antifungal and antibacterial effects that can discourage insect feeding.

Biochemical compounds play a crucial role in the survival and reproduction of plants under biotic stress (Wilson and Smith, 1976; Hedin and McCarty, 1990; Borkar and Verma, 1991; Bhat, 1997; Chakrabarty et al., 2002; Singh and Agarwal, 2004; Beniwal et al., 2006; Acharya and Singh, 2008; Govindappa et al., 2008; Ajmal et al., 2011; Anuradha, 2014). Although their association with plant response to biotic stresses has been extensively studied, little research has been conducted on the response of plants to virus-induced diseases (Kumar et al., 2020; Kumar et al., 2021; Kumar et al., 2022). To address this gap, we investigated the biochemical response of cotton plants to CLCuD by examining the production of various primary and secondary metabolites. This study can provide valuable insights into the mechanism involved in the resistance against CLCuV.

2 Materials and methods

2.1 Plant genotypes and analytical parameters

Four commercially grown cotton cultivars were selected for the study based on their disease incidence and plant types. Two hybrids,

HS6 and H 1236, and two genetically transformed *Bacillus thuringiensis* (Bt) varieties with Bt genes against bollworms (RCH-134 BG-II and Bunty) were chosen for the present study. Based on the previous studies on response against CLCuV, the cultivars H 1236 and Bunty were considered resistant, whereas HS 6 and RCH-134 BG-II were the susceptible sources in the present study (Anonymous, 2018). The experiment was conducted during the summer (*Kharif*) season using a randomized block design in plots measuring 5×4 m^2 in four replications. The disease appeared in 1-month-old plants along with an observed buildup of white fly populations. The disease was allowed to spread under natural epiphytic conditions (Supplementary Figures 1A, B). Standard biochemical methods were used to analyze the levels of sugar (total and reducing sugar), proteins, chlorophyll-a and chlorophyll-b, gossypol, total phenols, and tannins. Plants were scored on a disease grade scale ranging from 1 to 6, with grades 1–2 indicating a resistant (R) response, grade 3 indicating a moderately resistant (MR) response, grade 4 indicating a moderately susceptible (MS) response, and grades 5–6 indicating a susceptible (S) response to CLCuD (Table 1). Representative leaf samples of the CLCuD diseased plants of the four cotton varieties raised in the field conditions were collected. Plants with disease grades 0, 2, 4, and 6 of all four cultivars were selected at 40, 60, 90, and 120 days after sowing to observe the response of plants to disease infection at different growth stages.

2.2 Leaf sample preparation

Symptomless leaf samples were collected from resistant cultivars, while leaves of different disease grades (2, 4, and 6) were used from susceptible cultivars for analysis. In order to ensure a fair comparison, leaves without symptoms from susceptible cultivars were used as controls from the experimental plots under natural epiphytic exposure to white fly (vector of CLCuV) and the virus. The collected leaves were cleaned with sterilized water to remove any foreign material from the surface and sun-dried for 3 days. The dried samples were subjected to oven drying at 60°C for 5 days until completely dried. The leaves were then crushed into a fine powder for biochemical analysis, whereas fresh leaf samples were taken for chlorophyll estimation. The plants of susceptible cultivars exhibited a higher disease index of grade 4 after 30 days of sowing; therefore, biochemical response for various parameters for highly diseased plants was performed during the second stage of sampling.

2.3 Quantitative determination of primary metabolites

2.3.1 Sugar determination

Each test tube containing 100 mg of powdered leaf samples was added with 5 ml of 80% ethanol. These tubes were then placed in a hot water bath for 25–30 min at 80°C and mixed well. After cooling to room temperature, the tubes were centrifuged at 4,000 rpm for 10 min. The resulting supernatant was transferred to another set of test tubes for each sample and made up to a final volume of 10 ml with distilled water. The sugar content was estimated using the phenol-sulfuric acid method (DuBois et al., 1956).

2.3.2 Protein determination

The 100 mg of leaf extract was taken and poured into a 150-ml digestion flask. A 10-ml solution of H_2SO_4 and $HClO_4$ in the ratio of 4:1 was then gently poured along the walls of the flask. The mixture was left undisturbed for 24 h. Afterward, the flask was heated on a hot plate until the solution became colorless and was then allowed to cool at room temperature. The final volume was made 100 ml by adding distilled water and was transferred to the distillation apparatus. The total protein content was analyzed from the leaves using the Kjeldahl method as described by AOAC (Helrich, 1990).

2.3.3 Chlorophyll-a and chlorophyll-b determination

The determination of chlorophyll-a and b was carried out following the method of Hiscox and Israelstam (1979), and the formulas proposed by Arnon (1949) were used to calculate the total chlorophyll-a and chlorophyll-b as follows:

Total chlorophyll (mg g^{-1})

$$= \frac{(20.2 \ x \ A_{645}) + (8.02 \ x \ A_{663}) \times V}{(1,000 \times W)}$$

TABLE 1 Disease scale used for grading of CLCuD.

Grade of disease	Reaction response	Plant response
1	R	Thickening of small veins
2		Grade 1 + main vein thickening and little leaf curling
3	MR	From top 1/4 of the plant showing leaf curling
4	MS	Upper 1/2 of the plant affected by leaf curling
5	S	From top 3/4 of the plant affected by leaf curling
6		Severe stunting of plant with leaf curling

Chlorophyll-a (mg g^{-1})

$$= \frac{(12.7 \ x \ A_{663}) \ x \ (2.69 \ x \ A_{645}) \ \times \ V}{(1,000 \ \times \ W)}$$

Chlorophyll-b (mg g^{-1})

$$= \frac{(22.9 \ x \ A_{645}) + \ (4.69 \ x \ A_{663}) \ \times \ V}{1,000 \ \times \ W}$$

where

A_{663} and A_{645} = absorbance at wavelengths 645 and 663 nm, respectively;

V = volume of solution; and

W = weight of sample.

2.4 Quantitative determination of secondary metabolites

2.4.1 Gossypol determination

For each sample, 500 mg of powdered cotton leaves was taken and added to a 25-ml conical flask. Then, 10 ml of ethyl alcohol (95%) was added to the flask. The samples were subjected to a hot water bath for 5 min, filtered into fresh test tubes, and centrifuged at 8,000 rpm for 15 min at 18°C. Dilution was performed by adding 40% ethanol, and 1 N HCl was used to adjust the pH to 3.0. Using a separating funnel, 1.5 ml of diethyl ether at 10°C was mixed into the content of the test tubes. The extract was allowed to evaporate until the tubes were dried, and gossypol was estimated by using Diels–Alder reaction of hemigossypolone with myreene as per the method described by Bell (1986).

2.4.2 Phenol determination

Up to extract preparation for phenol determination, the method was the same as that used for sugar determination (*Section 2.3.1*). The phenol content was estimated using Folin-Ciocalteu's agent and the standard method described by Bray and Thorpe (1954).

2.4.3 Tannin determination

For each leaf extract, 100 mg was taken and added to a 10-ml oak ridge tube along with 5 ml of 70% acetone. The tubes were subjected to a hot water bath at 70°C for 25–30 min and then vortexed to ensure thorough mixing. After cooling to room temperature, the tubes were centrifuged at 4,000 rpm for 10 min. The resulting supernatant was transferred to fresh, empty oak ridge tubes for tannin estimation, following the method described by Porter et al. (1986).

2.5 Disease appearance, percent incidence, and progression

The disease appearance, incidence, and progression were recorded for 50 selected plants in the field for two susceptible cultivars grown in the same field. Weekly observations on disease development showed that the disease first appeared on June 21 (3rd week of crop stage) in both cultivars, and reached a maximum (100%) in the 9th week of the crop stage after infection (Table 2). In

TABLE 2 CLCuD disease incidence and periodical disease progression on two cotton cultivars.

Crop age	HS-6*			RCH 134 BG-II**		
Days after sowing	DS (%)	Disease incidence (%)	Disease progression (%)	DS (%)	Disease incidence (%)	Disease progression (%)
23	1.03	1.5	1.5	1.30	1.2	1.2
30	6.30	17.3	15.8	8.37	13.3	12.1
37	9.01	55.7	38.4	11.58	24.0	10.7
44	12.66	86.7	31.0	16.02	84.3	60.3
51	18.25	97.6	10.9	20.11	95.3	11.0
58	24.76	100.0	2.4	26.30	100.0	4.7
65	32.03	100.0	0.0	38.45	100.0	0.0
72	38.62	100.0	0.0	46.60	100.0	0.0
79	43.26	100.0	0.0	51.13	100.0	0.0
86	47.74	100.0	0.0	56.10	100.0	0.0
93	52.92	100.0	0.0	73.28	100.0	0.0
100	57.64	100.0	0.0	66.04	100.0	0.0
107	62.33	100.0	0.0	70.29	100.0	0.0
114	68.76	100.0	0.0	76.84	100.0	0.0
121	72.55	100.0	0.0	77.05	100.0	0.0

*Hybrid cotton, **Bt cotton.

the second-year trial, the disease appeared on June 30 (5th week of crop stage) and reached its maximum (100%) during the 10th week of the crop stage (Table 3). The varietal behavior of CLCuD was also recorded, revealing that both cultivars were susceptible to CLCuD, and there were no variations in the development of CLCuD.

2.6 Statistical analysis

The data obtained were analyzed using the online statistical tool OPSTAT (hau.ernet.in/about/opstat.php). Two-way ANOVA was performed to analyze the observations for both years. This analysis allowed for a comprehensive understanding of the data and enabled the identification of any significant differences or relationships between the variables studied.

3 Results

3.1 Sugar (total and reducing)

The maximum total sugar content of 14.9 mg g^{-1} was observed in symptomless plants of the susceptible cultivar RCH 134 BG-II at 90 DAS (as shown in Figure 1) under natural epiphytotic conditions. In contrast, the lowest sugar content of 1.5 mg g^{-1} was found in highly diseased plants of the susceptible hybrid HS 6 at 60 DAS. The resistant cultivars, Bunty, exhibited a decrease in total sugar at 120 DAS. Additionally, the reducing sugar in healthy plants of the susceptible Bt cultivar RCH 134 BG-II was the highest at 1.67 mg/g at 90 DAS (Figure 1). Conversely, the lowest value of 0.07 mg g^{-1} was observed at 60 DAS in highly diseased plants of the susceptible hybrid HS 6.

3.2 Protein

The maximum protein content of 26.3 mg g^{-1} was observed at 90 DAS in Bunty, followed by the resistant hybrid H 1236 with 25.1 mg g^{-1} (Figure 2). Even the healthy plants of the susceptible cultivars exhibited an increase in protein content. The susceptible cultivars HS 6 and RCH 134 BG-II, with lower disease incidence, exhibited more protein as compared to highly diseased plants. The lowest protein content was observed at 120 DAS in the susceptible cultivars HS 6 (9.4 mg g^{-1}) followed by RCH 134 BG-II (10.5 mg g^{-1}).

3.3 Chlorophyll (a and b)

An increase in chlorophyll-a (Chl-a) was observed with the progression of CLCuD symptoms and crop growth stages. HS 6 and RCH 134 BG-II exhibited increased Chl-a levels up to 90 DAS (Figure 3). Highly diseased plants of susceptible cultivars HS 6 (342.8 mg g^{-1}) and RCH 134 BG-II (299.1 mg g^{-1}) exhibited higher Chl-a levels at 90 DAS. In contrast, resistant cultivars H 1236 and Bunty exhibited 223.8 mg g^{-1} and 245.8 mg g^{-1} Chl-a, respectively, at 30 DAS. Chlorophyll-b (Chl-b) levels remained low in all cultivars up to 30 DAS.

TABLE 3 CLCuD disease incidence and periodical disease progression on two cotton cultivars during 2014.

Crop age	HS-6*			RCH 134 BG-II**		
Days after sowing	DS (%)	Disease incidence (%)	Disease progression (%)	DS (%)	Disease incidence (%)	Disease progression (%)
30	1.10	6.8	6.8	2.00	12.3	12.3
37	2.00	22.5	15.7	6.40	27.8	15.5
44	7.50	49.3	26.8	13.00	59.3	31.5
51	12.18	82.3	33.0	16.55	93.7	34.4
58	17.83	95.7	13.4	21.28	98.4	4.7
65	24.70	100.0	4.3	24.90	100.0	1.6
72	29.80	100.0	0.0	32.80	100.0	0.0
79	33.00	100.0	0.0	37.10	100.0	0.0
86	36.10	100.0	0.0	40.40	100.0	0.0
93	38.60	100.0	0.0	43.70	100.0	0.0
100	40.90	100.0	0.0	48.00	100.0	0.0
107	43.70	100.0	0.0	50.70	100.0	0.0
114	50.00	100.0	0.0	53.74	100.0	0.0
121	57.10	100.0	0.0	57.30	100.0	0.0

*Hybrid cotton, **Bt cotton.

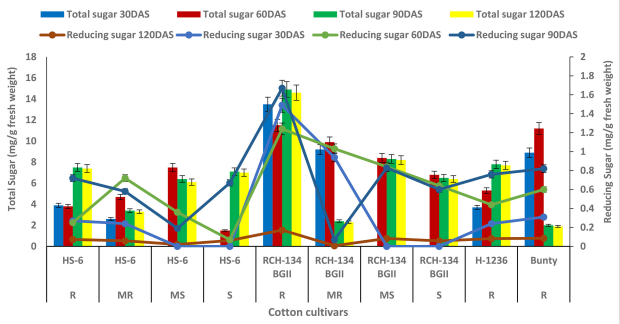

FIGURE 1
Total sugar (bars) and reducing sugar (lines) in cotton cultivars estimated at 30, 60, 90, and 120 days after sowing. The susceptible cultivars were Non-Bt (HS 6) and Bt (RCH 134 BGII). Non-Bt H1236 and Bt Bunty were taken as resistant cotton cultivars.

3.4 Phenol

The phenol content was observed to increase with plant growth up to 90 DAS, but decreased at 120 DAS (Figure 4). At 90 DAS, higher phenol content (0.70 mg g^{-1}) was observed in Bunty and H 1236, while highly diseased plants of HS 6 and RCH 134 BG-II exhibited the least phenol content (0.25 mg g^{-1}). Notably, highly diseased plants in susceptible cultivars showed lower phenol content compared to the resistant cultivars.

3.5 Gossypol

The concentration of gossypol increased in all four cultivars up to 90 DAS (Figure 5). The susceptible cultivar RCH 134 BG-II and the resistant cultivar Bunty exhibited the highest gossypol content, measuring 0.75 µg/g and 0.74 µg/g, respectively. At 90 DAS, the symptomless susceptible cultivars RCH 134 BG-II and HS 6 had the same gossypol content, measuring 0.72 µg/g. On the other hand, highly diseased plants of the same cultivars exhibited the lowest gossypol content.

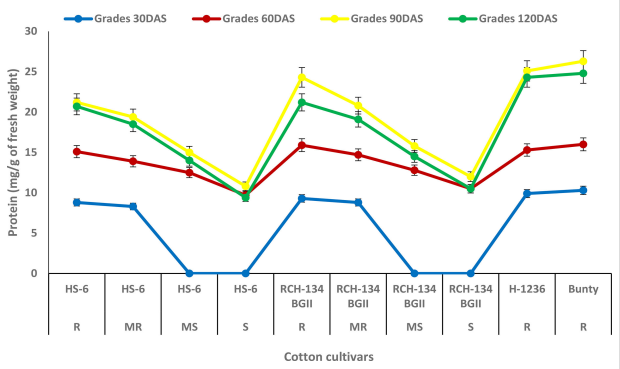

FIGURE 2
Protein content in cotton cultivars estimated at 30, 60, 90, and 120 days after sowing. The susceptible cultivars were Non-Bt (HS 6) and Bt (RCH 134 BGII). Non-Bt H1236 and Bt Bunty were taken as resistant cotton cultivars.

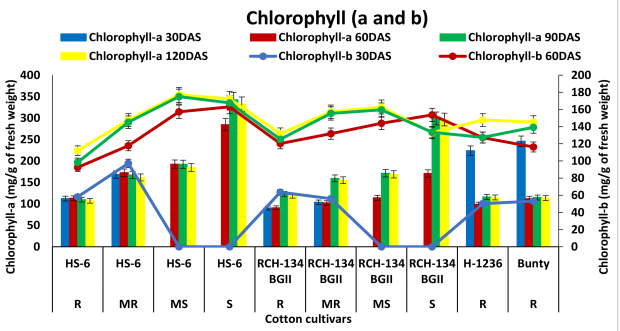

FIGURE 3
Chlorophyll-a (bars) and chlorophyll-b (lines) content in cotton cultivars estimated at 30, 60, 90, and 120 days after sowing. The susceptible cultivars were Non-Bt (HS 6) and Bt (RCH 134 BGII) with varied disease reactions. Non-Bt H1236 and Bt Bunty were taken as resistant cotton cultivars.

3.6 Tannin

The tannin content increased in all cultivars up to 60 DAS, after which it decreased over time at 90 and 120 DAS. Higher tannin content was observed in plants with fewer disease symptoms than in highly diseased plants (Figure 6). Healthy leaves of the susceptible hybrid HS 6 expressed a high tannin content (0.76 µg/g) compared to highly diseased plants with grade 6 symptoms (0.47 µg/g) at 60 DAS. Similarly, symptomless leaves of the susceptible Bt cultivar RCH 134 BG-II exhibited 0.93 µg/g tannin compared to the highly diseased plants of RCH 134 BG-II, which had 0.61 µg/g tannin.

3.7 Disease progression

The disease progression on two cultivars was observed weekly. The data presented in Table 2 show that disease progression reached a maximum of 38.4% up to 37 DAS in cultivar HS-6, and a maximum of 60.3% up to 44 DAS in RCH 134 BG-II in the first-year trial, after the appearance of the disease on 23 DAS. Thereafter, disease progression declined, and plants were fully infected after 58 days of sowing. Similarly, observations recorded in the second-year trials showed

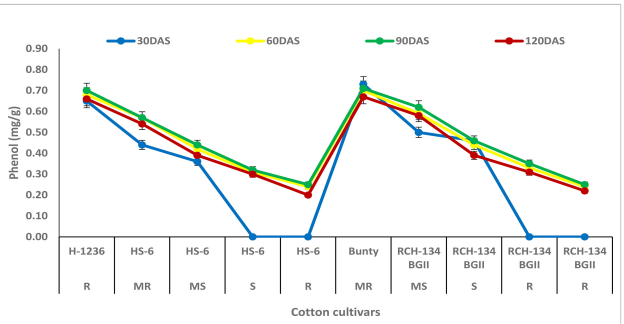

FIGURE 4
Phenol content in cotton cultivars estimated at 30, 60, 90, and 120 days after sowing. The susceptible cultivars were Non-Bt (HS 6) and Bt (RCH 134 BGII) with varied disease reactions. H1236 (Non-Bt) and Bunty (Bt) were taken as resistant cultivars.

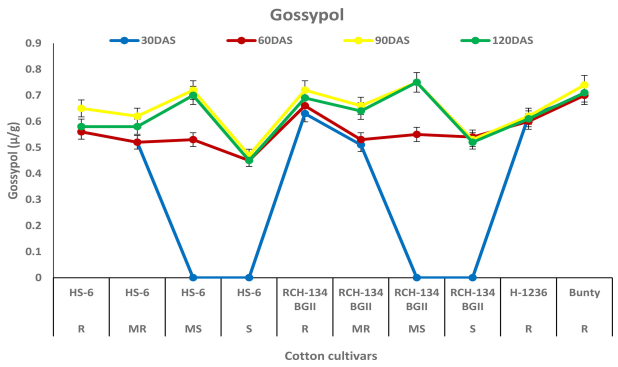

FIGURE 5
Gossypol in cotton cultivars estimated at 30, 60, 90, and 120 days after sowing. The susceptible cultivars were Non-Bt (HS 6) and Bt (RCH 134 BGII) with varied disease reactions. H1236 (Non-Bt) and Bunty (Bt) were taken as resistant cultivars.

that disease progression reached a maximum of 33.0% on HS-6 and 34.4% on RCH 134 BG-II up to 51 DAS, after the appearance of disease on 30 DAS. Thereafter, not much disease progression was recorded, and plants were fully infected. Perusal of data from both the trials revealed that the disease initiated around the 4th to 5th week and reached its maximum within 9–10 weeks of crop age in both the cultivars. It indicates that there was no significant difference between hybrid and Bt cotton regarding CLCuD infection and multiplication.

4 Discussion

In this study, sugar was investigated as part of the biochemical response to the virus due to its role as a source of energy for various physiological activities. However, our findings indicate that the total sugar content in resistant and susceptible cotton plants did not have a significant role in resistance against the virus. Interestingly, we observed variations in sugar content in plants, regardless of their reaction to the disease. Previous studies have reported high sugar content in susceptible plants (Klement and Goodman, 1967; Jayapal and Mahadevan, 1968; Patil et al., 2010; Lal et al., 2021), while in some cases, no significant association between sugar and disease resistance has been observed (Ashfaq et al., 2014). The limited understanding of the function of sugar in disease resistance remains a hindrance. While our study did not find sugar to be a contributing factor to the biochemical response against CLCuV, it may be worth investigating its role in the host–pathogen interaction phenomenon.

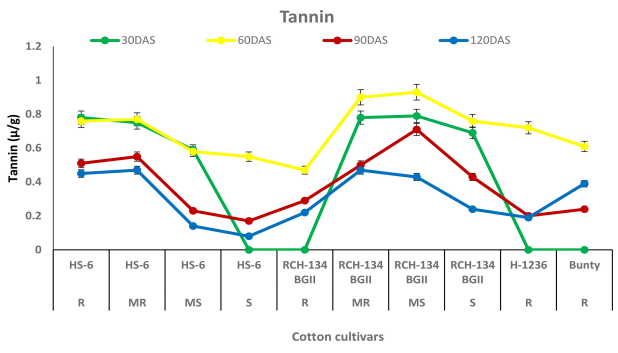

FIGURE 6
Tannin in resistant and susceptible cultivars of cotton estimated at 30, 60, 90, and 120 days after sowing. The susceptible cultivars were Non-Bt (HS 6) and Bt (RCH 134 BGII) with varied disease reactions. Non-Bt H1236 and Bt Bunty were taken as resistant cotton cultivars.

Protein biosynthesis in host plant interaction usually occurs in the incompatible reaction. It has been suggested that the high protein content in the infected plant may be due to the activation of host defense mechanisms between the host and pathogen (Agrios, 2005). The present study found that resistant cultivars H 1236 and Bunty had a high protein content, and even the less diseased plants of susceptible cultivars showed an increase in protein compared to highly diseased plants. This observation clearly indicates that protein plays a role in resistance against CLCuV infection. Our results are in agreement with previous findings that support the association of protein as one of the defense responses against CLCuV in cotton plants (Beniwal et al., 2006; Acharya and Singh, 2008; Siddique et al., 2014).

The physiological responses of stressed plants differ, and chlorophyll is one of the components that may be involved in their response to disease (Kumar et al., 2022). The present study demonstrated that chlorophyll levels increased with disease index and plant age. Research has shown that chlorophyll levels increase in diseased plants due to their role in the intercellular movement of viruses through symplastic pathways within the plant (Zhao et al., 2016). However, our study's findings did not align with this movement of the virus. Nevertheless, we observed a higher rise in chlorophyll in mature susceptible plants than in younger plants in all cultivars, indicating the accumulation of chlorophyll under CLCuV infection. Earlier studies also supported an increase in chlorophyll in susceptible plants (Devlin and Witham, 1983; Reddy et al., 2005; Kandhasamy et al., 2010; Ashfaq et al., 2014; Lal et al., 2021). Limited information exists on the role of chlorophyll in disease reaction; however, studies on its mechanism may provide insight into chlorophyll's involvement in both diseased and mature plants.

In host–pathogen interactions, phenols are considered to be the most important components in the defense response and play a key role in imparting resistance to plant diseases (Kumar et al., 2021). Our study found that resistant cultivars had a higher phenol content compared to susceptible cultivars. These findings are consistent with previous studies that have demonstrated an increase in phenol levels in resistant cultivars of cotton against CLCuV, indicating the secondary level of defense line in the plant (Ajmal et al., 2011). The possible explanation for this is that phenolic compounds help in the synthesis of lignin and suberin, providing mechanical strength to host cells and acting as physical barriers against pathogens (Ngadze et al., 2012; Singh et al., 2014). In our study, the increase in phenolic content also suggests a resistant reaction against CLCuV. Similar results have been observed in okra with high phenol content in the resistant reaction against OYVMV (Manju et al., 2021). However, the classification of phenolics involved in resistance was beyond the scope of this study. Nevertheless, previous research has suggested that phenol content could be used as reliable biochemical markers for early selection of genotype resistant to OELCuD (Yadav et al., 2020).

Gossypol is a toxic terpenoid aldehyde (TA) compound that is released in cotton and is known for its insecticidal properties against insect pests (Heinstein et al., 1979; Widmaier et al., 1980). As CLCuV is transmitted through whiteflies, we investigated the gossypol levels in cotton cultivars in the present study. Surprisingly, we found no evidence of any change in gossypol content in resistant and susceptible cotton plants against CLCuV. Although gossypol is toxic to various insect-pests, nematodes, and fungi (Bell, 1986), there are opportunities to explore its potential antimicrobial and antiviral properties in cotton. Similarly, tannins are an important group of secondary metabolic compounds that play a significant role in plant defense mechanisms against diseases and insect pests (Swain, 1979). In our study, we also analyzed the tannin content and found that susceptible cultivars exhibited a decrease in tannin content with an increase in disease, while resistant cultivars showed a higher tannin content. These results are consistent with the previous findings that tannins play a crucial role in imparting resistance to cotton cultivars against CLCuV (Beniwal et al., 2006; Acharya and Singh, 2008).

The results showed that while sugar and gossypol levels did not provide clear information on the resistance or susceptibility of the plants, other compounds such as protein, chlorophyll, phenols, and tannins can be used as markers for resistance against CLCuV. These findings offer insight into the role of primary and secondary metabolites in hybrid and Bt cotton's resistance to CLCuV.

5 Conclusions

The results showed that resistant cultivars activate proteins, phenols, and tannins against CLCuV, while sugar, gossypol, and chlorophyll, associated with basic physiological and metabolic mechanisms, did not play a significant role in resistance against CLCuV infection in cotton plants. Among the primary biochemical compounds, the activity of proteins was proposed as the first line of defense, while the secondary level of defense line in resistance exhibited the activity of phenols and tannins as the most significant in imparting resistance against CLCuV in cotton. The present study highlights the importance of biochemical studies in understanding the changes occurring in plants under biological stress due to viral infections. The findings provide valuable biochemical information to understand the mechanism of action involved in resistance against CLCuV and can serve as a source of information for the development and differentiation of resistance in cotton plants against CLCuV.

Data availability statement

The original contributions presented in the study are included in the article/Supplementary Material. Further inquiries can be directed to the corresponding authors.

Author contributions

PC and NM: Conceptualization, methodology, investigation, and writing—original draft preparation. RC and AK: Methodology, software, and visualization. RKT and RK: Reviewing and editing. ML: Data curation and revision. HS: Validation. All authors contributed to the article and approved the submitted version.

Acknowledgments

The authors express sincere thanks to the Department of Genetics and Plant Breeding, CCS Haryana Agricultural University, Hisar for providing access to biochemical laboratory for the smooth flow of the study. The authors are also thankful to the head of the Department of Genetics and Plant Breeding for providing analytical help in the results of the experiment. Lastly, the authors extend their acknowledgment to the Department of Plant Pathology of the University for providing timely guidance during the course (and in the writing) of this research.

Conflict of interest

The authors declare that the research was conducted in the absence of any commercial or financial relationships that could be construed as a potential conflict of interest.

Publisher's note

Supplementary material

The Supplementary Material for this article can be found online at: https://www.frontiersin.org/articles/10.3389/fpls.2023.1185337/full#supplementary-material

SUPPLEMENTARY FIGURE 1
CLCuD symptoms on infected plant **(A)** and enation at abaxial side of leaf with white fly infestation **(B)**.

References

Acharya, V. S., and Singh, A. P. (2008). Biochemical basis of resistance in cotton to the whitefly, bemisia tabaci genn. *J. Cotton Res. Dev.* 22 (2), 195–199.

Agrios, G. N. (2005). *Plant pathology. 5th ed* (New York: Elsevier Academic Press).

Ajmal, S., Perveen, R., Chohan, S., Yasmin, G., and Mehmood, M. A. (2011). Role of secondary metabolites biosynthesis in resistance to cotton leaf curl virus (CLCuV) disease. *Afr. J. Biotechnol.* 10 (79), 18137–18141. doi: 10.5897/AJB11.2502

Anonymous (2018). *50 years of cotton research in haryana* Vol. 125004 (Hisar (Haryana: Cotton Section, Department of Genetics and Plant Breeding, CCS Haryana Agricultural University), 102.

Anonymous (2019). "Cotton," in *OECD-FAO agricultural outlook 2019-2028*, (Paris: OECD Publishing), 217–226.

Anuradha (2014). *Genetical and biochemical basis of cotton leaf curl virus disease in gossypium hirsutum l* (Hisar: Department of Plant Pathology. CCS Haryana Agricultural University).

Arnon, D. I. (1949). Copper enzymes in isolated chloroplasts: polyphenoloxidase in beta vulgaris. *Plant Physiol.* 24, 1–15. doi: 10.1104/pp.24.1.1

Ashfaq, M., Khan, M. A., Mukhtar, T., and Sahi, S. T. (2014). Role of mineral metabolism and some physiological factors in resistance against urdbean leaf crinkle virus in blackgram genotypes. *Int. J. Agric. Biol.* 16, 189–194.

Barwale, R. (2016). A perspective on cotton crop in India – opportunities and challenges. *Cotton Stat News.* 10, 1–3.

Bell, A. A. (1986). *Physiology of secondary products* (Memphis, TN: Cotton Foundation).

Beniwal, J., Sharma, J., Kumar, A., and Talwar, G. (2006). Assessment of losses due to leaf curl virus (CLCuV) disease in cotton (Gossypium hirsutum). *J. Cotton Res. Dev.* 20 (2), 272–279.

Bhat, T. (1997). *Source-sink relationship as influenced by late leaf spot in groundnut genotypes* (Dharwad, India: University of Agricultural Science).

Borkar, S. G., and Verma, J. P. (1991). Dynamics of phenols and diphenoloxidase contents of cotton cultivars during hypersensitive and susceptible reaction induced by *Xanthomonas campestris* pv. *malvacearum*. *Indian Phytopathol.* 44 (3), 280–290.

Bray, H. G., and Thorpe, W. Y. (1954). "Analysis of phenolic compounds of interest in metabolism," in *Meth biochem. anal.* Ed. D. Glick (New York: Intersarnae Publishing Inc.), 27–52.

Chakrabarty, P. K., Mukewar, P. M., Raj, S., and Sravan, V. K. (2002). Biochemical factors governing resistance in diploid cotton against grey mildew. *Indian Phytopathol.* 55 (2), 140–146.

Devlin, R. M., and Witham, F. H. (1983). *Plant physiology. 4th ed* (California: PWS Publishers).

DuBois, M., Gilles, K. A., and Hamilton, J. D. (1956). Colorimetric method for determination of sugars and related substances. *Ann. Chern.* 28, 350–356. doi: 10.1021/ac60111a017

Farooq, A., Farooq, J., Mahmood, A., Shakeel, A., Rehman, A., Batool, A., et al. (2011). An overview of cotton leaf curl virus disease (CLCuD) a serious threat to cotton productivity. *Aust. J. Crop Science.* 5 (12), 1823–1831.

Govindappa, N., Hosagoudar, J., and Chattannavar, S. N. (2008). Biochemical studies in bt and non-bt cotton genotypes against *Xanthomonas axonopodis* pv. *malvacearum*. *J. Cotton Res. Dev.* 22 (2), 215–220.

Gupta, V. K., Sharma, R., Singh, S., Jindal, J., and Dilawari, V. K. (2010). Efficiency of bemicia tabaci (Gennadius) population from different plant-hosts for acquisition and transmission of cotton leaf curl virus. *Indian J. Biotechnol.* 9, 271–275.

Hedin, P. A., and McCarty, J. C. (1990). Possible roles of cotton bud sugars and terpenoids in oviposition by the boll we evil. *J. Chem. Ecol.* 16, 757–772. doi: 10.1007/BF01016487

Heinstein, P., Widmaier, R., Wegner, P., and Howe, J. (1979). "Biosynthesis of gossypol," in *Biochemistry of plant phenolics: recent advances in phytochemistry*. Eds. T. Swain, J. B. Harbone and C. F. Sumere (Boston, MA: Springer), 651.

Helrich, K. (1990). *Official methods of analysis of the association of official analytical chemists. 15th ed* (Arlington: Association of Official Analytical Chemists Inc.).

Hiscox, J. D., and Israelstam, G. F. (1979). A method for the extraction of chlorophyll from leaf tissue without maceration. *Can. J. Bot.* 57 (12), 1332–1334. doi: 10.1139/b79-163

Iqbal, Z., Iqbal, M. S., Hashem, A., Abd Allah, E. F., and Ansari, M. I. (2021). Plant defense responses to biotic stress and its interplay with fluctuating dark/light conditions. *Front. Plant Sci.* 12, 631810. doi: 10.3389/fpls.2021.631810

Jayapal, R., and Mahadevan, A. (1968). Biochemical changes in banana leaves in response of leaf spot pathogens. *Indian Phytopathol.* 21, 43–48.

Kandhasamy, S., Ambalavanan, S., and Palanisamy, M. (2010). Changes in physiology and biochemistry of mottle streak virus infected finger millet plants. *Arch. Phytopathol. Plant Protect.* 43, 1273–1285. doi: 10.1080/03235400802404833

Klement, Y., and Goodman, R. N. (1967). The hypersensitive reaction to infection of bacterial and plant pathogens. *Annu. Rev. Phytopathol.* 5, 17–44. doi: 10.1146/annurev.py.05.090167.000313

Kumar, R., Kaundal, P., Arjunan, J., Sharma, S., and Chakrabarti, S. K. (2020). Development of a visual detection method for potato virus s by reverse transcription loop-mediated isothermal amplification. *3 Biotech.* 10, 1–8. doi: 10.1007/s13205-020-02214-4

Kumar, R., Kaundal, P., Tiwari, R. K., Siddappa, S., Kumari, H., Lal, M. K., et al. (2022). Establishment of a one-step reverse transcription recombinase polymerase amplification assay for the detection of potato virus S. *J. Virol. Methods* 307, 114568.

Kumar, R., Kaundal, P., Tiwari, R. K., Lal, M. K., Kumari, H., Kumar, R., et al. (2023). Development of reverse transcription recombinase polymerase amplification (RT-RPA): a methodology for quick diagnosis of potato leafroll viral disease in potato. *Int. J. Mol. Sci.* 24 (3), 2511. doi: 10.3390/ijms24032511

Kumar, R., Tiwari, R. K., Jeevalatha, A., Siddappa, S., Shah, M. A., Sharma, S., et al. (2021). Potato apical leaf curl disease: current status and perspectives on a disease caused by tomato leaf curl new Delhi virus. *J. Plant Dis. Prot.* 128, 897–911. doi: 10.1007/s41348-021-00463-w

Lal, M. K., Sharma, N., Adavi, S. B., Sharma, E., Altaf, M. A., Tiwari, R. K., et al. (2022). From source to sink: mechanistic insight of photoassimilates synthesis and partitioning under high temperature and elevated [CO2]. *Plant Mol. Biol.* 110, 305–324. doi: 10.1007/s11103-022-01274-9

Lal, M. K., Tiwari, R. K., Kumar, R., Naga, K. C., Kumar, A., Singh, B., et al. (2021). Effect of potato apical leaf curl disease on glycemic index and resistant starch of potato (Solanum tuberosum l.) tubers. *Food Chem.* 359, 129939. doi: 10.1016/j.foodchem.2021.129939

Manju, K. P., Vijaya Lakshmi, K., Sarath Babu, B., and Anitha, K. (2021). Morphological and biochemical basis of resistance in okra to whitefly, bemisia tabaci and okra yellow vein mosaic virus (OYVMV). *J. Entomol. Zool. Stud.* 9 (1), 1719–1728.

Monga, D. (2014). "Cotton leaf curl virus disease," in *Technical bulletin* (Nagpur: Central Institute for Cotton Research), 34.

Ngadze, E., Coutinho, T. A., Icishahayo, D., and van der Waals, J. E. (2012). Role of polyphenol oxidase peroxidise, phenylalanine ammonia lyase, chlorogenic acid and total soluble. *Plant Dis.*. 96, 186–192. doi: 10.1094/PDIS-02-11-0149

Patil, L. C., Hanchinal, R. R., Lohithaswa, H. C., Nadaf, H. L., Kalappanavar, I. K., and Megeri, S. N. (2010). Biochemical relationship in resistant and susceptible cultivars of spot blotch infected tetraploid wheat. *Karnataka J. Agric. Sci.* 24 (4), 520–522.

Porter, L. J., Hrstich, L. N., and Chan, B. G. (1986). The conversion of procyanidins and prodelphinidins to cyanidin and delphinidin. *Phytochemistry.* 25, 223–230. doi: 10.1016/S0031-9422(00)94533-3

Qadir, R., Khan, Z. A., Monga, D., and Khan, J. A. (2019). Diversity and recombination analysis of cotton leaf curl multan virus: a highly emerging begomovirus in northern India. *BMC Genomics* 20, 274. doi: 10.1186/s12864-019-5640-2

Reddy, C., Tonapi, V. A., Varanasiappan, S., Navi, S. S., and Jayarajan, R. (2005). Influence of plant age on infection and symptomatological studies on urdbean leaf crinkle virus in urdbean (Vigna mungo). *Int. J. Agric. Sci.* 1, 1–6. Available at: http://oar.icrisat.org/id/eprint/5305.

Sharma, P., and Rishi, N. (2003). Host range and vector relationship of cotton leaf curl virus from northern India. *Indian Phytopathol.* 56, 496–499.

Siddique, Z., Akhtar, K. P., Hameedb, A., Sarwar, N., Imran, U.-H., and Khan, S. A. (2014). Biochemical alterations in leaves of resistant and susceptible cotton genotypes infected systemically by cotton leaf curl burewala virus. *J. Plant Interact.* 9 (1), 702–711. doi: 10.1080/17429145.2014.905800

Singh, R., and Agarwal, R. A. (2004). "Role of chemical components of resistant and susceptible genotypes of cotton and okra in ovipositional preference of leaf hoppers," in *Cotton breeding*. Ed. P. Singh (New Delhi: Kalyani Publishers), 136–146.

Singh, H. P., Kaur, S., Batish, D. R., and Kohli, R. K. (2014). Ferulic acid impairs rhizogenesis and root growth, and alters associated biochemical changes in mung bean (Vigna radiata) hypocotyls. *J. Plant Interact.* 9, 267–274. doi: 10.1080/17429145.2013.820360

Swain, T. (1979). Phenolics in the environment. *Recent Adv. Phytochem.* 12, 617–640. doi: 10.1007/978-1-4684-3372-2_19

Widmaier, R., Howe, J., and Heinstein, P. (1980). Prenyltransferase from *Gossypium hirsutum*. *Arch. Biochem. Biophys.* 200 (2), 609–616. doi: 10.1016/0003-9861(80)90394-X

Wilson, F. D., and Smith, J. N. (1976). Some genetic relationship between gland density and gossypol content in g. hirsutum. *Crop Sci.* 16, 830–832. doi: 10.2135/cropsci1976.0011183X001600060023x

Yadav, Y., Maurya, P. K., and Bhattacharjee, T. (2020). Inheritance pattern of okra enation leaf curl disease among cultivated species and its relationship with biochemical parameters. *J. Genet.* 99 (84), 1–12. doi: 10.1007/s12041-020-01241-7

Yang, J. W., Yi, H. S., Kim, H., Lee, B., Lee, S., Ghim, S. Y., et al. (2011). Whitefly infestation of pepper plants elicits defence responses against bacterial pathogens in leaves and roots and changes the below-ground microflora. *J. Ecol.* 99, 46–56. doi: 10.1111/j.1365-2745.2010.01756.x

Zhao, J., Zhang, X., Hong, Y., and Liu, Y. (2016). Chloroplast in plant-virus interaction. *Front. Microbiol.* 7, 1565. doi: 10.3389/fmicb.2016.01565

frontiers | Frontiers in Plant Science

TYPE Original Research
PUBLISHED 07 June 2023
DOI 10.3389/fpls.2023.1176513

OPEN ACCESS

EDITED BY
Ravinder Kumar,
Central Potato Research Institute (ICAR), India

REVIEWED BY
Subhas Hajeri,
Citrus Pest Detection Program, United States
Susheel Kumar Sharma,
Indian Agricultural Research Institute (ICAR), India
Madhurababu Kunta,
Texas A&M University Kingsville, United States

*CORRESPONDENCE
Ester Marco-Noales
marco_est@gva.es

RECEIVED 28 February 2023
ACCEPTED 05 May 2023
PUBLISHED 07 June 2023

CITATION
Morán F, Herrero-Cervera M, Carvajal-Rojas S and Marco-Noales E (2023) Real-time on-site detection of the three '*Candidatus* Liberibacter' species associated with HLB disease: a rapid and validated method.
Front. Plant Sci. 14:1176513.
doi: 10.3389/fpls.2023.1176513

Real-time on-site detection of the three '*Candidatus* Liberibacter' species associated with HLB disease: a rapid and validated method

Félix Morán[1], Mario Herrero-Cervera[1], Sofía Carvajal-Rojas[2] and Ester Marco-Noales[1*]

[1]Instituto Valenciano de Investigaciones Agrarias (IVIA), Centro de Protección Vegetal y Biotecnología, Unidad de Bacteriología, Moncada, Valencia, Spain, [2]Universidad de Costa Rica (UCR), Centro de Investigación en Biología Celular y Molecular (CIBCM), Laboratorio de Fitopatógenos Obligados y sus Vectores (LaFOV), San José, Costa Rica

Huanglongbing (HLB) is a devastating disease that affects all commercial citrus species worldwide. The disease is associated with bacteria of three species of the genus '*Candidatus* Liberibacter' transmitted by psyllid vectors. To date, HLB has no cure, so preventing its introduction into HLB-free areas is the best strategy to control its spread. For that, the use of accurate, sensitive, specific, and reliable detection methods is critical for good integrated management of this serious disease. This study presents a new real-time recombinase polymerase amplification (RPA) protocol able to detect the three '*Ca*. Liberibacter' species associated with HLB in both plant and insect samples, validated according to European and Mediterranean Plant Protection Organization (EPPO) guidelines and tested on 365 samples from nine different geographic origins. This new protocol does not require nucleic acid purification or specialized equipment, making it ideal to be used under field conditions. It is based on specific primers and probe targeting a region of *fusA* gene, which shows a specificity of 94%–100%, both *in silico* and *in vitro*, for the '*Ca*. Liberibacter' species associated with HLB. The analytical sensitivity of the new protocol is excellent, with a reliable detection limit in the order of 10^1 copies per microliter in HLB-infected plant and insect material. The repeatability and reproducibility of the new methods showed consistent results. Diagnostic parameters of the new RPA protocol were calculated and compared with the gold standard technique, a quantitative real-time PCR, in both crude extracts of citrus plants and insect vectors. The agreement between the two techniques was almost perfect according to the estimated Cohen's kappa index, with a diagnostic sensitivity and specificity of 83.89% and 100%, respectively, and a relative accuracy of 91.59%. Moreover, the results are obtained in less than 35 min. All these results indicate the potential of this new RPA protocol to be implemented as a reliable on-site detection kit for HLB due to its simplicity, speed, and portability.

KEYWORDS

Huanglongbing, rapid-screening test, in situ, KIT, RPA (recombinase polymerase amplification)

1 Introduction

Citrus is the most widely grown fruit crop in the world, so threats to this crop pose a risk to the socio-economic network of many countries. One of the weak points of citrus is its vulnerability to fungi, bacteria, and viruses (Ghosh et al., 2022), which can alter the normal growth of the plant, the development of leaves and branches, and the organoleptic properties of the fruit.

To date, one of the most destructive diseases for citrus is the Huanglongbing (HLB), also known as citrus greening, which affects all commercial citrus species and cultivars, severely reducing both crop yield and tree longevity (Bové, 2006).

HLB disease is associated with three uncultured bacterial species of the genus *Liberibacter* (family Rhizobiaceae, class Alphaproteobacteria, order Rhizobiales): '*Candidatus* Liberibacter asiaticus' (CaLas), '*Candidatus* Liberibacter africanus' (CaLaf), and '*Candidatus* Liberibacter americanus' (CaLam). These bacteria live in the plant phloem and are mainly transmitted by sap-sucking insects of the family Psyllidae. Specifically, the Asian citrus psyllid *Diaphorina citri* (Hemiptera: Liviidae) is the natural vector of CaLas and CaLam, and the African citrus psyllid *Trioza erytreae* (Hemiptera: Triozidae) is the natural vector of CaLaf, although, under experimental conditions, the African psyllid is capable to transmit CaLas (Massonie et al., 1976; Reynaud et al., 2022), and the Asian citrus psyllid is capable of transmitting CaLaf (Lallemand et al., 1986).

The three '*Ca*. Liberibacter' species associated with HLB are spread across several countries in Asia, Africa, and the Americas (EPPO Global Database, 2023), where they are causing devastation to millions of citrus trees in major citrus-producing countries (Das, 2008; Das et al., 2014; Neupane et al., 2016; da Costa et al., 2021). At present, none of these three bacteria have been reported in the Mediterranean Basin or Australia. However, in recent years, as a result of globalization, climate change, and the presence of the two insect vectors in the Mediterranean Basin (Pérez Otero et al., 2015; Wang, 2020; Ministry of Agriculture and Rural Development of Israel, 2022), HLB disease has become the most serious threat to the citrus sector in this area, especially for important European citrus-exporting countries, such as Spain.

Typical symptoms of HLB include diffuse yellow mottling of leaves, reduction in fruit size, and loss of organoleptic quality, as well as stunting of trees (Bové, 2006; Dala-Paula et al., 2019). As bacteria move slowly along vessels with a heterogeneous distribution throughout the different parts of the tree (Tatineni et al., 2008), symptoms appear several years after the first infection, making detection a challenge. Moreover, the asymptomatic spread of the disease hinders its control (Lee et al., 2015).

At present, the HLB citrus disease has no cure, and the best way to prevent its spread is to implement integrated disease management, applying a combination of strategies that include the early detection of bacteria in order to eradicate infected trees (Alquezar et al., 2022). In this context, it is essential the development of efficient, accurate, and rapid HLB diagnostic tools for specific bacterial detection.

Over the years, many different techniques have been developed for HLB diagnosis (Valdés et al., 2016; Ghosh et al., 2022), but molecular techniques are currently the most widely used for the diagnosis of plant pathogenic bacteria, including those associated with HLB, as they have a higher sensitivity and specificity than others (Sapre et al., 2021). Within the molecular detection techniques, the polymerase chain reaction (PCR) is the gold standard reference technique for HLB diagnosis (Valdés et al., 2016; Morán et al., 2020). In this regard, according to the latest HLB diagnostic protocols published by the European and Mediterranean Plant Protection Organization (EPPO) and the International Plant Protection Convention (IPPC), PCR protocols that amplify partial regions of several genes (Jagoueix et al., 1996; Hocquellet et al., 1999; Teixeira et al., 2005; Li et al., 2006; Lin et al., 2010; Morgan et al., 2012; Zheng et al., 2016; de Chaves et al., 2023) are the most recommended for the detection of '*Ca*. Liberibacter' spp. in both symptomatic and asymptomatic plant samples and insect vectors (EPPO, 2021b; IPPC-FAO, 2022).

Although PCR-based detection methods are indeed the most appropriate for laboratory screening, they have several limitations when used outside of a laboratory setting (Ivanov et al., 2021), as they require specialized equipment, trained personnel, and, in most cases, a nucleic acid purification step, making them not the most suitable tool for a first quick *in situ* diagnosis. Therefore, it is necessary to look for alternative techniques that involve less sample processing time and simple equipment for rapid on-site diagnosis.

In the last decade, new techniques based on isothermal amplification of nucleic acids have emerged, and their use has increased in the diagnosis of plant pathogenic microorganisms (Patel et al., 2022). They are a good option for rapid field detection. In recent years, several HLB detection protocols based on isothermal amplification have been developed: eight LAMP protocols (Li et al., 2012; Rigano et al., 2014; Ghosh et al., 2016; Wu et al., 2016; Qian et al., 2017; Choi et al., 2018; Stolowicz et al., 2022; Thoraneenitiyan et al., 2022) and three recombinase polymerase amplification (RPA) protocols (Ghosh et al., 2018; Li et al., 2022; Rattner et al., 2022). All these isothermal amplification methods were designed to detect a single species of '*Ca*. Liberibacter' associated with HLB, CaLas, probably because it is the most widespread species, is the most related to huge economic losses, and has the highest potential for spread (Lee et al., 2015; Taylor et al., 2019; Ajene et al., 2020). However, climate change and the consequences of accelerated globalization could increase the possibility of other HLB-associated bacteria invading disease-free areas as well. Thus, for HLB-free regions, such as the Mediterranean Basin and Australia, CaLam and CaLaf also pose a serious hazard that should not be underestimated, even more so when the African vector, *T. erytreae*, is already present and expanding in Spain and Portugal. In addition, it is very important that a method of such significance be validated according to the standards of organizations in the scope of agriculture and plant protection, which guarantees its robustness and reliability.

Therefore, the objective of this work has been the development and validation, according to EPPO guidelines, of a rapid, sensitive, and specific detection method for the diagnosis of HLB, which can be applicable in on-site conditions. For this purpose, we have used real-time RPA methodology, selecting highly specific primers and probe for the three species of '*Ca*. Liberibacter' associated with this devastating citrus disease.

2 Material and methods

2.1 Plant and insect material

A total of 141 plant and insect samples and bacterial suspensions were quantified by real-time PCR (de Chaves et al., 2023) and comparatively analyzed by the new real-time RPA developed in this work (Supplementary Table S1). Particularly, 131 samples of nine different '*Ca*. Liberibacter' spp. hosts from nine different geographic origins were used for the evaluation of the analytical specificity of the new detection method.

More precisely, a total of 76 positive samples used for validation included the following: i) symptomatic and asymptomatic plant material from species *Citrus sinensis* cv. Valencia, *Citrus hystrix*, *Citrus* sp., and Rusk citrange from Brazil (São Paulo and Paraná), Costa Rica (Alajuela), Cuba (Artemisa), and the plant collection of National Research Institute for Agriculture Food and the Environment (INRAE); and ii) insect samples of the species *D. citri* from the USA. A total of 65 negative samples included plant material of the species *C. sinensis* cv. Lane Late, *Citrus clementina* cv. Clemenules, and *Citrus limon* cv. Fino Mesero from Spain (Valencia) and insect samples of *D. citri* from the USA (Florida) and *T. erytreae* from Spain and South Africa. In addition, four suspensions at 10^6 CFU/ml of bacterial species *Agrobacterium tumefaciens* (strain C58/ATCC 33970), *Agrobacterium vitis* (strain 339), *Liberibacter crescens* (strain BT-1), '*Ca*. Liberibacter solanacearum', *Xylella fastidiosa* subsp. *pauca* (CFBP 8072), *X. fastidiosa* subsp. *fastidiosa* (IVIA 5770), *X. citri* subsp. *citri* (CFBP 2911), *Spiroplasma citri* (NCPPB 3095), and *Pseudomonas syringae* pv. *syringae* (IVIA 2827) were used as bacterial negative controls.

In order to evaluate the new detection method under field conditions, a total of 226 samples were collected in three random surveys performed in two countries where HLB disease is present and one country where the disease is absent: 140 samples were collected in Brazil (Matão, São Paulo), 66 in Costa Rica (Santa Eulalia, Alajuela), and 20 in Spain (Moncada, Valencia) (geographical coordinates, DD, according to Google Maps: −21.53, −48.6; 10.02, −84.36; and 39.58, −0.39 respectively). Surveys were conducted on private land, with permission of the owners, and in accordance with current national and international legislation, as no special permits were required.

The presence/absence and absolute quantification of '*Ca*. Liberibacter spp.' in all samples were determined using the real-time qPCR detection protocol described by de Chaves et al. (2023) from DNA purification of each sample. The identification of the '*Ca*. Liberibacter' species associated with HLB was performed by partial Sanger sequencing of the 16S rRNA gene following the protocol described by Morán et al. (2020).

2.2 Crude extract preparation and DNA purification

Plant samples were prepared from five citrus leaf petioles, which were placed and ground in individual plastic bags (Bioreba, Reinach, Switzerland) containing phosphate-buffered saline (PBS) (8.0 g of NaCl, 2.9 g of $Na_2HPO_4{\cdot}12\ H_2O$, 0.2 g of KH_2PO_4, and 0.2 g of KCl; pH 7.2) at a rate of 1:5 (w:v). Insect samples were prepared from individual specimens, which were squashed on Whatman paper (GE Healthcare, Europe), according to the method described by Bertolini et al. (2014); the membranes were then resuspended with 100 µl of 0.05% Tween 20.

Fresh crude plant extracts and insect extracts were used as direct samples for RPA analysis and to perform DNA purifications. DNA was purified from 400 µl of crude plant extracts and 90 µl of squashed insect extracts following the cetyl trimethylammonium bromide (CTAB) method recommended by the EPPO protocol PM7/121 (2) (EPPO, 2021b), without the addition of beta-mercaptoethanol. Quantification of total DNA was performed using a DeNovix DS-11 spectrophotometer (DeNovix Inc., Wilmington, DE, USA). Crude plant and squashed insect extracts and DNA purifications were stored at −20°C until use.

2.3 Complete genome analysis and design of primers and probe for recombinase polymerase amplification

The search for a highly conserved region was performed by multiple alignments of 11 complete genomes (accessed January 2023) using the package MAUVE (Darling et al., 2004). Specifically, nine complete genomes of '*Ca*. Liberibacter asiaticus' (GenBank accession numbers: NZ_CP010804.2, NC_020549.1, NZ_AP014595.1, NZ_CP019958.1, NC_012985.3, NZ_CP061535.1, NZ_CP040636.1, NZ_CP054558.1, and NZ_CP041385.1) (Zhou et al., 2011; Lin et al., 2013; Katoh et al., 2014; Zheng et al., 2014; Petrone et al., 2019; Lu et al., 2021; Wang et al., 2021; Zheng et al., 2022a; Zheng et al., 2022b), one of '*Ca*. Liberibacter africanus' (NZ_CP004021.1) (Lin et al., 2015), and one of '*Ca*. Liberibacter americanus'(NC_022793.1) (Wulff et al., 2014) were aligned. To select the most appropriate RPA target region, the level of conservation of 17 housekeeping genes (*rplL*, *rplJ*, *rpoB*, *rpoC*, *recA*, *glnA*, *fumC*, *gyrA*, *gyrB*, *metG*, *fusA*, *infB*, *mutS*, *grpE*, *dnaA*, *dnaG*, and *atpD*) was evaluated based on their alignment identity percentage (AIP) values.

The Proksee tool (Proksee, n.d.) was used to visualize the genomic map by BLAST comparison of the different isolates of '*Ca*. Liberibacter' spp.

The design of primers and probe of RPA was accomplished following the recommendations stipulated in the TwistAmp® Assay Design Manual (TwistAmp®, 2018). The free online tool OligoAnalyzer™ 3.1 (Owczarzy et al., 2008) (OligoAnalyzer Tool - IDT) was used to check the GC content percentage and melting temperature and to identify the secondary structures of the primers and probe.

Primers and probe of the new real-time RPA were designed in a region of *fusA* gene targeting a sequence of 201 bp. Primers designed were RPA-HLB-F2 (5′-ATAAAARTCCGC[deoxyinosine]CCCATCTTATCCATTTTATTG-3′) and RPA-HLB-R2 (5′-TATTGATACTCCTGG[deoxyinosine]CARGTTGATTTTACTA-3′), and the probe for detection of the amplification product was RPA-HLB-P2 (5′-ATACTTATCAGCCTGACGCCATACCGTTTC

[FAM-dT][THF][BHQ1-dT]TTGCGGTTCAACACC[Spacer3]-3′). To detect the three '*Ca.* Liberibacter' spp. associated with HLB, deoxyinosine molecules were included in both primers as internal modifications.

2.4 Primer test by conventional PCR and basic RPA

To evaluate the new primers designed for RPA, they were tested in conventional PCR and RPA formats. Conventional PCR was performed using GoTaq® Hot Start Polymerase (Promega Corporation, USA). The reaction mixture contained 1× GoTaq® Hot Start Polymerase PCR buffer, 3 mM of $MgCl_2$, 0.2 mM of each dNTP, 600 mM of each RPA primer, and 2.5 U of GoTaq® DNA polymerase in a total volume of 25 µl with 50 ng of DNA template. PCR amplification was performed in a Veriti 96 Well thermal cycler (Applied Biosystems, Foster City, CA, USA), and conditions consisted of one initial denaturalization cycle of 3 min at 94°C followed by 40 cycles of 30 s at 94°C, 40 s at 50°C, and 45 s at 72°C, with a final extension step of 72°C for 10 min.

Basic RPA was performed using TwistAmp Liquid Basic kit (TwistDx, Maidenhead, UK) following the manufacturer's indications. Optimized reaction mix consisted of 1× reaction buffer, 0.5 mM of each dNTP, 1× Basic E-mix, 1× Core Reaction Mix, 600 mM of each RPA primer, and 19 mM of MgOAc in a total volume of 50 µl with 1 µl of crude extract. RPA amplification conditions were adjusted in a Veriti 96 Well thermal cycler (Applied Biosystems, Foster City, CA, USA), consisting of a single incubation of 30 min at 45°C. All mixtures were shaken 5 min after the start of the reaction.

Amplicons were purified using mi-PCR Purification Kit (Metabion International AG, Germany) and visualized in 1.5% (w/v) agarose gel with GoodView™ staining (SBS Genetech Co., Ltd., China) after electrophoresis in 0.5× TAE buffer (40 mM of Tris; 20 mM of CH_3COOH; 1 mM of EDTA, pH 7.6).

2.5 Real-time RPA

For real-time RPA, the TwistAmp Liquid Exo kit (TwistDx, Maidenhead, UK) was used according to the manufacturer's instructions. The optimized reaction mix consisted of 1× reaction buffer, 0.45 mM of each dNTP, 1× Probe E-mix, 600 mM of each RPA primer, 200 nM of RPA probe, 1× Core Reaction Mix, 1× Exo, and 19 nM of MgOAc in a total volume of 50 µl with 1 µl of crude extract. Reaction incubation and fluorescence signal reading were performed using fluorimeters AmplifyRP® XRT (Agdia, Île-de-France, France) or Genie® II (OptiGene, Horsham, UK), consisting of 45°C for 35 min. All mixtures were shaken 5 min after the start of the reaction.

2.6 Validation of real-time RPA

The real-time RPA method developed in this study was validated according to the guidelines described in the EPPO diagnostic protocol for regulated pests PM 7/98 (5) (EPPO, 2021a) about the specific requirements for laboratories preparing accreditation for a plant pest diagnostic activity.

Thus, the following parameters were evaluated: i) analytical sensitivity, ii) analytical specificity, iii) selectivity, iv) repeatability, v) reproducibility, vi) diagnostic sensitivity and specificity, and vii) relative accuracy.

2.6.1 Analytical sensitivity

Analytical sensitivity of real-time RPA was evaluated by testing, in triplicate, 10-fold serial dilutions of healthy extracts of *C. sinensis* cv. Lane spiked with known amounts (10^5 to 4 copies/µl) of synthetic gBlocks (Integrated DNA Technologies, USA) containing the RPA target sequence (223 bp) of *fusA* gene from species CaLas, CaLaf, and CaLam (NZ_CP019958.1; NZ_CP004021.1 and NC_022793.1) (Supplementary Material). Avogadro constant was used to estimate the number of double- stranded DNA (dsDNA) copies (6.023×10^{23} molecules/mol) in each dilution.

Analytical sensitivity was also evaluated in plant and insect material by two approaches: one using HLB-infected material diluted in healthy extracts and the other using crude healthy extracts spiked with synthetic dsDNA. For HLB-infected material, three replicates of 10-fold serially diluted (from 10^{-1} to 10^{-6}) crude CaLas-infected extracts (samples 12,112.6 and 11,661.7) in healthy extracts were analyzed. Absolute quantification of CaLas was performed in each dilution by real-time PCR according to de Chaves et al. (2023).

Furthermore, in order to evaluate the limit of detection (LOD) in infected samples, 76 positive samples infected with CaLas, CaLaf, and CaLam isolates were quantified by real-time qPCR (de Chaves et al., 2023), and the absolute result was compared with the new real-time RPA protocol.

2.6.2 Analytical specificity and selectivity

Inclusivity was evaluated by analyzing a range of different isolates of '*Ca.* Liberibacter' species from Brazil, Cuba, Costa Rica, INRAE collection, and the USA, infecting *C. sinensis* cv. Valencia, *Citrus* × *hystrix*, *Citrus* × *reshni*, Rusk citrange, *Citrus* sp., and *D. citri*. A total of 35 amplicons positive by real-time RPA, which were selected as representative of different origins and hosts, were purified as described above and sequenced through Sanger sequencing methods in both directions (forward and reverse DNA strands) using the new RPA primers designed (see Section 3.1).

Sequences were analyzed using Geneious Prime 2022 software (Biomatters Ltd., Auckland, New Zealand) and submitted to GenBank database. In addition, *in silico* inclusivity and exclusivity were evaluated by BLASTN comparison of the designed RPA primers and probe against nucleotide NCBI database of RefSeq genomes of Rhizobiaceae family (NCBI:txid82115 accessed January 2023).

The exclusivity of real-time RPA was assessed by analyzing a set of relevant non-target bacteria composed of species phylogenetically close to those associated with HLB (*L. crescens* and '*Ca.* Liberibacter solanacearum') and citrus pathogenic species (*P. syringae* pv. *syringae*, *X. fastidiosa*, *X. citri* subsp. *Citri*, and *S. citri*) (Supplementary Table S1).

Real-time RPA selectivity was evaluated by testing extracts of HLB-infected samples from four different citrus cultivars and one vector species from five different geographical origins (Supplementary Table S1). In addition, symptomatology in plant material was taken into account in random surveys performed in countries where HLB is present, in order to test the detection capability of real-time RPA in both symptomatic and asymptomatic plants.

2.6.3 Repeatability and reproducibility

The repeatability and reproducibility of real-time RPA were evaluated using 10 plant samples (473, 607, 614, 615, 623, 627, 631, 633, 635, and 641) of *C. sinensis* cv. Valencia, originating from Costa Rica (Alajuela), infected with relatively low CaLas titers (low Cqs values, according to the real-time qPCR test by de Chaves et al. (2023). Each crude extract sample selected was analyzed using two fluorimeters: AmplifyRP® XRT (Agdia, Île-de-France, France) and Genie® II (OptiGene, Horsham, UK). For each instrument, three independent replicates were carried out on different days and by two different operators.

2.6.4 Diagnostic sensitivity and specificity

Validation of real-time RPA, by comparison with real-time qPCR (de Chaves et al., 2023), was performed on 226 total samples collected in two random surveys conducted in Costa Rica and Brazil, as described in Section 2.1. Each sample was analyzed in triplicate by real-time qPCR and real-time RPA. In order to confirm the correct *fusA* gene amplification by real-time RPA, a selection of 27 positive samples from random surveys were sequenced as described in Section 2.6.2.

Correlation results (PA, positive agreement; PD, positive deviation; ND, negative deviation; NA, negative agreement) were used to calculate the diagnostic sensitivity (PA/[PA + ND]), diagnostic specificity (NA/[NA + PD]), and relative accuracy ([PA + NA]/[PA + PD + ND + NA]) of real-time RPA. The agreement between techniques was evaluated using Cohen's kappa index (Cohen, 1960), which indicates the proportion of agreement beyond that expected by chance. The benchmarks of Landis and Koch (Landis and Koch, 1977) were used to categorize Cohen's kappa index, where < 0.00 is poor agreement, 0 to 0.2 is slight agreement, 0.21 to 0.40 is fair agreement, 0.41 to 0.60 is moderate agreement, 0.61 to 0.80 is substantial agreement, and 0.81 to 1.00 is almost perfect agreement.

3 Results

3.1 Design and evaluation of RPA primers and probe

Complete genome alignment of 11 '*Ca.* Liberibacter' isolates associated with HLB disease (psy62, gxpsy, A4, Ishi-1, JXGC, JRPAMB1, TaiYZ2, CoFLP, ReuSP1, PTSAPSY, and São Paulo) was used to select the most appropriate RPA target region. Genes *rplL*, *rplJ*, *glnA*, *gyrA*, *metG*, *infB*, *mutS*, *grpE*, *dnaA*, and *dnaG* were discarded for having AIP values ≤ 93%. Since high AIP values increase the probability of finding conserved regions that allow the design of oligos capable of hybridizing only with the three *Liberibacter* species associated with HLB, housekeeping genes *rpoB*, *rpoC*, *recA*, *fumC*, *fusA*, *gyrB*, and *atpD*, with AIP values ≥ 93%, were initially selected for primer and probe design (Figure 1). Finally, *fusA* gene, with AIP 93.7%, was the one that presented a more appropriate region for the design of the primers and the probe, which are usually large (30–36 nt for primers and 46–52 nt for probe). The gene *fusA*, which is present in a single copy per genome, encodes the elongation factor G, a molecule involved in the protein translation process in prokaryotes.

The results of the *in silico* specificity evaluation of the RPA primers, performed by BLASTN against RefSeq genomes of the Rhizobiaceae family, showed high inclusivity and exclusivity. Percentage identity ranged from 85% to 100% only with '*Ca.* Liberibacter' species, and no nucleotide homologies were found with any other species of the family Rhizobiaceae. Specifically, the primers showed 94%–100% identities with the '*Ca.* Liberibacter' spp. associated with HLB and identity values below 91% with '*Ca.* Liberibacter solanacearum'. While *in silico* evaluation of the specificity of the RPA probe showed good inclusivity, with 85%–100% sequence homology with the HLB-associated '*Ca.* Liberibacter' spp. with respect to exclusivity, the RPA probe showed identity homologies lower than 85% with other bacterial species of the Rhizobiaceae family, such as *Ensifer mexicanus*, *A. vitis*, *Rhizobium glycinendophyticum*, and *Rhizobium croatiense*, whose hosts are not citrus plants.

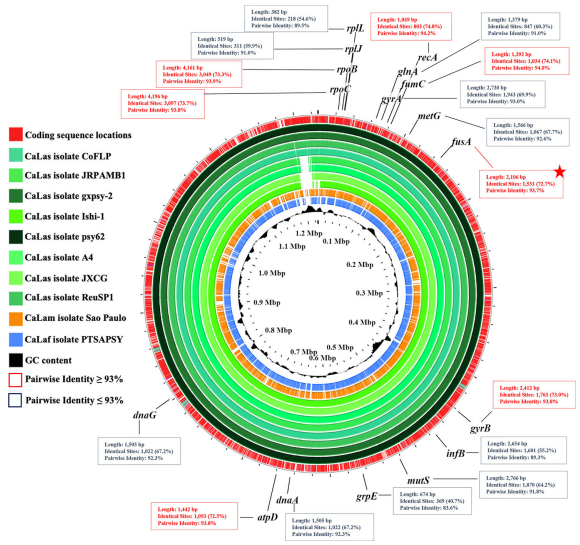

FIGURE 1
Genomic map, performed by BLASTN with Proksee tool, of 11 '*Candidatus* Liberibacter' isolates associated with Huanglongbing (HLB) disease from different origins (isolates psy62, gxpsy, A4, Ishi-1, JXGC, JRPAMB1, TaiYZ2, CoFLP, ReuSP1, PTSAPSY, and São Paulo). The map shows the 17 housekeeping genes evaluated for the design of primers for RPA technique (*rplL*, *rplJ*, *rpoB*, *rpoC*, *recA*, *glnA*, *fumC*, *gyrA*, *gyrB*, *metG*, *fusA*, *infB*, *mutS*, *grpE*, *dnaA*, *dnaG*, and *atpD*), with their MAUVE alignment pairwise identity percentage values. Genes with pairwise identity values ≥ 93% are highlighted in red boxes, and red star shows the target gene selected for the design of primers and probe.

With respect to *in vitro* specificity evaluation of RPA primers, performed by conventional PCR and RPA, amplification of total DNA from 35 positive control samples selected among citrus plant material and insect vectors (Supplementary Table 1) showed the expected single product of 201 bp in all of them, while in negative samples there was an absence of non-specific amplifications (Supplementary Figure 1). In addition, positive and negative results obtained by both conventional methods coincided in all the control samples analyzed. The 35 PCR products sequenced from different bacterial hosts originating from Brazil, Costa Rica, Cuba, and the USA showed sequences identities of 98.5 to 100% with *fusA* gene of '*Ca*. Liberibacter' spp. associated with HLB disease.

3.2 Validation of the new real-time RPA

3.2.1 Analytical sensitivity

Analytical sensitivity results, evaluated on healthy crude extracts spiked with known amounts of synthetic dsDNA, showed that the real-time RPA can detect synthetic sequences of the three species associated with HLB (CaLas, CaLam, and CaLaf) with a LOD that was at units of copies per microliter (4 to 8 copies/µl). More consistent LOD results were obtained with synthetic dsDNA of CaLas-gBlocks, in which the three replicates evaluated were positive, than with CaLaf- and CaLam-gBlocks, in which of the three replicates only two and one, respectively, were positive (Table 1).

The results of analytical sensitivity on HLB-infected material, diluted in healthy extract, showed amplifications in a time period ranging from 4 to 20 min, with a real-time RPA LOD at tens of copies per microliter (3.95×10^1 to 4.37×10^1 copies/µl), in both crude extracts of citrus plants and insect vectors. With the real-time qPCR by de Chaves et al. (2023), units of copies per microliter (3.95 to 4.37 copies/µl) from total DNA purified were detected (Table 2) (Supplementary Figure 2). LOD results of real-time RPA in HLB-infected plant material were more consistent than in HLB-infected insect material since in plant material two of three replicates were positive, while in insect material it was only one. With HLB-infected material (non-diluted), similar results were obtained since the new real-time RPA technique was capable of detecting up to tens of copies per microliter, between 2.6×10^6 and 1.08×10^1 copies/µl, but not bacterial titers lower than 7 copies/µl (Supplementary Table 1).

3.2.2 Analytical specificity and selectivity

Regarding the inclusivity results of the new real-time RPA, it was able to detect CaLas, CaLaf, and CaLam on HLB-infected samples from nine different origins (São Paulo and Paraná of Brazil, Alajuela of Costa Rica, Florida of the USA, Artemisa of Cuba, and INRAE collection) and five different HLB-hosts (*C. sinensis* cv. Valencia, Rusk citrange, *C. hystrix*, *Citrus* sp., and *D. citri*).

All the sequence analyses of the 35 real-time RPA products, selected as representing different origins and hosts of HLB, corresponded to *fusA* gene of '*Ca*. Liberibacter' species. Identity percentage sequences obtained by BLASTN showed values ranging from 99.2% to 100% with CaLas (isolate A4), 98.5% to 100% with CaLam (isolate São Paulo), and 98.5% to 100% with CaLaf (isolate PTSAPSY). New obtained partial sequences of *fusA* gene were submitted to GenBank database (GenBank accession numbers: OQ507405 to OQ507466).

Concerning the exclusivity, the non-target bacteria *A. vitis* (IVIA 339/26), *A. tumefaciens* (strain C58), *Liberibacter crecens* (strain BT-1), and '*Ca*. Liberibacter solanacearum' did not show amplification with the new real-time RPA protocol. The same results were obtained when evaluating the strains of citrus phytopathogenic bacteria *X. fastidiosa* subsp. *pauca* (strain CFBP 8072), *X. fastidiosa* subsp. *fastidiosa* (IVIA 5770), *X. citri* subsp. *citri* (CFBP 2911), *P. syringae* pv. *syringae* (IVIA 2827), and *S. citri* (NCPPB 3095). Also, there were no specific amplifications in negative samples of *C. sinensis* cv. Lane Late, *C. clementina* cv. Clemenules, *C. limon* cv. Finomesero, *Citrus reshni*, *D. citri*, and *T. erytreae*. These results coincided with the real-time qPCR results obtained (Supplementary Table 1).

Regarding the selectivity of the real-time RPA protocol, it was able to detect isolates of '*Ca*. Liberibacter' spp. on five HLB-infected

TABLE 1 Analytical sensitivity evaluation of the new real-time RPA protocol, performed with known amounts of synthetic dsDNA spiked in healthy crude extracts of *Citrus sinensis* cv. Lane.

Real- time RPA results (total copy number of target analyzed)*							
Synthetic DNA	Dilutions of healthy extracts of *C. sinensis* cv. Lane spiked with synthetic DNA						
	10^{-1}	10^{-2}	10^{-3}	10^{-4}	10^{-5}	10^{-6}	10^{-7}
CaLas-gBlocks	+++	+++	+++	+++	+++	+++	+++
	(4×10^5)	(4×10^4)	(4×10^3)	(4×10^2)	(4×10^1)	(40)	(4)
CaLaf-gBlocks	+++	+++	+++	+++	+++	+++	++-
	(6×10^5)	(6×10^4)	(6×10^3)	(6×10^2)	(6×10^1)	(60)	+- -
CaLam-gBlocks	+++	+++	+++	+++	+++	++-	+–
	(8×10^5)	(8×10^4)	(8×10^3)	(8×10^2)	(8×10^1)	(80)	(8)

RPA, recombinase polymerase amplification.
*Avogadro constant was used to estimate the number of double- stranded DNA (dsDNA) (6.023×10^{23} molecules/mol) in each dilution.
Upper row of each box: RPA reaction of each of three replicates (positive reaction, +; negative reaction, -); lower row: copy number as quantified by real-time PCR from de Chaves et al. (2023).

TABLE 2 Analytical sensitivity evaluation of the new real-time RPA and absolute quantification by real-time PCR of HLB-infected citrus and insect material 10-fold serial diluted on healthy material.

Host	Dilutions in healthy plant extracts	Real- time RPA	Quantification by real-time PCR (copies/µl)*
		Crude extract	Total DNA purified
Citrus hystrix (sample 12112.6)	1:10	+++	2.55×10^5
	1:100	+++	6.67×10^4
	1:1000	+++	4.51×10^3
	1:10,000	+++	4.95×10^2
	1:100,000	++-	2.95×10^1
	1:1.000,000	- - -	3.95
	Healthy plant material	- - -	- - -
Diaphorina citri (sample 11661.7)	1:10	+++	6.35×10^5
	1:100	+++	7.62×10^4
	1:1000	+++	2.17×10^3
	1:10,000	+++	3.84×10^2
	1:100,000	+ - -	5.61×10^1
	1:1,000,000	- - -	4.37
	Healthy insect material	- - -	- - -

RPA, recombinase polymerase amplification; HLB, Huanglongbing.
* Absolute quantification performed with efficiency > 95% of real-time PCR by de Chaves et al. (2023).
The results by real-time RPA are coded with + for positive reactions, and - for negative reactions, in three replicates per diltuion of each sample.

different citrus species and cultivars, as well as different insect specimens of *D. citri*. Specifically, the results showed that the new real-time RPA was able to detect '*Ca.* Liberibacter' spp. in 125 samples of *C. sinensis* cv. Valencia, one Rusk citrange, three *C. hystrix*, three *Citrus* spp., and 35 *D. citri* samples from the USA and Cuba.

3.2.3 Repeatability and reproducibility

Repeatability and reproducibility were assessed by analyzing 10 samples infected with relatively low concentrations of CaLas, with Cqs values ranging from 21.1 to 36.7. Technical replicates of each sample were analyzed using two different fluorimeters, Genie® II and AmplifyRP® XRT, and by two different operators. The Cqs values obtained by real-time qPCR and results obtained by real-time RPA in the two pieces of equipment are shown in Table 3. All infected samples showed positive results in both fluorimeters. Only one sample showed different results between the two devices: sample 607 showed negative results in one of the replicates analyzed in Genie® II, while in AmplifyRP® XRT, it was positive in all replicates.

3.2.4 Diagnostic sensitivity and specificity

The evaluation of diagnostic sensitivity and specificity was carried out by analyzing healthy and HLB-infected samples, both symptomatic and asymptomatic, collected randomly from three different origins (Brazil, Costa Rica, and Spain). A total of 226 citrus samples were analyzed by real-time qPCR (de Chaves et al., 2023) and the new real-time RPA design. Out of the total samples collected, 118 were positive and 88 were negative by real-time PCR, while 99 were positive and 107 were negative by real-time RPA. All partial sequences of *fusA* gene obtained from the 27 real-time RPA positive samples selected corresponded to CaLas and were submitted to the GenBank database (GenBank accession numbers: OQ507440 to OQ507466). Results from a correlation between both detection methods showed that the real-time RPA has a diagnostic sensitivity of 83.89%, a diagnostic specificity of 100%, and a relative accuracy of 91.59% in comparison with the gold standard method (Table 4). The agreement between the real-time qPCR (de Chaves et al., 2023) and the real-time RPA developed in this study was almost perfect, as Cohen's kappa index was 0.83.

4 Discussion

The HLB disease and its vectors, aided by intense international trade and climate change, are spreading rapidly, and HLB continues to decimate citrus productivity, with a devastating impact on the crop in important citrus growing areas. In fact, in countries where the disease is present, different control strategies have been carried out without significant success (Andrade et al., 2020; Bassanezi et al., 2020). Therefore, the best strategy against HLB disease remains to prevent the introduction and establishment rather than to cure it (Bové, 2006; Wang, 2020). Therefore, the threat of this disease to free areas, such as the Mediterranean Basin and Australia, requires that preventive measures be taken to at least delay the entry of the bacterium. For this purpose, it is essential to have sensitive, specific, and accurate techniques for early detection and containment. It is also very important that they have potential

TABLE 3 Evaluation of repeatability and reproducibility of the real-time RPA (in Genie II and AmplifyRP XRT) with 10 samples of Citrus sinensis cv. Valencia plants infected with 'Candidatus Liberibacter asiaticus'.

Sample ID	Real-time PCR according to de Chaves et al., 2023 (C_q average ± SE)	Genie® II	AmplifyRP® XRT
473	23.49 ± 0.24	+++	+++
607	24.17 ± 0.54	++-	+++
614	21.22 ± 0.96	+++	+++
615	22.76 ± 0.24	+++	+++
623	21.76 ± 0.86	+++	+++
627	22.23 ± 0.31	+++	+++
631	21.15 ± 0.45	+++	+++
633	21.91 ± 0.21	+++	+++
635	21.15 ± 0.71	+++	+++
641	22.64 ± 0.23	+++	+++
875	35.87 ± 0.11	++-	++-
874	36.71 ± 0.21	+++	+++
Infected extract of *C. sinensis* cv. Valencia	21.98 ± 0.38	+++	+++
Healthy extract of *C. sinensis* cv. Lane	- - -	- - -	- - -

RPA, recombinase polymerase amplification.
The results by real-time RPA are coded with + for positive reactions, and - for negative reactions, in three replicates per sample.

application at the front line, at the point of need in the field, and that they are rapid and robust with good cost-effectiveness.

The main requirements for a detection technique to be used at the point of care are a specificity of approximately 100% (absence of false positives), a sensitivity as high as possible (limited false-negative results), an easy implementation in a short time, and a limited cost (Cesbron et al., 2022). In this work, a fast on-site detection protocol, based on real-time recombinase polymerase amplification of gene *fusA*, which requires minimal and portable instrumentation and has a short reaction time, has been designed and developed for the detection of the three '*Ca.* Liberibacter' species associated with HLB. Although none of these three species are currently present in Europe, the two main insect vectors are already established and expanding in the Mediterranean Basin (Pérez Otero et al., 2015; Wang, 2020; Ministry of Agriculture and Rural Development of Israel, 2022). This, along with the continued movement of plant material imports worldwide, poses a serious threat to the introduction of HLB-associated bacteria into HLB-free regions. This threat is from both CaLas and CaLaf and, probably to a lesser extent, CaLam. The developed real-time RPA method allows the detection of the three species with excellent sensitivity and specificity, in addition to very fast reaction time, which makes it ideal for inspection in border points, local farms, or greenhouses since its use would increase the possibility of intercepting infected material, both insect and plant tissues.

In recent years, new molecular protocols for HLB detection have been developed and could be conveniently used on-site (Li et al., 2012; Rigano et al., 2014; Ghosh et al., 2016; Wu et al., 2016; Qian et al., 2017; Choi et al., 2018; Stolowicz et al., 2022; Thoraneenitiyan et al., 2022). However, all these protocols have

TABLE 4 Evaluation of diagnostic sensitivity and specificity of the new real-time RPA by comparison with a validated real-time PCR (de Chaves et al., 2023).

		Real-time PCR according to de Chaves et al. (2023)		
		Positive	Negative	Total
Real-time RPA	**Positive**	99	0	99
	Negative	19	108	127
	Total	118	108	226
Diagnostic sensitivity		83.89%		
Diagnostic specificity		100%		
Relative accuracy		91.59%		

RPA, recombinase polymerase amplification.

been designed to detect only CaLas and are predominantly based on loop-mediated isothermal DNA amplifications, and only three are based on recombinase polymerase amplification. Although these protocols are highly valuable for on-site detections in areas where CaLas is established, they may not provide complete protection against HLB in regions where the three '*Ca*. Liberibacter' species pose a potential risk. The new real-time RPA method developed in this study can detect CaLas, CaLaf, and CaLam in both plant and insect samples and can be easily applied for on-site detection, as it requires simple, portable equipment and no DNA purification step. All this displays real-time results in as little as 35 min.

The primers and probe designed for this new protocol target *fusA* gene, a highly conserved gene among HLB-associated bacterial species. The sequence is unique, conserved, and highly specific; it matches multiple genomes of each species and has been found to be specific. Moreover, it was observed that primers are specific to target HLB pathogens and do not cross- react with other major citrus pathogens. Unlike the 16S rRNA gene, which is known to produce false- positive results (Morán et al., 2020), the use of *fusA* gene offers a more specific detection method according to the findings of this study. The specificity of primers and probe designed for this new real-time RPA protocol was evaluated both *in silico* and *in vitro*. Results showed a high specificity degree since amplification was obtained with all samples containing HLB-associated '*Ca*. Liberibacter' spp., while no non-specific amplification was obtained in the samples not infected by HLB. The sequencing of the products obtained by conventional PCR showed the selective amplification of CaLas, CaLaf, and CaLam. In addition, the newly developed real-time RPA has been validated following the guidelines set by the EPPO standards (EPPO, 2021a), comparing it with the gold standard method (real-time PCR). This fact is very relevant since it implies that the newly developed real-time RPA is the only protocol for on-site detection of HLB that complies with EPPO standards to date, which is a guarantee of quality management requirements.

The new protocol showed a high analytical sensitivity, both in the evaluations carried out with synthetic dsDNA and in infected plant and insect material. In the case of synthetic dsDNA, the new RPA method was capable of detecting 4–8 copies/µl, while in infected material, it was capable of detecting amounts on the order of 10^1 copies/µl, which is a value similar to that obtained in other recent works with RPA in other pathosystems (Cesbron et al., 2022). The different sensitivity between synthetic dsDNA and natural samples can be due to the fact that the synthetic dsDNA is not encapsulated in a lipid membrane, contrary to what occurs with naturally infected material, where the DNA target is inside cells. Therefore, it can be said that the reliable detection limit of this protocol is approximately the order of 10^1 copies/µl, one order of magnitude lower than the LOD of the real-time qPCR with which it was compared (de Chaves et al., 2023). Evaluation of the diagnostic sensitivity of the new RPA method with a random selection of healthy and infected plant samples from three different countries, with a range of different target inoculum levels, revealed a concordance of 83.89% with the gold standard method. The lower sensitivity of the new protocol with respect to real-time qPCR is possibly due to the fact that detection below the order of magnitude of 10^1 copies/µl is subject in RPA to a random factor, as suggested by the results obtained during the evaluation of the analytical sensitivity.

Regarding the analytical specificity of the new RPA protocol, inclusivity results suggest that it can detect a broad range of HLB-associated '*Ca*. Liberibacter' isolates representing the diversity of the three species, as it was able to recognize target isolates from nine different origins, including São Paolo and Paraná of Brazil, Alajuela of Costa Rica, Florida of the USA, Artemisa of Cuba, and the INRAE collection (France). Furthermore, the new real-time RPA was able to detect '*Ca*. Liberibacter' isolates infecting at least five different plant hosts, such as *C. sinensis* cv. Valencia, Rusk citrange, *C. hystrix*, *Citrus* sp., and *D. citri* insect, suggesting that variations in the host-matrix, assessed in this study, do not affect the throughput of the new protocol. The exclusivity results indicate that the relevant phylogenetically close non-target bacterial species ('*Ca*. Liberibacter solanacearum', *L. crescens*, *A. tumefaciens*, and *A. vitis*) and phytopathogenic citrus bacterial species (*X. fastidiosa* subsp. *pauca*, *X. fastidiosa* subsp. *fastidiosa*, *X. citri* subsp. *citri*, and *P. syringae* pv. *syringae*) do not cause the occurrence of non-specific amplifications with the newly developed protocol. Moreover, the diagnostic specificity results showed 100% agreement with the gold standard method.

All these specificity results suggest that the new real-time RPA could detect with high confidence the three HLB-associated bacterial species and different isolates, being able to discriminate from other important citrus pathogens. Finally, regarding the repeatability and reproducibility of the new protocol, the high level of consistency in the results of the technique makes it ideal for obtaining reliable and comparable performance even when the technique is used by different operators and on different fluorimeters. Therefore, all these results suggest that the new real-time RPA protocol could be effectively used as a first rapid screening technique at strategic entry points, mainly in HLB-free regions where the three species of '*Ca*. Liberibacter' is a potential threat.

This new protocol developed in this study is not intended to replace other more sensitive molecular methods, such as real-time PCR, but rather to be an additional tool to support HLB diagnosis within the management systems of this serious disease. It is a prototype with great potential for use at points of care, within HLB prevention strategy plans, and in regions where there is a high risk of introduction or spread of the disease. It can be used as a first screening test for the detection of HLB in suspicious samples, such as symptomatic samples or samples from areas where the disease is present. This prototype overcomes the need for extensive technical expertise and complex infrastructure. In addition, the advantage of not requiring DNA purification provides greater cost-effectiveness than other technologies and allows the end user to feasibly perform screening tests at the point of need.

In conclusion, the results presented in this study demonstrate that the new real-time RPA protocol is a highly sensitive, specific, and accurate tool for the rapid diagnosis of HLB that can be used with easy-to-use portable equipment. This makes it very suitable for rapid point-of-care detection, especially useful for those disease-free countries with a high risk of introduction of any of the three '*Ca*. Liberibacter' species associated with HLB.

Data availability statement

The datasets presented in this study can be found in online repositories. The names of the repository/repositories and accession number(s) can be found in the article/Supplementary Material.

Author contributions

Conceptualization and methodology: FM and EM-N. Validation: FM, MH-C and SC-R. Formal analysis: FM and EM-N. Investigation: FM, EM-N, MH-C and SC-R. Resources: FM and EM-N. Data curation: FM and EM-N. Writing—original draft preparation: FM. Writing—review and editing: FM, EM-N, MH-C and SC-R. Funding acquisition: EM-N. All authors contributed to the article and approved the submitted version.

Funding

LIFE18 CCA/ES/001109 (Development of sustainable control strategies for citric under threat of climate change AND preventing entry of HLB in EU-LIFE Vida for Citrus-), PID2021-124145OR-C21 (Breeding, selection and evaluation of new citrus materials for more sustainable plantations in the face of emerging threats due to global change— FORTECITRUS), and IVIA-GVA 52202D (SOSTENIBLE) from Instituto Valenciano de Investigaciones Agrarias (project susceptible of being co-financed by the European Union through the ERDF Program 2021-2027 Comunitat Valenciana).

Acknowledgments

The authors express their sincere gratitude to several individuals and organizations whose contributions made this study possible. First, the authors would like to thank the European Commission initiative, innovation Radar, for recognizing this study as a high-potential innovation EU-funded research (https://www.innoradar.eu/innovation/38305). This acknowledgment is a testament to the support received from the European Commission, and the authors remain grateful for their assistance. Furthermore, the authors extend their appreciation to the Spanish Society of Phytopathology (Sociedad Española de Fitopatología, SEF) for awarding the "Ricardo Flores" prize to this study at the XX Congress of the Society. This recognition has encouraged our team to continue striving for excellence in research. The authors thank the Spanish Ministry of Agriculture for the support of the National Reference Laboratory of Phytopathogenic Bacteria (IVIA Bacteriology Laboratory). The authors would also like to express their gratitude to the following individuals for their contributions: Dr. Alejandro Tena, Dr. Alberto Urbaneja, and Dr. Meritxel Pérez-Hedo (IVIA-Spain) for providing insect samples; Dr. Edson Bertolini (UFRGS-Brazil), Dr. Maritza Luis-Pantoja, and Camilo Paredes (IIFT-Cuba) for providing insect and plant DNA samples; and Dr. Silvio Aparecido (Fundecitrus-Brazil), Laura Garita, Willian Villalobos, Dr. Carlos Chacón, and Dr. Mauricio Montero-Astúa (UCR-Costa Rica) for their help in conducting surveys. Their generous contributions have been invaluable to our research. The authors thank B. Davenport and M. Amato for technical advice. Finally, the authors would like to extend their gratitude to Dr. Silvia Barbé and MSc. Nerea García Moreno (IVIA-Spain) for their technical support. Their assistance has been necessary for the successful completion of this study.

Conflict of interest

The authors declare that the research was conducted in the absence of any commercial or financial relationships that could be construed as a potential conflict of interest.

Publisher's note

Supplementary material

The Supplementary Material for this article can be found online at: https://www.frontiersin.org/articles/10.3389/fpls.2023.1176513/full#supplementary-material

References

Ajene, I. J., Khamis, F., van Asch, B., Pietersen, G., Rasowo, B. A., Ekesi, S., et al. (2020). Habitat suitability and distribution potential of liberibacter species (`*Candidatus* liberibacter asiaticus´ and `*Candidatus* liberibacter africanus´) associated with citrus greening disease. *Divers. Distrib* 26, 575–588. doi: 10.1111/DDI.13051

Alquezar, B., Carmona, L., Bennici, S., Miranda, M. P., Bassanezi, R. B., and Peña, L. (2022). Cultural management of huanglongbing: current status and ongoing research. *Phytopathology* 112, 11–25. doi: 10.1094/PHYTO-08-21-0358-IA

Andrade, M., Li, J., and Wang, N. (2020). `*Candidatus* liberibacter asiaticus´: virulence traits and control strategies. *Trop. Plant Pathol.* 45, 285–297. doi: 10.1007/S40858-020-00341-0/METRICS

Bassanezi, R. B., Lopes, S. A., de Miranda, M. P., Wulff, N. A., Volpe, H. X. L., and Ayres, A. J. (2020). Overview of citrus huanglongbing spread and management strategies in Brazil. *Trop. Plant Pathol.* 45, 251–264. doi: 10.1007/S40858-020-00343-Y/METRICS

Bové, J. M. (2006). Huanglongbing: a destructive, newly-emerging, century-old disease of citrus. *Source: J. Plant Pathol.* 88, 7–37.

Bertolini, E., Felipe, R. T.A., Sauer, A. V., Lopes, S. A., Arilla, A., Vidal, E., et al (2014). Tissue-print and squash real-time PCR for direct detection of 'Candidatus Liberibacter' species in citrus plants and psyllid vectors. *Plant Pathol.* 63, 1149–1158. doi: 10.1111/PPA.12197

Cesbron, S., Dupas, E., and Jacques, M.-A. (2022). Evaluation of the AmplifyRP® XRT+ kit for the detection of xylella fastidiosa by recombinase polymerase amplification (RPA). *PhytoFrontiers*. doi: 10.1094/PHYTOFR-03-22-0025-FI

Choi, C. W., Hyun, J. W., Hwang, R. Y., and Powell, C. A. (2018). Loop-mediated isothermal amplification assay for detection of `*Candidatus* liberibacter asiaticus´, a causal agent of citrus huanglongbing. *Plant Pathol. J.* 34, 499. doi: 10.5423/PPJ.FT.10.2018.0212

Cohen, J. (1960). A coefficient of agreement for nominal scales. *Educ. Psychol. Meas* 20, 37–46. doi: 10.1177/001316446002000104

da Costa, G. V., Neves, C. S. V. J., Bassanezi, R. B., Junior, R. P. L., and Telles, T. S. (2021). Economic impact of huanglongbing on orange production. *Rev. Bras. Frutic* 43. doi: 10.1590/0100-29452021472

Dala-Paula, B. M., Plotto, A., Bai, J., Manthey, J. A., Baldwin, E. A., Ferrarezi, R. S., et al. (2019). Effect of huanglongbing or greening disease on orange juice quality, a review. *Front. Plant Sci.* 9. doi: 10.3389/FPLS.2018.01976/BIBTEX

Darling, A. C. E., Mau, B., Blattner, F. R., and Perna, N. T. (2004). MAUVE: multiple alignment of conserved genomic sequence with rearrangements. *Genome Res.* 14, 1394–1403. doi: 10.1101/GR.2289704

Das, A. K. (2008). "Citrus greening (Huanglongbing) disease in India: present status and diagnostic efforts," in *Proceedings International Research Conference on HLB 2008* Ed. Plant Management Network (Florida) 129–133.

Das, A. K., Nerkar, S., Bawage, S., and Kumar, A. (2014). Current distribution of huanglongbing (citrus greening disease) in India as diagnosed by real-time PCR. *J. Phytopathol.* 162, 402–406. doi: 10.1111/JPH.12195

de Chaves, M. Q.-G., Morán, F., Barbé, S., Bertolini, E., de la Rosa, F. S., and Marco-Noales, E. (2023). A new and accurate qPCR protocol to detect plant pathogenic bacteria of the genus `*Candidatus* liberibacter´ in plants and insects. *Sci. Rep.* 13, 1–12. doi: 10.1038/s41598-023-30345-0

EPPO (2021a). PM 7/98 (5) specific requirements for laboratories preparing accreditation for a plant pest diagnostic activity. *EPPO Bull.* 51, 468–498. doi: 10.1111/EPP.12780

EPPO (2021b). PM 7/121 (2) `*Candidatus* liberibacter africanus´, `*Candidatus* liberibacter americanus´ and `Candidatus liberibacter asiaticus´. *EPPO Bull.* 51, 267–282. doi: 10.1111/EPP.12757

EPPO Global Database (2023). Available at: https://gd.eppo.int/ (Accessed February 8, 2023).

Ghosh, D. K., Bhose, S., Warghane, A., Motghare, M., Sharma, A. K., Dhar, A. K., et al. (2016). Loop-mediated isothermal amplification (LAMP) based method for rapid and sensitive detection of `*Candidatus* liberibacter asiaticus´ in citrus and the psyllid vector, *Diaphorina citri* kuwayama. *J. Plant Biochem. Biotechnol.* 25, 219–223. doi: 10.1007/S13562-015-0332-8/METRICS

Ghosh, D. K., Kokane, S. B., Kokane, A. D., Warghane, A. J., Motghare, M. R., Bhose, S., et al. (2018). Development of a recombinase polymerase based isothermal amplification combined with lateral flow assay (HLB-RPA-LFA) for rapid detection of `Candidatus liberibacter asiaticus´. *PloS One* 13, e0208530. doi: 10.1371/JOURNAL.PONE.0208530

Ghosh, D., Kokane, S., Savita, B. K., Kumar, P., Sharma, A. K., Ozcan, A., et al. (2022). Huanglongbing pandemic: current challenges and emerging management strategies. *Plants 2023* 12, 160. doi: 10.3390/PLANTS12010160

Hocquellet, A., Toorawa, P., Bové, J. M., and Garnier, M. (1999). Detection and identification of the two *Candidatus* liberobacter species associated with citrus huanglongbing by PCR amplification of ribosomal protein genes of the beta operon. *Mol. Cell Probes* 13, 373–379. doi: 10.1006/MCPR.1999.0263

IPPC-FAO (2022) *Diagnostic protocols for regulated pests 31: `Candidatus liberibacter´ spp. on citrus spp*. Available at: https://www.ippc.int/es/publications/90935/ (Accessed February 8, 2023).

Ivanov, A. V., Safenkova, I. V., Zherdev, A. V., and Dzantiev, B. B. (2021). The potential use of isothermal amplification assays for in-field diagnostics of plant pathogens. *Plants* 10, 2424. doi: 10.3390/PLANTS10112424/S1

Jagoueix, S., Bové, J. M., and Garnier, M. (1996). PCR detection of the two "*Candidatus*" liberobacter species associated with greening disease of citrus. *Mol. Cell Probes* 10, 43–50. doi: 10.1006/MCPR.1996.0006

Katoh, H., Miyata, S. I., Inoue, H., and Iwanami, T. (2014). Unique features of a Japanese `*Candidatus* liberibacter asiaticus´ strain revealed by whole genome sequencing. *PloS One* 9. doi: 10.1371/JOURNAL.PONE.0106109

Lallemand, J., Fos, A., and Bové, J. M. (1986). Transmission de la bactérie associée à la forme africaine de la maladie du "Greening" par le psylle asiatique *Diaphorina citri* kuwayama. *Fruits* 41, 341–343.

Landis, J. R., and Koch, G. G. (1977). The measurement of observer agreement for categorical data. *Biometrics* 33, 159. doi: 10.2307/2529310

Lee, J. A., Halbert, S. E., Dawson, W. O., Robertson, C. J., Keesling, J. E., and Singer, B. H. (2015). Asymptomatic spread of huanglongbing and implications for disease control. *Proc. Natl. Acad. Sci. U.S.A.* 112, 7605–7610. doi: 10.1073/PNAS.1508253112/SUPPL_FILE/PNAS.1508253112.SAPP.PDF

Li, W., Hartung, J. S., and Levy, L. (2006). Quantitative real-time PCR for detection and identification of `*Candidatus* liberibacter´ species associated with citrus huanglongbing. *J. Microbiol. Methods* 66, 104–115. doi: 10.1016/J.MIMET.2005.10.018

Li, H., HuaNan, S., KeZhi, T., AiJun, H., ChangYong, Z., and ZhongAn, L. (2012). Establishment and application of loop-mediated isothermal amplification assay for the detection of citrus huanglongbing. *J. Fruit Sci.* 29, 1121–1126.

Li, M., Qin, H., Long, Y., Cheng, M., Li, L., Huang, A., et al. (2022). Field-deployable `Candidatus liberibacter asiaticus´ detection using recombinase polymerase amplification combined with CRISPR-Cas12a. *J. Vis. Exp.* 2022. doi: 10.3791/64070

Lin, H., Chen, C., Doddapaneni, H., Duan, Y., Civerolo, E. L., Bai, X., et al. (2010). A new diagnostic system for ultra-sensitive and specific detection and quantification of `*Candidatus* liberibacter asiaticus´, the bacterium associated with citrus huanglongbing. *J. Microbiol. Methods* 81, 17–25. doi: 10.1016/J.MIMET.2010.01.014

Lin, H., Han, C. S., Liu, B., Lou, B., Bai, X., Deng, C., et al. (2013). Complete genome sequence of a Chinese strain of `*Candidatus* liberibacter asiaticus´. *Genome Announc* 1. doi: 10.1128/GENOMEA.00184-13

Lin, H., Pietersen, G., Han, C., Read, D. A., Lou, B., Gupta, G., et al. (2015). Complete genome sequence of `*Candidatus* liberibacter africanus´, a bacterium associated with citrus huanglongbing. *Genome Announc* 3. doi: 10.1128/GENOMEA.00733-15

Lu, J., Delatte, H., Reynaud, B., Beattie, G. A. C., Holford, P., Cen, Y., et al. (2021). Genome sequence resource of `*Candidatus* liberibacter asiaticus´ from *Diaphorina citri* kuwayama (Hemiptera: liviidae) from la réunion. *Plant Dis.* 105, 1171–1173. doi: 10.1094/PDIS-09-20-1998-A

Massonie, G., Garnier, M., and Bové, J. M. (1976). "Transmission of Indian citrus decline by *Trioza erytreae* (Del guercio), the vector of south African greening," in International Organization of Citrus Virologists Conference Proceedings (1957-2010) ed. Open Access Publications from the University of California (Greece: California Digital Library (CDL)). doi: 10.5070/C54DH8X79M

Ministry of Agriculture and Rural Development of Israel (2022) *A new immigrant: the ministry of agriculture is fighting a new and destructive disease that has invaded Israel | ministry of agriculture and rural development*. Available at: https://www.gov.il/en/Departments/news/diaphorina_citri (Accessed February 8, 2023).

Morán, F., Barbé, S., Bastin, S., Navarro, I., Bertolini, E., López, M. M., et al. (2020). The challenge of environmental samples for PCR detection of phytopathogenic bacteria: a case study of citrus huanglongbing disease. *Agron. 2021* 11, 10. doi: 10.3390/AGRONOMY11010010

Morgan, J. K., Zhou, L., Li, W., Shatters, R. G., Keremane, M., and Duan, Y. P. (2012). Improved real-time PCR detection of `*Candidatus* liberibacter asiaticus´ from citrus and psyllid hosts by targeting the intragenic tandem-repeats of its prophage genes. *Mol. Cell Probes* 26, 90–98. doi: 10.1016/J.MCP.2011.12.001

Neupane, D., Moss, C. B., and van Bruggen, A. H. C. (2016). Estimating citrus production loss due to citrus huanglongbing in Florida. doi: 10.22004/AG.ECON.230093

OligoAnalyzer Tool - IDT. Available at: https://eu.idtdna.com/pages/tools/oligoanalyzer (Accessed February 10, 2023).

Owczarzy, R., Tataurov, A. v, Wu, Y., Manthey, J. A., Mcquisten, K. A., Almabrazi, H. G., et al. (2008). IDT SciTools: a suite for analysis and design of nucleic acid oligomers. *Nucleic Acids Res.* 36, 163–169. doi: 10.1093/nar/gkn198

Patel, R., Mitra, B., Vinchurkar, M., Adami, A., Patkar, R., Giacomozzi, F., et al. (2022). A review of recent advances in plant-pathogen detection systems. *Heliyon* 8. doi: 10.1016/J.HELIYON.2022.E11855

Pérez Otero, R., Mansilla Vázquez, J. P., and del Estal, P. (2015). Detección de la psila africana de los cítricos, *Trioza erytreae* (Del guercio 1918) (Hemiptera: psylloidea: triozidae), en la península ibérica. *Arquivos Entomolóxicos* 13, 119–122.

Petrone, J., Munoz-Beristain, A., Russell, J., Rios-Glusberger, P., and Triplett, E. (2019) *Direct submission - `Candidatus liberibacter asiaticus´ isolate JRPAMB1 chromosome, complete - nucleotide - NCBI*. Available at: https://www.ncbi.nlm.nih.gov/nuccore/NZ_CP040636.1 (Accessed February 9, 2023).

Proksee. Available at: https://proksee.ca/ (Accessed February 9, 2023).

Qian, W., Meng, Y., Lu, Y., Wu, C., Wang, R., Wang, L., et al. (2017). Rapid, sensitive, and carryover contamination-free loop-mediated isothermal amplification-coupled visual detection method for `*Candidatus* liberibacter asiaticus'. *J. Agric. Food Chem.* 65, 8302–8310. doi: 10.1021/ACS.JAFC.7B03490/SUPPL_FILE/JF7B03490_SI_001.PDF

Rattner, R. J., Godfrey, K. E., Hajeri, S., and Yokomi, R. K. (2022). An improved recombinase polymerase amplification coupled with lateral flow assay for rapid field detection of `*Candidatus* liberibacter asiaticus´. *Plant Dis.* 106, 3091–3099. doi: 10.1094/PDIS-09-21-2098-RE

Reynaud, B., Turpin, P., Molinari, F. M., Grondin, M., Roque, S., Chiroleu, F., et al. (2022). The African citrus psyllid *Trioza erytreae*: an efficient vector of `*Candidatus* liberibacter asiaticus´. *Front. Plant Sci.* 13. doi: 10.3389/FPLS.2022.1089762/BIBTEX

Rigano, L. A., Malamud, F., Orce, I. G., Filippone, M. P., Marano, M. R., do Amaral, A. M., et al. (2014). Rapid and sensitive detection of `*Candidatus* liberibacter asiaticus´ by loop mediated isothermal amplification combined with a lateral flow dipstick. *BMC Microbiol.* 14, 1–9. doi: 10.1186/1471-2180-14-86/TABLES/4

Sapre, S., Gontia-Mishra, I., Thakur, V. V., Sikdar, S., and Tiwari, S. (2021). "Molecular techniques used in plant disease diagnosis," in *Food security and plant disease management* A. Kumar and S. Droby (Chennai: Woodhead Publishing), 405–421. doi: 10.1016/B978-0-12-821843-3.00001-5

Stolowicz, F., Larocca, L., Werbajh, S., Parma, Y., Carrillo, C., Ogas, L., et al. (2022). A colorimetric, sensitive, rapid, and simple diagnostic kit for the HLB putative causal agent detection. *Front. Agron.* 4. doi: 10.3389/FAGRO.2022.984360/BIBTEX

Tatineni, S., Sagaram, U. S., Gowda, S., Robertson, C. J., Dawson, W. O., Iwanami, T., et al. (2008). In planta distribution of `*Candidatus* liberibacter asiaticus´ as revealed by polymerase chain reaction (PCR) and real-time PCR. *Phytopathology* 98, 592–599. doi: 10.1094/PHYTO-98-5-0592

Taylor, R. A., Ryan, S. J., Lippi, C. A., Hall, D. G., Narouei-Khandan, H. A., Rohr, J. R., et al. (2019). Predicting the fundamental thermal niche of crop pests and diseases in a changing world: a case study on citrus greening. *J. Appl. Ecol.* 56, 2057–2068. doi: 10.1111/1365-2664.13455

Teixeira, D. C., Saillard, C., Eveillard, S., Danet, J. L., Ayres, A. J., and Bové, J. M. (2005). "A new liberibacter species, `*Candidatus* liberibacter americanus sp. nov.´, is associated with citrus huanglongbing (Greening disease) in são paulo state, Brazil," in *International Organization of Citrus Virologists Conference Proceedings (1957-2010)* ed. Open Access Publications from the University of California (Mexico: California Digital Library (CDL)), 325–340. doi: 10.5070/C50DD5F2RT

Thoraneenitiyan, N., Choopara, I., Nuanualsuwan, S., Kokpol, S., and Somboonna, N. (2022). Rapid visual `*Candidatus* liberibacter asiaticus´ detection (citrus greening disease) using simple alkaline heat DNA lysis followed by loop-mediated isothermal amplification coupled hydroxynaphthol blue (AL-LAMP-HNB) for potential local use. *PloS One* 17, e0276740. doi: 10.1371/JOURNAL.PONE.0276740

TwistAmp® (2018). DNA Amplification kits assay design manual. *TwistAmp®*, 1–32. Available at: https://www.twistdx.co.uk/wp-content/uploads/2021/04/twistamp-assay-design-manual-v2-5.pdf. [Accessed February 9, 2023].

Valdés, R. A., Ortiz, J. C. D., Beache, M. B., Cabello, J. A., Chávez, E. C., Pagaza, Y. R., et al. (2016). A review of techniques for detecting huanglongbing (Greening) in citrus. *Can. J. Microbiol.* 62, 803–811. doi: 10.1139/CJM-2016-0022/ASSET/IMAGES/CJM-2016-0022TAB1.GIF

Wang, N. (2020). A perspective of citrus huanglongbing in the context of the Mediterranean basin. *J. Plant Pathol.* 102, 635–640. doi: 10.1007/S42161-020-00555-W/FIGURES/1

Wang, Y., Kondo, T., He, Y., Zhou, Z., and Lu, J. (2021). Genome sequence resource of `*Candidatus* liberibacter asiaticus´ from *Diaphorina citri* kuwayama (Hemiptera: liviidae) in Colombia. *Plant Dis.* 105, 193–195. doi: 10.1094/PDIS-06-20-1249-A

Wu, X., Meng, C., Wang, G., Liu, Y., Zhang, X., Yi, K., et al. (2016). Rapid and quantitative detection of citrus huanglongbing bacterium `*Candidatus* liberibacter asiaticus´ by real-time fluorescent loop-mediated isothermal amplification assay in China. *Physiol. Mol. Plant Pathol.* 94, 1–7. doi: 10.1016/J.PMPP.2016.03.001

Wulff, N. A., Zhang, S., Setubal, J. C., Almeida, N. F., Martins, E. C., Harakava, R., et al. (2014). The complete genome sequence of `*Candidatus* liberibacter americanuS´, associated with citrus huanglongbing. *Mol. Plant Microbe Interact.* 27, 163–176. doi: 10.1094/MPMI-09-13-0292-R

Zheng, Z., Deng, X., and Chen, J. (2014). Whole-genome sequence of `*Candidatus* liberibacter asiaticus´ from guangdong, China. *Genome Announc* 2. doi: 10.1128/GENOMEA.00273-14

Zheng, Z., Deng, X., and Chen, J. (2022a)Direct submission - `*Candidatus* liberibacter asiaticus´ strain JXGC chromosome, complete gen. Available at: https://www.ncbi.nlm.nih.gov/nuccore/NZ_CP019958.1 (Accessed February 9, 2023). NCBI Reference Sequence.

Zheng, Z., Li, T., and Narit, T. (2022b)Direct submission - first genome sequence source of `*Candidatus* liberibacter asiaticus´ from Thailand. Available at: https://www.ncbi.nlm.nih.gov/nuccore/NZ_CP041385.1 (Accessed February 9, 2023).

Zheng, Z., Xu, M., Bao, M., Wu, F., Chen, J., and Deng, X. (2016). Unusual five copies and dual forms of *nrdB* in `*Candidatus* liberibacter asiaticus´: biological implications and PCR detection application. *Sci. Rep.* 6, 1–9. doi: 10.1038/srep39020

Zhou, L., Powell, C. A., Hoffman, M. T., Li, W., Fan, G., Liu, B., et al. (2011). Diversity and plasticity of the intracellular plant pathogen and insect symbiont `*Candidatus* liberibacter asiaticus´ as revealed by hypervariable prophage genes with intragenic tandem repeats. *Appl. Environ. Microbiol.* 77, 6663–6673. doi: 10.1128/AEM.05111-11

Frontiers in
Plant Science

Cultivates the science of plant biology and its applications

The most cited plant science journal, which advances our understanding of plant biology for sustainable food security, functional ecosystems and human health.

Discover the latest Research Topics

See more →

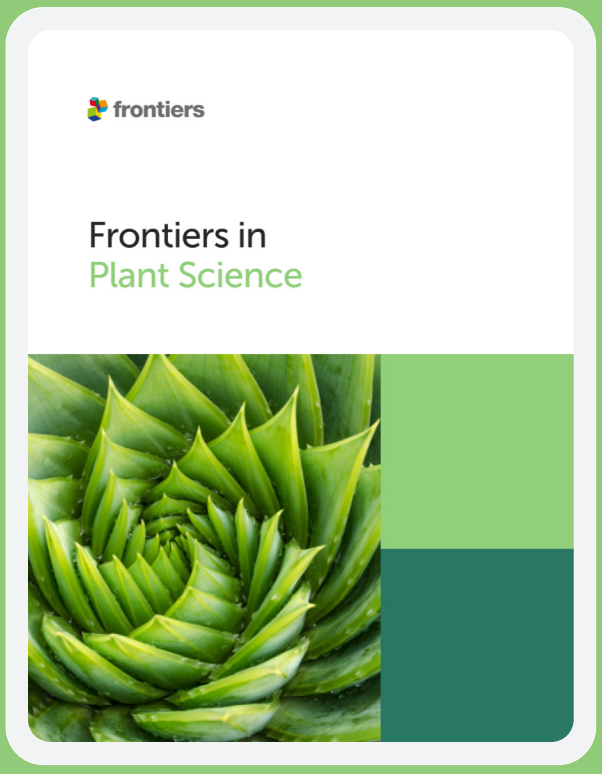

Frontiers

Avenue du Tribunal-Fédéral 34
1005 Lausanne, Switzerland
frontiersin.org

Contact us

+41 (0)21 510 17 00
frontiersin.org/about/contact